UCSF
UC San Francisco Electronic Theses and Dissertations

**Title**
Organelle transport

**Permalink**
https://escholarship.org/uc/item/0kd71551

**Author**
Niclas, Joshua,

**Publication Date**
1995

Peer reviewed|Thesis/dissertation

eScholarship.org Powered by the California Digital Library
University of California

Organelle Transport: Motor Proteins and Regulatory Mechanisms

by

Joshua Niclas

**DISSERTATION**

**Submitted in partial satisfaction of the requirements for the degree of**

**DOCTOR OF PHILOSOPHY**

**in**

Cell Biology

**in the**

**GRADUATE DIVISION**

**of the**

**UNIVERSITY OF CALIFORNIA**

**San Francisco**



copyright (1995)

by

Joshua Niclas

I dedicate this thesis to my mother, Elka, my father, Karl, my brother, Daniel, and my long-time friend and companion, Patty.

# ACKNOWLEDGEMENTS

I would like to start off by thanking my advisor, Dr. Ronald Vale for all the time and effort that he has put into my development as a scientist. Ever since starting in his lab back in my early medical school days, he has been both a teacher and a friend, something I have always valued. I am extremely thankful to Ron, for always having made time to talk to me whenever I needed to discuss the direction of my experiments. This is a quality that all graduate advisors should have. In addition, I am grateful to Ron for having cared enough to maintain a relatively conflict-free atmosphere in the lab by choosing new lab members carefully and consulting the lab first before making decisions. I would also like to thank Ron for those times when he helped me to see the positive side of experiments that appeared to have ended in utter failure, but actually provided small nuggets of useful information. Lastly, I can't thank Ron enough for having given me the opportunity to spend a summer doing research with him at the Woods Hole Marine Biological Laboratories. These were truly some of the most enjoyable times of my graduate years. In those three months, Ron taught me almost everything that I know about microscopy and developing in vitro assays for studying organelle transport. In addition, through this experience, I was able to meet some of the nicest and most enthusiastic scientists in my field. My memories of that experience have always been a continuous source of enthusiasm for scientific research.

It is hard to put into words, how thankful I am to my parents for all that they have done for me over the years. They have supported me in all my intellectual endeavors since my early days. There is no question that I would have never been an M.D.-Ph.D. student at a university like UCSF

without their support and nudging me along throughout my years in school. I thank them for having been there to lift me up during all those times of self-doubt and thinking that I merely got to be where I am by accident. I am also thankful for their home being a periodic escape from stress and the fog of doom that frequently curses those of us who live on the west side of UCSF. I am immensely thankful to them for not having complained during recent years about how long my schooling has taken, although I know that they are very happy now that it is nearing a conclusion. In addition to thanking my parents, I would also like to thank my brother, Daniel, also a graduate student in the biological sciences, for always being able to send me into fits of uncontrolled laughter with his unending supply of hilarious stories and his refreshingly unique and different views of graduate school, people and life.

I would like to thank Drs. Tim Mitchison, Andrew Murray and Vishu Lingappa for serving on my thesis committee. I feel fortunate to have had a committee that always provided useful, intelligent suggestions and helped me to make hard decisions about the path that my project was to take. It was nice to have a committee that made me feel like they cared about my work. In particular, I would like to thank Tim for the many ideas that he shared with me and for always being willing to set aside time to talk to me. Andrew deserves special mention of his ability to read my thesis committee meeting outline at the beginning of the meeting, digesting it and then coming up with the key questions to ask me all in under 3 minutes. Lastly, I would like to thank Vishu for being the MSTP council member on my committee, providing an "outside reviewer's" perspective on my project and thoughtful discussions of the topic of science and medicine.

Then there are the many members of the Vale lab that I have had the pleasure of knowing through the years. Many thanks go to Francesca Navone

for the many years of enjoyable international collaboration; to Gretchen McCaffrey for the many discussion about PCR and cloning; to Fady Malik, for his common sense advice, his unlimited willingness to help me when I was learning the basics of microscopy and reminding me to always look at the big picture; to Nora Hom-Booher, for being a great collaborator on all the kinesin cloning work, fun to work with and the greatest technician the Vale lab has ever had; to Lynne Sparks, for helping me with the initial cloning of uKHC and bringing a lot of cheer into the lab;to Harris Bernstein for all his advice and help with cloning the uKHC gene as well as being one of the nicest, good-natured persons that I have ever met; to Frank McNally, for demonstrating to me that rewards can come from persevering through years of absolutely brutal experiments in the face of seemingly insurmountable odds (I have come to understand you more and more since you left the lab.); to Nira Pollock for being the first long term fellow lab member working on organelle transport who I could have in depth discussions with on the topic; to Dara Friedman for being the first long term fellow lab member working on kinesin molecular biology and vesicle motility who I also could have in depth discussions with on that topic. She also deserves thanks for being a source of positivity in the lab. To Laura Romberg, thank you for all the entertaining discussions on your mouse behavior experiments; to Guenther Woehlke, for fun conversations about photography; to Chris Coppin for bailing me out of numerous computer disasters and for all his surgery stories that have lead to my eager anticipation of that clinical rotation; and to Rohit, who like Frank, taught me the virtues of being a hardworking, focused and dedicated labworker. And lastly, I have to thank a group individuals who are members of what could be called "The Glove Club". These include, Jim Wilhelm, Jim Hartman, Geno de Hostos and Dan Pierce. I can't thank you all enough for

the unending humor and entertainment that has come from something as ridiculous as the snap of a latex glove. To Jim Wilhelm, someone who seems to share the same brain that I use, thank you for becoming my fellow ultra-late night labworker and thanks for all the enjoyable discussions of low-brow science and late night bad TV. To Jim Hartman, thank you for also being a late night lab companion, a crazed audiogear maniac and beerlover like myself, and for all the millions of times you have helped me with my computer troubles. To Geno de Hostos, thank you so much for your 'snapping' sense of humor, teaching me that it is better to give than to receive, and for showing to me that a human being can endure unimaginable levels of pain and experimental hell and still attain success. To Dan Pierce, for having immediately understood the glove theme without any explanation and for always emphasizing to me that the rational, easiest, fastest approach is always the best approach.

The next round of thanks go to my fellow classmates. To Chris Vulpe, Jeff Lefstin and Elena Levine, thanks for all the times that you dragged me out of lab to remind me that there is a world outside of the Health Science Towers, and also thanks to Jeff for some of the wackiest scientific discussions I have ever been a part of; to Suzanne Noble for being an understanding and patient listener to my periodic ventings; to Bruce Cree for being a true friend during some of my worst moments, i.e. helping me to cope with an unexpected last minute major secondary orals proposal change and teaching me everything that I needed to know about yeast genetics two days before my oral qualifying exams; and to Jon Kull, for being my always helpful and friendly computer and Phaser expert.

From my Woods Hole days, I would like to express many thanks to Dr. Bob Palazzo for being a great teacher and friend to me and instilling in me a

great deal of the enthusiasm I have for scientific research. Jon Sheetz also deserves special mention for helping me with my experiments, being a good friend with a refreshing view of life, and providing me with the wildest high speed sailboat ride of my life.

Although they don't know me, I would like to thank three San Francisco musicians, Jim Thomas, Allen Whitman and Martyn Jones, who call themselves The Mermen. Their music has kept my brain awake during many late nights in lab and on numerous occasions provided the needed energy and inspiration to finish grueling experiments even if it meant seeing the sun come up.

And finally, I can't thank enough my dearest Patty. Over the last ten years, she has been a nonstop pillar of support and stability in my life. It is impossible to imagine having gone through the last 6 years of graduate school and 2 years of medical school without her there to help me maintain my sanity. She was always there to pull me out of my darkest moments and invariably made the good times great. I owe her a great deal for being a continuous source of energy and enthusiasm which I have been able to apply to all aspects of my life including my work.

# Organelle Transport: Motor Proteins and Regulatory Mechanisms

by

Joshua Niclas

**ABSTRACT**

Eukaryotic cells contain an elaborate transportation system for delivering membrane-bound organelles to their proper destination in the cytoplasm. Much of this transport is driven by motor proteins that attach to organelles and translocate along microtubule filaments. Two of these motor proteins, kinesin and cytoplasmic dynein, transport organelles towards the plus and minus ends of microtubules, respectively. This thesis presents work addressing the functions of kinesin in neuronal and non-neuronal cells as well as the regulation of cytoplasmic-dynein based organelle transport.

A human kinesin heavy chain expressed in all mammalian tissues (termed ubiquitous kinesin or uKHC) was cloned and different domains expressed in CV-1 cells. The C-terminal tail domain was unexpectedly found to bind to cytoplasmic microtubules, suggesting a microtubule crossbridging and sliding role for ubiquitous kinesin. Experiments with antisense oligonucleotides demonstrated a function in vesicle motility. Suppressing uKHC expression in neurons resulted in inhibition of neurite outgrowth and axonal transport of GAP-43 and synapsin I containing vesicles. Although a single kinesin was thought to serve all cell types, a second conventional KHC was discovered and found to be neuron-specific (nKHC). Like uKHC, nKHC is a nucleotide-dependent, microtubule-binding protein that partially cofractionates with membranes. In brain tissue, nKHC is highly enriched in

subsets of neurons; in cultured neurons, uKHC is distributed uniformly throughout the cell body and processes, whereas nKHC is concentrated in the cell body. The expression of nKHC was found to increase dramatically upon differentiation and axon-outgrowth of neuron-like cells (PC12 cells) in culture. These results demonstrate that mammalian neurons contain two conventional kinesin motors that may serve distinct functions in microtubule-based transport.

The mechanism by which cytoplasmic dynein-based organelle transport is controlled by the cell cycle was examined in extracts of Xenopus laevis eggs. In metaphase extracts, there is a dramatic reduction in organelle transport when compared to interphase. Cytoplasmic dynein was demonstrated by biochemical studies to be the minus-end motor in frog egg extracts. Analysis of purified membranes showed that cytoplasmic dynein and its activator dynactin detach from the membrane surface in metaphase extracts. In addition, one of the dynein light chains was found to be heavily phosphorylated in metaphase, but not interphase extracts. These studies suggest that cell cycle dependent phosphorylation may regulate organelle transport by modulating dynein's association with membranes.

T. J. Mitchison 9/18/95

Tim Mitchison, Ph.D.
Committee Chairman

Ronald Vale Sept 18, 1995

Ronald Vale, Ph.D.
Advisor

# TABLE OF CONTENTS

INTRODUCTION.....1

**PART 1:**

**The Ubiquitous and Neuronal Kinesins**

CHAPTER 1.....27

Cloning and Expression of a Human Kinesin Heavy Chain Gene: Interaction of the COOH-terminal Domain with Cytoplasmic Microtubules in Transfected CV-1 Cells

APPENDIX 1.....42

Characterization of a Human Kinesin Heavy Chain Gene

APPENDIX 2.....60

Suppression of Kinesin Expression in Cultured Hippocampal Neurons Using Antisense Oligonucleotides

CHAPTER 2.....74

Cloning and Localization of a Conventional Kinesin Motor Expressed Exclusively in Neurons

APPENDIX 3.....90

Differential Expression of Ubiquitous and Neuronal Kinesin Heavy

Chains During Differentiation of Neuroblastoma and PC12 Cells

## PART 2:
## Regulation of Microtubule-based Organelle Transport

CHAPTER 3.....121

Cell Cycle Regulation Of Dynein Association With Membranes Modulates Microtubule-Based Organelle Transport

APPENDIX 4.....158

Isolation Of Activators Of Dynein-Based Organelle Transport

CONCLUSIONS.....164

REFERENCES.....189

# LIST OF TABLES

**APPENDIX 2**

Table 1:

Effect of kinesin antisense oligonucleotides (50 μM) on neuritic growth after 2 days in culture.....67

**APPENDIX 3**

Table 1:

Expression of uKHC and nKHC in differentiated versus undifferentiated SH-SY5Y, IMR32 and PC12 cell lines.....109

**CHAPTER 3**

Table 1:

Organelle and bead transport in UV-vanadate photocleaved interphase *Xenopus* egg extracts.....147

# LIST OF FIGURES

**INTRODUCTION**

Figure 1:
Cartoon depictions of kinesin and cytoplasmic dynein.....25

**CHAPTER 1**

Figure 1:
Alignment of the human and invertebrate sequences.....32

Figure 2:
Nonmotor region comparison between the KHCs and the kinesin-like protein *bimC*.....33

Figure 3:
Immunofluorescence distribution of endogenous kinesin in nontransfected CV-1 cells.....33

Figure 4:
Indirect immunofluorescence of CV-1 cells expressing the entire KHC or portions of the KHC.....34

Figure 5:
Indirect immunofluorescence micrographs illustrating the distribution of expressed kinesin proteins in CV-1 cells after detergent permeabilization.....35

Figure 6:
Distributions of microtubules, vimentin filaments, and the expressed kinesin tail (pSVRT) in CV-1 cells....37

Figure 7:
Immunofluorescence localization of the microtubules and the expressed pSVKin after nocodazole or taxol treatment of CV-1 cells transfected with pSVKin....38

**APPENDIX 1**

Figure 1:
Generation of human kinesin heavy chain probe....50

Figure 2:
Schematic representation of human kinesin heavy chain cDNAs....52

Figure 3:
Nucleotide and deduced amino acid sequence of the human kinesin heavy chain cDNA....54

Figure 4:
Southern blots of human DNA probed with hKHC domain-specific probes....56

Figure 5:
Northern blots of human RNA probed with hKHC domain-

specific probes.....58

**APPENDIX 2**

Figure 1:

Hippocampal neurons double labeled with polyclonal tubulin antibody and the kinesin mAb SUK4.....64

Figure 2:

Hippocampal neurons fixed after 48 hr in culture under sense and antisense conditions.....66

Figure 3:

Dot immunobinding to quantitate rat kinesin, tubulin and dynein under sense and antisense conditions.....67

Figure 4:

Total neurite length measured as a function of time in culture.....67

Figure 5:

A dose-response curve illustrating neurite length as a function of the dose of kinesin antisense oligonucleotide.....67

Figure 6:

Recovery from antisense oligonucleotide treatment.....68

Figure 7:

GAP-43 staining of kinesin sense and antisense oligonucleotide

treated neurons.....69

Figure 8:
Synapsin I staining of kinesin sense and antisense oligonucleotide treated neurons.....70

**CHAPTER 2**

Figure 1:
Alignment and comparison of the amino acid sequences of human and *Drosophila* KHCs.....77

Figure 2:
Tissue-specific expression of the two human KHC genes.....78

Figure 3:
Tissue distribution of the uKHC and nKHC proteins.....79

Figure 4:
Cofractionation of uKHC and nKHC with microtubules and membranes.....80

Figure 5:
nKHC and MAP2 immunofluorescence in 10 μM thick coronal sections of rat brain.....81

Figure 6:
Distribution of nKHC and uKHC in primary cultures of

hippocampal neurons from newborn rats.....82

Figure 7:
Double immunofluorescence micrographs comparing the distributions of nKHC with tubulin, MAP2, and synaptotagmin.....83

**APPENDIX 3**

Figure 1:
Morphological appearance of control and differentiated neuroblastoma and PC12 cells by phase contrast microscopy.....110

Figure 2:
Expression of uKHC and nKHC in human neuroblastoma SH-SY5Y cells before and after pharmacological differentiation with retinoic acid.....112

Figure 3:
Expression of uKHC and nKHC in rat pheochromocytoma PC12 cells before and after treatment with NGF.....114

Figure 4:
Quantitative analysis of the expression of uKHC (black columns) and nKHC (hatched columns) in differentiated versus undifferentiated SH-SY5Y, IMR32 and PC12 cells.....116

Figure 5:
Expression of uKHC and nKHC transcripts in control and

differentiated SH-SY5Y and PC12 cells.....118

**CHAPTER 3**

Figure 1:
UV-vanadate photocleavage of cytoplasmic dynein in *Xenopus* egg extracts.....148

Figure 2:
Polarized array of microtubules nucleated by a *Spisula* egg centrosome.....150

Figure 3:
Restoring minus-end directed transport to UV-photocleaved extracts with purified *Xenopus* egg dynein.....152

Figure 4:
Decreased minus-ended motility as well as decreased association of dynein with cytosolic membranes in metaphase extracts.....154

Figure 5:
Cell cycle-dependent phosphorylation of a dynein light chain.....156

UNIVERSITY OF CALIFORNIA, SAN FRANCISCO

BERKELEY • DAVIS • IRVINE • LOS ANGELES • RIVERSIDE • SAN DIEGO • SAN FRANCISCO

SANTA BARBARA • SANTA CRUZ

JOSHUA NICLAS
DEPARTMENT OF BIOCHEMISTRY AND BIOPHYSICS, BOX 0448
UNIVERSITY OF CALIFORNIA, SAN FRANCISCO
513 PARNASSUS AVENUE
SAN FRANCISCO, CA 94143-0448

Tel. (415) 476-6381
Fax. (415) 502-1391 (lab)
Fax (415) 476-5292 (dept.)
Email: niclas@socrates.ucsf.edu

6/16/95

The Journal of Cell Biology
The Rockefeller University Press
222 East 70th Street
New York, NY 10021

To whom it may concern,

I would like permission to include in my PhD dissertation a copy of the papers cited below which were published in The Journal of Cell Biology in May and June of 1992. The dissertation will be microfilmed by University Microfilms Incorporated, and they request permission to supply single copies on demand.

Ferreira, A., Niclas, J., Vale, R. D., Banker, G., & Kosik, K. S. 1992. Suppression of Kinesin Expression in Cultured Hippocampal Neurons Using Antisense Oligonucleotides. *J. Cell Biol.* 117:595-606.

Navone, F., Niclas, J., Hom-Booher, N., Sparks, L., Bernstein, H., McCaffrey, G., & Vale, R. D. 1992. Cloning and Expression of a Human Kinesin Heavy Chain Gene: Interaction of the COOH-terminal Domain with Cytoplasmic Microtubules in Transfected CV-1 Cells. *J. Cell Biol.* 117:1263-1275.

Please respond by fax to 415-502-1391 (or 415-476-5292) or by mail to the address above. If there are any problems, I can be reached by Email at niclas@socrates.ucsf.edu. Thank you very much.

Sincerely,

Joshua Niclas

Joshua Niclas

The Rockefeller
University Press
222 East 70th Street
New York, New York 10021
(212) 327-7938
(Fax) 327-7944

10 July 1995

Dear Dr. Niclas:

We shall be glad to grant you permission for the reproduction of the material referred to in your letter of 6 July 1995*.

Our only requirements are that you also obtain permission from the author(s) and give suitable acknowledgment to the source in the following manner: Reproduced from **The Journal of Cell Biology, year, vol., pp.** by copyright permission of The Rockefeller University Press.

Sincerely Yours,

THE JOURNAL OF
CELL BIOLOGY

Iris Vallecilla
Permissions

Dr. Joshua Niclas
University of California-San Francisco
Box 0448
513 Parnassus Avenue
San Francisco,CA 94143-0448

*JCB-vol:117,595-606,1992
JCB-vol:117,1263-1275,1992
Articles to be used for PhD dissertion.

UNIVERSITY OF CALIFORNIA, SAN FRANCISCO

BERKELEY • DAVIS • IRVINE • LOS ANGELES • RIVERSIDE • SAN DIEGO • SAN FRANCISCO

SANTA BARBARA • SANTA CRUZ

JOSHUA NICLAS
DEPARTMENT OF BIOCHEMISTRY AND BIOPHYSICS, BOX 0448
UNIVERSITY OF CALIFORNIA, SAN FRANCISCO
513 PARNASSUS AVENUE
SAN FRANCISCO, CA 94143-0448

Tel. (415) 476-6381
Fax. (415) 502-1391 (lab)
Fax (415) 476-5292 (dept.)
Email: niclas@socrates.ucsf.edu

6/15/95

Neuron
Cell Press
50 Church Street
Cambridge, MA 02138

To whom it may concern,

I would like permission to include in my PhD dissertation a copy of the paper cited below which was published in Neuron in May of 1994. The dissertation will be microfilmed by University Microfilms Incorporated, and they request permission to supply single copies on demand.

Niclas, J., Navone, F., Hom-Booher & Vale, R. D. (1994). Cloning and Localization of a Conventional Kinesin Motor Expressed Exclusively in Neurons. Neuron *12*, 1059-1072.

Please respond by fax to 415-502-1391 (or 415-476-5292) or by mail to the address above. If there are any problems, I can be reached by Email at niclas@socrates.ucsf.edu. Thank you very much.

Sincerely,

Joshua Niclas

Joshua Niclas

W:\EMAIL.IN\1647 6/27/95

From niclas@cgl.ucsf.EDU Mon Jun 26 16:29:47 1995
Received: from socrates.ucsf.EDU by world.std.com (5.65c/Spike-2.0)
id AA13194; Tue, 27 Jun 1995 02:29:52 -0400
Received: (from niclas@localhost) by socrates.ucsf.EDU (8.6.12/GSC4.24)
id XAA06657 for Neuron@cell.com; Mon, 26 Jun 1995 23:29:47 -0700
Date: Mon, 26 Jun 1995 23:29:47 -0700
From: niclas@cgl.ucsf.EDU
Message-Id: <199506270629.XAA06657@socrates.ucsf.EDU>
To: Neuron@cell.com
Subject: 6/15/95 letter

To whom it may concern,

I sent a letter on 6/15/95 regarding a request for permission to include a copy of the following Neuron paper in my PhD thesis:

Niclas, J., Navone, F., Hom-Booher & Vale, R. D. (1994). Cloning and Localization of a Conventional Kinesin Motor Expressed Exclusively in Neurons. Neuron 12, 1059-1072.

we have received all correspondence ✓ 6/28/95

I was wondering if I could get confirmation of your having received that request. In addition, I wanted to update the fax number info that I sent with that initial letter. Since our lab moved to another building, one of our fax numbers has changed.

done ✓

The lab fax number is still 415-502-1391
The new departmental fax number is 415-476-5233.

Permission granted subject to citation of the original manuscript, and notation that copyright is held by Cell Press. (Our permission is contingent on permission of the author.)

Thanks,
Josh Niclas

Josh Niclas
Dept. of Biochemistry
Box 0448
University of California
San Francisco, CA 94143-0448

415-476-8712 or
415-476-6381

# INTRODUCTION

This thesis has been divided into two parts, both of which involve studies of microtubule-based motor proteins that participate in organelle transport. The first part represents efforts to determine the cytosolic targets and *in vivo* functions of ubiquitous kinesin. This work also lead to the identification and characterization of neuronal kinesin, a homolog of ubiquitous kinesin. The second part discusses a set of experiments designed to understand the mechanism by which organelle transport is regulated in extracts of the *Xenopus* egg. In this case, cytoplasmic dynein was the motor being studied.

In order to provide the proper background for the two parts of this thesis, the introduction includes sections covering kinesin, cytoplasmic dynein, and the regulation of organelle transport. At the end of the introduction, I discuss the broader range significance of understanding motor proteins and then summarize the goals of these projects and the resulting discoveries.

## Microtubule-based Organelle Transport

The cytoplasm of all living eukaryotic cells contains a complex arrangement of different organelles that is required for carrying out the many processes that ensure cell viability, growth and differentiation. The Golgi apparatus, for example, maintains a perinuclear localization, whereas the endoplasmic reticulum stretches out towards the plasma membrane. Observations of cells over 20 years ago by light microscopy revealed that the cytoplasm contains moving particles as small as 200 nm in size (Rebhun, 1972). About ten years later, the technique of video-enhanced differential interference contrast light microscopy made it possible to visualize moving vesicles smaller than 100 nm in diameter (Allen et al., 1981; Inoue, 1981).

This technique has demonstrated that a wide variety of cells contain very active populations of moving vesicles that appear to be translocating along microtubules (Brady et al., 1982; Hayden et al., 1983; Schliwa, 1984; Schnapp et al., 1985). Although these studies demonstrated that cytoplasmic organelles are actively transported along microtubules, they established neither the identity of the motile structures nor the identity of the factors responsible for their transport. The following two sections describe what is known about the two best characterized organelle-translocating factors, kinesin and dynein (Figure 1), which are also known as motor proteins. The proteins themselves have been extensively characterized by biochemical means, however, their in vivo functions and the means by which they are regulated is not well characterized.

## Kinesin

*Identification of a plus-end directed motor that moves on microtubules*

Kinesin was the first organelle-associated, microtubule-based motor protein to be purified. Using an *in vitro* motility assay derived from extracts of squid giant axon and optic lobes, kinesin was purified based upon its ability to translocate microtubules along a glass surface or carboxylated beads along microtubules (Vale et al., 1985). Kinesin was termed a plus-end directed motor since it was found to transport beads unidirectionally towards the plus-ends of microtubules (Vale et al., 1985), a process also referred to as anterograde transport in neurons. Transport by this motor requires energy in the form of ATP and its ATPase activity is stimulated by the presence of microtubules (Brady, 1985; Kuznetsov and Gelfand, 1986). Kinesin is inhibited by adenylyl imidophosphate (AMP-PNP), a non-hydrolyzable analog of ATP and, in fact, it was the rigorlike bond that kinesin forms with

microtubules in the presence of AMP-PNP that facilitated the purification of this motor by microtubule-affinity (Vale et al., 1985). This enriched fraction of kinesin could be released from microtubules in the presence of ATP and was the source for further purification.

*Structure of kinesin*

Since the initial isolation of kinesin, it has been purified and extensively characterized from a number of organisms and tissues. Kinesin is a dimer of two identical heavy chains (110-130 kDa) and two light chains (60-70 kDa) (Bloom et al., 1988; Cyr et al., 1991; Kuznetsov et al., 1988). Further analysis of kinesin purified from brain has shown that the majority of molecules contains two light chains, but that there also exists a smaller fraction that has no light chains (Hackney et al., 1991) Electron microscopy (EM) has shown that kinesin is an elongate rod-shaped structure of approximately 80 nm in length having two globular heads (~10 nm diameter), a thin stalk with a flexible hinge in the middle, and a fan-shaped tail (Amos, 1987; Hirokawa et al., 1989; Scholey et al., 1989). In addition, with the use of antibodies specific for different subunits, it was shown that the two heavy chains are arranged in parallel, forming the two heads and the tail region separated by a stalk domain, while the light chains are part of the fan-shaped tail (Hirokawa et al., 1989).

Kinesin heavy chain genes have been cloned and completely sequenced from *Drosophila* (Yang et al., 1988), squid (Kosik et al., 1990), sea urchin egg (Wright et al., 1991), mouse (Kato, 1990) (Genbank accession number X61435), *Caenorhabditis elegans* (Patel et al., 1993) and human (this thesis) (Navone et al., 1992; Niclas et al., 1994) Secondary structure predictions using the derived amino acid sequences and biochemical studies

of expressed fragments have provided support for the structural data from EM analysis. The heavy chain consists of three distinct domains: an N-terminal globular domain that contains the ATP- and microtubule-binding sites (Yang et al., 1989), a long α-helical coiled coil domain that enables the two heavy chains to dimerize (de Cuevas et al., 1992), and a small globular tail domain at the C-terminus. The N-terminal domain when expressed as a fusion protein in *Escherichia coli* is capable of transporting microtubules along a glass surface, implying that it serves as the functional motor domain of kinesin (Yang et al., 1990). The functions of the remainder of the molecule are still poorly defined, although the C-terminal globular domain as well as perhaps part of the α-helical coiled coil are thought to interact with the light chains (Gauger and Goldstein, 1993; Hirokawa et al., 1989), microtubules (this thesis) (Andrews et al., 1993; Navone et al., 1992) and membranes (Skoufias et al., 1994) possibly via a membrane-bound receptor (Kumar et al., 1995; Toyoshima et al., 1992)

*In vivo functions of kinesin*

A growing body of evidence supports the idea that kinesin transports organelles along microtubules *in vivo.* Immunolocalization studies indicate that at least a portion of kinesin is associated with membrane-bounded vesicles (Brady et al., 1990; Hirokawa et al., 1991; Hollenbeck, 1989; Pfister et al., 1989; Wright et al., 1991). In addition, ligation of a peripheral nerve was found to cause an accumulation of kinesin-immunoreactive organelles on the proximal side of the ligature, suggesting that kinesin is associated with anterogradely moving organelles (Hirokawa et al., 1991). Biochemical studies also suggests that at least a subset of kinesin is tightly associated with membrane vesicles. Not even 1 M potassium iodide or alkaline pH is able to

extract a subpopulation of kinesin from squid giant axon organelles (Schnapp et al., 1992).

Inhibition of kinesin function with antibodies or anti-sense oligonucleotides has provided evidence that kinesin not only interacts with membranous organelles, but is involved in transporting them as well. Macrophages contain an extensive microtubule-dependent array of tubular lysosomes that extend towards the cell periphery. Scrape-loading these cells with two different anti-kinesin antibodies caused the centripetal collapse of the lysosomal network (Hollenbeck and Swanson, 1990). Furthermore, in specialized cells called melanophores, certain extracellular signals are able to induce the uniform dispersion of pigment granules. When anti-kinesin antibodies are microinjected into these cells, the dispersion of these organelles is inhibited (Rodionov et al., 1991). Golgi-to-ER but not ER-to-Golgi membrane transport also can be inhibited by microinjected anti-kinesin antibodies, suggesting that kinesin powers the microtubule plus end-directed recycling of membrane to the ER, and remains inactive on pre-Golgi intermediates that move toward the Golgi complex (Lippincott-Schwartz et al., 1995). Bidirectional organelle transport in extruded axoplasm from the squid giant axon is also inhibited by anti-kinesin antibody treatment (Brady et al., 1990). Suppression of kinesin levels in neurons using anti-sense oligonucleotides resulted in phenotypic defects that are consistent with kinesin playing a role in transporting macromolecules to the nerve terminal (this thesis) (Amaratunga et al., 1995; Amaratunga et al., 1993; Ferreira et al., 1992). Together, these different approaches provide substantial evidence supporting a role for kinesin in the transport of different organelles in a variety of cell types.

Genetic analysis of kinesin has provided insight into its *in vivo* roles. Mutations in the heavy chain of kinesin in *Drosophila* result in motor and sensory defects, paralysis and then death during larval or pupal stages (Saxton et al., 1991). These results suggested that kinesin is essential for viability and has important functions in the nervous system. Subsequent studies showed that mutations in the heavy chain of kinesin inhibit action potential propagation and neurotransmitter release at synapses (Gho et al., 1992). However, these mutations had no effect on the numbers of synaptic vesicles in axonal termini. Hence, kinesin may play a role in the anterograde transport of organelles carrying ion channels and other components needed at the synaptic terminal, but this motor does not appear to be involved in delivery of synaptic vesicles.

*Kinesin-like motor proteins that translocate organelles*

Since the first kinesin heavy chain was cloned (Yang et al., 1989), a number of other genes have been isolated that demonstrate homology (30-50% amino acid identity) with the motor domain of kinesin (for reviews, see (Endow and Titus, 1992; Goldstein, 1993; Goldstein, 1991). These newly described kinesin-like proteins, however, do not show any amino acid homology outside of the kinesin heavy chain motor domain. Hence, the term "conventional kinesin" is used to refer to kinesin heavy chains that are homologous throughout their length to the *Drosophila* kinesin heavy chain prototype that was first sequenced. The term "kinesin-like proteins" or kinesin-related proteins" is used to signify proteins that share homology with *Drosophila* kinesin heavy chain only within in the motor domain. Most of the kinesin-related proteins characterized so far appear to play force-generating roles in the mitotic or meiotic spindle (for reviews, see (Endow

and Titus, 1992; Goldstein, 1993; Skoufias and Scholey, 1993). However, there is now a growing family of kinesin-related proteins that appear to be at least partly membrane associated and involved in anterograde transport in the axon. In *C. elegans*, mutational analysis demonstrated that the product of the unc-104 gene transports synaptic vesicles (Hall and Hedgecock, 1991). KIF3A (Kondo et al., 1994) and KIF4 (Sekine et al., 1994) are both plus-end transporters of as yet poorly characterized populations of membrane in axons of mouse neurons, the latter being heavily expressed in young differentiated neurons. KIF2 (Noda et al., 1995) appears to transport organelles that are distinct from synaptic vesicles as well as organelles carried by kinesin heavy chain and KIF3A. KIF1A (Okada et al., 1995) and KIF1B (Nangaku et al., 1994) have been shown to be the plus-end motors for synaptic vesicle precursors and mitochondria, respectively.

## Cytoplasmic dynein

*Identification of a minus-end directed motor that moves on microtubules*

Not long after the discovery of kinesin, another microtubule-based motor called cytoplasmic dynein was discovered. It was originally referred to as microtubule-associated protein 1C (MAP 1C) since it is one of five high molecular weight brain proteins that copurify with microtubules (Bloom et al., 1984; Olmsted, 1986). It was purified from this group of MAPs by using microtubule-affinity in the absence of nucleotide, followed by GTP extraction to remove contaminating kinesin and then extraction with ATP to release cytoplasmic dynein (Paschal et al., 1987). As is the case for kinesin, dynein cofractionated with a microtubule-activated ATPase activity and a microtubule-translocating activity. However, in an *in vitro* assay directionality assay, cytoplasmic dynein moved along microtubules towards

the minus-ends (Paschal and Vallee, 1987). In addition, MAP1C was demonstrated to be a relative of axonemal dynein by displaying a similar sensitivity to photocleavage when irradiated with ultraviolet light in the presence of micromolar concentrations of vanadate ion (Euteneuer et al., 1988; Lye et al., 1987; Paschal et al., 1987; Porter et al., 1988)

*Structure of dynein*

Cytoplasmic dynein is a ~1.2 X $10^6$ Da protein complex composed of two heavy chains of ~500 kDa, and several intermediate (70-80 kDa) and light chains (50-60 kDa) (Lye et al., 1987; Paschal et al., 1987). Scanning transmission electron microscopy revealed that cytoplasmic dynein has two large globular head domains (13.4 nm diameter) that are linked by stalk-like structures to a smaller basal domain (Vallee et al., 1988). These head domains most likely represent part of the heavy chains while the base is probably made up of the intermediate and light chains. In addition to these polypeptides, a more loosely associated 150 kDa protein also copurifies with cytoplasmic dynein in sucrose gradients (Collins and Vallee, 1989; Steuer et al., 1990). This protein, now called dynactin, was eventually purified as part of a large 20S multisubunit complex which stimulates vesicle transport by cytoplasmic dynein (Gill et al., 1991; Schroer and Sheetz, 1991).

Cytoplasmic dynein heavy chains have been cloned and completely sequenced from *Dictyostelium* (Koonce et al., 1992), rat (Mikami et al., 1993; Zhang et al., 1993), *Saccharomyces cerevisiae* (Eshel et al., 1993), *Aspergillus nidulans* (Xiang et al., 1994) and *Drosophila* (Li et al., 1994). In addition, partial sequences are available for human (Vaisberg et al., 1993), sea urchin (Gibbons et al., 1994) and *Paramecium* (Asai et al., 1994) Although several axonemal dynein heavy chain genes have been found in a given organism,

only one cytoplasmic homolog has been identified so far (Asai et al., 1994; Gibbons et al., 1994; Rasmusson et al., 1994). The predicted protein sequences reveal the presence of four ATP-binding domain consensus sequences (GXXXXGK(S/T)) in the middle third of the protein. Cytoplasmic dyneins and axonemal dyneins only share homology in the latter two-thirds of the molecule suggesting that this region may constitute the globular force-generating head domain. The amino-terminus may be part of the tail of the motor and might interact with the intermediate and light chains as well as cytosolic targets.

Genes for the intermediate and light chains have also been characterized. The predicted sequence of the rat 74 kDa intermediate chain revealed homology in the carboxyl-terminal half of a 70 kDa intermediate chain of *Chlamydomonas* flagellar dynein (Paschal et al., 1992). Since this flagellar intermediate chain seems to be involved in anchoring dynein within the flagella, the cytoplasmic intermediate chain may play a role in modulating the interaction of cytoplasmic dynein with intracellular cargo. A gene encoding one of the light chain isoforms displays no homology to other known proteins, but has a consensus nucleotide binding site (Gill et al., 1994; Hughes et al., 1995). Whether the light chains function to regulate dynein's enzymatic activity or its interactions with potential cargo is still unclear.

*Cellular functions of dynein*

Using *in vitro* vesicle motility assays, it has been demonstrated that cytoplasmic dynein is a minus-end motor for organelle transport. Treating extracts with ultraviolet light and vanadate ion results in the strong inhibition of minus-end organelle transport (Schnapp and Reese, 1989; Schroer et al., 1989). Addition of purified cytoplasmic dynein to photocleaved

extracts restores a large proportion of the original motility demonstrating that dynein is the predominant retrograde organelle motor (Schroer et al., 1989). Dynein is a peripheral membrane protein on synaptic vesicles and purified soluble dynein is capable of binding to alkaline pH-stripped synaptic vesicles (Lacey and Haimo, 1992). It is also associated with lysosomes (Lin and Collins, 1992) and with the Golgi apparatus (Fath et al., 1994) where it functions to maintain the pericentriolar localization of this organelle (Corthesy-Theulaz et al., 1992).

Cytoplasmic dynein displays a dual-purpose nature by also participating in the dynamics of the mitotic spindle. Cytoplasmic dynein localizes to the mitotic spindle fibers, centrosomes, and chromosome kinetochores during mitosis (Pfarr et al., 1990; Steuer et al., 1990). Inhibition of dynein motor activity with microinjected anti-dynein antibodies in mitotic mammalian cells blocks spindle formation in prophase, but has no effect on bipolar spindles or chromosome motion during anaphase, suggesting that this motor is necessary for bipolar spindle formation (Vaisberg et al., 1993). In *Saccharomyces cerevisiae*, disruption of the dynein heavy chain gene (DYN1) resulted in the misalignment of the mitotic spindle relative to the bud neck and abnormal distribution of dividing nuclei between the mother cell and the bud (Eshel et al., 1993). In a similar study, it was also observed that mutations in the yeast dynein heavy chain gene (called DHC1 by this group) lead to abnormal spindle movement into the bud, but had no effect on spindle assembly (Li et al., 1993). This may represent a difference in dynein function between yeast and mammals. A possible role for dynein in anaphase has been suggested by the requirement for the combined products of the yeast DHC1, CIN8 and KIP1 genes for proper chromosome segregation (Saunders et al., 1995). Examination of nuclear distribution mutants in filamentous fungi

lead to the discovery that ro-1 of *Neurospora crassa* and nudA of *Aspergillus nidulans* encode cytoplasmic dynein heavy chains (Plamann et al., 1994; Xiang et al., 1994). Although the role of cytoplasmic dynein in mitosis appears quite convincing, it is not clear if this motor plays any role in vesicle transport in these lower eukaryotes.

## Regulation of organelle transport

The majority of membranous organelles in the cytoplasm are transported along a polarized microtubule array to specific destinations within the cell. The complexity of this membrane traffic must require precise means of regulating both the levels and directionality of such microtubule-based motility. Microtubule motor proteins as well as the organelles themselves represent likely targets for such regulation. The motor itself could be controlled by modulating its ATPase activity or the conversion of ATP hydrolysis energy into force generation. Mechanisms may also be operative at the level of motor affinity for microtubules or the affinity and specificity of motors for different organelles.

### *Regulating organelle motility*

Physiological regulation of organelle transport has been most clearly demonstrated in fish chromatophores, a specialized cell that in response to extracellular signals is capable of aggregating (minus-end transport) or dispersing (plus-end transport) pigment granules along polarized microtubules. Phosphorylation of a 57 kDa protein by a cAMP-dependent kinase pathway (Lynch et al., 1986; Lynch et al., 1986; Rozdzial and Haimo, 1986) has been shown to be involved in the dispersion of pigment granules, while dephosphorylation of this 57 kDa factor mediated by the phosphatase

calcineurin (Thaler and Haimo, 1990) and increased intracellular $Ca^{2+}$ (Kotz and McNiven, 1994) has been implicated in the aggregation of these particles. How phosphorylation of this 57 kDa protein regulates pigment granule motility has yet to be determined.

Phosphorylation may control organelle transport in other cells as well. The protein phosphatase inhibitor okadaic acid enhances overall organelle transport in mammalian cells in culture (Hamm-Alvarez et al., 1993) and greatly increases the number of movements of endoplasmic reticulum (ER) tubules in frog egg extracts (Allan, 1995). In the latter case, the sensitivity of ER tubule translocation to this drug suggested that inhibition of protein phosphatase 1 was responsible for this stimulation. Since these ER tubules move exclusively in the minus-end direction, cytoplasmic dynein may be the target of regulation. If so, enhancement of transport is a result of increased motor activity and not increased affinity for membrane, since okadaic acid does not cause an increase in association of dynein with membranes (Allan, 1995). Okadaic acid also increases lytic granule transport in extracts of T cells (McIlvain et al., 1994). An increase in motor activity was suggested by an observed increase in microtubule gliding activity on glass. Organelle motility is also regulated by phosphorylation during the cell cycle. High $p34^{cdc2}$ kinase activity suppresses bidirectional organelle motility in metaphase frog egg extracts (Allan and Vale, 1991).

Possible means of regulation that do not directly involve phosphorylation have also been studied. A potential role for GTP-binding proteins in organelle transport been examined in the giant axon of squid. Treatment of extruded axoplasm with GTPγS, a non-hydrolyzable analog of GTP, resulted in a decrease in organelle transport velocities, suggesting that

cycles of GTP hydrolysis and exchange play a part in modulating motility in the axon (Bloom et al., 1993).

*Regulation of kinesin and dynein by phosphorylation*

Protein motors, the ATP-hydrolyzing enzymes that power the movement of organelles on microtubules, represent likely targets for regulation of vesicle transport. The two best studied organelle motors, dynein (Paschal et al., 1987; Paschal and Vallee, 1987) and kinesin (Brady, 1985; Vale et al., 1985), move membrane-bound compartments towards the minus (Schnapp and Reese, 1989; Schroer et al., 1989) and plus ends (Hollenbeck and Swanson, 1990; Rodionov et al., 1991) of microtubules, respectively. Both kinesin (Hollenbeck, 1993; Matthies et al., 1993; Okada et al., 1995) and dynein (Dillman and Pfister, 1994) are phosphorylated in cells, although the kinases involved and the functional consequences of such phosphorylation still remain largely unresolved. Modulation of dynein and kinesin activity by phosphorylation, however, has been suggested by several studies. For kinesin, specific phosphoisoforms are found selectively bound to membranes and their levels are increased during neurite outgrowth after addition of nerve growth factor (Lee and Hollenbeck, 1995). Kinesin that has been phosphorylated *in vitro* by cAMP-dependent kinase shows a 2-fold decrease in binding to synaptic vesicles and these vesicles display a 2-fold lower frequency of association with microtubules (Sato-Yoshitake et al., 1992). A similar reduction in anterograde vesicles movements was observed *in vivo* when cAMP-dependent protein kinase activity was stimulated in crayfish giant axons (Okada et al., 1995). Hence, in contrast to pigment granule transport, this preliminary data suggest that plus-end motility of axonal vesicles could be inhibited by this kinase via decreased affinity for its cargo.

In the case of dynein, the heavy chain was found to be less phosphorylated on anterogradely moving vesicles in rat optic nerves compared to the total cellular pool of vesicles, suggesting that dephosphorylation may inactivate dynein so that it could be carried by plus-end directed motors to the nerve terminal (Dillman and Pfister, 1994). In a second study on rat kidney fibroblasts, okadaic acid was found to increase phosphorylation of the cytoplasmic dynein heavy chain as well as change the dynein immunofluorescence pattern from a vesicular staining to a more diffuse pattern (Lin et al., 1994). The amount of dynein on Triton X-100 soluble membrane decreased by about 2-fold. While this result suggests that dynein is released from the organelle surface, the stimulation of organelle transport by okadaic acid (Allan, 1995) implies that the dynein that dissociated from the membrane could represent an inactivate storage pool of the motor (Lin et al., 1994).

*Regulation of dynein by interactions with phospholipids*

In addition to phosphorylation, the activity of dynein also appears to be regulated by interactions with phospholipids. Dynein's ATPase activity is increased by up to 2-fold in the presence of phosphatidylserine or phosphatidylcholine containing liposomes, suggesting that dynein increases its ATP hydrolyzing and force-generating activity when it binds to an organelle (Ferro and Collins, 1995). This might represent one way of repressing the ATPase activity of this motor until it becomes associated with its cargo.

*Regulation of kinesin and dynein by motor-associated factors*

Organelle transport may also be regulated by motor-associated factors, some of which have been purified or partially purified using *in vitro* assays (Schroer and Sheetz, 1991). The best characterized activator is a multi-subunit factor called the dynactin complex which is required for dynein function in minus-end directed organelle motility (Gill et al., 1991) as well as in the mitotic spindle (Muhua et al., 1994; Plamann et al., 1994). Kinesin activity also appears to be modulated by associated factors. Three proteins that copurify with kinesin were found to be more heavily phosphorylated under conditions in which plus-ended organelle motility was enhanced (McIlvain et al., 1994). So far, the mechanisms of action of these accessory factors are unknown.

The dynactin complex is a 20S macromolecular structure made up of polypeptides of 150, 135, 62, 50, 45, 37 and 32 kDa (Gill et al., 1991; Paschal et al., 1993). Preparations of dynein that contain dynactin ($p150^{Glued}$) support the transport of vesicles *in vitro*; however, dynein that has been purified away from dynactin (as well as the associated proteins of the complex) loses much of its ability to promote minus-ended motility (Gill et al., 1991). Although it is not known how dynactin stimulates the activity of dynein, it is known that dynactin is capable of interacting with microtubules (Waterman-Storer et al., 1995). Its microtubule-binding region (amino acids 39-150) might act by increasing the affinity of dynein for microtubules or possibly increasing the processivity of vesicle motility by preventing diffusion away from the microtubule. In lower eukaryotes, genetic studies have provided evidence for the dynactin complex playing a role in dynein-based motility in the mitotic spindle. Mutations in the *ro-3* and *ro-4* genes of *Neurospora crassa* have identical phenotypes to mutations in the *ro-1* gene which encodes cytoplasmic dynein (Plamann et al., 1994). *ro-3* encodes a homologue of

dynactin ($p150^{Glued}$) and *ro-4* encodes a homologue of the 45 kDa centractin (also called actin-RPV or Arp-1), a novel form of actin that is part of the dynactin complex. It is not known how centractin (Clark and Meyer, 1992; Lees-Miller et al., 1992) functions with dynein to stimulate organelle motility or proper nuclear distribution.

Three kinesin-associated proteins have also been implicated in regulation of organelle movement, since their phosphorylation levels increase in conjunction with a 2-fold increase in lytic granule movement along microtubules after okadaic acid treatment (McIlvain et al., 1994). These polypeptides called KAPP150, KAPP79 and KAPP73 (kinesin-associated phosphoproteins of 150, 79 and 73 kDa) copurify with kinesin by microtubule-affinity and MgATP elution. Since microtubule gliding on glass was also stimulated about 2-fold, the increase in granule motility probably represents an increase in motor activity as opposed to an increase in affinity of kinesin for vesicles. As for the activators of dynein, how these KAPPs act upon kinesin is not known.

## The broader significance of studying motor proteins

The study of microtubule-based motor proteins is increasing our understanding of such diverse cellular processes as organelle transport and cell division. We are learning how motor proteins convert chemical energy into mechanical energy in order to move different intracellular structures along microtubule filaments so that they are delivered to their proper location in the cell. In the last few years, the size of the microtubule-based motor family has increased dramatically, demonstrating that many processes in the cell are dependent on force generation. In addition, we are beginning to understand the elaborate mechanisms used by the cell to control the

activity of these mechanochemical enzymes. The more immediate gains from this work are a better understanding of the functions of these proteins at the cellular level. However, the knowledge gained from these studies may also have much longer reaching consequences as well. Advances in areas such as medicine and engineering are possible, but have yet to be achieved.

Several microtubule-based motor proteins appear to be required for the anterograde and retrograde transport of membrane-bound organelles in the axons of neurons and, hence, mutations in the corresponding genes may be involved in neurodegenerative disorders. It is generally believed that impairment of axonal transport to the nerve terminal of materials synthesized in the cell body as well as inhibition of motility in the opposite direction leads to a degeneration of the axon starting at the axon terminus. Many of the diseases that display this phenotype have not been characterized at the molecular level, but of those that have, defects in microtubule-based motor proteins have so far not been found. However, other cytoskeletal proteins have been implicated in motor neuron diseases. For example, the abnormal assembly of neurofilaments in motor neuron cell bodies and axons is one of the most common, conspicuous findings in most cases of human motor neuron disease (Hirano, 1991). In fact, overexpression of neurofilament proteins in mice causes severe defects in the axonal transport of organelles and cytoskeletal elements, resulting in axonal degeneration (Collard et al., 1995). However, it is not clear if the neurofilament phenotype in motor neuron disease is the initial cause of the disease or is merely a secondary effect. It is easy to imagine that excessive quantities of neurofilaments might be capable of creating a barrier to the motor protein-driven movement of structures through the axon. Another example of an abnormal cytoskeletal protein causing a neurological defect was discovered

when the mouse *dilute* locus was found to encode a member of the myosin V class of proteins (Mercer et al., 1991). Mice with mutations in this locus display seizures and die by 2-3 weeks of age. This motor appears to play a role in vesicle transport since the yeast homologue (MYO2) is required for vesicle transport into daughter cells (Johnston et al., 1991); it is also very interesting that mutations in this gene can be suppressed by mutations in SMY1, a gene encoding a kinesin-like protein (Lillie and Brown, 1992). Hence, a defect in transport of vesicles in neurons by this myosin motor may explain the neurological phenotype displayed by the *dilute* mouse.

If partially defective motors are shown to cause the slow axonal degeneration seen in certain neurological disorders, a detailed understanding of the motors and their corresponding genes might help in the design of treatments. For example, a detailed characterization of the ATPase activity and the structure of the ATP binding site might allow the development of compounds which enhance the ATPase activity and consequently the organelle transport by the weakened motor. An understanding of the regulation of expression of the motor would help in the identification of agents that stimulate its expression, with the possible end result of overcoming protein instability with a higher concentration of motor. Such approaches might help to slow the progression of axonal deterioration.

Motors of the mitotic spindle represent potential targets for anti-cancer agents. Since mitotic motors are responsible for generating the forces needed for proper spindle formation and chromosome segregation, inhibiting their activity might also inhibit the uncontrolled cell division that occurs in tumors. The obvious targets on the motor molecule would be the ATPase site and the tail domain which interacts with a specific cargo. Since, it may be difficult to find an inhibitor that acts specifically against the ATPase site of a

particular motor, the tail domain represents a more promising target since this domain is much more unique for any given motor (Goldstein, 1993). Such drugs might represent promising new cancer treatments, if they can be designed to be very specific for the mitotic motors that they inhibit and not have the many side effects of the current cell division-inhibiting drugs.

Studies of the nanometer-scale movements as well as the crystal structures of motors may prove helpful to engineers who's goal it is to design microscopic motors. There already exists a growing field of nanotechnology that is capable of creating miniaturized objects such as gears and tubes. At present, motors to move these structures do not exist. Understanding the mechanics of biological motors may allow for the successful designing of microscopic synthetic motors that would likely find many applications in the computer and microchip industry as well as in medicine. In the ever increasing need to fit more transistors onto a microchip, one could imagine synthetic motors performing micro-manipulations of hardware for microcircuitry manufacture. For medical applications, these tiny motors might be used to construct micro-pumps that could be implanted into any organ in the body for the purpose of controlled release of deficient hormones, for example.

Although some of these ideas may seem a bit far-fetched and may take many years to be achieved, they nonetheless represent very exciting possibilities. Considering how relatively young the field of motor proteins is and how little we actually know about them, the proposed applications presented above will probably pale in comparison to what will be accomplished years from now.

## Summary

*The Ubiquitous and Neuronal Kinesins*

At present, a great deal is know about the motor protein, kinesin. EM studies, *in vitro* assays and the cloning of the heavy and light chains have greatly contributed to our understanding of its structure and biochemical activities. However, its *in vivo* roles are much less well understood. The identity of the cargo which kinesin transports is only beginning to be determined. The mechanism by which kinesin interacts with its appropriate cargo and how that interaction is regulated is still unclear.

In an effort to understand the roles performed by kinesin in the cell, I sought to identify the cytoplasmic structures with which the different domains of the kinesin heavy chain interact. To accomplish this goal in a mammalian tissue culture system, a human kinesin heavy chain gene was isolated so that transient transfections of the different domains into CV-1 cells could be performed. This collaborative project between Francesca Navone and myself (Chapter 1) resulted in the discovery that not only does the N-terminal motor domain colocalize with microtubules, but the C-terminal tail domain does as well. In contrast, the α-helical coiled coil rod domain only showed diffuse localization. In another collaborative project (Appendix 2), Adriana Ferreira and I examined the function of kinesin in developing neurons. Treating embryonic hippocampal neurons with anti-sense oligonucleotides to suppress kinesin heavy chain expression led to the inhibition of neurite outgrowth and anterograde transport of synapsin I and GAP43 containing vesicles to neurite termini. Subsequent to this work, I identified a second conventional human kinesin heavy chain that is only expressed in neurons (Chapter 2) unlike the first KHC that I cloned which is expressed in all cells. It had been believed that a single conventional kinesin motor powers anterograde organelle transport, but this result showed that

there are two such motors that probably serve distinct functions in microtubule-based axonal transport.

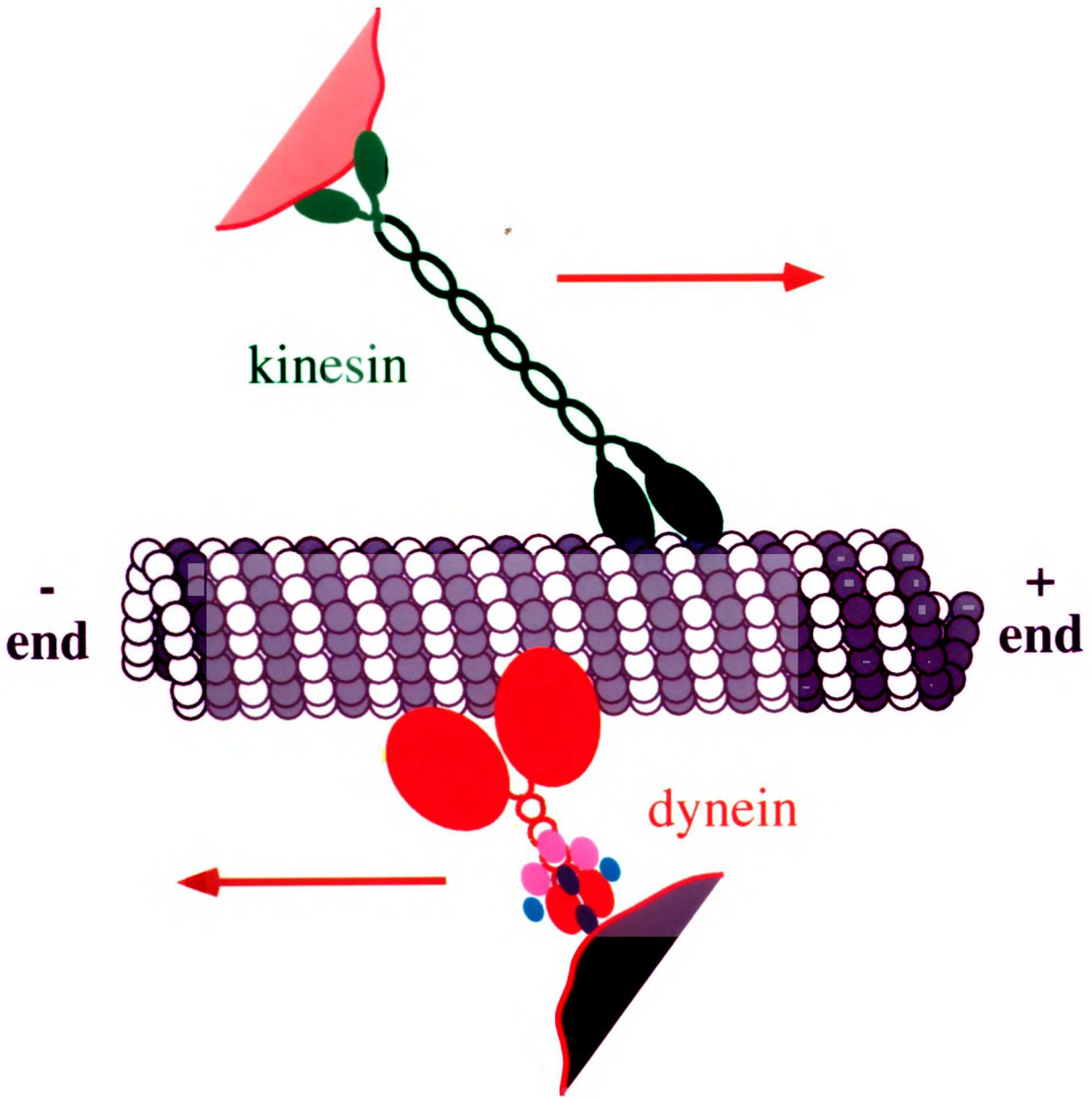
*Regulation of Microtubule-based Organelle Transport*

Despite the extensive characterization of kinesin and dynein, the regulation of organelle transport by these motors is poorly understood. There are many examples of physiological modulation of membrane transport, but the proteins involved and the mechanisms employed are largely unknown. In many of these cases, however, it is quite clear that phosphorylation events and motor-associated factors are involved in controlling kinesin and dynein-based movement. Since phosphorylation plays a part in this regulation, there must be a number of kinases and phosphatases that act to switch these motors on and off. This could occur by inactivation of the ATPase activity or by altering the affinity of the motor for microtubules or organelles.

In order to determine how organelle transport is turned on and off, I chose to study organelle motility in interphase or metaphase extracts of *Xenopus laevis* eggs. In previous work, interphase-arrested egg extracts were shown to support 10-fold higher levels of bidirectional motility compared to metaphase extracts (Allan and Vale, 1991). Regulation of this activity must involve post-translational modifications, since changes in the level of organelle transport were observed when the cell cycle state of the extract was converted in the presence of protein synthesis inhibitors. In Chapter 3, I show that cytoplasmic dynein is the predominant minus-end organelle motor in *Xenopus* egg extracts and that cytoplasmic dynein and its activator dynactin detach from the membrane surface when interphase extracts are converted to a metaphase state. By measuring organelle transport in the same extracts, I found that the reduction in membrane-associated dynein

correlates well with the decrease in minus-end directed organelle transport in metaphase extracts. My collaborator, Viki Allan, looked at the phosphorylation of dynein purified from interphase and metaphase extracts. While cell-cycle dependent phosphorylation of the dynein heavy and intermediate chains was not observed, a ~12-fold increase in phosphorylation of a dynein light chain was observed in metaphase compared to interphase extracts. These results suggest that dynein-based organelle transport is controlled by cell-cycle dependent phosphorylation events that regulate the attachment of dynein to intracellular membranes.

**Figure 1.** Cartoon depictions of kinesin and cytoplasmic dynein. Kinesin, a plus-end microtubule motor, is a dimer of two heavy chains and two light chains. Cytoplasmic dynein, a minus-end microtubule motor, is a complex of two heavy chains, and a number of intermediate and light chains. Both appear to transport membranous organelles by converting energy in the form of ATP into force which results in transport along microtubules.


kinesin
-
end
+
end
dynein

# PART 1:

# The Ubiquitous and Neuronal Kinesins

# CHAPTER 1

# Cloning and Expression of a Human Kinesin Heavy Chain Gene: Interaction of the COOH-terminal Domain with Cytoplasmic Microtubules in Transfected CV-1 Cells

Chapter 1 represents a collaboration between Francesca Navone and myself. The cloning and characterization of the human kinesin heavy chain cDNAs was my work while Francesca used this gene as a reagent for the transfection and immunolocalization experiments. Nora Hom-Booher and Lynne Sparks contributed to the library screening and sequencing efforts. Harris Bernstein and Gretchen McCaffrey provided critical advice and reagents that lead to the successful isolation of kinesin heavy chain cDNAs. By isolating a mammalian kinesin heavy chain gene, I found that there is a high level of amino acid sequence conservation in the motor and tail regions when compared with invertebrate kinesins, implying the presence of important sequences that are involved in force generation by the motor domain and attachment to cytosolic cargo via the tail domain. Other interesting features of this gene are presented as well. By transfecting the different domains (head or motor domain, rod domain and tail domain) into CV-1 cells, it was found that not only did the motor domain interact with microtubules as expected, but the tail domain did as well. This result suggested that kinesin is capable of cross-bridging microtubules via the motor and tail domains and sliding them relative to each other. This chapter is reproduced from The Journal of Cell Biology, 1992, vol. 117, pp. 1263-1275 by copyright permission of The Rockefeller University Press.

# Cloning and Expression of a Human Kinesin Heavy Chain Gene: Interaction of the COOH-terminal Domain with Cytoplasmic Microtubules in Transfected CV-1 Cells

**Francesca Navone,*‡ Joshua Niclas,* Nora Hom-Booher,* Lynne Sparks,* Harris D. Bernstein,* Gretchen McCaffrey,* and Ronald D. Vale***

*Departments of Pharmacology and Biochemistry, University of California, San Francisco, San Francisco, California 94143; and ‡C. N. R. Center of Cytopharmacology, Department of Medical Pharmacology, Milano, Italy

***Abstract.*** To understand the interactions between the microtubule-based motor protein kinesin and intracellular components, we have expressed the kinesin heavy chain and its different domains in CV-1 monkey kidney epithelial cells and examined their distributions by immunofluorescence microscopy. For this study, we cloned and sequenced cDNAs encoding a kinesin heavy chain from a human placental library. The human kinesin heavy chain exhibits a high level of sequence identity to the previously cloned invertebrate kinesin heavy chains; homologies between the COOH-terminal domain of human and invertebrate kinesins and the nonmotor domain of the *Aspergillus* kinesin-like protein *bimC* were also found. The gene encoding the human kinesin heavy chain also contains a small upstream open reading frame in a G-C rich 5′ untranslated region, features that are associated with translational regulation in certain mRNAs. After transient expression in CV-1 cells, the kinesin heavy chain showed both a diffuse distribution and a filamentous staining pattern that coaligned with microtubules but not vimentin intermediate filaments. Altering the number and distribution of microtubules with taxol or nocodazole produced corresponding changes in the localization of the expressed kinesin heavy chain. The expressed $NH_2$-terminal motor and the COOH-terminal tail domains, but not the α-helical coiled coil rod domain, also colocalized with microtubules. The finding that both the kinesin motor and tail domains can interact with cytoplasmic microtubules raises the possibility that kinesin could crossbridge and induce sliding between microtubules under certain circumstances.

KINESIN, a plus end–directed microtubule motor protein (Vale, 1987), has been characterized extensively using biochemical and molecular biological techniques. Mammalian kinesin is composed of two identical heavy chains (110–120 kD) and two identical light chains (60–70 kD) (Kuznetsov et al., 1988; Bloom et al., 1988) which together form an elongated structure with globular domains at either end (Amos, 1987; Hirokawa et al., 1989; Scholey et al., 1989). The heavy chain can be subdivided into three domains: a globular $NH_2$-terminal domain, a long rod domain, and a globular COOH-terminal tail domain (Yang et al., 1989; Kosik et al., 1990). The $NH_2$ terminal domain, which contains a consensus sequence for nucleotide binding (Yang et al., 1989), has been shown to generate microtubule movement in vitro (Yang et al., 1990) and has microtubule-stimulated ATPase activity (Kuznetsov et al., 1989); this region of kinesin is hence referred to as the motor domain. The middle of the kinesin heavy chain (KHC)[1] folds into a long α-helical coiled coil (rod domain) that enables the two heavy chains to dimerize (de Cuevas et al., 1992). The COOH-terminal globular tail domain interacts with the light chains (Hirokawa et al., 1989) and possibly other cytoplasmic components. Domains homologous to the kinesin motor have been found in a variety of other proteins, which are thought to be members of a large superfamily of microtubule-based motors (Vale and Goldstein, 1990; Endow, 1991; Goldstein, 1991). (In this paper, we shall refer to homologues as kinesin-like motors and refer to the originally described motor simply as kinesin).

Based upon in vitro observations that kinesin transports latex beads to the plus ends of microtubules (Vale et al., 1985), it was proposed that kinesin powers anterograde transport of organelles. Several recent experimental findings support this hypothesis. First, light and electron immunolocalization studies indicate that at least some of the kinesin is associated with membrane-bounded vesicles (Pfister et al., 1989; Hollenbeck, 1989; Wright et al., 1991; Hirokawa et al., 1991). Second, antikinesin antibodies cause the centripetal collapse of tubular lysosomes in macrophages (Hollenbeck and Swanson, 1990), inhibit pigment granule dispersion when microinjected into melanophores (Rodionov et al.,

1. *Abbreviations used in this paper*: hKHC, human kinesin heavy chain; KHC, kinesin heavy chain; ORF, open reading frame; PCR, polymerase chain reaction; VSV, vesicular stomatitis virus.

1991), and inhibit organelle transport when added to squid axoplasm (Brady et al., 1990). Finally, inhibition of kinesin expression in hippocampal neurons by antisense oligonucleotides (Ferreira et al., 1992) and the creation of mutations in the *Drosophila* kinesin gene (Saxton et al., 1991) both result in neuronal defects that are consistent with impaired axonal transport. In addition to transporting membrane vesicles, kinesin may have other biological functions. Kinesin, for example, was found to crossbridge and produce sliding between microtubules (Urrutia et al., 1991) and may transport intermediate filaments to the cell periphery (Gyoeva and Gelfand, 1991).

To understand the biological roles performed by kinesin, it is important to determine its interactions with subcellular structures and decipher how these interactions are regulated. In this study, we have isolated and sequenced a human cDNA encoding a gene that shows a high degree of amino acid sequence identity to the previously cloned invertebrate KHC genes (Yang et al., 1989; Kosik et al., 1990; Wright et al., 1991). Different domains of this KHC were expressed in CV-1 African green monkey kidney epithelial cells and their subcellular localizations determined. While the rod domain shows a predominantly soluble distribution, we find that the entire KHC, the motor domain, and the COOH-terminal tail domain all can interact with cytoplasmic microtubules.

## Materials and Methods

### Generation of Mammalian KHC Probe

The KHC nucleotide probe used for screening a human cDNA library was generated by the polymerase chain reaction (PCR) (Mullis et al., 1986). Specifically, MDCK cell first-strand cDNA was incubated with 500 pmol of a 128-fold degenerate 20 mer (5'-GA[GA]GA[GATC]ACCGT[GC]GC-[GATC]AA[GA]GA-3') and 18 mer (5'-[TC]TGCA[GA][GA]TC[TC]TG-[GATC]AC[GA]AA-3') (these two sequences were based upon amino acids 781–787 and 798–803 of the *Drosophila* KHC, respectively) in 67 mM Tris-HCl, pH 8.8, 6.7 mM $MgCl_2$, 16.6 mM ammonium sulfate, 10 mM 2-mercaptoethanol, 6.7 μM EDTA, 10% DMSO, 1.25 mM each of dNTP and 1 U Taq polymerase (Perkin-Elmer Cetus Instrs., Norwalk, CT) in a 50-μl reaction. Reactions were carried out for 50 cycles (93°C for 60 s, 48°C for 60 s, 55°C for 30 s) and then analyzed by PAGE. For sequencing of the PCR products, the reactions were run as above, but the degenerate 20 mer was endlabeled with $^{32}P$ (Maniatis et al., 1982). The radiolabeled PCR products were separated by PAGE as before, and a band of the expected size was excised from the gel. The radiolabeled fragment was extracted and then sequenced (Maxam and Gilbert, 1977) and found to encode a portion of a protein that was highly homologous to invertebrate KHCs.

### cDNA Library Screening

A radioactive probe for library screening was prepared from the PCR-generated fragment. Specifically, 100 ng of the 20 mer and 18 mer, 5 U of the Klenow fragment of DNA polymerase I (Bethesda Research Laboratories, Gaithersburg, MD), 100 ng of the PCR fragment, 0.1 mM each of dGTP, dCTP, and dTTP, and 200 μCi of α[$^{32}P$]dATP (ICN Biomedicals, Inc., Costa Mesa, CA) were combined in 20 mM Tris-HCl, pH 7.5, 10 mM $MgCl_2$, 5 mM DTT, and incubated for 1 h at 23°C. This probe was then used to screen a human placental λgt11 cDNA library (generous gift from J. Evan Sadler, Washington University, St. Louis, MO) by plaque hybridization (Maniatis et al., 1982).

### Sequence Analysis and Structure Prediction

Sequencing templates were generated by restriction fragment subcloning into M13 vectors or by making nested deletions with exonuclease III (Henikoff, 1987). Both strands of all clones were sequenced by the dideoxy chain termination technique (Sanger et al., 1977) using the USB Sequenase kit. Sequence analysis programs (Molecular Biology Information Resource, Department of Cell Biology, Baylor College of Medicine, Houston, TX) and structure prediction programs (Feiner-Moore and Stroud, 1984) were used as described. The computer search comparing different sequences of kinesin and kinesin-like proteins was performed using a Dayhoff scoring matrix (Lawrence and Goldman, 1988).

### Construction of Vectors Expressing Human Kinesin Heavy Chain (hKHC)

Various portions of the human kinesin cDNA were synthesized using PCR; the full-length kinesin cDNA clone served as a template. The 5' PCR oligonucleotide in each reaction included an Xba site, the Kozak consensus sequence (Kozak, 1987), and the first 18 bases of the desired segment of the coding region. In the reactions for clones with an epitope tag, the 3' PCR oligonucleotide corresponded to the last 18 bases of the desired coding region, 39 bases encoding glycine and proline (as a flexible linker) and then vesicular stomatitis virus (VSV) G protein epitope tag (5'-CTTTCCAAG-ACGATTCATTTCGATGTCGGTGGGCCCCTGG-3'), a stop codon, and the SacI site. The 3' PCR oligonucleotide for the clones without an epitope tag included the last 18 bases of the desired coding region, a stop codon, and a BamHI site. The PCR reactions were done under the following conditions: 10 ng of cesium gradient-purified plasmid DNA was added to a mix containing 10 mM Tris, pH 8.3, 50 mM KCl, 2 mM $MgCl_2$, 0.01% gelatin, 0.2 mM dNTP, and 50 pmol of each oligonucleotide. The reactions were carried out at 94°C (60 s), 50°C (60 s), 72°C (3 min), for 30 cycles. The PCR products were subcloned into the SV-40 expression vector pSVL51 using either the XbaI, SacI, or BamHI sites (Huylebroeck et al., 1988).

### Cell Culture

Unless otherwise indicated, CV-1 cells were grown in Dulbecco's minimum essential medium supplemented with 10% FCS, 4 mM L-glutamine, 100 U/ml penicillin, 100 μg/ml streptomycin, and 10 μg/ml gentamicin. Cells were maintained at 37°C under a 10% $CO_2$ atmosphere.

### Transient Transfection of CV-1 Cells

20–24 h before DNA transfer, 70–80% confluent CV-1 cells were seeded 1:3 or 1:5 on acid-cleaned sterile glass coverslips. Transfections were performed following a DEAE–dextran precipitation method (Friederich et al., 1989; Huylebroeck et al., 1988). In all experiments, cesium chloride–purified plasmid DNA was dissolved to a final concentration of 20 μg/ml in minimum essential medium (with Earle's salts, 25 mM Hepes, L-glutamine) (MEM-Hepes, pH 7.15), without serum or sodium carbonate, but containing the same antibiotics as above. The DNA/MEM-Hepes solution was slowly added to an equal volume of 1 mg/ml DEAE-dextran (molecular mass 500,000; Pharmacia LKB Biotechnology Inc., Uppsala, Sweden) in MEM-Hepes (pH 7.25) and incubated for 30 min at room temperature after agitation. Cells were removed from the incubator, rinsed twice with MEM-Hepes, pH 7.25, and 100–150 μl of the DNA/DEAE-dextran mixture was added to each coverslip. After a 30-min incubation at room temperature, an excess of MEM-Hepes (pH 7.25) was added, the medium was removed, and cells were washed twice in the same medium. Supplemented Dulbecco's minimum essential medium containing 0.1 mM chloroquine diphosphate (Sigma Chem. Co., St. Louis, MO) was added, and cells were placed at 37°C for 3–4 h. The chloroquine treatment was followed by an overnight exposure of the cells to 0.1 mM sodium butyrate (Sigma Chem. Co.) in supplemented Dulbecco's minimum essential medium. Finally, cells were rinsed extensively with supplemented Dulbecco's minimum essential medium and grown for 24–48 h in the same medium before being analyzed. Proteins of the expected sizes were expressed in CV-1 cells from pSVTail, pSVRod, and pSVRT plasmids when examined by immunoblot analysis using a monoclonal antibody against the VSV G peptide.

### Immunofluorescence Labeling

24–72 h after DNA transfer, cells were rinsed with PBS (140 mM NaCl, 2.7 mM KCl, 1.5 mM $KH_2PO_4$, 8.1 mM $Na_2HPO_4$, pH 7.2) and fixed by sequential immersions for 4 min each in methanol and acetone at −20°C. Cells were then immediately rehydrated in PBS before the staining reactions. When fixation was preceded by permeabilization, cells were treated in either one of the following ways: (*a*) after rinsing with PBS, coverslips were dipped four times for 25 s into four different breakers, each containing microtubule stabilizing buffer (80 mM Pipes-KOH, 1 mM EGTA, 1 mM $MgCl_2$, pH 6.8), 10% glycerol, and 0.5% Triton X-100 (modified from

Kreis [1986]); or (*b*) after rinsing with PBS, cells were incubated at 37°C for 10 min in 1% Triton X-100 in the same buffer as above (protocol modified from Hollenbeck [1989]). Both treatments produced similar results. Detergent treatment was then followed by methanol-acetone fixation. For immunofluorescence labeling, cells were processed through the following steps: (*a*) incubation with primary antibodies (see below) diluted in PBS (2 h); (*b*) wash with PBS (three to four times for 15 min); (*c*) incubation with affinity-purified Texas red-conjugated goat anti-rabbit IgGs and/or FITC-conjugated goat anti-mouse IgG (Axell Accurate Chemical Sci. Corp., Westbury, NY) (45 min; room temperature) (the rat monoclonals were efficiently recognized by the anti-mouse secondary IgGs); (*d*) washes with PBS (3–4 times for 15 min); and (*e*) a quick rinse in distilled water before mounting. Cells were observed using a photomicroscope III (Carl Zeiss, Inc., Thornwood, NY) equipped with epifluorescence, and photographs were taken using Tmax 400 film (Eastman Kodak Co., Rochester, NY).

The following primary antibodies were used in this study: (*a*) a polyclonal serum raised against squid KHC that was affinity purified against the bovine brain KHC by the method of Olmsted (1981); (*b*) monoclonal and affinity-purified polyclonal antibodies that recognize the COOH-terminal 10-amino acid epitope of the VSV G protein (Kreis, 1986), which were a kind gift from Drs. T. Kreis and R. Duden (EMBL, Heidelberg, Germany); (*c*) a rat antitubulin mAb (YL1/2) was a kind gift from Dr. J. Kilmartin (MRC, Cambridge, England), and; (*d*) a mAb against vimentin obtained from Boehringer Mannheim Corp. (Indianapolis, IN).

### *Quantitation of the Level of Kinesin Expression*

The relative levels of kinesin expression were compared by quantitative video analysis. Cells containing the transiently expressed kinesin and/or endogenous kinesin were prepared for immunofluorescence as described above and reacted with the affinity-purified polyclonal antiserum against the squid KHC. The fluorescence signal was imaged with a Hamamatsu silicon-intensified target camera. The gain of the silicon-intensified target camera was first set so that the fluorescence signal from endogenous kinesin in the untransfected cells was within the linear range of the camera. At this gain, the fluorescence signal from the transfected cells generally saturated the camera. To bring the signal within the same linear range, neutral density filters were placed in the epifluorescence light path. The transmission characteristics of the filters were calibrated, so that signal could be normalized and the relative intensities from the transfected and nontransfected cells estimated. The images from the camera were stored digitally and analyzed using a Macintosh computer-based image analysis program (IMAGE - version 1.32; available from the National Technical Information Service, Springfield, VA). The average fluorescence intensities were measured for cells whose boundaries were marked manually.

### *SDS Gel Electrophoresis and Immunoblot Analysis*

Proteins of total homogenates of CV-1 cells were separated on polyacrylamide gels under denaturing and reducing conditions (Laemmli, 1970) and immunoblotted (Towbin et al., 1979). Immunolabeling was performed using 5% nonfat dry milk, 10 mM Tris, pH 7.4, 150 mM NaCl, and 0.1% Tween-20 for all washes and incubations. Rabbit antibodies were detected by $^{125}$I-conjugated protein A (Amersham Corp., Arlington Heights, IL) and autoradiography.

## *Results*

### *Isolation of an hKCH cDNA*

To obtain a hKHC cDNA, a nucleotide probe for screening cDNA libraries was first obtained by PCR. After comparing sequences of the *Drosophila* and squid KHC genes, two 128-fold degenerate pools of primers were synthesized based upon a highly conserved 35-amino acid sequence in the COOH-terminal domain (see Materials and Methods). With these primers, a unique fragment of the expected size (69 bp) was generated using first-strand cDNA derived from MDCK cells as a template. The sequence of this amplified DNA was ~75% identical at the nucleotide level and 100% identical at the amino acid level to the corresponding region of the squid (Kosik et al., 1990) or the *Drosophila* KHC genes (Yang et al., 1989), suggesting that the PCR product encoded a portion of a mammalian KHC gene.

The PCR-generated DNA fragment was used to screen a human placental λgt11 cDNA library. A 1.5-kb clone (λHK-3) obtained from the initial screen contained a large open reading frame that showed considerable homology to the COOH-terminal half of the squid and *Drosophila* KHCs and contained the sequence of the PCR fragment that was used as the probe. Rescreening of the library with a 5′ EcoRI–NcoI fragment of this partial clone produced a 3-kb clone (λHK-21), which contained the sequences of λHK-3 as well as an additional 1,250 nucleotides of coding sequence and 250 nucleotides in the 3′ untranslated region. Since λHK-21 did not encode a full-length KHC, a third screening using the 5′ NcoI–ApaLI fragment of λHK-21 was performed. This screen yielded a 1.4-kb clone (λHK-H8), which had a 700-nucleotide overlap with the 5′ end of λHK-21, the 5′ end of the coding sequence, and 313 nucleotides of the 5′ untranslated region. Another clone was later obtained that was identical to λHK-H8, except that it contained an additional 127 nucleotides at the 5′ end of the untranslated region. A hKHC cDNA (3.7 kb) containing the entire coding region as well as 313 bp of 5′ uncoding sequence and 482 bp of 3′ uncoding sequence (including an 82-base poly[A] tail) was created by joining λHK-H8 and λHK-21 together using a common PstI site.

### *Sequence Analysis and Comparison*

The largest open reading frame (ORF) of the hKHC cDNA encodes a polypeptide of 963 amino acids (Fig. 1), which is similar in size to *Drosophila* (975 aa; Yang et al., 1989), squid (967 aa; Kosik et al., 1990), and sea urchin (1,031 aa; Wright et al., 1991) KHCs. The amino acid and nucleotide sequences are accessible through Genbank (accession number X65873). The amino acid sequence of hKHC displays a considerable identity throughout its length to the invertebrate KHCs (63% when compared with *Drosophila*) (Fig. 1). Even where amino acid sequences are different, many of the changes are conservative in nature. Secondary structure predictions using the method of Finer-Moore and Stroud (1984) also suggest that hKHC has an overall domain organization similar to that of previously described invertebrate KHCs (Yang et al., 1989; Kosik et al., 1990). Amino acids 1–413 of human kinesin (which contain a consensus sequence for ATP binding [aa 85–101]) are predicted to form a globular domain containing both α helices and β sheets. Adjacent to this putative motor domain is a long stretch of amino acids (aa 414–890; the rod domain) containing heptad repeats with hydrophobic amino acids prevalent in positions 1 and 4. The amphipathic nature of the helix is broken between residues 566 and 582 (the hinge region of the rod domain) and is weak between residues 460 and 470, 730 and 770, and 815 and 835. The COOH-terminal domain of hKHC (aa 890–963) is predicted to contain α helices, β sheets, and turns, which are suggestive of a more globular configuration. Based upon the high degree of primary and secondary structure similarities with invertebrate KHCs, we believe that our cloned cDNA encodes a human homologue of the KHC.

KHCs have not been found to share homology with a variety of kinesin-like proteins outside of their motor domains.

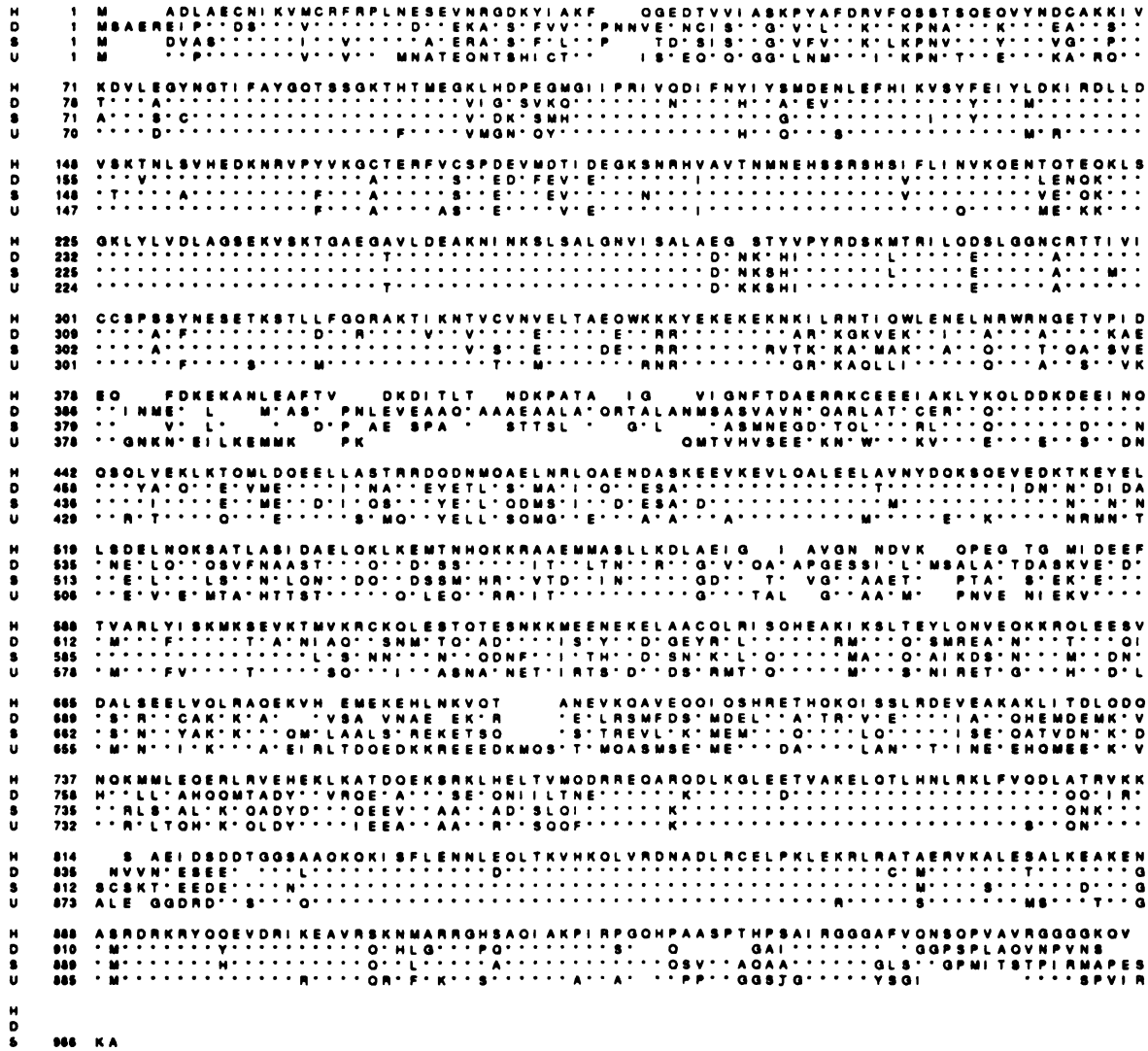


*Figure 1.* Alignment of the human and invertebrate KHC sequences. The three invertebrate KHCs—*Drosophila* (*D*), squid (*S*), and sea urchin (*U*)—were compared with the human (*H*) KHC sequence. Amino acids are numbered in the left margin. The one-letter amino acid code is used. Asterisks represent amino acid identities between a given invertebrate sequence and human. Blank spaces represent gaps that were introduced to maximize homology.

We reexplored this issue by aligning smaller segments of the hKHC with the kinesin-like genes *bimC* (Enos and Morris, 1990), KAR3 (Meluh and Rose, 1990), *cut7* (Hagan and Yanagida, 1990), *uncl04* (Otsuka et al., 1991), *ncd* (McDonald and Goldstein, 1990; Endow et al., 1990), and *nod* (Zhang et al., 1990). Our analyses revealed that *bimC* of *Aspergillus* (but none of the above kinesin-like proteins) contained segments of homology with the KHCs (Fig. 2). Two regions of similarity were noted. The first was a 14-amino acid stretch within the highly conserved end of the rod (aa 780–793 in human), which has seven identical residues, and three conservative changes in common with a region in the tail of *bimC* (aa 730–743). Another segment of 23 amino acids in the tail of KHC (aa 891–913 in human) also displayed significant homology to a region in the globular tail of *bimC* (aa 789–811). These findings suggest that the tail domains of *bimC* and the KHCs of higher eukaryotes have regions that may perform similar functions.

The 5′-untranslated region of hKHC has several features that are rarely found in eukaryotic mRNAs. This region, which is at least 440 nucleotides long, is longer than the 5′ untranslated regions found in most mammalian mRNAs (Kozak, 1987). It also contains unusually long stretches of G-C rich sequence (89.5% for nt −7 to −44, 75% for nt −53 to −96; 85.4% for nt −113 to −160; and 84.2% for nt −227 to −283) that may have the potential to form extensive secondary structure. The most unusual feature of the 5′-untranslated region, however, is the presence of three AUGs

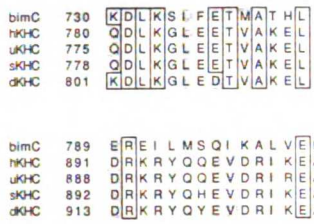



*Figure 2.* Nonmotor region comparison between the KHCs and the kinesin-like protein *bimC*. Comparison of the COOH-terminal domain of the human (*hKHC*), sea urchin (*uKHC*), squid (*sKHC*), and *Drosophila* (*dKHC*) KHCs to the nonmotor domains of *bimC* yielded these two regions of potentially meaningful homology. Amino acids are numbered in the left margin. Amino acid identity between *bimC* and any of the conventional KHCs is shown as a box. Shading indicates a conservative amino acid change. The SD scores for the upper and lower regions are 2.8 and 2.1, respectively, which indicates the number of SDs from that expected by a chance occurrence.

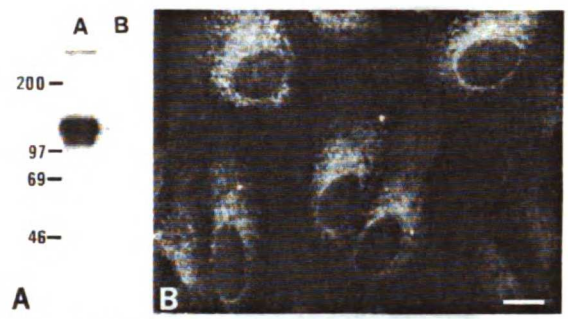



*Figure 3.* Immunofluorescence distribution of endogenous kinesin in nontransfected CV-1 cells (*A*) An immunoblot showing that an anti-KHC polyclonal antibody recognizes a unique band in a total homogenate of CV-1 cells (lane *B*; loading of 40 $\mu$g protein) which comigrates with purified bovine brain kinesin (lane *A*; loading of 1.5 $\mu$g protein). The migration of molecular weight standards are noted at the left. (*B*) Localization of endogenous kinesin in CV-1 cells as demonstrated by indirect immunofluorescence, using the same polyclonal serum as in *A*. CV-1 cells were grown to subconfluence on glass coverslips and fixed by methanol–acetone at −20°C. Bar, 1 $\mu$m.

upstream from the KHC start codon (at nt −226, −217, and −214) followed by an in-frame termination codon at nt −203 (GCCGCCGCCATGGCTGCCATGATGGATCGGAAGTGA). This small open reading frame could encode a polypeptide of no more than eight amino acids. The first AUG of the upstream ORF is contained within a consensus initiation sequence (GCCGCCPuCCAUGG; [Kozak, 1987]).

### *Transient Expression of the hKHC Gene in CV-1 Cells*

To study the interaction of different domains of the KHC with cytoplasmic structures, we expressed the hKHC gene or portions of the gene in CV-1 monkey kidney epithelial cells and examined the localization of the expressed proteins by immunofluorescence microscopy. Constructs containing the hKHC gene were prepared in the pSVL51 vector, which drives expression from a late SV-40 promoter and which replicates in CV-1 cells by virtue of expressing the SV-40 large T antigen. Constructs containing the following portions of the hKHC gene were used in this study: (*a*) the entire coding region of hKHC (pSVKin; aa 1–963), (*b*) the motor domain (pSVMot; aa 1–426), (*c*) a portion of the $\alpha$-helical rod domain (pSVRod; aa 511–766), (*d*) the strongly conserved COOH-terminal portion of the $\alpha$-helical coiled coil rod and the tail domain (pSVTail; 767–963), and (*e*) the COOH-terminal half of the protein containing the majority of the rod and the entire tail domain (pSVRT; 511–963). To localize the expressed protein unambiguously, nucleotides encoding the last 10 amino acids of the VSV G protein followed by a termination codon were added to the 3′ end of the above constructs. Monoclonal and polyclonal antibodies that recognize this peptide specifically (Kreis, 1986) were used to determine the location of the expressed protein by immunofluorescence.

Before examining the localization of the expressed hKHC, the distribution of the endogenous kinesin protein in CV-1 cells was determined using an affinity-purified polyclonal anti-KHC serum (originally prepared against SDS–polyacrylamide gel denatured squid KHC). By immunoblot analysis, the affinity-purified polyclonal antibody recognized a single 120-kD polypeptide in CV-1 crude extracts, which is the size expected for the KHC (Fig. 3 *A*). At a threefold greater protein loading, a very faint 45-kD band was also detected (not shown), which is the same size as a common proteolytic fragment of kinesin (Kuznetzov et al., 1989; Scholey et al., 1989). Immunofluorescence staining with the polyclonal antibody after methanol–acetone fixation revealed a diffuse distribution with some reticular features; neither filamentous nor vesicular staining was detected (Fig. 3 *B*). The faint reticular staining was retained after treatment with saponin (0.02%), but was substantially reduced by Triton X-100 (0.5%) permeabilization before fixation (not shown). This distribution of kinesin in nonextracted cells is similar to that reported by Hollenbeck (1989) in chicken embryo fibroblasts.

When CV-1 cells were transfected with pSVKin and fixed by methanol-acetone 24 h later, a strong immunofluorescence signal with the anti-VSV G peptide antibody was detected in ~10% of the cells, which are the ones believed to have been transfected with the plasmid (Fig. 4). The fluorescent signal from the remainder of the cells was extremely faint and only slightly greater than that produced by secondary antibody alone. This same weak staining is seen in cells that did not undergo the transfection procedure and thus probably represent untransfected cells in the population.

The distribution of hKHC expressed from pSVKin was somewhat different from that described above for the endogenous protein. A large amount of the expressed heavy chain was diffusely distributed throughout the cytoplasm; however, a filamentous pattern superimposed upon this diffuse staining was visible in most cells (Fig. 4 *A*). Filaments were not obvious in some cells, perhaps because of their prominent background staining. Filamentous patterns were also observed when the kinesin COOH-terminal tail (pSVTail) was expressed in CV-1 cells (Fig. 4 *C*). The filamentous patterns of the expressed KHC and the KHC tail domain coaligned with microtubules in these cells (Fig. 4, *B* and *D*). On the other hand, the kinesin rod domain (pSVRod) and the motor domain (pSVMot) displayed only a diffuse staining

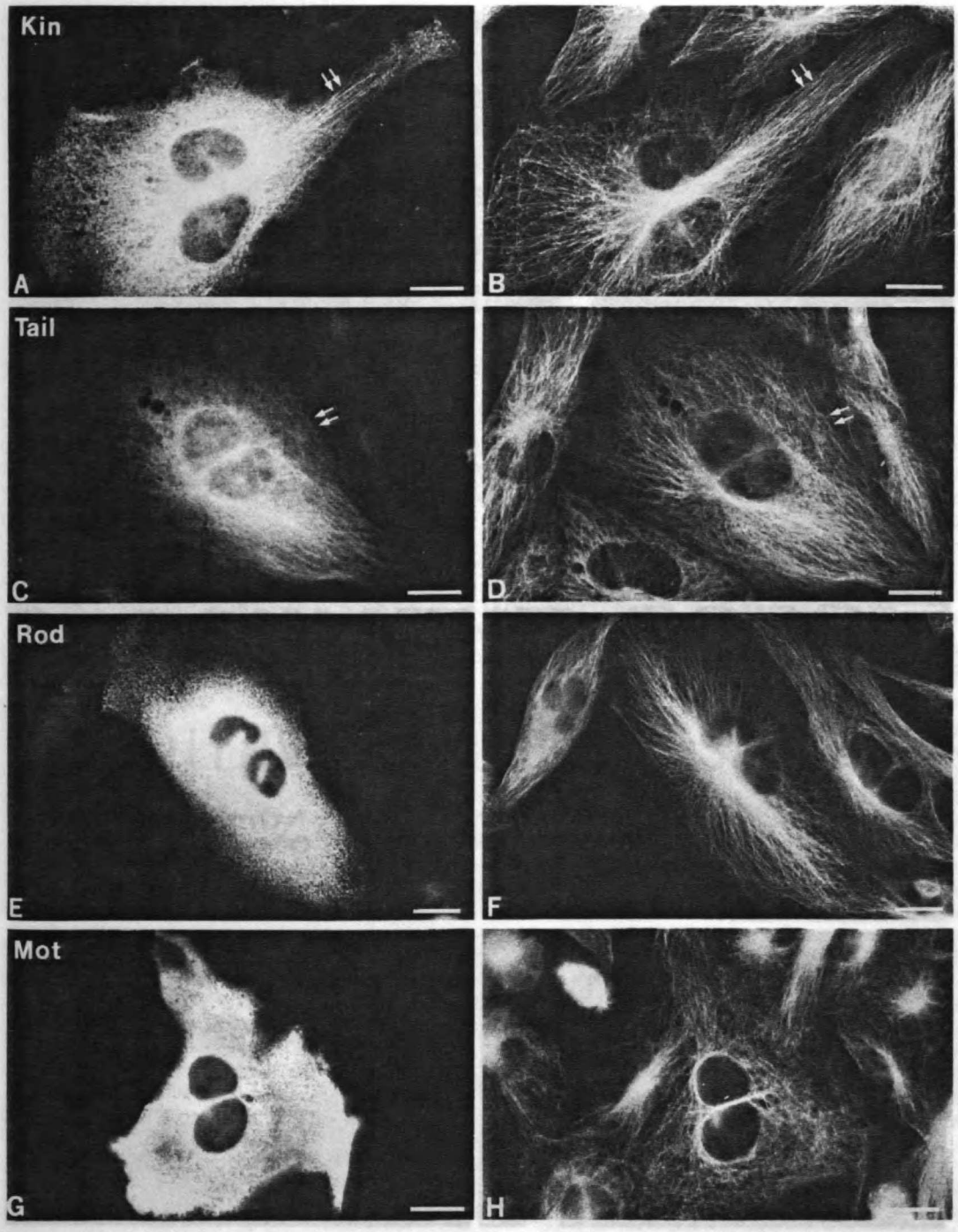



*Figure 4.* Indirect immunofluorescence of CV-1 cells expressing the entire KHC or portions of the KHC. Cells were transfected with the following constructs: (*A* and *B*) pSVKin; (*C* and *D*) pSVTail; (*E* and *F*) pSVRod; (*G* and *H*) pSVMot. All cells were fixed 24 h after transfection in methanol–acetone at −20°C. Cells were then double-labeled for the expressed kinesin proteins with rabbit polyclonal IgG against the VSV G peptide epitope (*C*, *E*, and *G*) and for tubulin with a monoclonal rat IgG (*B*, *D*, *F*, and *H*). In *A*, the expressed kinesin was visualized with the antikinesin polyclonal antibody; similar results were obtained with this construct with the anti-VSV G peptide polyclonal antibody. While the antitubulin antibody labels microtubules in all cells, the anti-VSV G peptide or antikinesin antibody produces an intense staining only in the transfected cells. In cells transfected with pSVKin (*A*) and pSVTail (*C*), the expressed kinesin proteins show a diffuse or faintly reticular distribution throughout the cytoplasm; superimposed on this pattern, filamentous staining is also evident (*A* and *C*, *arrows*) which coincides with microtubules (*B* and *D*, *arrows*). In cells transfected with pSVRod (*E*) and pSVMot (*G*), the expressed proteins are distributed throughout the cytoplasm and, in both cases, filamentous patterns were not observed. A greater percentage of transfected cells had multiple nuclei than untransfected cells, as shown in this figure. Multinucleate and uninucleate transfected cells, however, showed similar distributions of the expressed kinesin proteins. Bars, 2 μm.

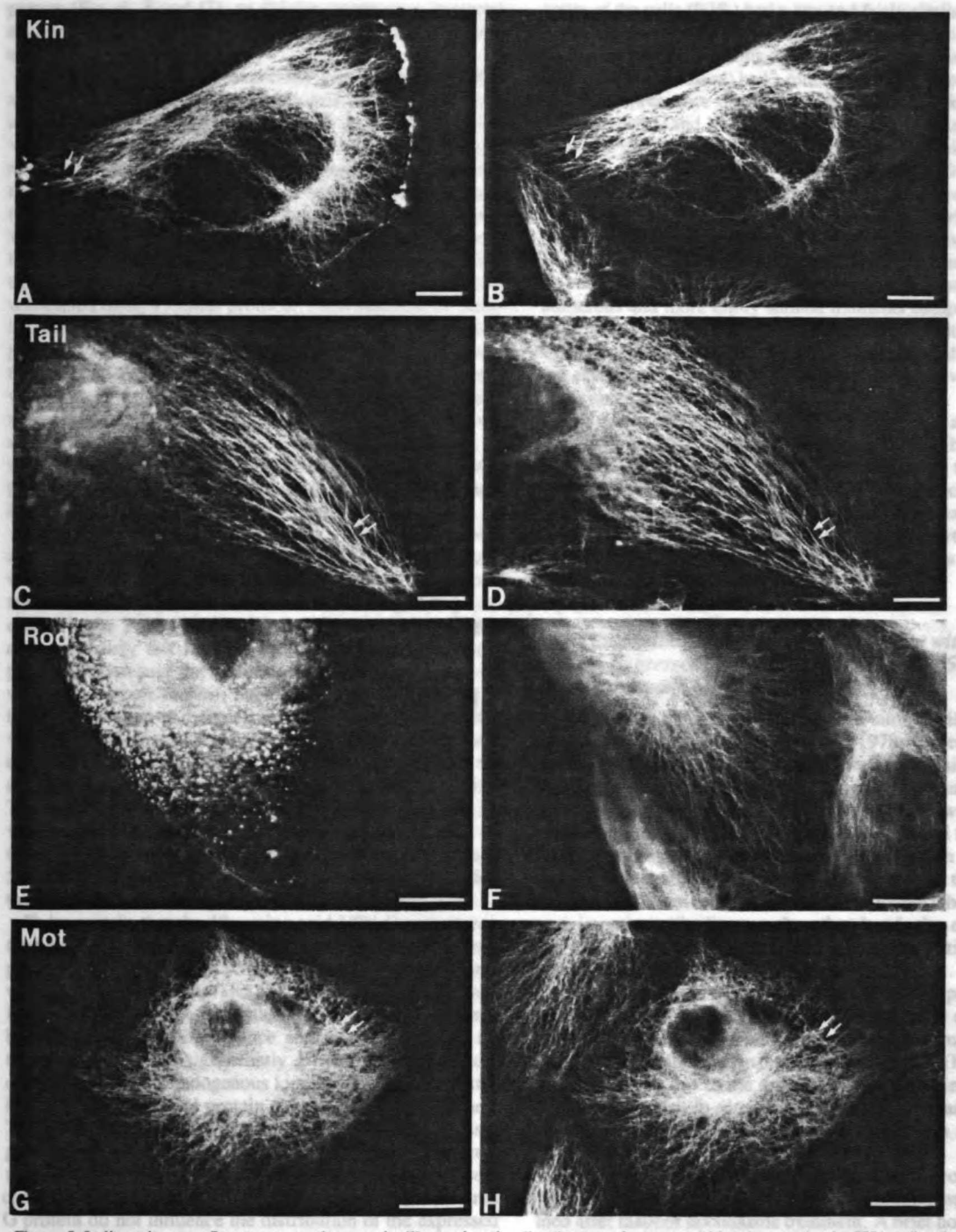



*Figure 5.* Indirect immunofluorescence micrographs illustrating the distribution of expressed kinesin proteins in CV-1 cells after detergent permeabilization. Cells were transfected with the following constructs: (*A* and *B*) pSVKin; (*C* and *D*) pSVTail; (*E* and *F*) pSVRod; (*G* and *H*) pSVMot. Cells were permeabilized with either 0.5% or 1% Triton X-100 in 80 mM Pipes, 1 mM EGTA, and 1 mM $MgCl_2$ before fixation in methanol–acetone at −20°C. Cells were then double-labeled for the expressed kinesin proteins with the polyclonal anti-G protein epitope antibody (*A*, *C*, *E*, and *G*) and for tubulin with the rat monoclonal (*B*, *D*, *F*, and *H*). In cells transfected with pSVKin (*A*) and pSVTail (*C*), treatment with Triton X-100 before the methanol–acetone fixation greatly reduces the diffuse and reticular staining of the cytoplasm which was evident in Fig. 7 (compare Fig. 7, *A* and *C*, with Fig. 8, *A* and *C*). The filamentous staining pattern for pSVKin, pSVTail, and pSVMot expressed proteins and the coalignment with microtubules is clearly evident (*A–D*, *G*, and *H*, *arrows*). In cells transfected with pSVRod that were Triton X-100 permeabilized before fixation, very few cells were found that displayed a strong immunofluorescence staining, probably because the soluble protein was removed by detergent treatment. The few cells that had a prominent immunofluorescence signal displayed an aggregated but not a filamentous staining pattern (*E*). The fine particulate immunofluorescence in *E* is probably due to artefactual precipitation of the expressed protein. Bars, 2 μm.

pattern (Fig. 4, *E* and *G*), as did the cytoplasmic bacterial enzyme β-galactosidase when expressed in CV-1 cells (not shown).

The localization of the expressed protein from pSVKin and pSVTail to filamentous cytoplasmic elements was clear in virtually all cells when soluble and membrane proteins were first extracted with Triton X-100 before fixation with methanol-acetone (Fig. 5, *A* and *C*). Saponin permeabilization and glutaraldehyde fixation produced identical results (not shown). The coalignment of these filamentous elements with microtubules also became more apparent after permeabilization (Fig. 5, *B* and *D*). The endogenous kinesin in untransfected cells did not show this filamentous distribution when fixed using a similar protocol. Such filamentous staining was also not observed with the expressed protein from pSVRod; in fact, very few immunoreactive cells could be detected, probably because the rod was soluble and hence washed away by the detergent treatment. In the few cells where immunoreactivity was detected, an aggregated but not a filamentous pattern was observed (Fig. 5, *E* and *F*). A small percentage (10%) of transfected cells exhibited large punctate staining suggestive of aggregated protein, regardless of the construct used or the fixation conditions.

After Triton X-100 permeabilization, the expressed motor domain demonstrated a filamentous staining that colocalized with microtubules (Fig. 5, *G* and *H*). This filamentous pattern, however, was not detected when 5 mM MgATP was included in the Triton X-100 permeabilization buffer; in this case, extremely few immunoreactive cells were observed, presumably because the motor domain was soluble and was washed away (not shown). Such ATP-dependent binding of the motor domain to cytoplasmic microtubules is consistent with biochemical experiments demonstrating that the motor domain exhibits a high affinity for microtubules only in the absence of ATP (Yang et al., 1989; Kuznetsov et al., 1989). The cellular concentrations of ATP probably account for why the motor domain does not localize to microtubules after direct methanol–acetone fixation (Fig. 4 *G*). Inclusion of 5 mM MgATP in the permeabilization buffer did not affect the colocalization of the tail domain with microtubules.

To be certain that the 10–amino acid VSV G protein epitope tag did not influence the distribution of the expressed proteins, the pSVKin and pSVRT constructs were prepared without the epitope tag and the expressed proteins were localized with the affinity-purified anti-KHC polyclonal antibody. The immunofluorescence signal obtained from the transfected cells was significantly greater than that of cells expressing only the endogenous kinesin, and thus the distribution of the expressed protein could be easily established. The immunofluorescence pattern observed for the expressed proteins without the epitope tag was indistinguishable from those shown in Figs. 4 and 5 (data not shown). Thus, we conclude that the 10 amino acids of the vesicular stomatitis virus G protein do not influence the distribution of the expressed kinesin proteins.

We also examined whether the level of KHC expression affected its distribution. pSVKin-expressed protein was compared to the endogenous KHC by performing immunofluorescence with the kinesin polyclonal antibody, imaging the cells with a video camera, and analyzing the relative intensities of stored digital images of cells using a computer program (see Materials and Methods). The majority of the cells (90%) had a low and fairly similar fluorescence signal attributable to the endogenous kinesin in the untransfected cells (100 cells analyzed). The transfected cells (10% of the population) had a much greater fluorescence signal; the fluorescence signal from 26% of the transfected cells was between 4- and 10-fold greater than that of untransfected cells, the signal from 47.3% of cells was 10–100-fold greater, and the signal from 26.7% of the cells was 100–500-fold greater (116 cells analyzed in total). All transfected cells exhibited both a cytoplasmic and a filamentous distribution of the expressed kinesin, regardless of the level of expression. In general, the cells expressing low levels of kinesin (four- to sixfold greater than endogenous kinesin) showed less numerous and more dimly stained filaments compared with high expressing cells, but these filaments were still always superimposable with microtubules. Thus, colocalization of the expressed KHC with microtubules was observed over a wide range of expression levels.

The transfected cells were generally larger (an average of 2.9-fold greater surface area) and more frequently binucleate than the untransfected cells. However, many of the transfected cells were small and contained only one nucleus; neither the size nor number of nuclei in the cell appeared to be correlated with the level of kinesin expression. Furthermore, the distribution of the KHC or KHC domains was not influenced by cell size.

### *The Filamentous Elements That Colocalize with Protein Expressed by pSVKin, pSVTail, and pSVRT Are Cytoplasmic Microtubules*

As intermediate filaments often show a similar distribution to microtubules (Hynes and Destree, 1978; Geuens et al., 1983), we examined whether the filamentous staining pattern of the expressed KHC proteins reflects an interaction with intermediate filaments. Fig. 6, *A* and *B*, shows that the rod–tail protein (pSVRT), like the tail domain and the entire KHC, demonstrated a filamentous staining pattern that very closely reflected the microtubule distribution in the transfected cells. When transfected cells were double labeled with antivimentin antibodies, on the other hand, the expressed rod–tail domain colocalizes extensively but not entirely with vimentin intermediate filaments (Fig. 6, *C* and *D*). The lack of colocalization is particularly evident in the periphery, where the vimentin filament network had partially collapsed towards the cell center. This partial collapse was more common in the transfected than the untransfected cells (Fig. 6 *D*), which could be due to the expressed kinesin tail interfering with a kinesin-driven extension of intermediate filaments towards the periphery along microtubules (Gyoeva and Gelfand, 1991).

To further establish that the expressed KHC colocalizes with cytoplasmic microtubules, its distribution was examined after taxol or nocodazole treatment. A brief nocodazole treatment (20 min; 10 μM) was used to depolymerize the majority of the cytoplasmic microtubules (Fig. 7 *A*); this short incubation did not collapse the intermediate filament network. The microtubules that remained intact (many of which were in the perinuclear region) probably correspond to a subset of stable microtubules that have been described in other studies (Schulze and Kirschner, 1987; Kreis, 1987). The expressed KHC (pSVKin) colocalized with the nocoda-

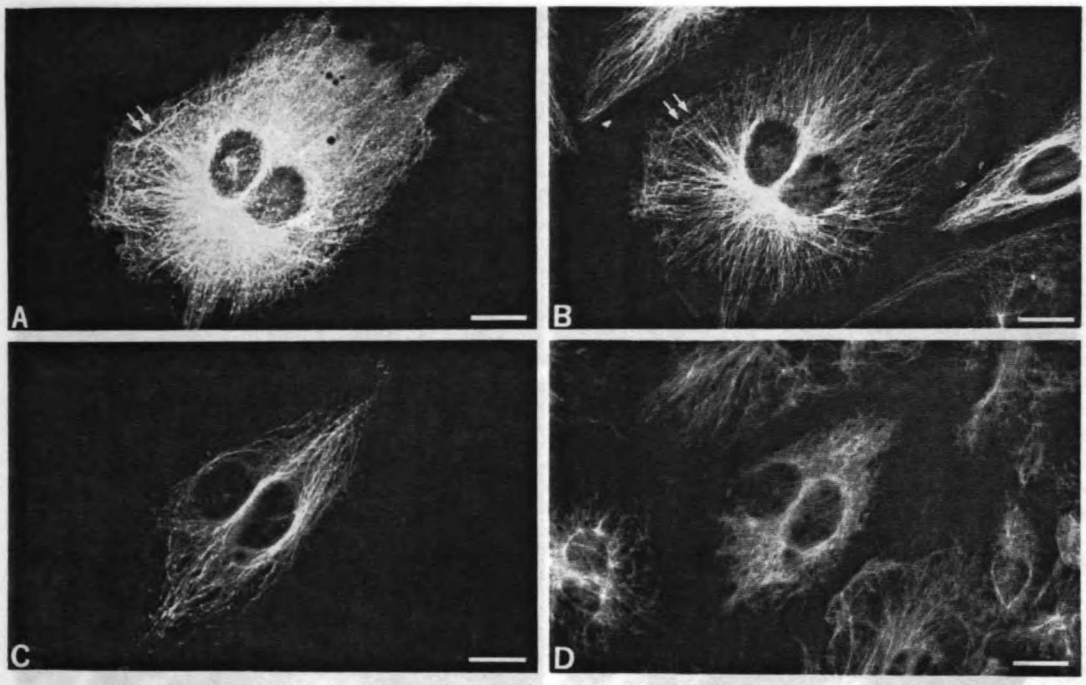



*Figure 6.* Distributions of microtubules, vimentin filaments, and the expressed kinesin tail (pSVRT) in CV-1 cells. All cells were fixed with methanol–acetone at −20°C and double-labeled with the following primary antibodies: polyclonal IgG against the VSV G protein epitope (*A* and *C*), monoclonal rat IgG against tubulin (*B*), and monoclonal mouse IgG to vimentin (*D*). The pattern of immunofluorescence for the expressed kinesin protein (*A* and *C*) shows a filamentous distribution similar to that of microtubule (*B*), but different from the one of intermediate filaments (*D*). In *A*, a diffuse immunofluorescence is observed throughout the cytoplasm similar to the staining obtained for pSVKin and pSVTail in the same fixation conditions and shown in Fig. 7, *A* and *C*. Such diffuse immunofluorescence is less evident in *C* probably because of a better extraction obtained in these cells with methanol–acetone. Individual filaments decorated by the VSV G peptide antibody appear to coalign with single microtubules (arrows in *A* and *B*), but not with intermediate filaments. Bar, 2 μm.

zole-resistant microtubules surrounding the nucleus (Fig. 7 *A*); the filamentous staining of KHC which normally extends towards the periphery in the transfected cells, (Figs. 5 *A* and 7 *E*) was no longer observed after nocodazole treatment. With a longer nocodazole incubation (1–2 h), neither microtubule nor filamentous KHC staining was evident (not shown). Taxol (20 μM) causes the polymerization of noncentrosomal microtubules, which often become bundled (Fig. 7 *D*) (DeBrabander et al., 1981). In transfected cells treated with taxol, the pSVKin expressed protein colocalized with the taxol-induced microtubule bundles (Fig. 7, *C* and *D*). Similar changes in the distribution of the tail domain expressed from pSVTail were observed after nocodazole and taxol treatment (not shown). The change in distribution of the pSVKin and pSVTail expressed proteins after taxol or nocodazole treatment further supports the notion that these proteins interact with cytoplasmic microtubules or microtubule-associated proteins.

Cells transfected with pSVKin frequently displayed unusual spatial arrangements of cytoplasmic microtubules that were rarely seen in the untransfected cells. In untransfected cells or cells expressing the motor, tail, or the rod–tail domains, microtubules generally emanate from the centrosomal region of the cell and extend towards the periphery (Fig. 5, *D*, *F*, and *H*). In ~50% of the cells expressing the entire KHC, the connection of microtubules to the centrosome was less obvious and the microtubules seemed more disorganized than those in the nontransfected cells (Fig. 7 *E* and *F*).

## Discussion

### Comparison of Human and Invertebrate KHC Sequences

In this study, we have cloned and characterized the gene encoding the human homologue of the KHC. Comparisons of the human KHC sequence with *Drosophila* (Yang et al., 1989), squid (Kosik et al., 1990), and sea urchin (Wright et al., 1991) KHC sequences reveal a high level of amino acid sequence identity over the entire molecule. The degree of similarity between the invertebrate and mammalian KHCs is particularly striking in the motor domain, where very long stretches of nearly 100% amino acid identity are observed. These domains of high conservation presumably play important roles in ATP hydrolysis, microtubule binding, and force production. The COOH-terminal tail domain also displays extensive segments of nearly complete identity, indicating that it must serve an important, although still unidentified function. This region has been proposed to interact with light chains, organelles, and possibly microtubules. The rod displays significantly less primary sequence homology, except at its COOH-terminal end, which is almost identical in all of the cloned KHCs.

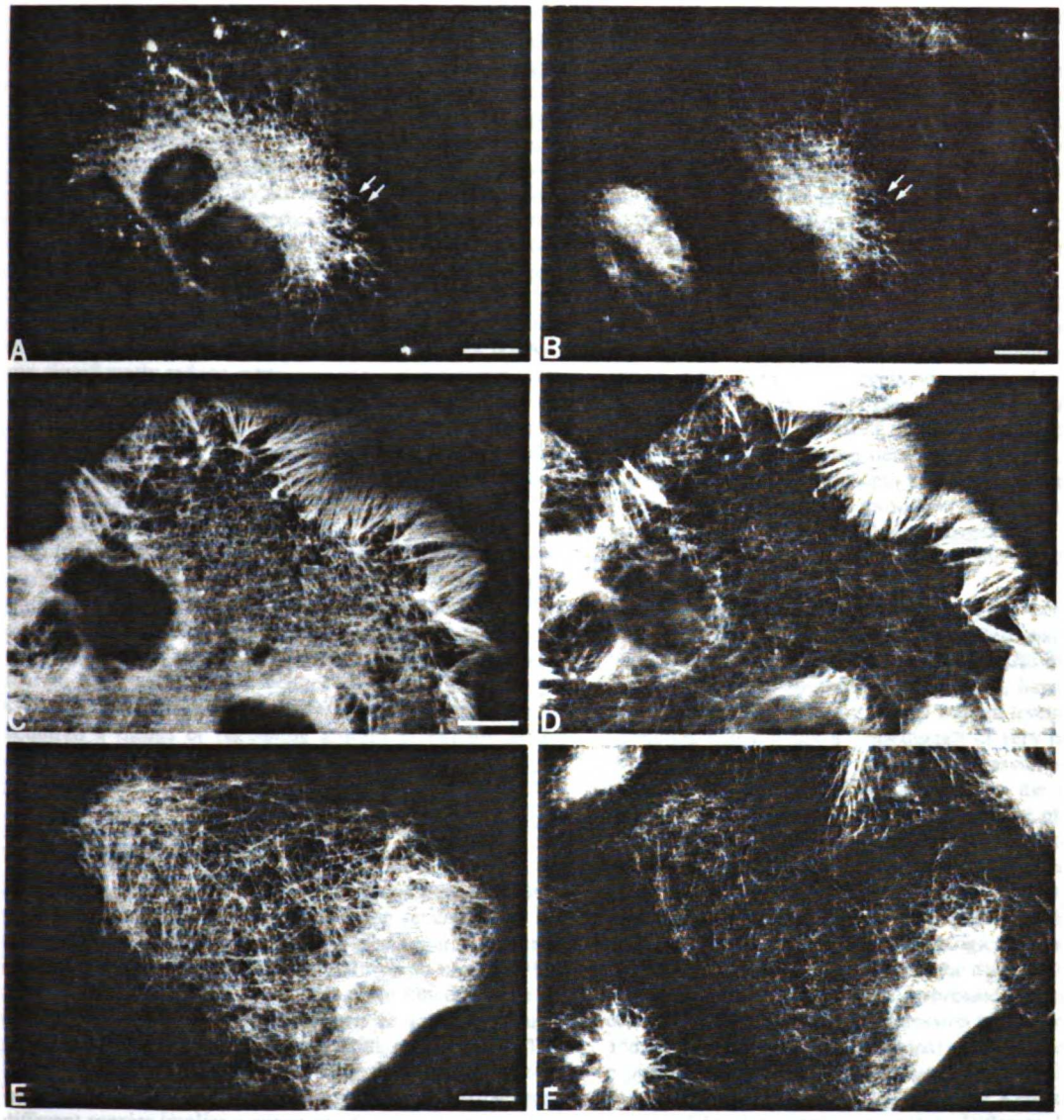



*Figure 7.* Immunofluorescence localization of the microtubules and the expressed pSVKin after nocodazole or taxol treatment of CV-1 cells transfected with pSVKin. In *A* and *B*, cells were incubated for 6 min in the presence of 10 μM nocodazole; in *C* and *D* they were treated with 20 μM taxol (National Cancer Institute) for 2 h (both at 37°C). Cells in *E* and *F* did not receive any drug treatment. All cells were permeabilized with 0.5% Triton X-100 in 80 mM Pipes, 1 mM EGTA, 1 mM $MgCl_2$ and then fixed in methanol–acetone at −20°C. Cells were double-labeled for the expressed kinesin with the polyclonal anti-VSV G protein epitope antibody (*A*, *C*, and *E*) and for tubulin with the rat monoclonal antibody (*B*, *D*, and *F*). The pattern of distribution of the expressed KHC appears very similar to that of microtubules even when the organization of the microtubular network is modified by nocodazole or taxol treatments. In *A*, filaments decorated with the expressed kinesin coincide with microtubules in *B* that have not yet depolymerized (see arrows for an example). In *C* and *D*, taxol-induced microtubules bundles coincide with localization pattern seen with the anti-VSV G peptide antibody. Cells transfected with pSVKin often show a disorganized microtubule network that does not originate from the centrosomal area (*E* and *F*). The distributions of the expressed kinesin protein and tubulin again appear to coincide. Bars, 2 μm.

We have also found two short stretches (14 and 23 amino acids) of sequence homology between the nonmotor domains of the KHCs and *bimC* (a kinesin-like gene from *Aspergillus* [Enos and Morris, 1990]) that were not noted in previous sequence comparisons. In the 14-amino acid stretch located at the COOH-terminal end of the human KHC rod domain, 10 amino acids are either identical or are similar to those found within a region of the nonmotor domain of *bimC*. In contrast, no sequence homologies were observed between the nonmotor domains of the KHCs and a variety of other kinesin-like motor proteins. Although the regions of sequence similarity between human KHC and *Aspergillus bimC* are relatively small, they nonetheless suggest that the nonmotor domains of these two proteins may have a similar property or function.

We have also identified an upstream ORF and a G-C rich

leader sequence in the 5′ untranslated region of hKHC that may be important for translational regulation. The upstream ORF (nt −226 to −203) contains three tandemly arranged potential start codons which are in the same reading frame; the nucleotides surrounding the first start codon form a perfect consensus sequence for ribosomal initiation of translation (Kozak, 1987). Upstream AUG codons are rare among eukaryotic mRNAs and are not found in the published 5′ untranslated regions of *Drosophila*, squid, and sea urchin kinesins. The ability of upstream ORFs to regulate mRNA translation has been most clearly shown for GCN4, a yeast gene involved in the control of amino acid biosynthesis (for review see Hinnebusch, 1990). In mammalian systems, AUG codons introduced into the 5′-untranslated region of mRNAs can significantly reduce expression of the downstream reading frame (Kozak, 1984; Liu et al., 1984). In addition to the upstream ORF, the human KHC 5′-untranslated region contains regions that are very G-C rich, a characteristic that at least in one case (the c-*sis*/PDGF 2 transcript) has been shown to inhibit translation (Rao et al., 1988). The presence of upstream AUGs and G-C rich regions in the 5′-untranslated region of kinesin mRNA may pose an obstacle to initiation by a ribosome scanning mechanism and could signify internal initiation of translation, as has been documented for mRNAs encoding BiP (Macejak and Sarnow, 1991) and polio virus proteins (Pelletier and Sonnenberg, 1988). Since invertebrate KHC cDNAs have neither upstream ORFs nor the G-C rich leader sequence, it is possible that vertebrates have acquired a means of regulating kinesin expression at the translational level.

### *Interaction of the Kinesin Motor and Tail Domains with Cytoplasmic Microtubules*

Although a good deal is known about the properties of kinesin's motor domain, the functions of the remainder of the molecule are poorly understood. Based upon the overall structure of kinesin (Amos, 1987; Hirokawa et al., 1989; Scholey et al., 1989), the tail is thought to function as an attachment domain, anchoring kinesin to macromolecular structures that are to be transported along microtubules. The fact that the tail domain shows the same degree of amino acid homology as the motor domain amongst kinesins from different species implies a conserved function, possibly that of binding to specific target proteins. One of its binding partners is the kinesin light chain, which has been localized by electron microscopy to the kinesin tail (Hirokawa et al., 1989). However, the tail domain of the KHC may likely interact with other proteins that are important for the biological activities of this motor protein.

In this study, we have found that the KHC and the KHC tail domains expressed in CV-1 cells colocalize with cytoplasmic microtubules but not with vimentin filaments. The distribution patterns of these expressed proteins and of microtubules change in similar ways when cells are treated with taxol or nocodazole, reinforcing the notion that these expressed proteins interact with microtubules and not some other cytoplasmic filamentous network. The expressed KHC proteins containing the tail domain also show a soluble distribution, suggesting possibly that these expressed proteins have a relatively weak affinity for microtubules in a cellular environment.

The expressed motor domain also associates with cytoplasmic microtubules, but only after detergent permeabilization in a nucleotide-free buffer. This treatment most likely produces a rigor-like association between kinesin and the cytoplasmic microtubules. The finding that the motor domain does not localize to microtubules in cells fixed in methanol–acetone or in cells permeabilized with Triton X-100 and MgATP indicates that the expressed motor domain exhibits normal ATP-sensitive microtubule binding. The localization of the tail domain with microtubules, on the other hand, does not seem to be influenced by ATP, suggesting that its interaction with microtubules is not nucleotide sensitive.

An important concern is whether the interaction of the kinesin tail domain with microtubules reflects a specific and biologically meaningful interaction. Microtubule colocalization of the expressed proteins was observed with or without Triton X-100 permeabilization and under two different fixation conditions, indicating that this localization pattern is not a fixation artefact. Furthermore, the expressed kinesin rod domain and the cytoplasmic enzyme β-galactosidase are both randomly distributed throughout the cytoplasm and do not colocalize with microtubules, suggesting at least some specificity of the interaction between the tail domain and microtubules.

The levels of kinesin expression from the vector pose another possible concern. Quantitative video analysis reveals that expression levels vary by more than 100-fold between different cells. Microtubule colocalization, however, is evident in cells expressing low as well as high levels of protein, indicating that it is not a consequence of very high overexpression. The lowest level of kinesin expression in the transfected cells, although fourfold greater than the endogenous kinesin levels, is also not necessarily beyond physiological concentrations. Hollenbeck (1989) has shown that kinesin levels in sympathetic neurons are eightfold greater than those in epidermal fibroblast cells and such levels are probably comparable to those found in some of the transfected cells. Although these levels may be physiological in neurons, one can not rule out the possibility that the different localization patterns of the endogenous and expressed kinesins in CV-1 cells is due to their different expression levels. For example, additional factors (e.g., light chains) could be needed for the proper localization of KHC and their levels may be insufficient to complex with the KHC or KHC tail domain produced by the expression vector. Different localization patterns could also occur if the endogenous and transfected KHCs are products of distinct genes.

Whether the expressed kinesin tail domain is binding to microtubules or indirectly to microtubule-associated proteins is not clear. Several studies with purified kinesin, however, suggest that kinesin's tail domain can bind directly to microtubules. After examining kinesin bound to microtubules with AMP-PNP by electron microscopy, Amos (1987), Hisanaga et al. (1989), and Andrews, B., P. Gallant, B. Schnapp, and T. Reese (personal communication) all suggested that the tail as well as the motor domain can bind to microtubules in vitro. The dark-field scanning transmission electron microscopy study by Andrews et al. clearly shows that single kinesins can crossbridge two microtubules through interactions at opposite ends of the molecule. The *Drosophila* kinesin tail domain produced by in vitro translation did not cosediment with microtubules under the conditions used in these experiments (Yang et al., 1989); however, the bacterially expressed COOH-terminal domain of the sea

urchin KHC recently was found to cosediment with microtubules in an ATP-independent manner (Skoufias, D., and J. Scholey, personal communication). Thus, our observations, taken together with the above in vitro experiments, suggest a microtubule-binding activity of the kinesin COOH-terminal tail domain.

The nonmotor domains of other kinesin-like molecules may also bind to microtubules. This has been demonstrated most convincingly for the $NH_2$-terminal (nonmotor) domain of KAR3, which when expressed as a $\beta$-galactosidase fusion protein in yeast colocalized with cytoplasmic microtubules (Meluh and Rose, 1990). Although the $NH_2$-terminal domain of KAR3 (aa 1–109) and the COOH-terminal domain of hKHC (890–963) share no sequence similarity, they both contain a large number of basic (His, Arg, Lys: 21% in KAR3 and 25% in hKHC) and proline (8% both in KAR3 and hKHC) residues and relatively few acidic (Asp, Glu: 5.5% both in KAR3 and hKHC) residues; these features are common in other microtubule-binding proteins (Lee et al., 1989; Lewis et al., 1988).

Since kinesin is thought to transport organelles, our expectation was that the expressed KHC or its tail domain would colocalize with cytoplasmic membranes. Several difficulties, however, make it difficult to assess whether any of the expressed KHC is associated with membranes in these experiments. First, a weak membrane association, similar to that of endogenous kinesin, would be difficult to detect amidst the more prominent levels of soluble and microtubule-associated kinesin protein in the transfected cells. Furthermore, an association with small membrane vesicles would be difficult to discern because of the presence of small punctate aggregates of expressed kinesin that arise possibly as an artefact of fixation or overexpression.

Although the results presented in this study do not resolve whether kinesin associates with membranes, the localization of the kinesin and its tail domain to microtubules raises the possibility that kinesin may participate in movements of the microtubule cytoskeleton. The ability of the kinesin COOH-terminal domain to bind to microtubules and the $NH_2$-terminal domain to bind to and generate movement along microtubules suggests that kinesin could crossbridge and induce sliding between microtubules. In accordance with this notion, purified kinesin causes microtubule–microtubule bending motions in solution (Vale et al., 1985) and has been shown to induce unipolar microtubule asters, presumably by inducing sliding between adjacent microtubules (Urrutia et al., 1991). Furthermore, the disorganization of microtubules in CV-1 cells expressing the intact KHC might somehow arise from microtubule movements generated by a functional motor.

Possible in vivo situations where microtubule sliding may occur include anaphase B type movements in the microtubule overlap zone (Cande and Hogan, 1989) and the sliding of microtubules in neuronal processes (Reinsch et al., 1991). Since kinesin is abundant in neurons, the latter phenomenon represents a particularly intriguing role for a kinesin motor. In their study, Reinsch et al. (1991) show that fluorescently tagged microtubules are transported towards the nerve terminal, the expected direction for slow anterograde transport of the cytoskeleton. Although the mechanism of this transport is unknown, axonal microtubules, whose plus ends are oriented towards the terminal, could be anterogradely transported along a subpopulation of stationary microtubules. Such transport could be mediated by a plus-end motor, such as kinesin, that is anchored onto microtubules via a tail domain and moves along stationary microtubules through a force-generating crossbridge cycle.

Whether or not kinesin participates in microtubule sliding in vivo, however, has not yet been established. We and others (Pfister et al., 1989; Neighbors et al., 1988) have not found an obvious colocalization of endogenous kinesin with cytoplasmic microtubules by immunofluorescence. Although Hollenbeck (1989) documented a colocalization of endogenous kinesin with cytoplasmic microtubules after saponin permeabilization, this pattern may represent an interaction with microtubule-associated membranes rather than with microtubules themselves. Thus, if kinesin crossbridges microtubules and induces microtubule sliding in cells, the immunolocalization data suggest that it must either be driven by a subset of the kinesin motors or must be regulated so as to occur only under certain circumstances. Thus, further work is required to establish whether the microtubule binding activity of the tail domain actually is manifested under physiological conditions.

We are indebted to Jon Kull for his assistance in the secondary structure predictions, Dr. G. Fungalli for assistance with quantitative analysis of the fluorescence images, and Dr. V. Sheffield for assistance with PCR. We also thank Drs. K. Kosik and L. Goldstein for sharing kinesin sequence information before publication; Drs. T. Kreis, R. Duden, and J. Kilmartin for antibodies; the National Cancer Institute for their gift of taxol; and P. Tinelli for photographic assistance. F. Navone is also grateful to Drs. A. Zanini and N. Borgese for encouragement and discussion.

This work was supported by a National Institutes of Health grant (GM38499) and fellowships from the Klingenstein and Rita Allen Foundations.

Received for publication 27 November 1991 and in revised form 13 March 1992.

### *References*

Amos, L. A. 1987. Kinesin from pig brain studied by electron microscopy. *J. Cell Sci.* 87:105–111.

Bloom, G. S., M. C. Wagner, K. K. Pfister, and S. T. Brady. 1988. Native structure and physical properties of bovine brain kinesin and identification of the ATP-binding subunit polypeptide. *Biochemistry.* 27:3409–3416.

Brady, S. T., K. K. Pfister, and G. S. Bloom. 1990. A monoclonal antibody against kinesin inhibits both anterograde and retrograde fast axonal transport in squid axoplasm. *Proc. Natl. Acad. Sci. USA.* 87:1061–1065.

Cande, W. Z., and C. J. Hogan. 1989. The mechanism of anaphase spindle elongation. *Bioessays.* 11:5–9.

DeBrabander, M., G. Geuens, R. Nuydens, R. Willebrords, and J. DeMey. 1981. Taxol induces the assembly of free microtubules in living cells and blocks the organizing capacity of centrosomes and kinetochores. *Proc. Natl. Acad. Sci. USA.* 78:5608–5611.

de Cuevas, M., T. Tao, and L. S. B. Goldstein. 1992. Evidence that the stalk of Drosophila kinesin heavy chain is an $\alpha$-helical coiled coil. *J. Cell Biol.* 116:957–965.

Endow, S. A. 1991. The emerging kinesin family of microtubule motor proteins. *Trends. Biochem. Sci.* 16:221–225.

Endow, S. A., S. Henikoff, and L. Soler-Niedziela. 1990. Mediation of meiotic and early mitotic chromosome segregation in Drosophila by a protein related to kinesin. *Nature (Lond.).* 345:81–83.

Enos, A. P., and N. R. Morris. 1990. Mutation of a gene that encodes a kinesin-like protein blocks nuclear division in *A. nidulans*. *Cell.* 60:1019–1027.

Ferreira, A., J. Niclas, R. D. Vale, G. Banker, and K. S. Kosik. 1992. Suppression of kinesin expression in cultured hippocampal neurons using antisense oligonucleotides. *J. Cell Biol.* In press.

Finer-Moore, J., and R. M. Stroud. 1984. Amphiphatic analysis and possible formation of the ion channel in an acetylcholine receptor. *Proc. Natl. Acad. Sci. USA.* 81:155–159.

Friederich, E., C. Huet, M. Arpin, and D. Louvard. 1989. Villin induces microvilli growth and actin redistribution in transfected fibroblasts. *Cell.* 59: 461–475.

Geuens, G., M. DeBrabander, R. Nuydens, and J. DeMey. 1983. The interac-

tion between microtubules and intermediate filaments in cultured cell treated with taxol and nocodazole. *Cell Biol. Int. Rep.* 7:35–47.

Goldstein, L. S. B. 1991. The kinesin superfamily: tails of redundancy. *Trends Cell Biol.* 1:93–98.

Gyoeva, F. K., and V. I. Gelfand. 1991. Coalignment of vimentin intermediate filaments with microtubules depends on kinesin. *Nature (Lond.).* 353:445–448.

Hagan, I., and M. Yanagida. 1990. Novel potential mitotic motor protein encoded by the fission yeast *cut7*+ gene. *Nature (Lond.).* 347:563–566.

Henikoff, S. 1987. Unidirectional digestion with exonuclease III in DNA sequence analysis. *Methods Enzymol.* 155:156–165.

Hinnebusch, A. G. 1990. Involvement of an initiation factor and protein phosphorylation in translational control of GCN4 mRNA. *Trends Biol. Sci.* 15:148–152.

Hirokawa, N., K. K. Pfister, H. Yorifuji, M. C. Wagner, S. T. Brady, and G. S. Bloom. 1989. Submolecular domains of bovine brain kinesin identified by electron microscopy and monoclonal antibody decoration. *Cell.* 56:867–878.

Hirokawa, N., R. Sato-Yoshitake, N. Kobayashi, K. K. Pfister, G. S. Bloom, and S. T. Brady. 1991. Kinesin associates with anterogradely transported membranous organelles. *J. Cell Biol.* 114:295–302.

Hisanaga, S., H. Murofushi, S. Okuhara, R. Sato, Y. Masuda, H. Sakai, and N. Hirokawa. 1989. The molecular structure of adrenal medulla kinesin. *Cell Motil. Cytoskeleton.* 16:264–272.

Hollenbeck, P. J. 1989. The distribution, abundance and subcellular localization of kinesin. *J. Cell Biol.* 108:2335–2342.

Hollenbeck, P. J., and J. A. Swanson. 1990. Radial extension of macrophage tubular lysosomes supported by kinesin. *Nature (Lond.).* 346:864–866.

Huylebroeck, D., G. Maertens, M. Verhoeyen, C. Lopez, A. Raeymakers, W. M. Jou, and W. Fiers. 1988. High-level transient expression of influenza virus proteins from a series of SV 40 late and early replacement vectors. *Gene (Amst.).* 66:163–181.

Hynes, R. O., and A. T. Destree. 1978. 10 nm filaments in normal and transformed cells. *Cell.* 13:151–163.

Kosik, K. S., L. D. Orecchio, B. Schnapp, H. Inouye, and R. L. Neve. 1990. The primary structure and analysis of the squid kinesin heavy chain. *J. Biol. Chem.* 265:3278–3283.

Kozak, M. 1984. Selection of initiation sites by eucaryotic ribosomes: effect of inserting AUG triplets upstream from the coding sequence for preproinsulin. *Nucleic Acids Res.* 12:3873–3893.

Kozak, M. 1987. An analysis of 5'-noncoding sequences from 699 vertebrate messenger RNAs. *Nucleic Acids Res.* 15:8125–8148.

Kreis, T. E. 1986. Microinjected antibodies against the cytoplasmic domain of vesicular stomatitis virus glycoprotein block its transport to the cell surface. *EMBO (Eur. Mol. Biol. Organ.) J.* 5:931–941.

Kreis, T. E. 1987. Microtubules containing detyrosinated tubulin are less dynamic. *EMBO (Eur. Mol. Biol. Organ.) J.* 6:2597–2606.

Kuznetsov, S. A., E. A. Vaisberg, N. A. Shanina, N. N. Magretova, V. Y. Chernyak, and V. I. Gelfand. 1988. The quarternary structure of bovine brain kinesin. *EMBO (Eur. Mol. Biol. Organ.) J.* 7:353–356.

Kuznetsov, S. A., Y. A. Vaisberg, S. W. Rothwell, D. B. Murphy, and V. I. Gelfand. 1989. Isolation of a 45-kDa fragment from the kinesin heavy chain with enhanced ATPase and microtubule-binding activity. *J. Biol. Chem.* 264:589–595.

Laemmli, U. 1970. Cleavage of structural proteins during assembly of the bacteriophage T4. *Nature (Lond.).* 227:680–685.

Lawrence, C. B., and D. A. Goldman. 1988. Definition and identification of homology domains. *Compot. Appl. Biosci.* 4:25–31.

Lee, G., R. L. Neve, and K. S. Kosik. 1989. The microtubule binding domain of tau. *Neuron.* 2:1615–1624.

Lewis, S. A., D. Wang, and N. J. Cowan. 1988. Microtubule-associated protein MAP2 shares a microtubule binding motif with tau protein. *Science (Wash. DC).* 242:936–939.

Liu, C.-C., C. C. Simonsen, and A. D. Levinson. 1984. Initiation of translation at internal AUG codons in mammalian cells. *Nature (Lond.).* 309:82–85.

Macejak, D. G., and P. Sarnow. 1991. Internal initiation of translation mediated by the 5' leader of a cellular mRNA. *Nature (Lond.).* 353:90–93.

Maniatis, T., E. F. Fritsch, and J. Sambrook. 1982. Molecular Cloning: A laboratory manual. Cold Spring Harbor Laboratory, Cold Spring Harbor, NY. 545 pp.

Maxam, A. M., and W. Gilbert. 1977. A new method for sequencing DNA. *Proc. Natl. Acad. Sci. USA.* 74:560–564.

McDonald, H. B., and L. S. B. Goldstein. 1990. Identification and characterization of a gene encoding a kinesin-like protein in Drosophila. *Cell.* 61:991–1000.

Meluh, P. M., and M. D. Rose. 1990. KAR3, a kinesin-related gene required for yeast nuclear fusion. *Cell.* 60:1029–1041.

Mullis, K., F. Faloona, S. Scharf, R. Saiki, G. Horn, and H. Erlich. 1986. Specific enzymatic amplification of DNA in vitro: the polymerase chain reaction. *Cold Spring Harbor Symp. Quant. Biol.* LI:263–273.

Neighbors, B. W., R. C. Williams, Jr., and J. R. McIntosh. 1988. Localization of kinesin in cultured cells. *J. Cell Biol.* 106:1193–1204.

Olmsted, J. B. 1981. Affinity purification of antibodies from diazotized paper blots of heterogenous protein samples. *J. Biol. Chem.* 256:11955–11957.

Otsuka, A. J., A. Jeyaprakash, J. Garcia-Anoveros, L. Z. Tang, G. Fisk, T. Hartshorne, R. Franco, and T. Born. 1991. The *C. elegans* unc-104 gene encodes a putative kinesin heavy chain-like protein. *Neuron.* 6:113–122.

Pelletier, J., and N. Sonnenberg. 1988. Internal initiation of translation of eukaryotic mRNA directed by a sequence derived from poliovirus RNA. *Nature (Lond.).* 334:320–325.

Pfister, K. K., M. C. Wagner, D. L. Stenoien, S. T. Brady, and G. S. Bloom. 1989. Monoclonal antibodies to kinesin heavy and light chains stain vesicle-like structures, but not microtubules, in cultured cells. *J. Cell Biol.* 108:1453–1464.

Rao, C. D., M. Pech, K. C. Robbins, and S. A. Aaronson. 1988. The 5' untranslated sequence of the c-sis platelet-derived growth factor 2 transcript is a potent translational inhibitor. *Mol. Cell. Biol.* 8:284–292.

Reinsch, S. S., T. J. Mitchison, and M. Kirschner. 1991. Microtubule polymer assembly and transport during axonal elongation. *J. Cell Biol.* 115:365–379.

Rodionov, V. L., F. K. Gyoeva, and V. I. Gelfand. 1991. Kinesin is responsible for centrifugal movement of pigment granules in melanophores. *Proc. Natl. Acad. Sci. USA.* 88:4956–4960.

Sanger, F., S. Nicklen, and A. Coulson. 1977. DNA sequencing with chain terminating inhibitors. *Proc. Natl. Acad. Sci. USA.* 74:5463–5467.

Saxton, W. M., J. Hicks, L. S. B. Goldstein, and E. C. Raff. 1991. Kinesin heavy chain is essential for viability and neuromuscular functions in Drosophila, but mutants show no defects in mitosis. *Cell.* 64:1093–1102.

Scholey, J. M., J. Heuser, J. T. Yang, and L. S. B. Goldstein. 1989. Identification of globular mechanochemical heads of kinesin. *Nature (Lond.).* 338:355–357.

Schulze, E., and M. Kirschner. 1987. Dynamic and stable populations of microtubules in cells. *J. Cell Biol.* 104:277–288.

Towbin, H., T. Staehelin, and J. Gordon. 1979. Electrophoretic transfer of proteins from polyacrylamide gels to nitrocellulose sheets: procedure and some applications. *Proc. Natl. Acad. Sci. USA.* 76:4350–4354.

Urrutia, R., M. A. McNiven, J. P. Albanesi, D. B. Murphy, and B. Kachar. 1991. Purified kinesin promotes vesicle motility and induces active sliding between microtubules *in vitro*. *Proc. Natl. Acad. Sci. USA.* 88:6701–6705.

Vale, R. D. 1987. Intracellular transport using microtubule-based motors. *Annu. Rev. Cell Biol.* 3:347–378.

Vale, R. D., and L. S. B. Goldstein. 1990. One motor, many tails: an expanding repertoire of force-generating enzymes. *Cell.* 60:883–885.

Vale, R. D., B. J. Schnapp, T. Mitchison, E. Steuer, T. S. Reese, and M. P. Sheetz. 1985. Different axoplasmic proteins generate movement in opposite directions along microtubules in vitro. *Cell.* 43:623–632.

Wright, B. D., J. H. Henson, K. P. Wedaman, P. J. Willy, J. N. Morand, and J. M. Scholey. 1991. Subcellular localization and sequence of sea urchin kinesin heavy chain: evidence for its association with membranes in the mitotic apparatus and interphase cytoplasm. *J. Cell Biol.* 113:817–833.

Yang, J. T., R. A. Laymon, and L. S. B. Goldstein. 1989. A three-domain structure of kinesin heavy chain revealed by DNA sequence and microtubule binding analyses. *Cell.* 56:879–889.

Yang, J. T., W. M. Saxton, R. J. Stewart, E. C. Raff, and L. S. Goldstein. 1990. Evidence that the head of kinesin is sufficient for force generation and motility in vitro. *Science (Wash. DC).* 249:42–47.

Zhang, P., B. A. Knowles, L. S. B. Goldstein, and R. S. Hawley. 1990. A kinesin-like protein required for distributive chromosome segregation in Drosophila. *Cell.* 62:1053–1062.

# APPENDIX 1

# Characterization of a Human Kinesin Heavy Chain Gene

The following appendix contains gene analysis data that was not included in the published work of Chapter 1. This includes the nucleotide sequence of the entire human kinesin heavy chain cDNA isolated from the placental library as well as characterization of its corresponding gene and expressed messenger RNAs by Southern blot and Northern blot analysis, respectively. In addition, figures depicting the cloning strategy have been included in order to complement the description of the cDNA isolation provided in Chapter 1, in the Results section entitled, "Isolation of an hKHC cDNA".

## RESULTS

### *Cloning and sequencing of human kinesin heavy chain cDNAs*

As described in Chapter 1, a library screening nucleotide probe was generated from MDCK cell (canine) first strand cDNA by the polymerase chain reaction (Mullis et al., 1986) using 128-fold degenerate 5' 20mer and 3' 18mer oligonucleotides (Figure 1). The degenerate oligonucleotides were designed based on a region (amino acids 807-813 and 824-829 of *Drosophila* kinesin heavy chain) in the tail domain that was found to be highly conserved between squid and *Drosophila* kinesin heavy chains. The resulting 69 nucleotide PCR fragment was used to screen a human placental λgt11 cDNA library (Figure 2). The clone HK-3 was obtained and the 5' EcoRI-NcoI fragment was used to rescreen the library giving rise to clone HK-21. A third screening using the 5' NcoI-ApaLI fragment from HK-21 lead to the isolation of HK-H8. HK-21 and HK-H8 were spliced together via a PstI site to create the hKHC cDNA containing a complete coding region. The complete nucleotide sequence of this cDNA is shown in Figure 3. The sequences corresponding to the two PCR primers are indicated as well the start codons and the stop codon of the small open reading frame located in the 5'-untranslated region of the mRNA (discussed in Chapter 1 in the Results section entitled "Sequence analysis and comparison".)

### *Southern Analysis of the hKHC gene*

Southern blot analysis was performed by hybridizing hKHC DNA corresponding to either the motor (nuc. -137 to 1094), rod (nuc. 1095 to 2398) or tail (nuc. 2399 to end of cDNA) domains to HeLa cell genomic DNA digested with 3 different restriction enzymes (Figure 4). With high stringency washes (see Materials and Methods), the motor domain probe hybridized to

one prominent band for each of the three digested DNA samples (not shown). Similarly, the tail domain probe hybridized to a single species of genomic DNA cut with either BamHI or SacI. These results suggest that a single KHC gene exists in the human genome. These results are supported by chromosome mapping studies in which the hKHC cDNA hybridized exclusively to a region on mouse chromosome 18 which is syntenic with human chromosome 18q (Justice et al., 1992). With lower stringency washes, the motor domain probe hybridized weakly to several bands (Figure 4), indicating that additional genes with sequences similar but not identical to the motor domain of hKHC are present in the genome. In contrast, the tail probe did not hybridize to additional bands under lower stringency conditions (Figure 4).

*The hKHC Gene Encodes Several RNA Transcripts*

Northern blot analysis of polyA$^+$ RNA from HeLa cells revealed that at least four mRNA species (6.2, 4.3, 3.9 and 1.7 kb) hybridized to the hKHC cDNA. The relative signal ratios of the four bands remained the same regardless of the stringency of hybridization (data not shown). Figure 5 shows that the motor, rod and tail domain probes all hybridized to the three larger transcripts, while only the motor domain probe hybridized to the 1.7 kb species. These bands have been observed in multiple RNA samples prepared by different methods, suggesting that they are not simply degradation products. The finding that the motor and tail probes hybridize with multiple RNA species (Figure 5) but one genomic DNA fragment (Figure 4) under similar hybridization conditions suggests that a single gene gives rise to multiple mRNA transcripts.

## DISCUSSION

### *The Human Kinesin Heavy Chain Gene*

Kinesin heavy chain appears to be encoded by a single copy gene in mammals, based upon high stringency Southerns. However, when the stringency is reduced, the KHC motor domain hybridizes to a variety of bands, suggesting the presence of a superfamily of kinesin-related motors in mammals as has been described in *Drosophila* and *S. cerevisiae* (Endow, 1991). Like the motor domain, the kinesin C-terminal tail, which is thought to attach kinesin to organelles or other intracellular components, shows a striking degree of amino acid identity amongst KHCs from different species. Although it is possible that the C-terminal domain belongs to a family of proteins that share similar attachment properties, the KHC tail probe did not hybridize to additional bands under low stringency conditions. This finding suggests that the tail domain may be unique or at least does not seem to be highly conserved throughout its length amongst a family of proteins.

### *Kinesin Expression in Mammalian Cells*

In contrast to invertebrates which express only a single KHC transcript (Wright et al., 1991; Yang et al., 1988), rats and humans have at least four mRNA species that are derived from a single copy gene. Three of these transcripts (6.2, 4.3, 3.9 kb) are large enough to encode the entire KHC protein (2.9 kb of coding sequence). The fourth is a minor 1.7 kb message that hybridizes to sequences derived exclusively from the motor domain. Interestingly, the *dilute* gene from mouse (which encodes a putative myosin motor) also has several transcripts, including a small one that corresponds to the motor region of the protein (Mercer et al., 1991). At present, it is not clear how the hKHC transcripts differ from one another. It is possible that the

larger mRNAs might have additional coding sequence, although we have not encountered any sequence heterogeneity among the cDNAs isolated. Alternatively, the 6.2 kb and 4.3 kb messages may simply have larger 5' or 3' untranslated regions.

The physiological significance of the multiple hKHC transcripts is not known. All hKHC transcripts were expressed in the same ratio in a variety of tissues, with the possible exception of the 3.9 kb transcript in heart. The four species of hKHC mRNA are found in both rat and human cells, however, suggesting that this pattern of expression has been conserved in recent evolution.

The human kinesin heavy chain gene represents a valuable tool for helping to understand the function of kinesin in mammalian cells. The kinesin cDNA can be used in transfection experiments to study kinesin localization (see Chapter 1), and anti-sense oligonucleotides directed against the KHC mRNA can be used to block kinesin expression (see Appendix 2). Both approaches have provided interesting results about the role that kinesin may be playing in the cell.

## MATERIALS AND METHODS

*Cloning and sequencing methods*

See Materials and Methods in Chapter 1.

*Motor, rod and tail-specific probes*

Motor, rod and tail domain probes were made by the following restriction enzyme digestions of the human kinesin heavy chain cDNA: motor domain probe- XmaI-SacI fragment (nuc. -137 to 1094); rod domain probe- SacI-FspI fragment (nuc. 1095 to 2398); tail domain probe- FspI-EcoRI fragment (nuc. 2399 to end of cDNA). DNA probes were labeled with {$\alpha$-$^{32}$P}-dCTP (~3000 Ci/mmol) (ICN Biomedicals) to a specific activity of >$10^9$ cpm/$\mu$g using the random primer technique (24), purified using a Nuctrap probe purification column (Stratagene, Inc.), denatured and then used for hybridization.

*Southern blot analysis*

Genomic DNA (generous gift from Bruce Cree, UCSF) isolated from HeLa cells was digested with either BamHI, EcoRI or SacI. Samples (10 $\mu$g per lane) were loaded onto a 0.7% agarose gel and run overnight at 30 V. HindIII-cut $\lambda$ DNA fragments (Bethesda Research Laboratory) served as molecular size standards. The gel was then treated with 0.25 M HCl for 20 min, 0.5 M NaOH/1.5 M NaCl for 30 min, 0.5 M Tris-HCl pH 7.5/1.5 M NaCl for 30 min and then blotted overnight onto a Hybond N nylon membrane (Amersham) with 10X SSC. After transfer, the blot was UV crosslinked (0.12 Joules/cm$^2$) using a Stratalinker (Stratagene) and then prehybridized (55$^o$C) in 3X SSCP (60 mM $NaPO_4$ pH 6.8, 45 mM Na citrate, 0.36 M NaCl), 10X Denhardt's solution (0.2% (w/v) Ficoll 400, 0.2% (w/v) polyvinylpyrrolidone, 0.2% bovine serum

albumin), 0.5% SDS and 250 μg/ml denatured salmon sperm DNA. Hybridization was performed in the same buffer as prehybridization but with 10% dextran sulfate (Pharmacia) and the radioactive probe at a concentration of 5 x $10^6$ cpm/ml. Southern blots were hybridized overnight at 55°C, washed at either low stringency (55°C, 2X SSC (0.3 M NaCl, 30 mM sodium citrate, pH 7)/0.1% SDS) or high stringency (65°C, 0.2X SSC/0.1% SDS) and then exposed to Kodak XAR-5 film with intensifying screens at -80°C.

*RNA isolation and Northern blot analysis*

RNA was extracted from monolayers of HeLa cells with guanidine isothiocyanate followed by purification using ultracentrifugation through a cesium chloride cushion (Sambrook et al., 1989). The poly(A)$^+$ mRNA fraction was selected using oligo(dT)-cellulose chromatography (InVitrogen, Inc.). RNA concentration and purity were quantitated spectrophotometrically. HeLa cell poly(A)$^+$ mRNA samples (3 μg per lane) were electrophoresed on 1% agarose, 2.2 M formaldehyde gels. RNA size standards were obtained from Bethesda Research Laboratory. Ethidium bromide staining was used to confirm that RNA samples were not degraded and that the expected amount of RNA was loaded. After electrophoresis, gels were treated with 50 mM NaOH for 25 min, 1 M Tris-HCl pH 7.5 for 30 min, 20X SSC for 15 min and then transferred to Hybond N nylon membranes (Amersham) with 20X SSC. After transfer, blots were UV-crosslinked (0.15 J/$cm^2$) by a Stratalinker (Stratagene, Inc.) and prehybridized and hybridized in the same buffers described for the Southern blots. Hybridizations were performed overnight at either 55°C, 65°C or 70°C in the presence of 5 x $10^6$ cpm/ml of radiolabelled probe and then washed at the same temperature in 0.2X SSC/0.1% SDS. Autoradiography was the same as for Southern blots.

**Figure 1.** Generation of human kinesin heavy chain probe.

The 18mer and 20mer are degenerate oligonucleotides that were used to generate a 69 nucleotide PCR fragment for the purpose of library screening. The amplified region is shown in relationship to the amino acid sequences of the *Drosophila* and squid kinesin heavy chain proteins.

**20mer:** 5'- GA A GA A A CC GT C GC A A A A GA -3'
G G G G G
C C
T T

**18mer:** 5'- T T GC A GG T C T T GG A C GA A -3'
C AA A A
T
C

**Drosophila kinesin protein:**

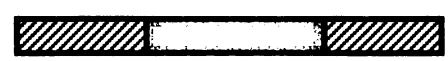



**Squid kinesin:** RREQAKQDLKGLEETVAKELQTLHNLRKLFVQDLQ

**Drosophila kinesin:** RREQARKDLKGLEDTVAKELQTLHNLRKLFVQDLQ

**20mer** **18mer**

**Corresponding amplified nucleotide sequence with primer sequences at ends:**



**20** **31** **18**

**Figure 2.** Schematic representation of human kinesin heavy chain cDNAs. The strategy used to obtain a cDNA containing the entire protein coding sequence is shown. Empty boxes represent coding regions. Stippled boxes indicate the 5' and 3' untranslated regions. The solid box represents the region amplified in the PCR experiments. Hatched boxes correspond to fragments used as probes in secondary and tertiary library screenings. The motor, rod and tail probes utilized in the Southern and Northern analysis (see figures 4 and 5) are indicated along the hKHC cDNA. Restriction enzyme sites of interest are indicated as well.

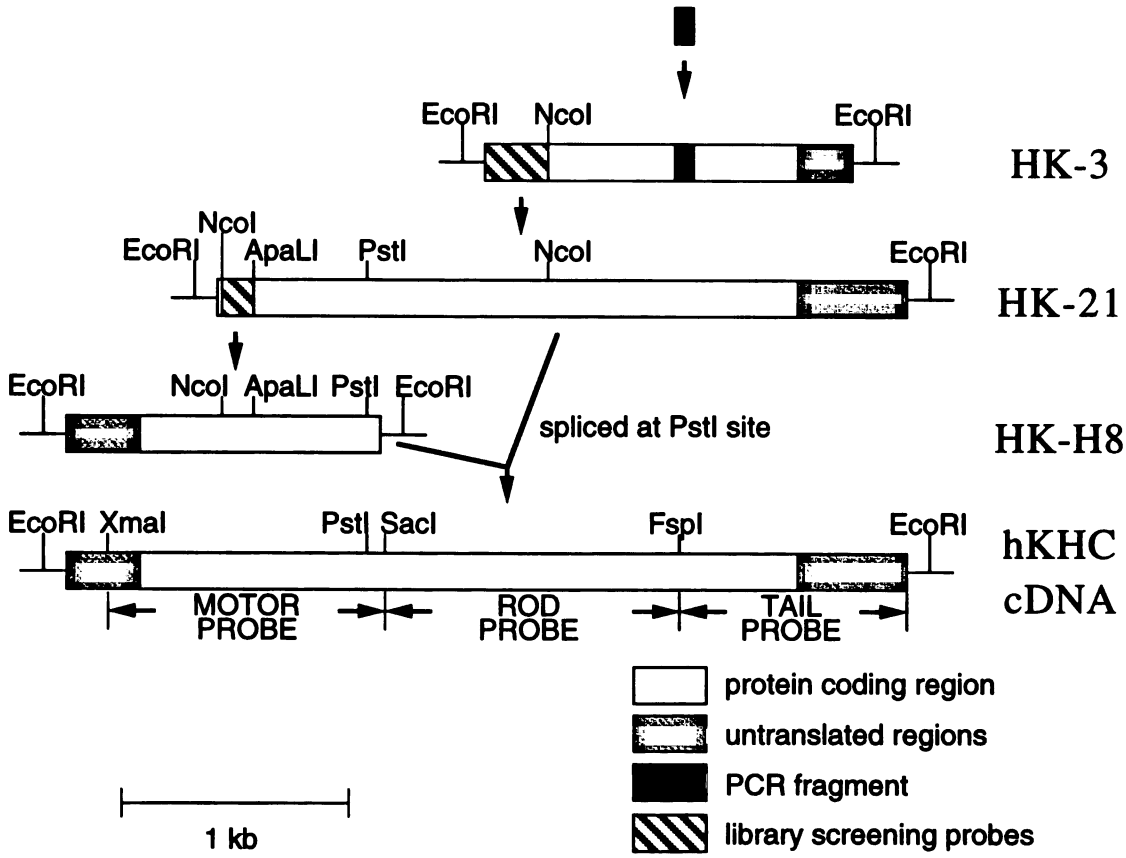

EcoRI
NcoI
EcoRI
HK-3
NcoI
EcoRI
ApaLI
PstI
NcoI
EcoRI
HK-21
EcoRI
NcoI
ApaLI
PstI
EcoRI
spliced at PstI site
HK-H8
EcoRI
XmaI
PstI
SacI
FspI
EcoRI
hKHC
cDNA
MOTOR
PROBE
ROD
PROBE
TAIL
PROBE
protein coding region
untranslated regions
PCR fragment
library screening probes
1 kb

**Figure 3.** Nucleotide and deduced amino acid sequence of the human kinesin heavy chain cDNA.

Nucleotides and amino acids are numbered in the left margin. The one letter amino acid code is used. The upstream in-frame start codons in the 5' untranslated region are underlined and the two in-frame stop codons are underlined and italicized. The arrows indicate the regions that correspond to the PCR oligonucleotides (20mer, nuc. 2356-2375; 18mer, nuc. 2407-2424).

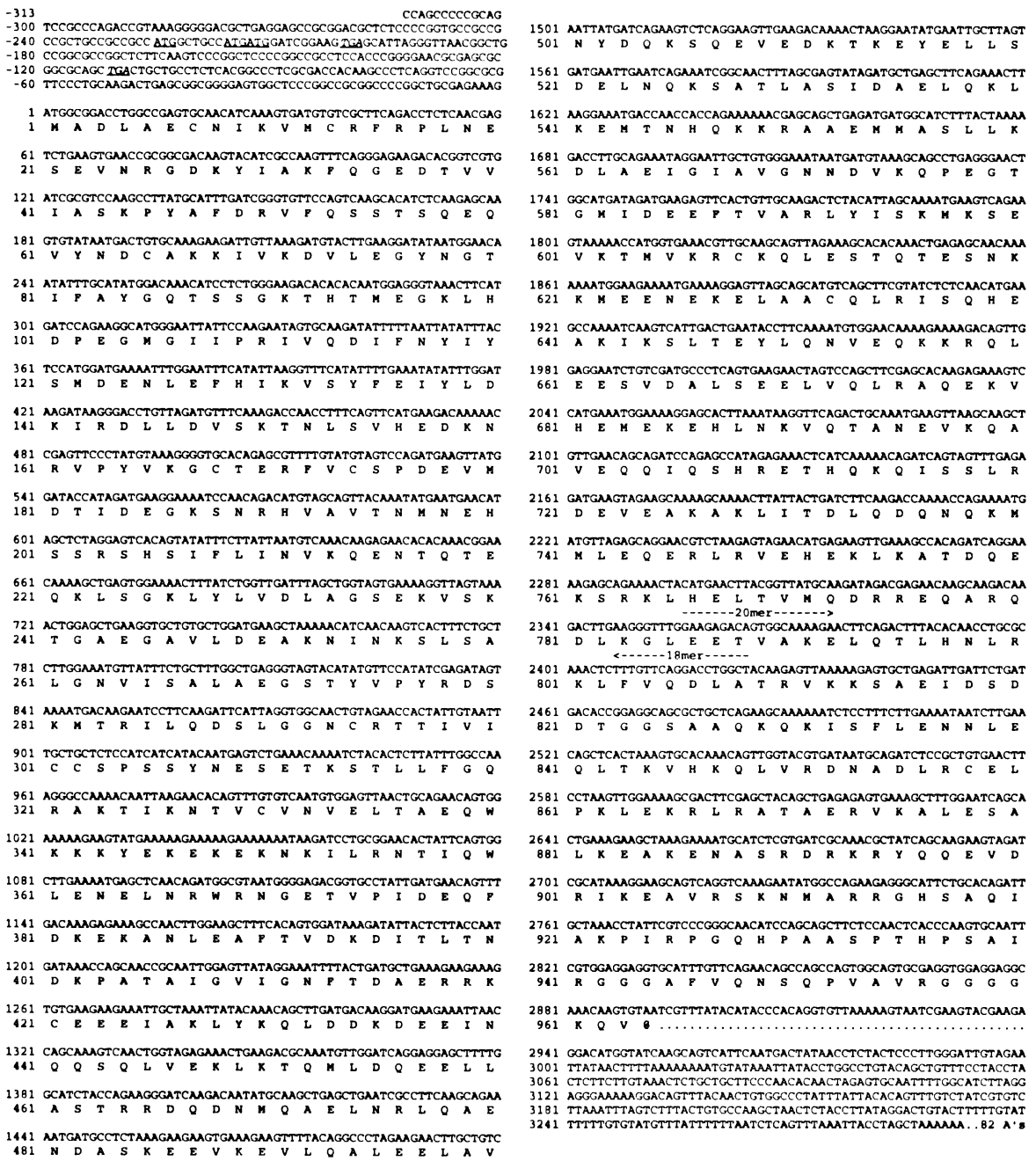

-313 CCAGCCCCCGCAG
-300 TCCGCCCAGACCGTAAAGGGGGACGCTGAGGAGCCGCGGACGCTCTCCCCGGTGCCGCCG
-240 CCGCTGCCGCCGCC ATGGCTGCC ATGATGGATCGGAAG TGAGCATTAGGGTTAACGGCTG
-180 CCGGCGCCGGCTCTTCAAGTCCCGGCTCCCCGGCCGCCTCCACCCGGGGAACGCGAGCGC
-120 GGCGCAGC TGACTGCTGCCTCTCACGGCCCTCGCGACCACAAGCCCTCAGGTCCGGCGCG
-60 TTCCCTGCAAGACTGAGCGGCGGGGAGTGGCTCCCGGCCGCGGCCCCGGCTGCGAGAAAG
1 ATGGCGGACCTGGCCGAGTGCAACATCAAAGTGATGTGTCGCTTCAGACCTCTCAACGAG
1 M A D L A E C N I K V M C R F R P L N E
61 TCTGAAGTGAACCGCGGCGACAAGTACATCGCCAAGTTTCAGGGAGAAGACACGGTCGTG
21 S E V N R G D K Y I A K F Q G E D T V V
121 ATCGCGTCCAAGCCTTATGCATTTGATCGGGTGTTCCAGTCAAGCACATCTCAAGAGCAA
41 I A S K P Y A F D R V F Q S S T S Q E Q
181 GTGTATAATGACTGTGCAAAGAAGATTGTTAAAGATGTACTTGAAGGATATAATGGAACA
61 V Y N D C A K K I V K D V L E G Y N G T
241 ATATTTGCATATGGACAAACATCCTCTGGGAAGACACACACAATGGAGGGTAAACTTCAT
81 I F A Y G Q T S S G K T H T M E G K L H
301 GATCCAGAAGGCATGGGAATTATTCCAAGAATAGTGCAAGATATTTTTAATTATATTTAC
101 D P E G M G I I P R I V Q D I F N Y I Y
361 TCCATGGATGAAAAATTTGGAATTTCATATTAAGGTTTCATATTTTGAAATATATTTGGAT
121 S M D E N L E F H I K V S Y F E I Y L D
421 AAGATAAGGGACCTGTTAGATGTTTCAAAGACCAACCTTTCAGTTCATGAAGACAAAAAC
141 K I R D L L D V S K T N L S V H E D K N
481 CGAGTTCCCTATGTAAAGGGGTGCACAGAGCGTTTTGTATGTAGTCCAGATGAAGTTATG
161 R V P Y V K G C T E R F V C S P D E V M
541 GATACCATAGATGAAGGAAAATCCAACAGACATGTAGCAGTTACAAATATGAATGAACAT
181 D T I D E G K S N R H V A V T N M N E H
601 AGCTCTAGGAGTCACAGTATATTTCTTATTAATGTCAAACAAGAGAACACACAAACGGAA
201 S S R S H S I F L I N V K Q E N T Q T E
661 CAAAAGCTGAGTGGAAAACTTTATCTGGTTGATTTAGCTGGTAGTGAAAAGGTTAGTAAA
221 Q K L S G K L Y L V D L A G S E K V S K
721 ACTGGAGCTGAAGGTGCTGTGCTGGATGAAGCTAAAAACATCAACAAGTCACTTTCTGCT
241 T G A E G A V L D E A K N I N K S L S A
781 CTTGGAAATGTTATTTCTGCTTTGGCTGAGGGTAGTACATATGTTCCATATCGAGATAGT
261 L G N V I S A L A E G S T Y V P Y R D S
841 AAAATGACAAGAATCCTTCAAGATTCATTAGGTGGCAACTGTAGAACCACTATTGTAATT
281 K M T R I L Q D S L G G N C R T T I V I
901 TGCTGCTCTCCATCATCATACAATGAGTCTGAAACAAAATCTACACTCTTATTTGGCCAA
301 C C S P S S Y N E S E T K S T L L F G Q
961 AGGGCCAAAACAATTAAGAACACAGTTTGTGTCAATGTGGAGTTAACTGCAGAACAGTGG
321 R A K T I K N T V C V N V E L T A E Q W
1021 AAAAAGAAGTATGAAAAAGAAAAAGAAAAAAATAAGATCCTGCGGAACACTATTCAGTGG
341 K K K Y E K E K E K N K I L R N T I Q W
1081 CTTGAAAATGAGCTCAACAGATGGCGTAATGGGGAGACGGTGCCTATTGATGAACAGTTT
361 L E N E L N R W R N G E T V P I D E Q F
1141 GACAAAGAGAAAGCCAACTTGGAAGCTTTCACAGTGGATAAAGATATTACTCTTACCAAT
381 D K E K A N L E A F T V D K D I T L T N
1201 GATAAACCAGCAACCGCAATTGGAGTTATAGGAAATTTTACTGATGCTGAAAGAAGAAAG
401 D K P A T A I G V I G N F T D A E R R K
1261 TGTGAAGAAGAAATTGCTAAATTATACAAACAGCTTGATGACAAGGATGAAGAAATTAAC
421 C E E E I A K L Y K Q L D D K D E E I N
1321 CAGCAAAGTCAACTGGTAGAGAAACTGAAGACGCAAATGTTGGATCAGGAGGAGCTTTTG
441 Q Q S Q L V E K L K T Q M L D Q E E L L
1381 GCATCTACCAGAAGGGATCAAGACAATATGCAAGCTGAGCTGAATCGCCTTCAAGCAGAA
461 A S T R R D Q D N M Q A E L N R L Q A E
1441 AATGATGCCTCTAAAGAAGAAGTGAAAGAAGTTTTACAGGCCCTAGAAGAACTTGCTGTC
481 N D A S K E E V K E V L Q A L E E L A V
1501 AATTATGATCAGAAGTCTCAGGAAGTTGAAGACAAAACTAAGGAATATGAATTGCTTAGT
501 N Y D Q K S Q E V E D K T K E Y E L L S
1561 GATGAATTGAATCAGAAATCGGCAACTTTAGCGAGTATAGATGCTGAGCTTCAGAAACTT
521 D E L N Q K S A T L A S I D A E L Q K L
1621 AAGGAAATGACCAACCACCAGAAAAAACGAGCAGCTGAGATGATGGCATCTTTACTAAAA
541 K E M T N H Q K K R A A E M M A S L L K
1681 GACCTTGCAGAAATAGGAATTGCTGTGGGAAATAATGATGTAAAGCAGCCTGAGGGAACT
561 D L A E I G I A V G N N D V K Q P E G T
1741 GGCATGATAGATGAAGAGTTCACTGTTGCAAGACTCTACATTAGCAAAATGAAGTCAGAA
581 G M I D E E F T V A R L Y I S K M K S E
1801 GTAAAAACCATGGTGAAACGTTGCAAGCAGTTAGAAAGCACACAAACTGAGAGCAACAAA
601 V K T M V K R C K Q L E S T Q T E S N K
1861 AAAATGGAAGAAAATGAAAAGGAGTTAGCAGCATGTCAGCTTCGTATCTCTCAACATGAA
621 K M E E N E K E L A A C Q L R I S Q H E
1921 GCCAAAATCAAGTCATTGACTGAATACCTTCAAAATGTGGAACAAAAGAAAAGACAGTTG
641 A K I K S L T E Y L Q N V E Q K K R Q L
1981 GAGGAATCTGTCGATGCCCTCAGTGAAGAACTAGTCCAGCTTCGAGCACAAGAGAAAGTC
661 E E S V D A L S E E L V Q L R A Q E K V
2041 CATGAAATGGAAAAGGAGCACTTAAATAAGGTTCAGACTGCAAATGAAGTTAAGCAAGCT
681 H E M E K E H L N K V Q T A N E V K Q A
2101 GTTGAACAGCAGATCCAGAGCCATAGAGAAACTCATCAAAAACAGATCAGTAGTTTGAGA
701 V E Q Q I Q S H R E T H Q K Q I S S L R
2161 GATGAAGTAGAAGCAAAAGCAAAACTTATTACTGATCTTCAAGACCAAAACCAGAAAATG
721 D E V E A K A K L I T D L Q D Q N Q K M
2221 ATGTTAGAGCAGGAACGTCTAAGAGTAGAACATGAGAAGTTGAAAGCCACAGATCAGGAA
741 M L E Q E R L R V E H E K L K A T D Q E
2281 AAGAGCAGAAAACTACATGAACTTACGGTTATGCAAGATAGACGAGAACAAGCAAGACAA
761 K S R K L H E L T V M Q D R R E Q A R Q
-------20mer-------->
2341 GACTTGAAGGGTTTGGAAGAGACAGTGGCAAAAGAACTTCAGACTTTACACAACCTGCGC
781 D L K G L E E T V A K E L Q T L H N L R
<------18mer------
2401 AAACTCTTTGTTCAGGACCTGGCTACAAGAGTTAAAAAGAGTGCTGAGATTGATTCTGAT
801 K L F V Q D L A T R V K K S A E I D S D
2461 GACACCGGAGGCAGCGCTGCTCAGAAGCAAAAAATCTCCTTTCTTGAAAATAATCTTGAA
821 D T G G S A A Q K Q K I S F L E N N L E
2521 CAGCTCACTAAAGTGCACAAACAGTTGGTACGTGATAATGCAGATCTCCGCTGTGAACTT
841 Q L T K V H K Q L V R D N A D L R C E L
2581 CCTAAGTTGGAAAAGCGACTTCGAGCTACAGCTGAGAGAGTGAAAGCTTTGGAATCAGCA
861 P K L E K R L R A T A E R V K A L E S A
2641 CTGAAAGAAGCTAAAGAAAATGCATCTCGTGATCGCAAACGCTATCAGCAAGAAGTAGAT
881 L K E A K E N A S R D R K R Y Q Q E V D
2701 CGCATAAAGGAAGCAGTCAGGTCAAAGAATATGGCCAGAAGAGGGCATTCTGCACAGATT
901 R I K E A V R S K N M A R R G H S A Q I
2761 GCTAAACCTATTCGTCCCGGGCAACATCCAGCAGCTTCTCCAACTCACCCAAGTGCAATT
921 A K P I R P G Q H P A A S P T H P S A I
2821 CGTGGAGGAGGTGCATTTGTTCAGAACAGCCAGCCAGTGGCAGTGCGAGGTGGAGGAGGC
941 R G G G A F V Q N S Q P V A V R G G G G
2881 AAACAAGTGTAATCGTTTATACATACCCACAGGTGTTAAAAAGTAATCGAAGTACGAAGA
961 K Q V @ .....
2941 GGACATGGTATCAAGCAGTCATTCAATGACTATAACCTCTACTCCCTTGGGATTGTAGAA
3001 TTATAACTTTTAAAAAAAAATGTATAAATTATACCTGGCCTGTACAGCTGTTTCCTACCTA
3061 CTCTTCTTGTAAACTCTGCTGCTTCCCAACACAACTAGAGTGCAATTTTGGCATCTTAGG
3121 AGGGAAAAAGGACAGTTTACAACTGTGGCCCTATTTATTACACAGTTTGTCTATCGTGTC
3181 TTAAATTTAGTCTTTACTGTGCCAAGCTAACTCTACCTTATAGGACTGTACTTTTTGTAT
3241 TTTTTGTGTATGTTTATTTTTTAATCTCAGTTTAAATTACCTAGCTAAAAAA..82 A's

**Figure 4.** Southern blots of human DNA probed with hKHC domain-specific probes.

Blots of HeLa genomic DNA (10 μg per lane) cut with BamHI, EcoRI or SacI were hybridized with either the motor, rod or tail probes (See Figure 2 and Materials and Methods). The molecular size standards (HindIII-cut λ DNA) are indicated on the left side.

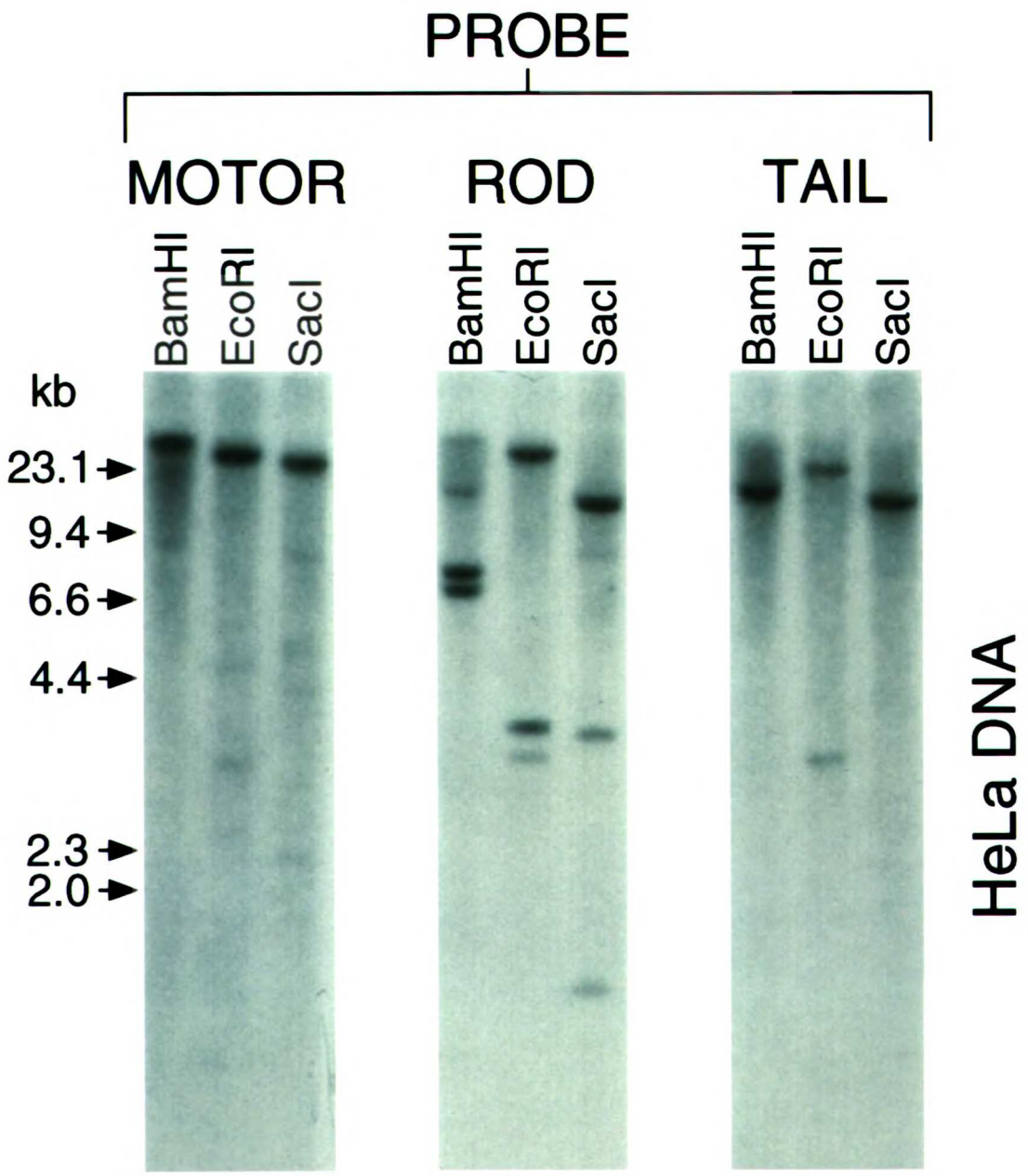
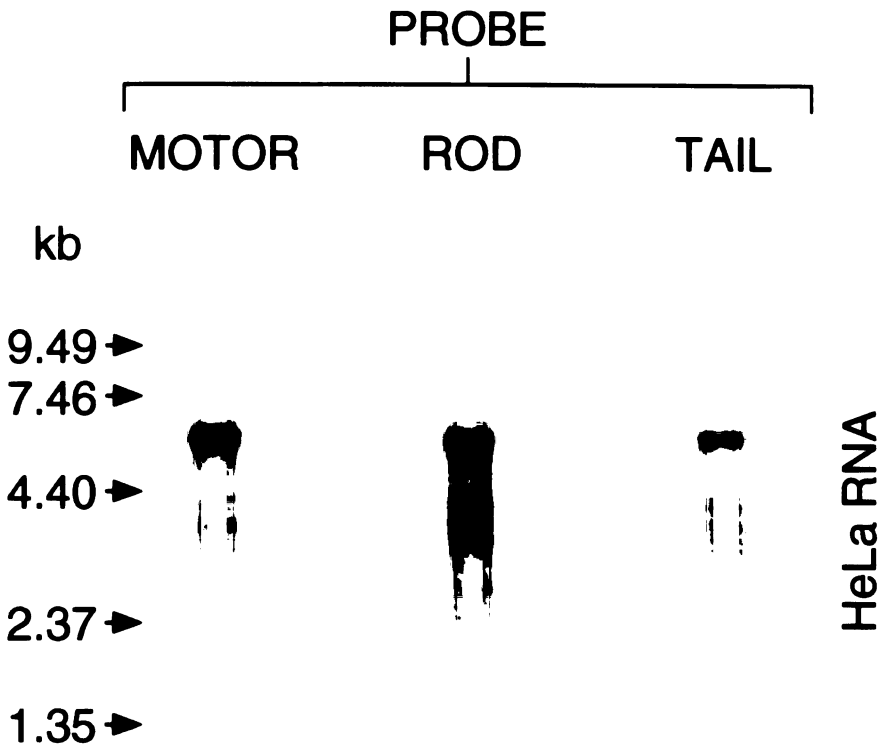

PROBE
MOTOR
ROD
TAIL
BamHI
EcoRI
SacI
BamHI
EcoRI
SacI
BamHI
EcoRI
SacI
kb
23.1
9.4
6.6
4.4
2.3
2.0
HeLa DNA

**Figure 5.** Northern blots of human RNA probed with hKHC domain-specific probes.

Blots of HeLa poly(A)$^+$ RNA (3 μg per lane) were probed with either the motor, rod or tail probes at a variety of temperatures (55°C, 65°C and 70°C). Since the hybridization patterns were indistinguishable at 55°C and 65°C and undetectable at 70°C, only the 55°C blots are shown. The molecular size standards (0.24-9.5 kb RNA ladder) are indicated on the left side.


PROBE
MOTOR
ROD
TAIL
kb
9.49
7.46
4.40
2.37
1.35
HeLa RNA

# APPENDIX 2

# Suppression of Kinesin Expression in Cultured Hippocampal Neurons Using Antisense Oligonucleotides

Appendix 2 presents the results of a collaborative project in which the function of kinesin in rat hippocampal neurons was examined by suppressing its expression using anti-sense oligonucleotides. In order to design appropriate anti-sense oligonucleotides, I first amplified the region around the start codon of the rat homolog of the human kinesin gene by PCR. Using the sequence obtained from this PCR fragment, I designed two different oligonucleotides that Adriana Ferreira used to successfully suppress kinesin expression in rat hippocampal neurons. Treatment of these cells with the oligonucleotides also lead to a profound inhibition of neurite outgrowth as well as the anterograde transport of GAP-43 and synapsin I containing vesicles. This appendix has been reproduced from The Journal of Cell Biology, 1992, vol. 117, pp. 595-606, by copyright permission of The Rockefeller University Press.

# Suppression of Kinesin Expression in Cultured Hippocampal Neurons Using Antisense Oligonucleotides

**Adriana Ferreira,* Joshua Niclas,‡ Ronald D. Vale,‡ Gary Banker,* and Kenneth S. Kosik§**

*Department of Neuroscience, University of Virginia School of Medicine, Charlottesville, Virginia 22908; ‡Departments of Pharmacology and Biochemistry, University of California, San Francisco, California; and §Department of Neurology (Neuroscience), Harvard Medical School and Center for Neurologic Diseases, Department of Medicine (Division of Neurology), Brigham and Women's Hospital, Boston, Massachusetts 02115

***Abstract.*** Kinesin, a microtubule-based force-generating molecule, is thought to translocate organelles along microtubules. To examine the function of kinesin in neurons, we sought to suppress kinesin heavy chain (KHC) expression in cultured hippocampal neurons using antisense oligonucleotides and study the phenotype of these KHC "null" cells. Two different antisense oligonucleotides complementary to the KHC sequence reduced the protein levels of the heavy chain by greater than 95% within 24 h after application and produced identical phenotypes. After inhibition of KHC expression for 24 or 48 h, neurons extended an array of neurites often with one neurite longer than the others; however, the length of all these neurites was significantly reduced. Inhibition of KHC expression also altered the distribution of GAP-43 and synapsin I, two proteins thought to be transported in association with membranous organelles. These proteins, which are normally localized at the tips of growing neurites, were confined to the cell body in antisense-treated cells. Treatment of the cells with the corresponding sense oligonucleotides affected neither the distribution of GAP-43 and synapsin I, nor the length of neurites. A full recovery of neurite length occurred after removal of the antisense oligonucleotides from the medium. These data indicate that KHC plays a role in the anterograde translocation of vesicles containing GAP-43 and synapsin I. A deficiency in vesicle delivery may also explain the inhibition of neurite outgrowth. Despite the inhibition of KHC and the failure of GAP-43 and synapsin I to move out of the cell body, hippocampal neurons can extend processes and acquire an asymmetric morphology.

KINESIN, a microtubule-based motor protein, is a heterotetramer consisting of two 110–130 kD heavy chains and two 60–70 kD light chains (Bloom et al., 1988; Kuznetsov et al., 1988). The primary structure of the heavy chain is conserved in four widely divergent species: *Drosophila* (Yang et al., 1989), squid (Kosik et al., 1990), sea urchin (Wright et al., 1991), and human (Navone et al., in press). Purified kinesin generates ATP-dependent microtubule gliding after being adsorbed onto glass coverslips (Vale et al., 1985*a*; Scholey et al., 1985; Porter et al., 1987) or induces the transport of latex beads along microtubules after adsorption onto the bead surface (Vale et al., 1985*a*). In experiments with purified bovine chromaffin granules, the addition of kinesin and ATP was sufficient to induce translocation of the granules along microtubules (Urrutia et al., 1991). Kinesin-coated objects move unidirectionally towards the plus end of microtubules (Vale et al., 1985*b*; Porter et al., 1987). This direction corresponds to anterograde transport in neurons, since axonal microtubules have their plus ends oriented distally (Filliatreau and DiGiamberdino, 1981; Heidemann et al., 1981; Baas et al., 1988).

Several experiments also support the idea that kinesin transports organelles in vivo. Microinjection of antibodies to kinesin heavy chain (KHC)[1] inhibit tubular lysosome extension in macrophages (Hollenbeck and Swanson, 1990), pigment granule dispersion in melanophores (Rodionov et al., 1991) and organelle transport in extruded axoplasm (Brady et al., 1990). An association of kinesin with membrane-bound organelles was suggested by the immunofluorescence localization of KHC to punctate and tubular Triton X-100 soluble structures (Pfister et al., 1989; Hollenbeck, 1989; Brady et al., 1990; Wright et al., 1991; Houliston and Elinson, 1991). Higher resolution analysis by immunogold EM has shown that KHC is associated with membrane-bounded organelles (Hirokawa et al., 1991). Furthermore, after ligation of a peripheral nerve, organelles that react with KHC antibodies collect on the proximal side of the ligature, implying that kinesin is associated with anterogradely moving organelles (Hirokawa et al., 1991).

Some clues concerning the in vivo functions of kinesin

A. Ferreira's present address is Brigham and Women's Hospital, 221 Longwood Ave., Boston, MA 02115.

1. *Abbreviations used in this paper*: KHC, kinesin heavy chain.

were obtained by examining the phenotype of KHC mutants. A *Drosophila* containing temperature-sensitive KHC mutant had impaired muscle activity and tactile sensitivity, most pronounced in the posterior region (Saxton et al., 1991). Mutations of the *unc*-104 locus in *C. elegans*, which encodes a kinesin-like molecule (Otsuka et al., 1991), also cause deficits in neuromuscular transmission, which appear to be secondary to a deficit in anterograde transport. These mutants exhibit a severe depletion of synaptic vesicles in presynaptic terminals and a corresponding accumulation of vesicles in nerve cell bodies (Hall and Hedgecock, 1991). Despite this defect, neurites are able to grow out and establish appropriate synaptic connections.

In this study, we examined the cellular functions of kinesin in mammalian neurons. To approach this problem, we created a pseudo-genetic null mutation of KHC in cultured rat hippocampal neurons by administering antisense oligonucleotides to suppress KHC expression. Cells treated with the KHC antisense oligonucleotides extended neurites which elongated and expressed polarity, but the neurites were significantly shorter than in untreated cells. In addition, neurons treated with KHC antisense oligonucleotides did not transport GAP-43 or synapsin I to the neurite tip, suggesting that kinesin is required for the normal anterograde transport of these molecules.

## Materials and Methods

### Cultures

Neuronal cultures were prepared from the hippocampi of embryonic day 18 rats as previously described (Bartlett and Banker, 1984; Goslin and Banker, 1991). In brief, cells from the dissected hippocampi were dissociated by trypsinization (0.25% for 15 min at 37°C) followed by trituration with a fire polished Pasteur pipette. For immunofluorescence, the cells were plated at a density of 100,000 cells per 60-mm petri dish on glass coverslips coated with poly-L-lysine (1 mg/ml) in MEM with 10% horse serum. In antisense experiments, cells were plated onto 12-mm-diameter coverslips that were placed with the cells facing up in 35-mm dishes with 1 ml of medium. After 2–4 h the medium was changed to MEM with N2 supplements (Bottenstein and Sato, 1979), ovalbumin (0.1%), and pyruvate (0.01 mg/ml) that had been conditioned in cultures of astroglial cells for 24 h. Long-term cultures used in immunolocalization studies were co-cultured with astroglia.

### Antisense Oligonucleotides

The initial experiments were performed with oligonucleotides (−11+14 hkin) based upon the sequence of the human KHC (Navone et al., In press). Because the neuronal cultures were taken from rat brain, these experiments were subsequently repeated using oligonucleotides corresponding to the rat KHC sequence. The rat sequence in the region of the initiator codon AUG was obtained by using nondegenerate, 18-mer human primers and performing polymerase chain reaction (PCR) on reverse transcribed rat brain mRNA. An amplified band of the expected size was obtained and the DNA was cloned and sequenced. Key experiments were repeated with rat sense and antisense oligonucleotides.

Antisense oligonucleotide −11+14 hkin, consisting of the sequence GCCAGGTCCGCCATCTTTCTCGCAG, is the inverse complement of the human nucleotides −11 to +14. Antisense oligonucleotide −11+14 rkin, consisting of the sequence GCCGGGTCCGCCATCTTTCTGGCAG, is the inverse complement of the rat nucleotides −11 to +14. Antisense oligonucleotide −35−12 rkin, consisting of the sequence CCGGGACTGCAGGCCGGGAGCCAC, is the inverse complement of the rat nucleotides −35 to −12. Nucleotides −11+14 hkin and −11+14 rkin, which identically straddle the initiator AUG of the KHC, differ by only two nucleotides. Oligonucleotide −35−12 rkin is a nonoverlapping oligonucleotide located entirely entirely within the 5′ untranslated region of rat KHC. The antisense oligonucleotide sequences did not have significant homology with any other sequence in the database (Sequence Analysis Software Package, version 6.1; Devereux et al., 1984). The oligonucleotides were synthesized on an Applied Biosystems 380B synthesizer (Applied Biosystems, Inc., Foster City, CA), purified over a NAP5 column (Pharmacia LKB Biotechnology, Inc., Piscataway, NJ), ethanol precipitated, and taken up in media.

The administration of the oligonucleotide was as follows: At 2–4 h after plating, when the cells were transferred to serum-free glial-conditioned medium, the oligonucleotide was added at 50 μM. The medium was supplemented with 25 μM additional oligonucleotide every 12 h from the time of plating for either 24 or 48 h. Controls were treated with the same concentration and dosage schedule of the corresponding sense strand oligonucleotide. In dose-response experiments additional antisense oligonucleotides were added every 12 h at half the initial dose.

### Immunodetection

For immunostaining, the cultures were fixed for 20 min with warm 4% formaldehyde in PBS containing 0.12 M sucrose, permeabilized in 0.3% Triton X-100 for 5 min at room temperature, and rinsed in PBS. Cultures were incubated with 10% BSA for 1 h at 37°C, then exposed to primary antibody (diluted in 1% BSA/PBS) overnight at 4°C.

The following primary antibodies with their dilutions were used for this study. For kinesin staining, SUK4 (1:10), a mAb raised against the sea urchin KHC (Ingold et al., 1988), and a polyclonal antiserum raised against the squid KHC (1:500), provided by Michael Sheetz (Duke University, Durham, NC) were used. An affinity purification of the immunoglobulin fraction was prepared from the polyclonal antiserum. Both of these antibodies crossreact with mammalian brain KHC on Western blots (data not shown). Also used were a mAb raised against the heavy chain of chick brain cytoplasmic dynein taken from a mouse hybridoma tissue culture supernatant (1:2) provided by Michael Sheetz (Steuer et al., 1990); mAb DM1B (1:4,000) (Boehringer Mannheim Biochemicals, Indianapolis, IN) raised against β-tubulin; a rabbit polyclonal antibody against α- and β-tubulin (1:1,000) from Sigma Chemical Co., St. Louis, MO), an affinity-purified rabbit polyclonal antibody against synapsin I (1:250) provided by Pietro de Camilli (de Camilli et al., 1983); mAb 9-1E12(1:2,000), which reacts monospecifically with GAP-43 on immunoblots of cultured hippocampal neurons, provided by D. Schreyer and J. H. P. Skene (Goslin and Banker, 1990), and a rabbit polyclonal antibody (1:1,000–1:10,000) raised against a fusion protein in which the amino terminal 16 amino acids of rat GAP-43 were replaced by 13 amino acids from the λ gt7 capsid protein, provided by Mark Willard (Washington University, St. Louis, MO).

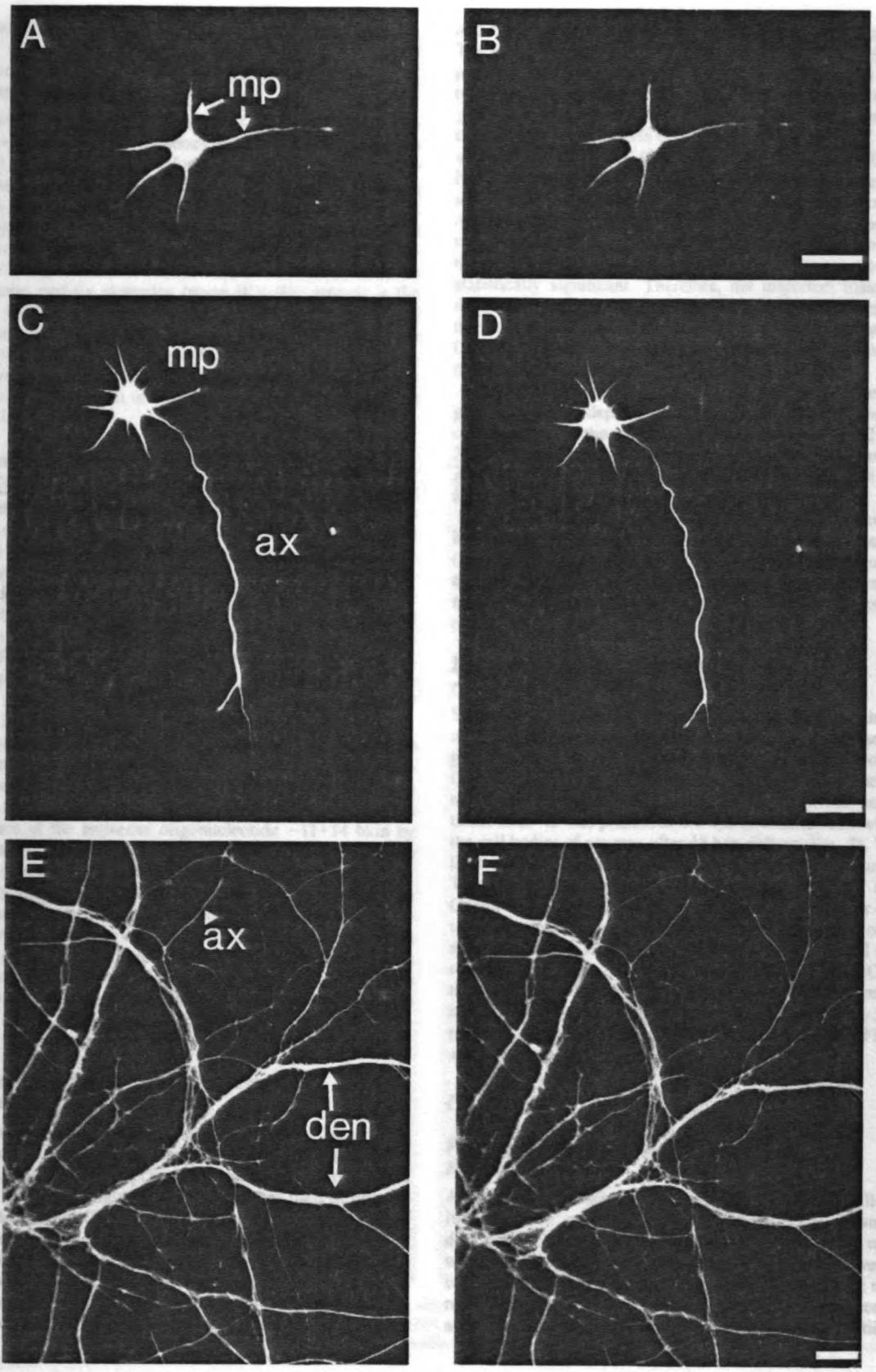
The following secondary antibodies were used. Rabbit anti-mouse IgG labeled with FITC (1:200) and goat anti-rabbit IgG labeled with rhodamine (1:200), both from Boehringer Mannheim Biochemicals. For synapsin I staining biotinylated goat anti-rabbit IgG (1:1,000) and avidin conjugated to fluorescein (1:500) (Vector Laboratories, Norwalk, CT) were used. Incubations in these antibodies were for 1 h at 37°C.

Dot immunobinding was performed with $^{125}$I-labeled protein A as originally described by Jahn et al. (1984) and modified by Ferreira et al. (1989). The KHC polyclonal antibody was used because of the avidity of rabbit IgG for protein A. The cultures were rinsed twice in warmed PBS, scraped into Laemmli buffer (Laemmli, 1970), homogenized in a boiling water bath for 5 min, and centrifuged at 33,000 rpm. The supernatant was removed and applied to nitrocellulose paper (Ferreria et al., 1989).

### Morphometric Analysis

Fixed cells were viewed from the inverted microscope by phase microscopy using a video camera and images were recorded on an optical memory disk recorder. Cells were selected at random, traced from the screen, and the lengths of their processes measured using a digitizing tablet.

*Figure 1.* Hippocampal neurons double labeled with polyclonal tubulin antibody (*A*, *C*, and *E*) and the kinesin mAb SUK4 (*B*, *D*, and *F*). Stage II neurons are shown in *A* and *B* with their minor processes (*mp*) indicated. Stage III neurons are shown in *C* and *D* with the axon (*ax*) indicated. Neurons at stage IV, when dendrites (*den*) become apparent, are shown in *E* and *F*. Bars, 20 μm.


A
mp
B
C
mp
ax
D
E
ax
den
F

## Results

### Immunolocalization of KHC in Cultured Rat Hippocampal Cells

Cultured rat hippocampal neurons from E18 rat brain represent a relatively homogeneous population of neurons in which pyramidal cells predominate. After plating, hippocampal neurons undergo predictable developmental changes (Dotti et al., 1988). At stage I, during the first few hours after plating, the neurons appear rounded. Stage II (Fig. 1) begins ~8 h after plating, when the neurons elaborate a symmetric array of neurites. After ~24 h in culture, one of the processes rapidly elongates (stage III); this process is the axon. During stage IV (72–96 h in culture), the remaining neurites differentiate into dendrites. Kinesin reactivity was observed at all of these stages (Fig. 1). It appeared to be homogeneously distributed, as was tubulin. Kinesin immunoreactivity was present in cell bodies and in both axonal and dendritic processes.

### Antisense Oligonucleotide Affect KHC Expression

The oligonucleotides (antisense and sense) were tested for their ability to inhibit KHC expression. The sequence sites selected for the design of the oligonucleotides were centered on the initiator AUG and a nonoverlapping site located immediately upstream in the 5′ untranslated region. Cells incubated with each of the antisense oligonucleotides described in Materials and Methods showed markedly reduced reactivity to a KHC mAb (SUK4), as assessed by immunofluorescence at 24 or 48 h after plating (Fig. 2). Neurons incubated with the sense oligonucleotides, on the other hand, appeared unaffected and showed a normal degree of KHC immunoreactivity by immunofluorescence.

To verify that KHC was depleted from cells after antisense treatment, the more sensitive technique of dot immunobinding was used for detection (Fig. 3). KHC was not detectable above the background level of counts in cells grown in the presence of the antisense oligonucleotide −11+14 hkin by the dot immunobinding assay. In contrast, cells treated with sense oligonucleotides were comparable in their immunoreactivity to untreated control cells. Exposure to the antisense oligonucleotides did not affect tubulin and dynein immunoreactivity by the same assay (Fig. 3). The presence of normal levels of tubulin and dynein in the kinesin-suppressed cells suggests that the effect of the antisense oligonucleotide was specific and that the regulation of the expression of the retrograde motor, dynein, was independent of kinesin.

### Effects of Antisense Oligonucleotides on Neurite Extension

Neurite extension was measured after either a 24- or 48-h exposure to the KHC oligonucleotides. Neurite elongation during the second 24-h period is considerably more affected by the antisense oligonucleotide treatment than during the first 24-h period (Fig. 4). At both time points nearly all of the neurons had two populations of neurites consisting of several short minor neurites and a single long neurite considered the axon. When the cells were exposed to the antisense oligonucleotide −11+14 hkin and fixed 24 h after plating, there was a 25% decrease in the lengths of the minor neurites and a 34% decrease in the length of the presumptive axon. The mean length of the presumptive axon was 74.5 ± 2.1 μm (compared with 111.7 ± 5.6 μm in sense-treated controls) and the summed length of the minor neurites was 79.6 ± 4.1 μm (compared with 105.2 ± 5.5 μm in sense-treated controls). Neurite growth of neurons exposed to KHC antisense oligonucleotides for 48 h is quantitated in Table I. Neurons treated with kinesin antisense oligonucleotides (50 μM) for 48 h exhibited a 50% decrease in both the lengths of the minor processes and the axon-like processes. The human antisense oligonucleotide was slightly less effective than the rat antisense oligonucleotide, but the difference was not statistically significant. Therefore, the imperfect match of the human antisense oligonucleotide, which differed in two nucleotides, did not significantly affect KHC suppression. On average the antisense-treated neurons had one less minor neurite than the sense-treated controls (Table I).

The KHC antisense oligonucleotides affected neurite outgrowth in a dose-dependent manner (Fig. 5). Increasing the concentration of the antisense oligonucleotide from 12.5 to 50 μM caused a progressive decrease in neurite outgrowth. At 12.5 μM the total neurite length was reduced 19% and at 50 μM it was reduced 50%.

The KHC antisense oligonucleotides, while suppressing KHC expression, did not irreversibly damage the neurons (Fig. 6). When, after 48 h, the cells were released from antisense inhibition by changing the medium, neurite extension resumed at a rate that paralleled that observed under control conditions.

### Distribution of GAP-43 and Synapsin in Antisense-treated Neurons

Since kinesin has been postulated to power anterograde axonal transport, we examined the effect of KHC antisense oligonucleotides on the immunocytochemical distribution of GAP-43 and synapsin, molecules that are transported to nerve termini by fast axonal transport. Under control conditions, GAP-43 was present at the tips of neurites and within the cell bodies of neurons after 48 h in culture (Fig. 7). Very little staining was detectable along the shafts of neurites. This pattern was similar to that described in Fig. 2 *H* of Goslin and Banker (1990). Likewise, synapsin I, under control conditions, was concentrated in the distal portion of the axon (Fig. 8), as described previously in hippocampal neurons (Fletcher et al., 1991). Following exposure to KHC antisense oligonucleotides, the GAP-43 and synapsin I immunoreactivities were largely restricted to the cell body; the neurites were essentially devoid of immunostaining (Fig. 7 and 8).

## Discussion

### Phenotype of Hippocampal Neurons After Kinesin Suppression

A powerful approach for understanding a protein's cellular function is to study the phenotype of a cell or organism deficient in that protein. Targeted gene deletion is the most widely used strategy for achieving these goals; however, such experiments are not readily possible in postmitotic neurons. Messenger RNA inactivation, either by expression of antisense RNAs or exposure to antisense oligonucleotides,

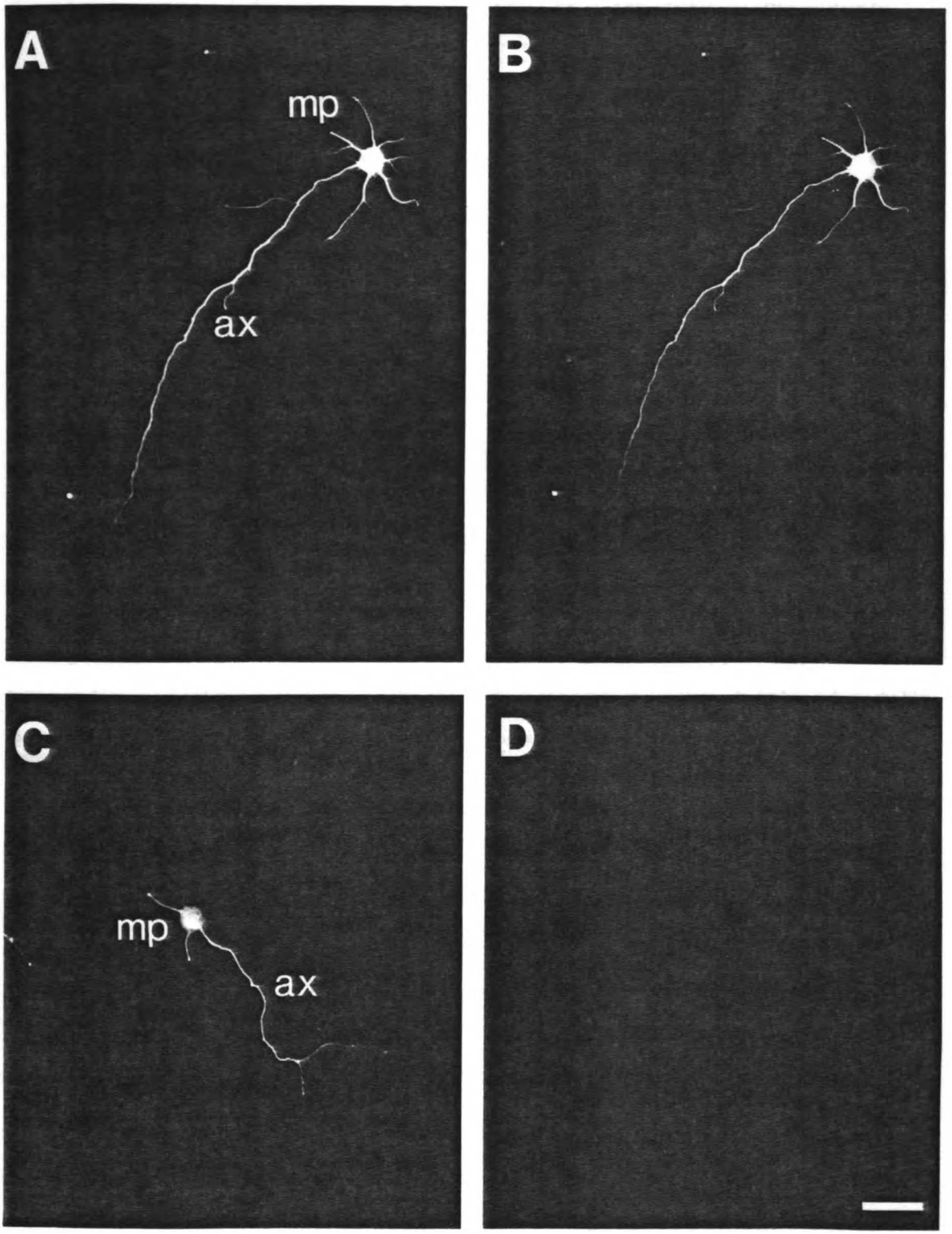



*Figure 2.* Hippocampal neurons fixed after 48 h in culture under sense (*A* and *B*) and antisense (*C* and *D*) conditions. The cells were double labeled with antibodies to tubulin (*A* and *C*) and kinesin SUK4 (*B* and *D*). The oligonucleotides used in this experiment were hkin −11+14 (sense) and −11+14 hkin (antisense). Identical results were observed with the other oligonucleotides. *ax*, axon; *mp*, minor process. Bar, 20 μm.

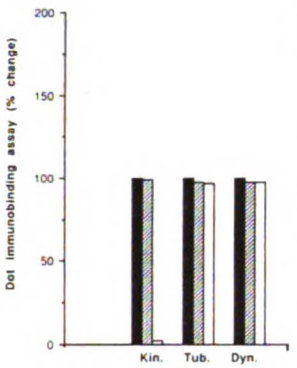



*Figure 3.* Dot immunobinding to quantitate rabbit kinesin (*Kin.*), tubulin (*Tub.*) (DM1B), and dynein (*Dyn.*) under sense and antisense conditions. The kinesin antibody used was the rabbit polyclonal and the tubulin antibody was DM1B. The control (■) refers to untreated cultures and the value in cpms for the control was considered 100%. The other values are expressed as a percentage of the control. ▨, sense kinesin; □, antisense kinesin.

provides an alternative means of reducing cellular concentrations of a specific protein. In this study, we have shown that exposure to antisense oligonucleotides causes a marked reduction in the levels of the KHC protein in rat hippocampal neurons. After a 24-h exposure to antisense, but not to sense oligonucleotides, the levels of KHC protein are not detectable above background by dot-immunobinding. Thus, antisense oligonucleotide treatment provides a means of creating a "null" kinesin phenotype in a mammalian neuronal cell.

The homogeneous pattern of KHC labeling in the cultured neurons is consistent with the reported large soluble pool (Hollenbeck, 1989). However other investigators have observed a punctate pattern consistent with localization to membranous organelles (Pfister et al., 1989; Wright et al., 1991). It seems likely that the punctate pattern results from some degree of extraction of KHC with the fixatives used. Brady (1991) has raised a number of plausible arguments that favor a predominant membrane localization for KHC, and has reconciled the solubility of the molecule by proposing an easily extractable relationship to membranes. The issue, however, remains problematic because recent data using extruded squid axoplasm suggests a tight association of plus-end motors with organelles that does not exchange with the soluble pool (Schnapp, B. J., T. S. Reese, and R. B. Bechtold. 1991. *J. Cell. Biol.* 115:40 Abstr.)

*Table I. Effect of Kinesin Antisense Oligonucleotides (50 μM) on Neuritic Growth after 2 d in Culture*

| Treatment | Length | | | Number of Minor Processes |
|---|---|---|---|---|
| | Total | Axonal | Minor Processes | |
| | (μm) | (μm) | (μm) | |
| None | 444 ± 16 | 247 ± 9 | 37 ± 2 | 4.8 ± 0.2 |
| Sense HK11-14 | 420 ± 12 | 216 ± 11 | 32 ± 1 | 4.8 ± 0.3 |
| Antisense HK11-14 | 215 ± 9 | 126 ± 6 | 20 ± 1 | 3.8 ± 0.3 |
| Sense RK11-14 | 390 ± 12 | 228 ± 11 | 31 ± 1 | 4.8 ± 0.4 |
| Antisense RK11-14 | 171 ± 7 | 116 ± 5 | 16 ± 1 | 3.3 ± 0.1 |
| Sense RK35-12 | 420 ± 8 | 254 ± 10 | 29 ± 2 | 4.6 ± 0.2 |
| Antisense RK35-12 | 180 ± 9 | 114 ± 7 | 17 ± 0.7 | 3.5 ± 0.6 |

Neurite length was determined in 100 cells for each experimental condition. Each value represents the mean ± SEM. For all of the length measurements comparisons with the controls were significant with $P < 0.005$. For the minor processes the comparison of the sense and antisense oligonucleotides HK 11-14 and RK 11-14 had a significance of $P < 0.01$, and for RK 35-12 a significance of $P < 0.05$.

Several results indicate that the phenotypic changes in hippocampal cells observed after KHC antisense oligonucleotide treatment can most likely be attributed to the reduced levels of KHC. First, the antisense oligonucleotides do not cause irreversible damage to the cell; neurons resume neurite outgrowth at normal rates following a change to medium free of the antisense oligonucleotide. Second, two different antisense oligonucleotides complementary to two different regions of the KHC mRNA produce identical morphological effects on hippocampal neurons. The finding reduces the likelihood that the observed cellular effects are because of the oligonucleotides hybridizing to an mRNA other than the KHC mRNA. Among the kinesin-like molecules sequenced to date, the most significant region of homology lies in the

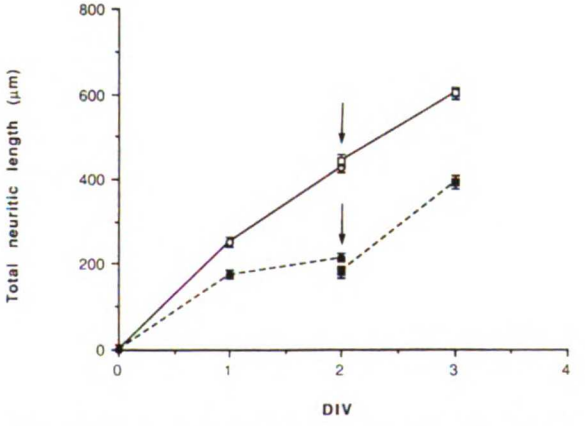



*Figure 4.* Total neurite length measured as a function of time in culture. The dotted line represents the antisense oligonucleotide-treated cells and the solid line represents the sense oligonucleotide-treated cells. Measurements were taken after 1 d of treatment and after 2 d of treatment. At times beyond the arrow, the medium was changed to a nucleotide-free medium. Continued neurite extension paralleled the control values.

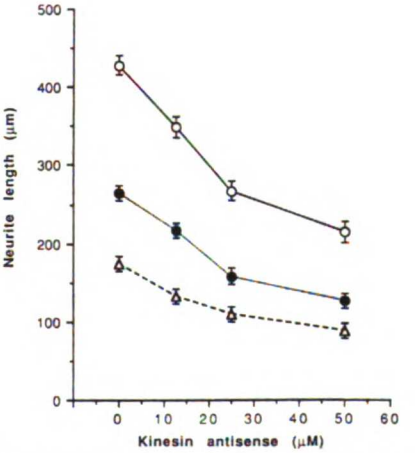



*Figure 5.* A dose-response curve illustrating neurite length as a function of the dose of kinesin antisense oligonucleotide. These cultures were analyzed at 48 h after plating. (–○–) Total neuritic length; (···●···) axonal length; (---△---) minor processes length.

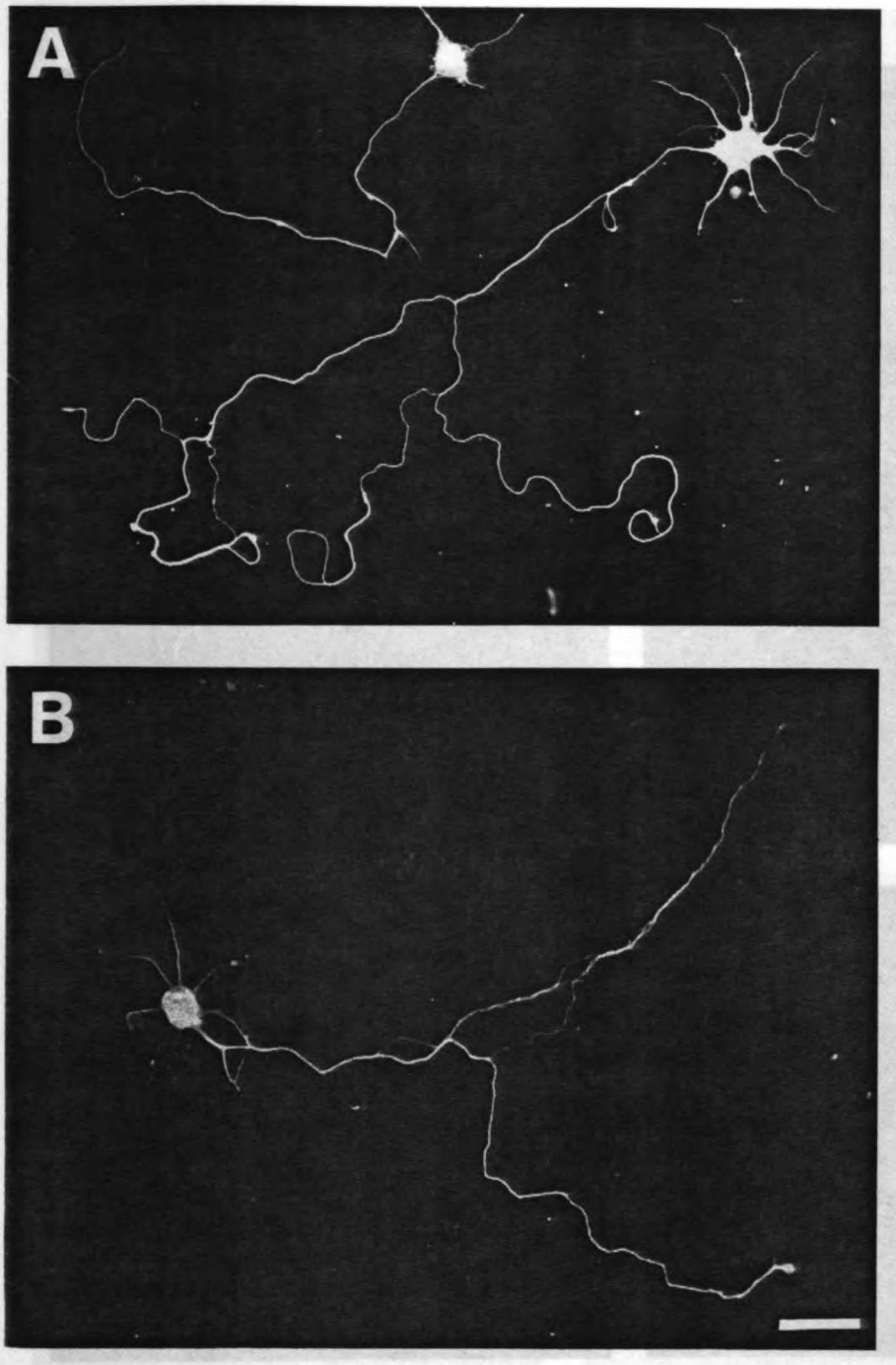



*Figure 6.* Recovery from antisense oligonucleotide treatment. The neurons in *A* were treated with kinesin sense oligonucleotides and in *B* with kinesin antisense oligonucleotides for 48 h. Then medium was changed and oligonucleotides were excluded. At 72 h the cells were fixed and stained with kinesin antibody (SUK4). Although the growth of the cell in *B* appears to lag behind the cells in *A*, recovery of kinesin immunoreactivity and morphological development is evident. Bar, 20 $\mu$m.

ATP- and microtubule-binding sites, not the region at the 5′ end from where we derived our antisense oligonucleotides. Third, tubulin and dynein protein levels remain normal suggesting that there is not a general reduction in protein synthetic activity.

The phenotype of KHC suppressed hippocampal neurons offers some insight into the normal physiological roles for kinesin in these cells. One striking finding is the altered distribution of synapsin I and GAP-43 in cells treated with KHC antisense oligonucleotides. In untreated cells or cells treated with sense oligonucleotides, synapsin I and GAP-43 are found in the neurites and are particularly concentrated in the termini. In antisense-treated cells, on the other hand, both proteins are confined to the cell bodies. Synapsin I and GAP-43 are both membrane-associated proteins (De Camilli et al., 1983; Valtorta et al., 1988; Gispen et al., 1985) and are

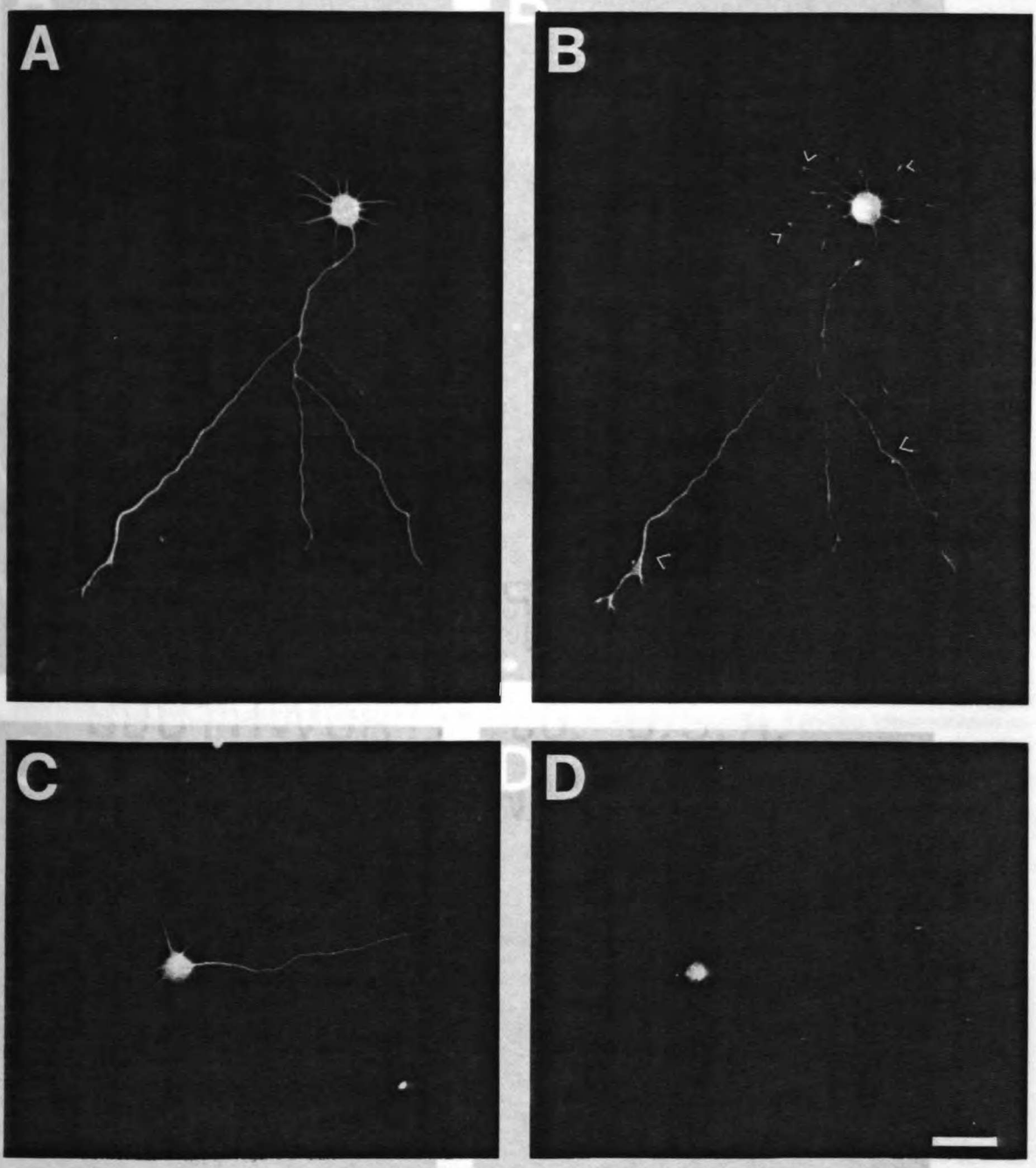



*Figure 7.* GAP-43 staining. *A* and *B* are kinesin sense oligonucleotide treated. *C* and *D* are kinesin antisense oligonucleotide treated. *A* and *C* are stained with the tubulin antibody and *B* and *D* are stained with the GAP-43 antibody (9-IE12). Bar, 20 $\mu$m.

delivered to neuronal termini by fast axonal transport (Baitinger and Willard, 1987; Skene and Willard, 1981; Benowitz et al., 1981). Microtubules in both minor neurites and axons are aligned with their plus ends distal to the cell body (Baas et al., 1989), so that translocation of organelles to the neurite terminus of both types of processes requires a plus-end–directed motor. The impaired delivery of synapsin I and GAP-43 to the neurite terminus under antisense conditions suggests that kinesin may serve as the plus-end motor involved in the anterograde transport of vesicles containing these proteins. This conclusion is consistent with recent findings that KHC is associated with vesicles traveling by anterograde transport that accumulate at the proximal side of a nerve ligation (Hirokawa et al., 1991). Alterna-

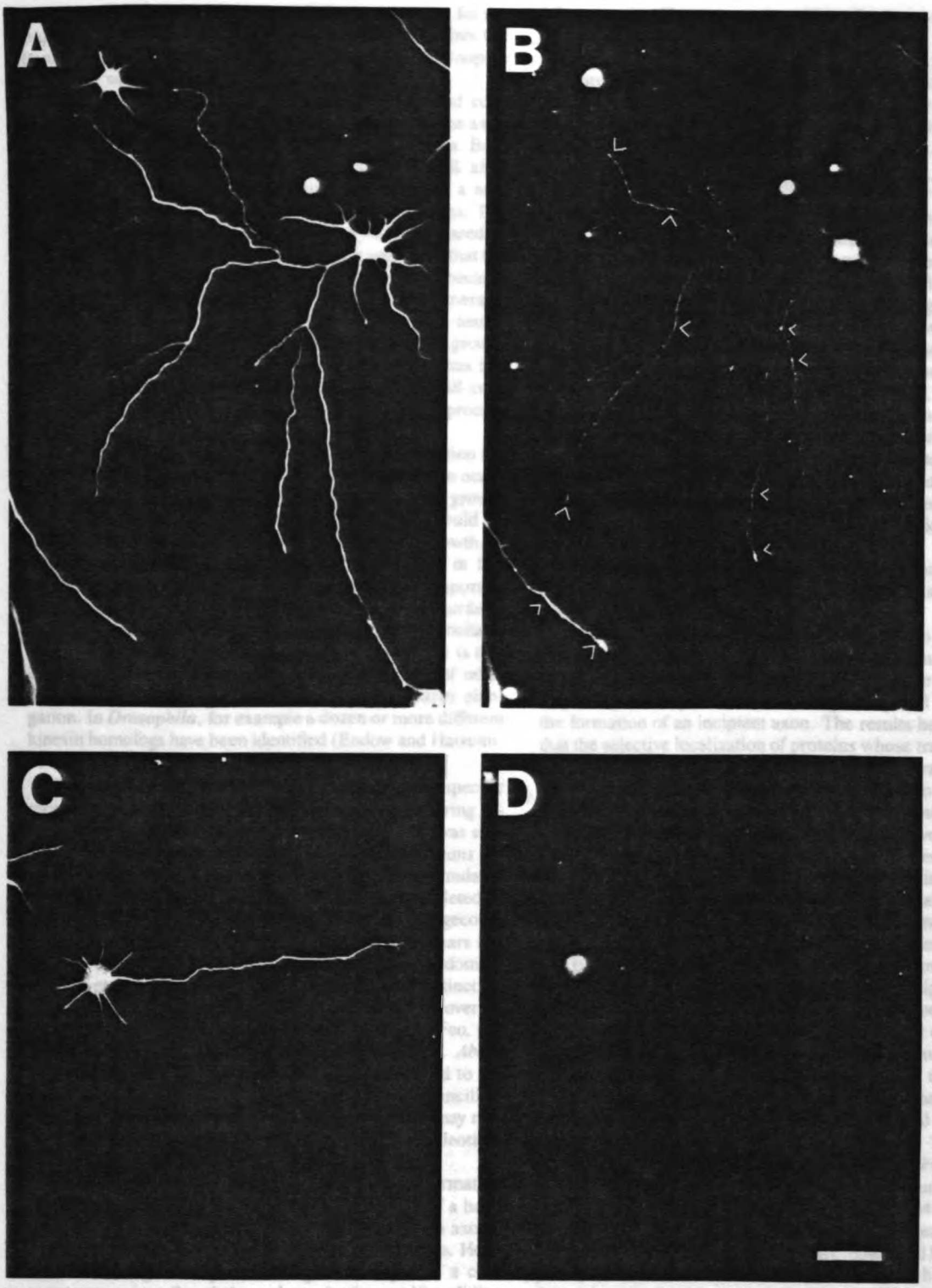



*Figure 8.* Synapsin I staining. *A* and *B* are kinesin sense oligonucleotide treated. *C* and *D* are kinesin antisense oligonucleotide treated. *A* and *C* are stained with the tubulin antibody (DM1B) and *B* and *D* are stained with the synapsin I rabbit antibody. Bar, 20 μm.

tively, it is formally possible that KHC is unnecessary for the transport of GAP-43 and synapsin I, but instead inhibits the transport of another protein that traps GAP-43 and synapsin I in distal neurites.

Another consistent change in the antisense-treated cells was a reduction in neurite length that affected both the axon and the minor processes which will become dendrites. Both classes of neurites were reduced in length by ~50% after 48 h in antisense-containing medium, but resumed a normal growth rate upon removal of the oligonucleotides. The greater effect on the minor neurites after 48 h compared to just 24 h in the antisense-containing media suggested that the longer the processes grew, the more dependent they became on kinesin for further elongation (Fig. 4). It is generally thought that the addition of new surface membrane necessary for neurite elongation occurs predominantly at growth cones (Pfenninger and Maylie-Pfenninger, 1981). Thus impaired anterograde transport of vesicles in KHC null cells may be the underlying cause for the reduced rate of process outgrowth.

If this explanation is correct, why is neurite elongation not entirely blocked? It may be that neurite outgrowth can occur in the absence of anterograde vesicle transport to growth cones. Membrane addition within the cell body could be sufficient to support a reduced rate of process outgrowth, at least for short distances (Small et al., 1984) and in fish epidermal keratocytes there is a rapid forward transport of concanavalin A–coated gold particles on the dorsal surfaces of lamellipodia that is blocked by treatment with cytochalasin D (Kucik et al., 1989). An alternative possibility is that a different anterograde motor drives the transport of other classes of organelles that can, in part, support neurite elongation. In *Drosophila*, for example a dozen or more different kinesin homologs have been identified (Endow and Hatsumi, 1991).

The particular class of organelles translocated by specific motors remains problematic, particularly in comparing diverse systems. Some degree of organelle specificity was suggested for the putative motor gene *unc*-104 in *C. elegans* because neurons from the mutant phenotype accumulated synaptic vesicles in nerve cell bodies and were depleted of such vesicles in presynaptic terminals (Hall and Hedgecock, 1991). The protein encoded by the *unc*-104 gene bears homology to KHC only in the force-generating head domain (Otsuka et al., 1991). *Unc*-116 in *C. elegans*, is a distinct locus, which encodes a kinesin that is 55% identical over its entire length to the *Drosophila* and squid KHC (de Feo, G., N. Patel, and J. R. Mancillas. 1991. *Soc. Neurosci. Abstr.* 17:58). One allele at this locus has defects restricted to the nervous system (de Feo, G., N. Patel, and J. R. Mancillas. 1991. *Soc. Neurosci. Abstr.* 17:58), and this mutant may represent a closer analogy to the defect in the oligonucleotide-induced KHC null neurons.

The ultimate loss of ribosomes during the transformation of a minor neurite into an axon, and thus the loss of a basis for local protein synthesis, places a high priority on axonal transport to support this rapidly elongating structure. However, some degree of process outgrowth might be a consequences primarily of the polymerization and/or sliding of microtubules. Microtubule polymerization can produce work in vitro (Hotani and Miyamoto, 1990) and appears to drive process formation in Sf9 cells that express high levels of $\tau$ protein (Knopps et al., 1991). Furthermore, recent studies (Tanaka and Kirschner, 1991) indicate that intact microtubules are pushed anterograde in neurons; such sliding forces may also contribute to process extension. It will be important to examine the growing tips of processes grown in KHC antisense conditions for the possibility that they are enriched in cytoskeletal structures but devoid of organelles.

### *Development of Neurite Asymmetry in Null Cells*

During their initial growth, hippocampal neurons extend several processes; one of these ultimately differentiates into a long and slender axon while the remainder become dendrites. The commitment of a neurite to an axonal identity occurs when that process becomes significantly longer than the others (Goslin and Banker, 1989). In this study we find that hippocampal neurons that lack detectable KHC nevertheless become polarized, at least as assessed by morphologic criteria. Although process length is reduced, the cells nonetheless exhibit a distinctly asymmetric form, with one neurite far longer than any of the others. Appropriate markers will be necessary to establish the identity of the long process as an axon. Because treatment with KHC antisense oligonucleotides prevents the transport of GAP-43 and synapsin I into neurites, these commonly used axonal markers cannot be utilized. Other markers, like MAP-2 and $\tau$ become segregated relatively late in the course of neuronal development in culture (Caceres et al., 1984; Kosik and Finch, 1987), too late for use in the present work.

Appropriate sorting of molecules must occur to create and maintain the molecular differences between axons and dendrites. The selective elongation of a single neurite is an early step in the development of neuronal polarity and represents the formation of an incipient axon. The results here suggest that the selective localization of proteins whose transport requires kinesin cannot be essential for the elaboration of an asymmetric array of neurites. GAP-43 appears to be among this class of proteins. The function of GAP-43, and its possible role in neurite outgrowth, remain controversial. Although it has been reported that GAP-43 antibodies delivered into neuroblastoma cells prevent neuritogenesis (Shea et al., 1991) and overexpression of GAP-43 accelerates neurite outgrowth in PC12 cells (Yankner et al., 1990), neurite outgrowth does occur normally in a PC12 line deficient in GAP-43 (Baetge and Hammang, 1991). GAP-43 normally accumulates in the axonal growth cones of cultured hippocampal neurons coincident with the emergence of the axon, suggesting that it could play a role in the establishment of polarity (Goslin and Banker, 1990). Since the inhibition of KHC expression resulted in the restriction of GAP-43 to the cell body, it is reasonable to suggest that GAP-43 need not be present in axons and their growth cones for axonal outgrowth and for the development of neurite asymmetry. There are, however, certain caveats to this interpretation. First, if the half-life of KHC is sufficiently long, then this motor protein may be present for some portion of the initial 24-h period. Some GAP-43 may have been transported into neurites during the first day in culture, before KHC levels had been completely reduced, but may have disappeared by 24 h, when we determined its localization. It is also possible that a small amount of GAP-43 was present in axons, but was below the level of detection by immunofluorescence.

The specific suppression of KHC expression by antisense

techniques permits the assessment of the role of this motor and the transport of specific molecules in neuronal development. Retained neuronal function in the absence of the motor suggests that additional motors or other mechanisms may be operative in neurite elongation and the development of polarity. Which classes of organelles are transported by kinesin and exactly what degree of cellular integrity is retained in a KHC-null state are compelling topics of further investigation.

We thank M. Willard for the polyclonal GAP-43 antibody and the members of his laboratory who contributed to generating the antibody, particularly Dr. Susan Schuh and Arlene Loewy. We thank J. Scholey for SUK4, M. Sheetz for the kinesin polyclonal antibody and the dynein antibody; and J. H. P. Skene for the monoclonal GAP-43 antibody.

This work was supported by Rita Allen Klingenstein, and National Institutes of Health (NIH) grants GM38499 to R. D. Vale, NS17112 to G. Banker, and NS29031 to K. S. Kosik.

Received for publication 1 November 1991 and in revised form 9 January 1992.

### *References*

Baas, P. W., J. S. Deitch, M. M. Black, and G. A. Banker. 1988. Polarity orientation of microtubules in hippocampal neurons: uniformity in the axon and nonuniformity in the dendrite. *Proc. Natl. Acad. Sci. USA.* 85:8335–8339.

Baas, P. W., J. S. Deitch, M. M. Black, and G. A. Banker. 1989. Changes in microtubule polarity orientation during the development of hippocampal neurons in culture. *J. Cell Biol.* 109:3085–3094.

Baetge, E. E., and J. P. Hammang. 1991. Neurite outgrowth in PC12 cells deficient in GAP-43. *Neuron.* 6:21–30.

Baitinger, C., and M. Willard. 1987. Axonal transport of synapsin I-like proteins in rabbit retinal ganglion cells. *J. Neurosci.* 7:3723–3735.

Bartlett, W. P., and G. A. Banker. 1984. Electron microscopic studies of axonal and dendritic development by hippocampal neurons in culture. I. Cells which develop without intercellular contacts. *J. Neurosci.* 4:1944–1953.

Benowitz, L. J., V. E. Shashoua, and M. G. Yoon. 1981. Specific changes in rapidly transported proteins during regeneration of the goldfish optic nerve. *J. Neurosci.* 1:300–307.

Bloom, G. S., M. C. Wagner, K. K. Pfister, and S. T. Brady. 1988. Native structure and physical properties of bovine brain kinesin and identification of the ATP-binding subunit polypeptide. *Biochemistry.* 27:3409–3416.

Bottenstein, J. E., and G. H. Sato. 1979. Growth of a rat neuroblastoma cell line in serum-free supplemented medium. *Proc. Natl. Acad. Sci. USA.* 76:514–517.

Brady, S. T., K. K. Pfister, and G. S. Bloom. 1990. A monoclonal antibody against the heavy chain of kinesin inhibits both anterograde and retrograde axonal transport in isolated squid axoplasm. *Proc. Natl. Acad. Sci. USA.* 87:1061–1065.

Brady, S. T. 1991. Molecular motors in the nervous system. *Neuron.* 7:521–533.

Caceres, A., G. A. Banker, O. Steward, L. Binder, and M. Payne. 1984. MAP2 is localized to the dendrites of hippocampal neurons which develop in culture. *Dev. Brain Res.* 13:314–318.

De Camilli, P., R. Cameron, and P. Greengard. 1983. Synapsin I (Protein I), a nerve terminal-specific phosphoprotein. I. Its general distribution in synapses of the central and peripheral nervous system demonstrated by immunofluorescence in frozen and plastic sections. *J. Cell Biol.* 96:1337–1354.

Devereux, J. R., P. Haeberli, and O. Smithies. 1984. A comprehensive set of sequence analysis programs for the VAX. *Nucl. Acids Res.* 12:387–395.

Dotti, C. G., C. A. Sullivan, and G. A. Banker. 1988. The establishment of polarity by hippocampal neurons in culture. *J. Neurosci.* 8:1454–1468.

Endow, S. A., and M. Hatsumi. 1991. A multimember kinesin gene family in Drosophila. *Proc. Natl. Acad. Sci. USA.* 88:4424–4427.

Ferreira, A., J. Bosciglio, and A. Caceres. 1989. Microtubule formation and neurite growth in cerebellar macroneurons which develop *in vitro*: evidence for the involvement of the microtubule-associated proteins, MAP-1a, HMW-MAP2, and tau. *Dev. Brain. Res.* 49:215–228.

Filliatreau, G., and L. DiGiamberdino. 1981. Microtubule polarity in myelinated axons as studied after decoration with tubulin. *Biol. Cell.* 42:69–72.

Fletcher, T. L., P. Cameron, P. De Camilli, and G. Banker. 1991. The distribution of synapsin I and synaptophysin in hippocampal neurons developing in culture. *J. Neurosci.* 11:1617–1626.

Gispen, W. H., J. L. M. Leunissen, A. B. Oestreicher, A. J. Verkleij, and H. Zwiers. 1985. Presynaptic localization of B-50 phospho-protein, the ACTH-sensitive protein kinase C substrate involved in rat brain phosphoinositide metabolism. *Brain Res.* 328:381–385.

Goslin, K., and G. A. Banker. 1989. Experimental observations on the development of polarity by hippocampal neurons in culture. *J. Cell Biol.* 108:1507–1516.

Goslin, K., and G. A. Banker. 1990. Rapid changes in the distribution of GAP-43 correlate with the expression of neuronal polarity during development and under experimental conditions. *J. Cell Biol.* 110:1319–1331.

Goslin, K., and G. A. Banker. 1991. Rat hippocampal neurons in low density culture. *In* Culturing Nerve Cells. G. Banker and K. Goslin, editors. The MIT Press, Cambridge, MA. 251–283.

Hall, D. H., and E. M. Hedgecock. 1991. Kinesin-related gene unc-104 is required for axonal transport of synaptic vesicles in C. elegans. *Cell.* 65:837–847.

Heidemann, S. R., J. M. Landers, and M. A. Hamborg. 1981. Polarity orientation of axonal microtubules. *J. Cell Biol.* 91:661–665.

Hirokawa, N., R. Sat-Yoshitake, N. Kobayashi, K. K. Pfister, G. S. Bloom, and S. T. Brady. 1991. Kinesin associates with anterogradely transported membranous organelles in vivo. *J. Cell Biol.* 114:295–302.

Hollenbeck, P. J. 1989. The distribution, abundance and subcellular localization of kinesin. *J. Cell Biol.* 108:2335–2342.

Hollenbeck, P. J., and J. A. Swanson. 1990. Radial extension of macrophage tubular lysosomes supported by kinesin. *Nature (Lond.).* 346:864–866.

Hotani, H., and H. Miyamoto. 1990. Dynamic features of microtubules as visualized by dark-field microscopy. *Adv. Biophys.* 26:135–156.

Houliston, E., and R. P. Elinson. 1991. Evidence for the involvement of microtubules, ER, and kinesin in the cortical rotation of fertilized frog eggs. *J. Cell Biol.* 114:1017–1028.

Ingold, A. L., S. A. Cohn, and J. M. Scholey. 1988. Inhibition of kinesin-driven microtubule motility by monoclonal antibodies to kinesin heavy chains. *J. Cell Biol.* 107:2657–2667.

Jahn, R., W. Schiebler, and P. Greengard. 1984. A quantitative dot-immunobinding assay for proteins using nitrocellulose membrane filters. *Proc. Natl. Acad. Sci. USA.* 81:1684–1687.

Knops, J., K. S. Kosik, G. Lee, J. D. Pardee, L. Cohen-Gould, and L. McConlogue. 1991. Overexpression of tau in a non-neuronal cell induces long cellular processes. *J. Cell Biol.* 114:725–733.

Kosik, K. S., and E. A. Finch. 1987. MAP2 and tau segregate into axonal and dendritic domains after the elaboration of morphologically distinct neurites: An immunocytochemical study of cultured rat cerebrum. *J. Neurosci.* 7:3142–3153.

Kosik, K. S., L. D. Orecchio, B. J. Schnapp, H. Inouye, and R. L. Neve. 1990. The primary structure and analysis of the squid kinesin heavy chain. *J. Biol. Chem.* 265:3278–3283.

Kucik, D. F., E. L. Elson, and M. P. Sheetz. 1989. Forward transport of glycoproteins on leading lamellipodia in locomoting cells. *Nature (Lond.).* 340:315–317.

Kuznetsov, S. A., E. A. Vaisberg, N. A. Shanina, N. N. Magvetova, V. X. Chernyak, and V. I. Gelfand. 1988. The quaternary structure of bovine brain kinesin. *EMBO (Eur. Mol. Biol. Organ.) J.* 7:353–356.

Laemmli, U. K. 1970. Cleavage of structural protein during the assembly of the head of the bacteriophage T4. *Nature (Lond.).* 227:680–685.

Navone, F., J. Niclas, N. Hom-Booher, L. Sparks, H. Bernstein, G. McCaffrey, and R. D. Vale. 1992. Expression of the human kinesin heavy chain gene in CV-1 cells: interaction of the carboxy terminal domain with cytoplasmic microtubules. In press.

Otsuka, A. J., A. Jeyaprakash, J. Garcia-Anoveros, L. Z. Tang, G. Fisk, T. Hartshorne, R. Franco, and T. Born. 1991. The C. elegans unc-104 gene encodes a putative kinesin heavy chain-like protein. *Neuron.* 6:113–122.

Pfenninger, K. H., and M. Mayle-Pfenninger. 1981. Lectin labeling of sprouting neurons. II. Relative movement and appearance of glycoconjugates during plasmalemmal expansion. *J. Cell Biol.* 89:547–559.

Pfister, K. K., M. C. Wagner, D. L. Stenoien, S. T. Brady, and G. S. Bloom. 1989. Monoclonal antibodies to kinesin heavy and light chains stain vesicle-like structures, but not microtubules, in cultured cells. *J. Cell Biol.* 108:1453–1463.

Porter, M. E., J. M. Scholey, D. L. Stemple, G. P. A. Vigers, R. D. Vale, M. P. Sheetz, and J. R. McIntosh. 1987. Characterization of the microtubule movement produced by sea urchin egg kinesin. *J. Biol. Chem.* 262:2794–2802.

Rodionov, V. I., F. K. Gyoeva, and V. I. Gelfand. 1991. Kinesin is responsible for centrifugal movement of pigment granules in melanophores. *Proc. Natl. Acad. Sci. USA.* 88:4956–4960.

Saxton, W. M., J. Hicks, L. S. B. Goldstein, and E. C. Raff. 1991. Kinesin heavy chain is essential for viability and neuromuscular functions in Drosophila, but mutants show no defects in mitosis. *Cell.* 64:1093–1102.

Scholey, J. M., M. E. Porter, P. M. Grissom, and J. R. McIntosh. 1985. Identification of kinesin in sea urchin eggs, and evidence for its localization in the mitotic spindle. *Nature (Lond.).* 318:483–486.

Shea, T. B., N. I. Perrone-Bizzozero, M. L. Beermann, and L. I. Benowitz. 1991. Phospholipid-mediated delivery of anti-GAP-43 antibodies into neuroblastoma cells prevents neuritogenesis. *J. Neurosci.* 11:1685–1690.

Skene, P. J. H., and I. Virag. 1989. Posttranslational membrane attachment and dynamic fatty acylation of a neuronal growth cone protein, GAP-43. *J. Cell Biol.* 108:613–624.

Skene, J. H. P., and M. Willard. 1981. Changes in axonally transported proteins during axon regeneration in toad retinal ganglion cell. *J. Cell Biol.* 89:86–95.

Small, R. K., M. Blank, R. Ghez, and K. H. Pfenninger. 1984. Components of the plasma membrane of growing axons. II. Diffusion of membrane protein complexes. *J. Cell Biol.* 98:1434–1443.

Steuer, E. R., L. Wordeman, T. A. Schroer, and M. P. Sheetz. 1990. Localization of cytoplasmic dynein to mitotic spindles and kinetochores. *Nature (Lond.).* 345:266–268.

Tanaka, E. M., and M. W. Kirschner. 1991. Microtubule behavior in the growth cones of living neurons during axon elongation. *J. Cell Biol.* 115:345–363.

Urrutia, R., M. A. McNiven, J. P. Albanesi, D. B. Murphy, and B. Kachar. 1991. Purified kinesin promotes vesicle motility and induces active sliding between microtubules *in vitro*. *Proc. Natl. Acad. Sci. USA.* 88:6701–6705.

Vale, R. D., T. S. Reese, and M. P. Sheetz. 1985*a*. Identification of a novel force generating protein, kinesin, involved in microtubule-based motility. *Cell.* 42:39–50.

Vale, R. D., B. J. Schnapp, T. Mitchison, E. Steuer, T. S. Reese, and M. P. Sheetz. 1985*b*. Different axoplasmic proteins generate movement in opposite directions along microtubules *in vitro*. *Cell.* 43:623–632.

Valtorta, F., A. Villa, R. Jahn, P. DeCamilli, P. Greengard, and B. Ceccarelli. 1988. Localization of synapsin I at the frog neuromuscular junction. *Neuroscience.* 24:593–603.

Wright, B. D., J. H. Henson, K. P. Wedaman, P. J. Willy, J. N. Morand, and J. M. Scholey. 1991. Subcellular localization and sequence of sea urchin kinesin heavy chain: evidence for its association with membranes in the mitotic spindle apparatus and interphase cytoplasm. *J. Cell Biol.* 113:817–833.

Yang, J. T., R. A. Laymon, and L. S. B. Goldstein. 1989. A three-domain structure of kinesin heavy chain revealed by DNA sequence and microtubule binding analyses. *Cell.* 56:879–889.

Yankner, B. A., L. I. Benowitz, L. Villa-Komaroff, and R. L. Neve. 1990. Transfection of PC12 cells with the human GAP-43 gene: effects on neurite outgrowth and regeneration. *Mol. Brain. Res.* 7:39–44.

# CHAPTER 2

# Cloning and Localization of a Conventional Kinesin Motor Expressed Exclusively in Neurons

The work presented in Chapter 2 is the product of a collaboration with Francesca Navone. My contribution was the cloning of a second conventional kinesin heavy chain, the characterization of its gene expression and biochemical characterization and subcellular fractionation of the expressed protein. Nora Hom-Booher contributed to the library screening and sequencing work. I showed that there is in fact more than one gene in the human genome that encodes a conventional kinesin and that this new kinesin is expressed only in neural tissue (hence the name neuronal KHC or nKHC). Francesca used the antibodies that I generated to immunolocalize our previously characterized kinesin (termed ubiquitous KHC or uKHC in this chapter) as well as nKHC in brain slices as well as dissociated hippocampal neurons. This chapter has been reproduced from the journal, Neuron, 1994, vol. 12, pp. 1059-1072 by copyright permission of Cell Press.

# Cloning and Localization of a Conventional Kinesin Motor Expressed Exclusively in Neurons

**Joshua Niclas,* Francesca Navone,† Nora Hom-Booher,* and Ronald D. Vale***
*Departments of Pharmacology and Biochemistry
University of California
San Francisco, California 94143
†CNR Center of Cytopharmacology
Department of Medical Pharmacology
Milano
Italy

## Summary

**Kinesin is a microtubule-based motor protein involved in organelle transport in neuronal and nonneuronal cells. Although a single kinesin motor has been thought to serve all cell types, we document here that neurons express a second conventional kinesin heavy chain (nKHC) that is 65% identical in amino acid sequence to the ubiquitously expressed kinesin heavy chain (uKHC). By preparing antibodies which distinguish between the two KHCs, we demonstrate that nKHC is a nucleotide-dependent microtubule-binding protein which partially cofractionates with membrane organelles. Immunolocalization experiments show that nKHC is distributed throughout the CNS but is highly enriched in subsets of neurons. In hippocampal neurons in culture, uKHC is distributed uniformly throughout the neuron, whereas nKHC is selectively concentrated in the cell body. These results demonstrate that mammalian neuronal tissue contains two conventional kinesin motors which may serve distinct functions in microtubule-based transport.**

## Introduction

Kinesin, a mechanochemical enzyme that moves toward the plus ends of microtubules in vitro, has been proposed to transport membranous organelles from the cell body toward the nerve terminal (anterograde fast axonal transport). A growing body of evidence substantiates this claim. First, immunocytochemical staining (Hirokawa et al., 1991) and biochemical studies (Schnapp et al., 1992) indicate that at least a subset of the kinesin in axons is tightly associated with membrane vesicles. Second, antibodies to kinesin inhibit organelle transport along microtubules when added to squid axoplasm (Brady et al., 1990). Finally, mutations in the kinesin gene in Drosophila (Gho et al., 1992), as well as reduction in kinesin levels by antisense oligonucleotide treatment (Ferreira et al., 1992; Amaratunga et al., 1993), produce phenotypic defects that are consistent with a role of kinesin in transporting macromolecules to the nerve terminal.

The biochemical properties of kinesin have been characterized in great detail (for reviews see Schroer and Sheetz, 1991; Brady, 1991; Skoufias and Scholey, 1993). Kinesin is a dimer of two identical heavy chains of ~120 kDa; in addition, the majority of kinesin isolated from brain contains two light chains of ~62 kDa (Kuznetsov et al., 1988; Bloom et al., 1988; Hackney et al., 1991; Cyr et al., 1991). The heavy chain contains three distinct domains: an N-terminal globular domain that contains ATP- and microtubule-binding sites (Yang et al., 1989), a long α-helical coiled coil domain that enables the two heavy chains to dimerize (De Cuevas et al., 1992), and a small globular tail domain at the C-terminus. The N-terminal domain expressed as a fusion protein in Escherichia coli transports microtubules along a glass surface, indicating that it serves as the functional motor domain of kinesin (Yang et al., 1990). The functions of the remainder of the molecule are still poorly defined, although the C-terminal globular domain as well as perhaps a portion of the α-helical coiled coil are thought to interact with the 60 kDa light chains (Hirokawa et al., 1989), microtubules (Navone et al., 1992; Andrews et al., 1993), and perhaps a membrane-bound receptor (Toyoshima et al., 1992). Kinesin heavy chain (KHC) genes have now been completely sequenced in a variety of species including Drosophila (Yang et al., 1989), squid (Kosik et al., 1990), sea urchin (Wright et al., 1991), mouse (Kato, 1990; Genbank accession number X61435), and human (Navone et al., 1992).

Since the first KHC gene was sequenced (Yang et al., 1989), a variety of other genes have been identified that contain a region of homology (28%–50% amino acid identity) with the kinesin motor domain (for reviews see Goldstein, 1991; Endow and Titus, 1992). These newly described kinesin-like proteins, however, show no amino acid homology outside of the KHC motor domain. For the sake of clarity, we use the term "conventional kinesin" to signify KHCs that exhibit homology throughout their length to the Drosophila KHC prototype which was first sequenced. The term "kinesin-related proteins" is used in reference to proteins that share homology with Drosophila KHC only within the motor domain. The majority of kinesin-related proteins characterized to date appear to be involved in force-generating events in mitosis and meiosis (Endow and Titus, 1992; Goldstein, 1993; Skoufias and Scholey, 1993); however, some kinesin-related proteins such as unc-104 from Caenorhabditis elegans participate in axonal transport of organelles (Hall and Hedgecock, 1991). The superfamily of kinesin motors appears to be large, with at least 11 members present in a single organism (Drosophila) (Endow and Hatsumi, 1991; Stewart et al., 1991).

Although many kinesin-related proteins have been documented, only one conventional kinesin gene has been uncovered within any given species. Hence, it has been believed that a single conventional kinesin motor powers anterograde organelle transport in a variety of cells and tissues. In this study, however, we show that mammals contain two genes which encode

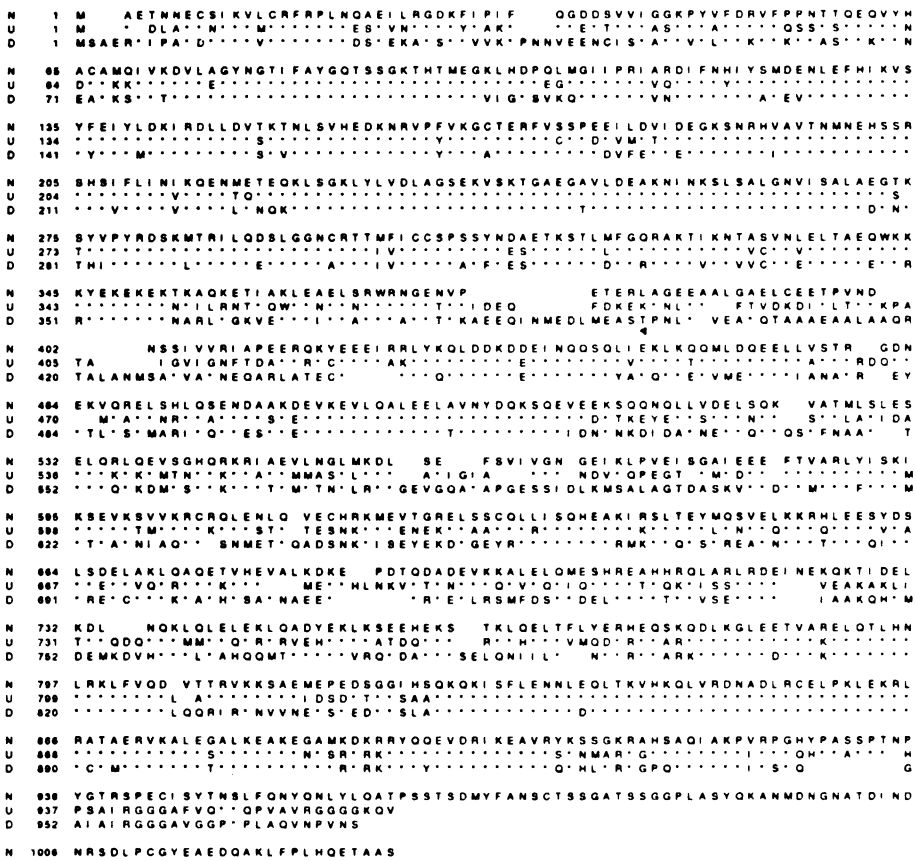


Figure 1. Alignment and Comparison of the Amino Acid Sequences of Human and Drosophila KHCs

Hippocampal library KHC (nKHC) (N), human placental library KHC (uKHC) (U), and Drosophila KHC (D). Amino acids are numbered in the left margin. Asterisks represent amino acid identity to the hippocampal KHC (nKHC), and blank spaces represent gaps that were introduced to maximize homology.

conventional kinesins. This is demonstrated by the cloning and sequencing of a second conventional human KHC gene that is distinct from the human KHC gene which we characterized in a prior study (Navone et al., 1992). Unlike the previously described KHC gene, which is expressed in all tissues examined, this newly identified KHC gene is expressed only in neurons. By preparing polyclonal antibodies that react selectively with either the ubiquitous KHC (uKHC) or the neuronal KHC (nKHC), we show that both KHC proteins are present in mammalian brain in approximately equal amounts, both exhibit nucleotide-dependent binding to microtubules, and both cosediment to a similar extent with membranous organelles. Immunolocalization studies on frozen rat brain sections show that nKHC is present throughout the brain, but is particularly enriched in subsets of neurons. In hippocampal neurons in culture, nKHC is present in cell bodies, dendrites, and axons, but is less abundant in growth cones. This newly uncovered kinesin may be involved in microtubule-based transport activities that are unique to neuronal cells.

## Results

### Cloning and Sequencing of a Second Human KHC Gene

We previously sequenced a cDNA encoding an entire conventional KHC from a human placental library (Navone et al., 1992). At approximately the same time, Adams et al. (1991) obtained a partial sequence (279 bp) of a cDNA (EST257) derived from a human hippocampal library; unexpectedly, we found that the sequence of EST257 differed from that which we obtained from the corresponding region of our human KHC cDNA. These findings suggested either that there is a second conventional KHC gene or that these two distinct cDNAs were derived by alternative splicing of a single transcript.

To investigate this question further, we sought to obtain a full-length cDNA containing the EST257 sequence from a human hippocampal cDNA library. Hybridization screenings using a 140 bp probe corresponding to the 5′ end of the 1.5 kb EST257 yielded two partial cDNA clones, 25 and 1b1. Clone 25, a

2.7 kb cDNA, contained 2020 bp of an open reading frame and 590 bp of a 3'-untranslated region that did not include a poly(A) tail. The sequence of this clone was identical to that of EST257 in the overlapping region. Clone 1b1, a 2.6 kb cDNA, contained 148 bp of 5'-untranslated sequence and a start codon; the 3' end of clone 1b1 was identical to the sequences of clone 25 and EST257 in the overlapping region. Clone 1b1, however, suffered a 29 bp deletion (from comparison with the placental library KHC sequence) that created a frame shift in the sequence. To obtain the missing sequence (nucleotides 404–432), primers flanking the deletion were used to amplify this region from a human whole-brain library using the polymerase chain reaction (PCR; see Experimental Procedures). To create a complete cDNA clone, the deleted region in clone 1b1 was replaced with the PCR product prior to ligating clones 1b1 and 25 together via an XhoI site at position 2420.

The hippocampal library cDNA encodes a predicted polypeptide of 1032 amino acids (the complete nucleotide sequence is available in GenBank under accession number U06698). The amino acid sequence of this gene is conserved throughout its length to the placental library KHC (65.3%) and Drosophila KHC (54%), indicating that this cDNA encodes a protein product that should be classified as a conventional KHC (Figure 1). A secondary structure prediction (Finer-Moore and Stroud, 1984) from the hippocampal library KHC amino acid sequence suggests that this protein, like the placental library KHC (Navone et al., 1992), contains an N-terminal ~410 amino acid globular motor domain and an ~180 amino acid C-terminal globular domain separated by an amphipathic helix which is predicted to form an α-helical coiled coil. Several regions throughout the sequence, particularly in the motor domain, display long stretches of nearly complete amino acid identity. Characteristic features of conventional kinesin, such as the phosphate-binding loop of the ATP-binding site (86–102) and a helix-breaking proline that creates a hinge in the middle of the α-helical coiled coil (amino acid 573), are also found in the hippocampal library KHC. A unique feature of the hippocampal library KHC sequence is that it contains a stretch of 69 amino acids at the very C-terminus which is absent in both the placental library KHC and Drosophila KHC.

Southern blot analysis and chromosome mapping experiments confirm that placental library KHC and brain library KHC are encoded by distinct genes. When Southern blots of restriction enzyme-digested HeLa DNA were hybridized with N-terminal or C-terminal domain probes from the two cDNAs, different patterns of bands were observed (data not shown). With certain restriction enzymes, single hybridization bands were observed for both cDNAs, implying that each is present as a single copy in the human genome. In chromosome mapping studies, the placental library cDNA hybridized to a region on mouse chromosome 18 which is syntenic with human chromosome 18q (Justice et al., 1992). The hippocampal library cDNA, on the other hand, hybridized to a region on mouse chromosome 2 that is syntenic with human chromosome 2 (N. Jenkins and N. Copeland, National Cancer Institute, personal communication).

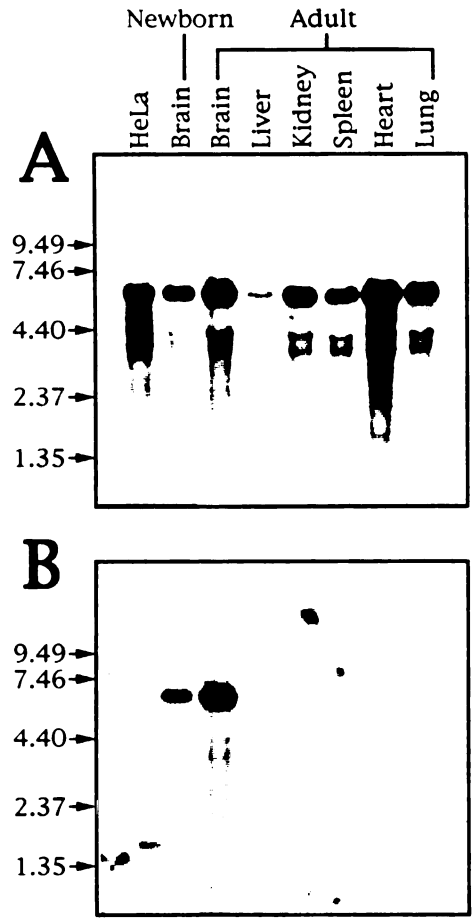



Figure 2. Tissue-Specific Expression of the Two Human KHC Genes

A Northern blot of HeLa poly(A)$^+$ RNA (3 μg) and various rat total RNA samples (10 μg) were probed with the complete human placental library KHC cDNA (uKHC) (A), or with the partial human hippocampal library KHC cDNA, EST257 (nKHC) (B). Lane 1, HeLa poly(A)$^+$ RNA; lane 2, newborn brain; lane 3, adult brain; lane 4, adult liver; lane 5, adult kidney; lane 6, adult spleen; lane 7, adult heart; lane 8, adult lung. Molecular size standards (0.24–9.5 kb ladder) are indicated on the left side.

### Tissue-Specific Expression of the Two Human KHC Genes

Northern blot analysis of total RNA from various rat tissues and poly(A)$^+$ HeLa RNA revealed that the placental and hippocampal library KHC genes have different tissue expression patterns. Whereas the placental library KHC gene is expressed in brain, liver, kidney, spleen, heart, lung, and HeLa cells, the hippo-

campal library KHC is expressed only in brain tissue (Figure 2). Even longer exposures (7 day) did not reveal an mRNA that hybridized with the hippocampal library KHC cDNA in the nonneuronal tissues tested. Based upon these findings (as well as immunoblotting and immunostaining experiments to be presented later), the placental library KHC and the hippocampal library KHC will be referred to as uKHC and nKHC, respectively.

Both the uKHC and nKHC cDNAs hybridized most strongly to 6.2 kb mRNAs. In addition, the uKHC cDNA hybridized to 4.3 kb, 3.9 kb, and 1.7 kb transcripts in all tissues examined. The nKHC cDNA also hybridized, albeit less strongly, to these smaller size mRNAs in brain tissue. Probes corresponding to the N-terminal and C-terminal domains of uKHC hybridized to the three largest transcripts (which are all large enough to encode a full-length KHC), whereas only the motor domain probe hybridized to the 1.7 kb species (data not shown). The finding that the cDNA probes hybridize with multiple RNA species, but only one genomic DNA fragment under similar hybridization conditions, suggests that the single uKHC and nKHC genes give rise to multiple transcripts.

### Preparation of Antibodies Specific for uKHC and nKHC

To characterize the uKHC and nKHC proteins, antibodies that react specifically against each KHC were generated. The less conserved regions of the α-helical coiled coil domains of the two KHCs (amino acids 523–773 of uKHC and amino acids 527–775 of nKHC) were cloned into the pMALcRI vector to create maltose-binding protein (MBP) fusions, which were then expressed in E. coli and used as antigens for immunization of rabbits. The polyclonal antisera raised against these purified antigens, however, reacted against both kinesin fusion proteins probably owing to the presence of anti-MBP antibodies as well as cross-reacting anti-KHC stalk antibodies. In addition, the anti-MBP-nKHC antiserum was found to react with both rat brain and kidney homogenates on immunoblots indicating a lack of specificity. To remove cross-reactive antibodies, the anti-MBP-uKHC antiserum was applied to a MBP-nKHC affinity column, whereas the anti-MBP-nKHC antiserum was applied to a MBP-uKHC affinity column. The flow-throughs from these columns were specific for their respective antigens (data not shown).

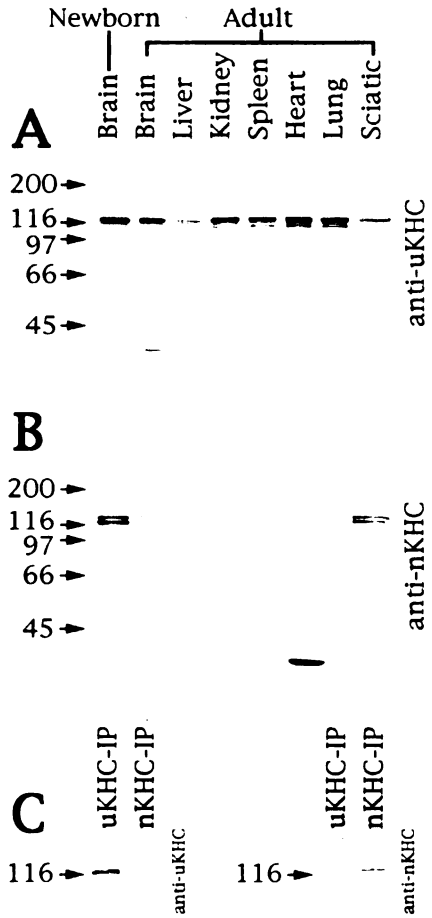



Figure 3. Tissue Distribution of the uKHC and nKHC Proteins

Immunoblots of various rat tissue extracts were probed with either anti-uKHC (A) or anti-nKHC (B) antiserum. The protein loaded per lane in (A) and (B) was 30 and 80 μg, respectively (except for the sciatic nerve lanes which contained ~40 μg). Lane 1, newborn brain; lane 2, adult brain; lane 3, adult liver; lane 4, adult kidney; lane 5, adult spleen; lane 6, adult heart; lane 7, adult lung; lane 8, adult sciatic nerve. Levels of expression of the two KHCs in sciatic nerve cannot be compared with those of the other tissues since the sciatic nerve samples were not run on the same immunoblot as the rest of the samples. Molecular size standards (kDa) are shown on the left side. In (C), immunoblots of anti-uKHC (uKHC-IP) and anti-nKHC (nKHC-IP) immunoprecipitates from rat brain high speed supernatants were probed with either affinity purified anti-uKHC antiserum or anti-nKHC antiserum at 1:100 dilutions. Note that very little nKHC is present in the anti-uKHC immunoprecipitate, and very little uKHC is present in the anti-nKHC immunoprecipitate, implying that the two KHCs selectively form homodimers.

### Tissue Distribution of uKHC and nKHC Proteins

The levels of expressed protein from the uKHC and nKHC genes in newborn brain, adult brain, liver, kidney, spleen, heart, lung, and sciatic nerve tissue homogenates were examined by immunoblot analysis. Consistent with the RNA analysis, anti-uKHC antiserum reacted against an ~120 kDa polypeptide in all of the above tissues (Figure 3A) as well as testes (data not shown). The anti-nKHC antiserum, on the other hand, reacted only against brain and sciatic nerve tissue as well as a low molecular weight band in heart tissue. In brain and sciatic nerve tissue, it recognized a doublet of ~120 kDa and ~133 kDa (see Figure 5b). The <45 kDa band seen in heart is probably an artifact, since Northern blot analysis showed that nKHC is not expressed in this tissue. The anti-nKHC antiserum did not react with proteins from testes (data not shown). By combining the two antisera and immunoblotting brain and kidney tissue, it is clear that the lower poly-

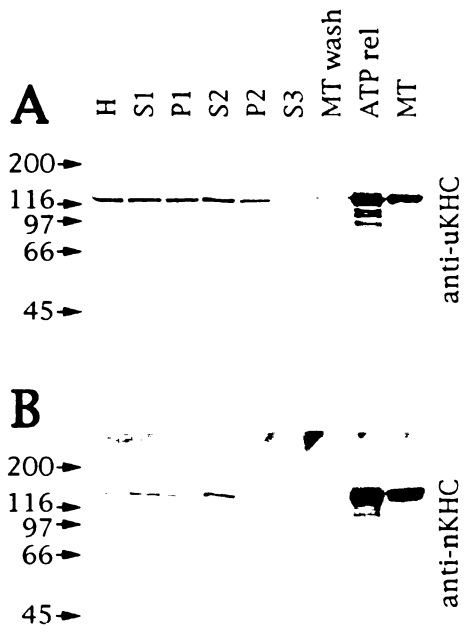



Figure 4. Cofractionation of uKHC and nKHC with Microtubules and Membranes

Immunoblots of fractions from a rat neuronal kinesin preparation (see Experimental Procedures for details) were blotted with either anti-uKHC (A) or anti-nKHC (B) antiserum. Lane 1, 40 μg of brain homogenate; lane 2, 40 μg of S1 (low speed [27,000 × g/hr] supernatant); lane 3, 40 μg of P1 (low speed [27,000 × g/hr] pellet); lane 4, 40 μg of S2 (high speed [250,000 × g/hr] supernatant); lane 5, 40 μg pf P2 (high speed [250,000 × g/hr] pellet); lane 6, 40 μg of S3 (microtubule-depleted S2); lane 7, MT wash (20 μl of nucleotide-free buffer wash of microtubules); lane 8, ATP rel (release) (10 μl of supernatant after a 10 mM Mg-ATP incubation and centrifugation of microtubules); lane 9, MT (10 μl of resuspended final microtubule pellet). Molecular size standards (kDa) are shown at the left.

peptide recognized by anti-nKHC antiserum and the polypeptide recognized by anti-uKHC antiserum have the same mobility in SDS-polyacrylamide gels (data not shown). The lower band recognized by anti-nKHC antiserum, which varied somewhat in amount from preparation to preparation, was not a cross-reaction with uKHC, since a band of this size did not appear in the other tissues tested. Since the nKHC cDNA predicts a protein of 1032 amino acids versus 963 amino acids for uKHC, the upper band most likely corresponds to the full-length product, whereas the lower band probably represents a degraded or specifically processed product.

The relative amounts of nKHC and uKHC in human adult brain tissue were determined by immunoblotting a human brain homogenate alongside known quantities of MBP-uKHC or MBP-nKHC fusion proteins. Quantitative densitometry of the signals revealed that adult human brain contains slightly more uKHC (3.6 pmol per mg total protein) than nKHC (2.4 pmol of both 120 and 133 kDa polypeptide bands per mg total protein).

We also examined whether nKHC and uKHC selectively form homodimers with their own polypeptides. To distinguish between homo- and heterodimer formation, nKHC and uKHC were immunoprecipitated from rat brain high speed supernatants, and the immunoprecipitated material was immunoblotted with the anti-nKHC and anti-uKHC antibodies. Figure 3C shows that the material immunoprecipitated with anti-nKHC antibodies contained mostly nKHC and very little uKHC; the converse results were obtained with the material immunoprecipitated with anti-uKHC antibodies. Thus, both KHCs preferentially form homodimers.

### Cofractionation of uKHC and nKHC with Microtubules and Membranes

To examine the association of nKHC and uKHC with membranes and microtubules, the partitioning of the two KHCs into membrane and microtubule fractions was monitored during the course of a kinesin purification from rat brain tissue. Figure 4 shows that similar amounts of uKHC and nKHC (38% and 22%, by densitometry) cosedimented with membranous organelles during a high speed (250,000 × g/hr) centrifugation. The majority of both KHCs (62% for uKHC; 78% for nKHC), however, remained in the supernatant. The supernatant was used to purify kinesin by microtubule affinity. Addition of microtubules to an ATP-depleted supernatant followed by centrifugation led to an almost quantitative depletion of both KHCs from the soluble fraction. Both microtubule-bound KHCs did not dissociate during an incubation with nucleotide-free buffer but were released after addition of 10 mM Mg-ATP (Figure 4). Quantitative immunoblotting and densitometry revealed that the ATP release fraction contained more uKHC (70 pmol/mg) than nKHC (39 pmol/mg). These results demonstrate that both nKHC and uKHC are nucleotide-dependent microtubule-binding proteins and thus are likely to be bona fide motor proteins.

### Distribution of nKHC Immunoreactivity in the CNS

The distribution of nKHC in the CNS was examined by indirect immunofluorescence on frozen sections of rat brain using affinity purified antibodies that are specific for neuronal kinesin (Figure 5). A diffuse fluorescence could be detected in virtually all regions of the gray and white matter examined, which included the cerebral cortex, hippocampus, and diencephalon. This fluorescence depended upon antibodies directed against nKHC, since only a very weak fluorescence, almost indistinguishable from the autofluorescence of the tissue, was observed when the sections were treated with secondary antibodies alone (data not shown). Figures 5a and 5b show a frozen coronal section of the CA4-CA3 region of rat hippocampus in the area of the hilus which was double-labeled with the affinity purified antibody against nKHC and a monoclonal antibody against MAP2, a microtubule-associated protein found in the perikarya and den-

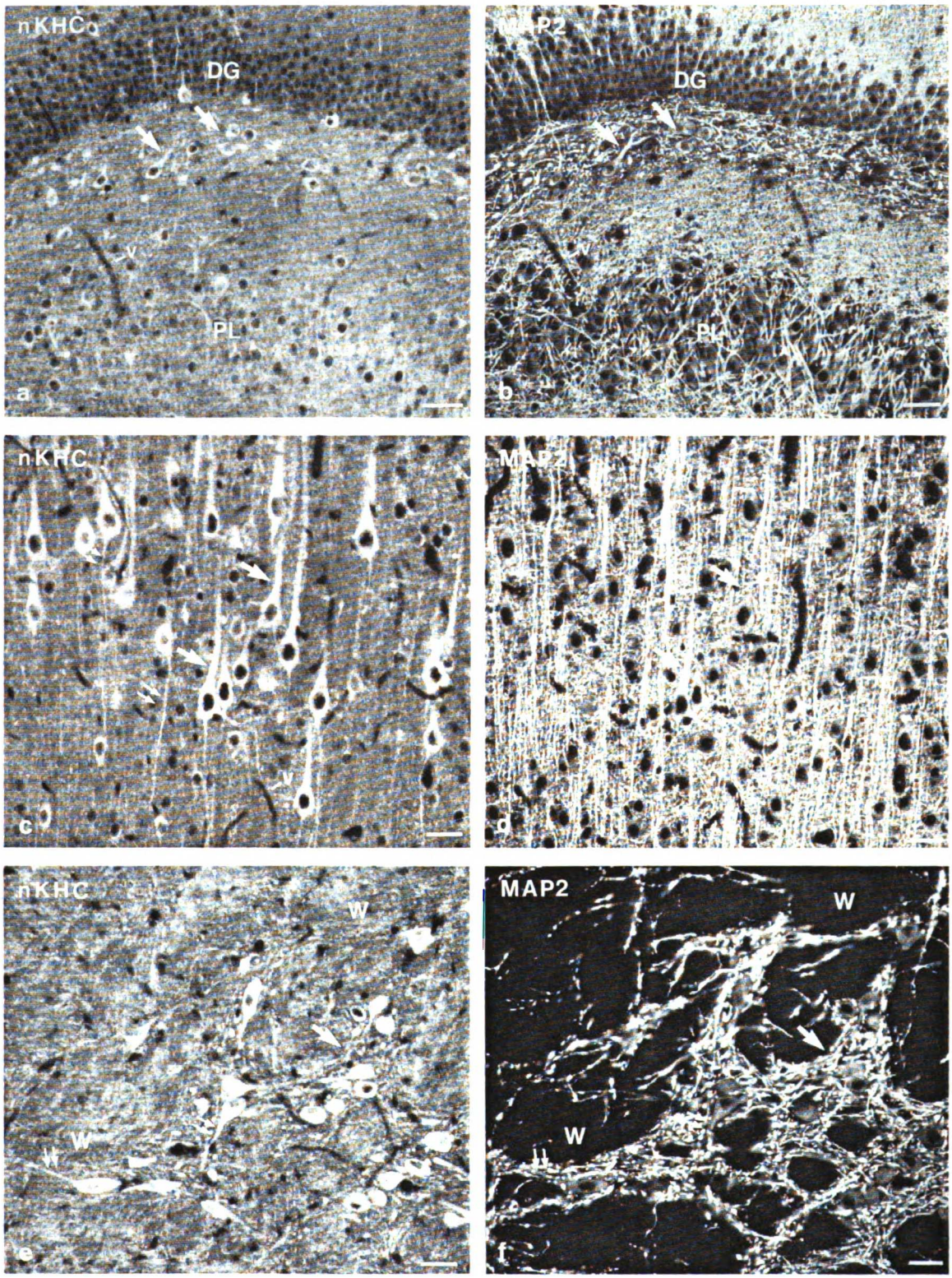



Figure 5. nKHC and MAP2 Immunofluorescence in 10 μm Thick Coronal Sections of Rat Brain

In this picture, immunoreactive material appears white. Sections were double-labeled with affinity purified anti-nKHC polyclonal antibodies (a, c, and e) and with the monoclonal anti-MAP2 antibody (b, d, and f).

(a and b) A section of the hippocampus in the region of the hilus. The pyramidal cell layer of the CA4–CA3 region (PL), the dentate

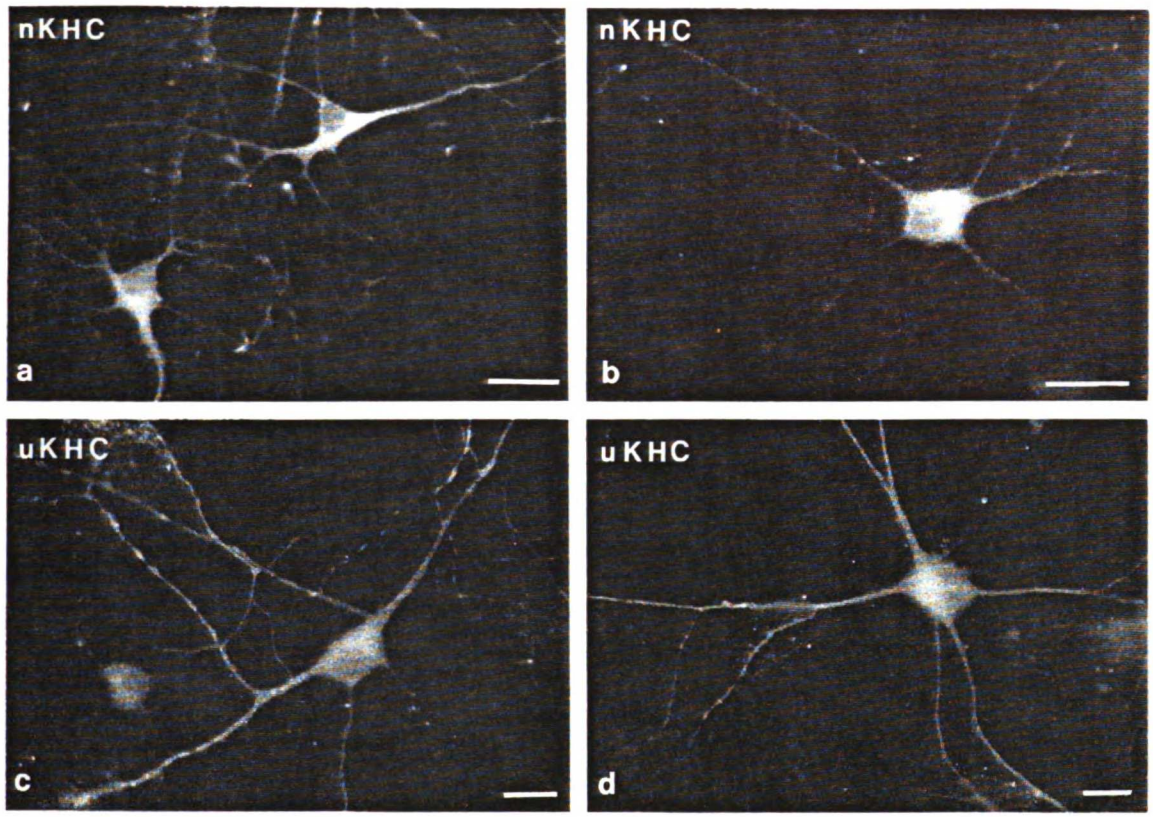



Figure 6. Distribution of nKHC and uKHC in Primary Cultures of Hippocampal Neurons from Newborn Rats

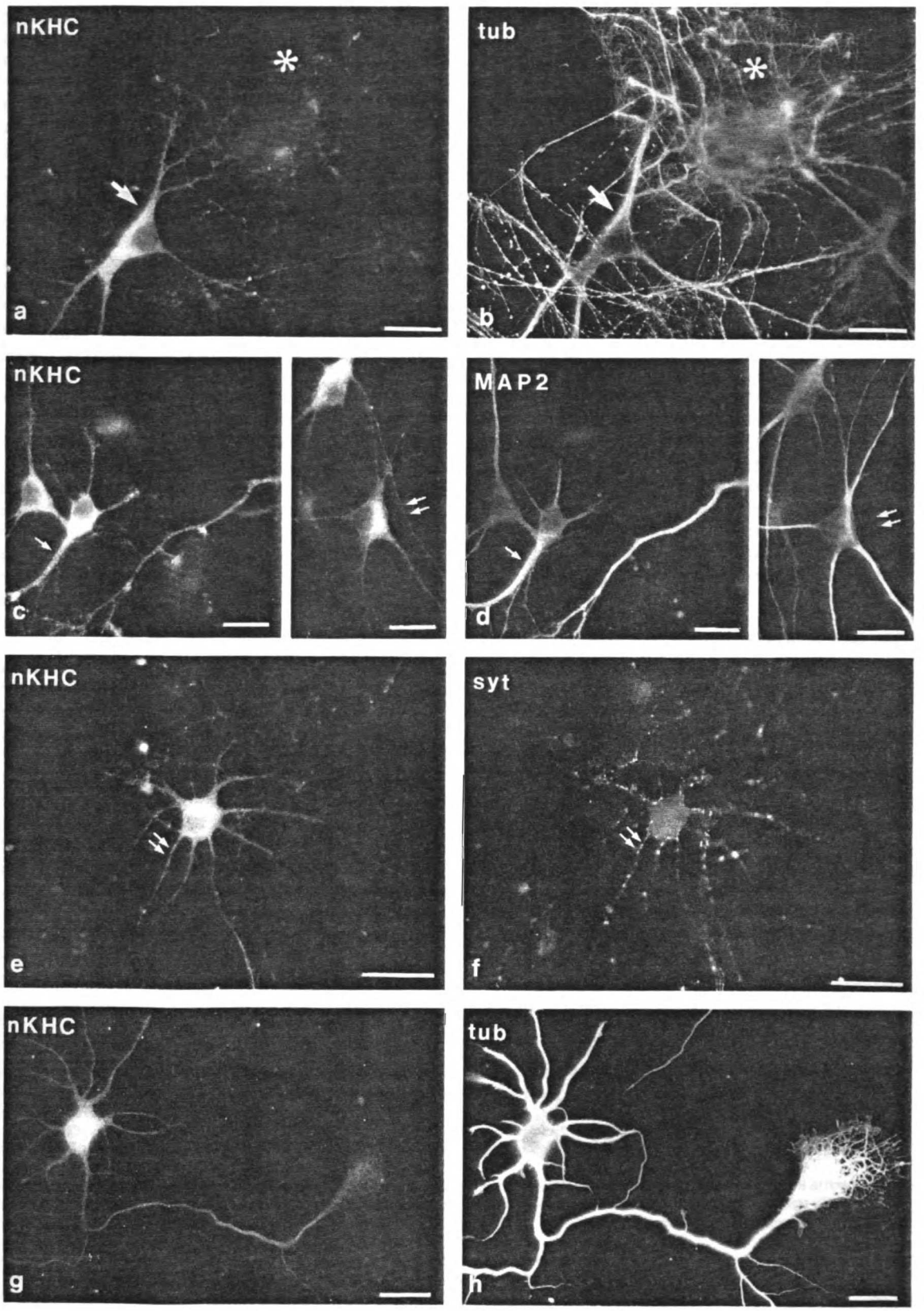
Immunofluorescence microscopy shows that uKHC (a and b) is uniformly distributed in the perikaryon and the neurites, whereas nKHC (c and d) is more abundant in the cell body. White halos that appear in the background represent nonspecific staining of cellular fragments and dirt on the slide. These white halos are particularly evident in (c) and (d), where they may be due to fragments of astrocytes which display uKHC, but not nKHC, immunoreactivity. Bars, 17 μm.

drites (De Camilli et al., 1984). A uniform distribution of nKHC immunoreactivity was found in the pyramidal cell layer, in the dentate gyrus, and throughout the neuropile (Figure 5a). A few neurons located just below the granule cells of the dentate gyrus stand out owing to the intense fluorescence of their perikarya and dendrites. These cells, some of which can be clearly recognized in the same section immunolabeled for MAP2 (Figure 5b), are likely to be the cells of the hilus of the dentate gyrus (Amaral and Witter, 1989). Figures 5c and 5d show a frozen section of the cerebral cortex double-labeled with anti-nKHC and anti-MAP2 antibodies, respectively. In contrast with MAP2 staining, which is similar in most cell bodies, neuronal kinesin immunoreactivity is particularly strong in a subset of cortical neurons. The fine processes that arise from the basal portion of the pyramidal neurons and that are intensely fluorescent with the anti-nKHC antibody are probably axons. Figures 5e and 5f show a frozen section of the diencephalic region of rat brain situated ventral to the thalamus. All neurons are intensely stained by anti-nKHC antibodies, and a uniform immunoreactivity is also evident in the surrounding neuropile. nKHC immunoflu-

gyrus (DG), and a blood vessel (v) are indicated. Below the dense granule cell layer in the dentate gyrus are the cells of hilus, which show a bright immunofluorescent signal for nKHC (arrows); they can also be recognized in (b), which is stained for MAP2.

(c and d) A group of pyramidal cells in layer V of the cerebral cortex. nKHC is particularly concentrated in some pyramidal cells, where it is evident in the cell bodies, the thick apical dendrites (arrows), and the fine axonal processes that arise from the basal portion of the perikarya (double arrows). Specific, although less intense, nKHC immunoreactivity is also present in the neuropile. MAP2 staining in (d) reveals the location of neuronal cell bodies and apical dendrites. v, unstained blood vessel.

(e and f) A section of the diencephalon situated ventral to the thalamus. The distribution of MAP2 immunoreactivity shows that neuronal cell bodies are surrounded by a network of dendritic processes (arrow) as well as tracts of white matter (W) that are MAP2 negative. nKHC immunoreactivity is homogeneously distributed throughout the gray and white matter, but is particularly intense in neuronal perikarya and the proximal portion of neuronal dendrites (double arrows). Bars, 40 μm (a and b); 30 μm (c–f).


nKHC
a
tub
b
nKHC
c
MAP2
d
nKHC
e
syt
f
nKHC
g
tub
h

orescence is present in MAP2-positive cell bodies and dendrites as well as MAP2-negative bundles of myelinated axons.

### Localization of uKHC and nKHC in Primary Cultures of Hippocampal Neurons

To obtain more information on the subcellular distribution of nKHC and uKHC, isoform-specific antibodies were used to stain cultured newborn hippocampal neurons. Whereas uKHC was distributed uniformly throughout the cell body and processes (Figures 6c and 6d), nKHC was distinctly more concentrated in the soma than in the neurites (Figures 6a and 6b; Figures 7a, 7c [right panel], and 7e). Within the cell body, nKHC appeared to be concentrated in the perinuclear region; this is particularly evident in neurons with relatively large and flat cell bodies, such as the one shown in Figure 7c (right panel).

The subcellular distribution of nKHC was further explored by comparing its localization with that of well-known markers for different subcellular compartments of neurons by double-label immunofluorescence. Staining of newborn rat hippocampal cultures with an anti-tubulin antibody (Figure 7b) revealed the outlines of a pyramidal neuron cell body surrounded by an intricate meshwork of axons and dendrites; astrocytes that lie beneath the neurons in these cultures can also be seen (Figure 7b, asterisk). Concomitant staining with the anti-nKHC antibody revealed immunoreactivity in pyramidal neurons but not in glial cells (Figure 7a), indicating that nKHC is a neuron-specific protein. Anti-uKHC antibodies, on the other hand, stained the glial cells in this culture (data not shown). Colocalization of nKHC and MAP2 shows that MAP2 is present in higher amounts in dendritic trunks than in cell bodies, whereas the converse was true for nKHC (Figures 7c and 7d). The anti-nKHC antibody also stained slender, MAP2-negative processes that are likely to be axons (double arrows in Figure 7c, right panel). To verify that nKHC is in both dendrites and axons, nKHC was localized in embryonic rat hippocampal neurons which extend morphologically distinguishable axons and dendrites in vitro (Banker and Cowan, 1977; Bartlett and Banker, 1984; Matteoli et al., 1992) (Figures 7g and 7h). Anti-tubulin staining outlines an embryonic neuron that has several shorter dendrites and a long axon that terminates in a growth cone-like structure (Mundigl et al., 1993). nKHC is concentrated in the cell body, but is also detectable in the axon and dendrites. However, staining is weak or absent in the lamellae of the growth cone-like structure itself. Consistent with this observation, the distribution of nKHC differs from that of synaptotagmin (Matthew et al., 1981), a synaptic vesicle-associated protein which is concentrated at axo-somatic and axo-dendritic contacts (Figures 7e and 7f).

## Discussion

### Expression of Two Conventional KHCs in Mammalian Brain

In this study, we have characterized a human KHC cDNA that is distinct from the human KHC cDNA which we previously isolated (Navone et al., 1992). The two human KHCs, which display a high degree of amino acid identity in their motor and nonmotor domains, are clearly encoded by different genes based on Southern blotting, chromosome mapping, and sequence analysis. The isolation of the nKHC gene represents the first clear evidence that there is more than one conventional KHC within the kinesin superfamily of motor proteins.

The two human KHCs differ dramatically in their tissue expression patterns. Whereas the uKHC gene is expressed in all tissues examined, the nKHC gene is expressed only in neurons. Surprisingly, however, the patterns of transcripts from nKHC and uKHC genes are very similar to one another (6.2, 4.3, 3.9, and 1.7 kb in size). This suggests that the nKHC and uKHC genes most likely arose from a duplication of a common ancestral gene and that nKHC acquired neuronal-specific promoter elements while maintaining similar transcription initiation/processing signals.

The three larger transcripts of the two KHC genes could potentially encode complete nKHC or uKHC proteins; differences between these mRNAs may reside in the untranslated regions, since heterogeneity in the coding region was never encountered in several

---

Figure 7. Double Immunofluorescence Micrographs Comparing the Distributions of nKHC with Tubulin, MAP2, and Synaptotagmin

The primary cultures of hippocampal neurons in (a)–(f) were from newborn rats, whereas (g) and (h) show neurons isolated from embryonic rats.

(a) shows nKHC labeling of a neuronal cell body (arrow) and its processes, but does not reveal specific staining of an astrocyte (asterisk) which can be seen by anti-tubulin staining in (b). The network of immunofluorescent processes superimposed on the glial cell originates from neurons located outside of the photographic field.

Double-labeling with nKHC and MAP2 in (c) and (d) show that MAP2 is more abundant in dendritic processes (small arrow) than in the cell body, whereas nKHC is more concentrated in the perikaryon. The flat neuron in the right side of (c) shows that nKHC is more concentrated in the perinuclear area of the cytoplasm. Double arrows indicate a fine neuronal process that is stained by anti-nKHC, but not by anti-MAP2, antibodies (see right panel in [d]) and hence is probably an axon.

(e) and (f) reveal distinct distributions of nKHC and of synaptotagmin, a synaptic vesicle membrane protein. Double arrows indicate a portion of a neuronal process where immunoreactivity for nKHC is uniformly distributed, whereas synaptotagmin immunoreactivity shows a punctate pattern.

(g) and (h) show an embryonic hippocampal neuron double-labeled with anti-nKHC and anti-tubulin antibodies. The growth cone-like structure delineated by the tubulin staining shows only a very faint immunofluorescence for nKHC. Bars, 22 μm.

nKHC and uKHC cDNAs that were isolated and sequenced. The 1.7 kb mRNA, on the other hand, does not hybridize to KHC probes that do not include the N-terminal motor domain. Interestingly, the *dilute* gene from mouse (which encodes a putative myosin motor) also has several transcripts, including one that corresponds only to the motor region of the protein (Mercer et al., 1991). The Drosophila KHC gene, on the other hand, only produces a 4 kb mRNA (Yang et al., 1988), implying that the mammalian KHC genes have acquired the capability for more complex transcriptional and/or translational control.

The human nKHC gene characterized in this study resembles other kinesin cDNAs isolated from mouse brain libraries. In a screen for cDNA clones with specific expression patterns in mouse brain, Kato (1990) isolated a cDNA (DN40) that was expressed predominantly in the cerebral and cerebellar cortices and the motor trigeminal nucleus. Subsequent sequencing by Kato revealed that DN40 encodes a conventional KHC (unpublished but available via Genbank accession number X61435). This mouse KHC is more homologous to human nKHC (94% amino acid identity) than human uKHC (71% amino acid identity) and also contains the additional C-terminal stretch of 69 amino acids that is present in nKHC but not in uKHC. DN40 may therefore represent the mouse homolog of human nKHC, although it was not established whether DN40 is expressed exclusively in neuronal tissue. In another study by Aizawa et al. (1992), a PCR fragment was isolated that encodes 156 amino acids of a mouse gene (KIF5) which is expressed only in brain and which demonstrates 88.5% and 98.7% amino acid identity to the motor domains of human uKHC and human nKHC, respectively. KIF5, which is clearly not the mouse homolog of uKHC based on its expression pattern, also differs from mouse DN40 (93.6% amino acid identity in the overlapping region). These results suggest that there may be two neuron-specific KHC genes, although it is still unclear whether the KIF5 gene truly encodes a conventional KHC since its nonmotor domain has not been sequenced.

### Properties of the nKHC and uKHC Proteins

To obtain more information on the amounts and properties of the two KHCs in the CNS, it is essential to have antibodies that distinguish between these two isoforms. In this study, we have prepared polyclonal antibodies against the α-helical coiled coil domains of the two KHCs and removed the cross-reactive antibodies using KHC affinity columns; the resultant polyclonal antibodies are highly selective for their respective KHCs. Immunoblot analysis shows that the anti-uKHC antiserum reacts against a single polypeptide of 120 kDa in all tissue homogenates examined, whereas anti-nKHC antiserum reacts against polypeptides of 133 kDa and 120 kDa only in brain and sciatic nerve homogenates. The 133 kDa polypeptide probably corresponds to the full-length product, whereas the 120 kDa polypeptide may represent a processed or degraded product.

In membrane and microtubule fractionation studies, the nKHC and uKHC gene products display similar properties. The majority of both KHCs are present in the soluble fraction although both KHCs also cosediment with membranes in a high speed centrifugation. The relative amounts of the two kinesins that partition between the high speed supernatant (78% of nKHC; 62% of uKHC) and pellet (22% of nKHC; 38% of uKHC) are consistent with the estimates of soluble and membrane-bound kinesin documented in other studies (Hollenbeck, 1989; Leopold et al., 1992). Whether the two KHCs interact with different types of membranes cannot be ascertained from this limited subcellular fractionation study. In addition, both uKHC and nKHC are depleted from high speed supernatants by microtubule affinity under conditions of ATP depletion and adenylyl-imidodiphosphate addition, and both KHCs require ATP to be released from the microtubules. These properties suggest that both KHCs are microtubule-based motor proteins.

Previous work has suggested that purified kinesin from neuronal tissue contains a mixture of heavy chain isotypes. In SDS-polyacrylamide gel electrophoresis, KHC often runs as a doublet, and two-dimensional gel electrophoresis reveals several KHC species that differ in charge as well as molecular weight (Wagner et al., 1989). Although some of these differences are probably caused by posttranslational modifications, it is clear from this study that KHC diversity observed in purified kinesin preparations is also generated by the presence of two different gene products which differ in size and charge (predicted pIs of 5.53 for nKHC and 6.05 for uKHC). The presence of two distinct KHCs in most neuronal kinesin preparations should be considered as a factor that can potentially complicate the quantitative analysis of kinesin's ATPase, motility, and binding interactions with microtubules and membranes.

### Distribution and Biological Roles of KHCs in the Nervous System

Immunostaining of frozen brain sections shows that nKHC is found in neurons throughout the CNS, although subpopulations of neurons are particularly enriched in this motor protein. Immunoblot analysis also reveals the presence of nKHC in peripheral nerves indicating that nKHC serves a general function in the nervous system. Glia, at least in primary tissue culture, express uKHC but not nKHC, indicating that the latter protein is indeed neuron specific. We have also found that uKHC and nKHC have different subcellular distributions within hippocampal neurons. Most notably, nKHC is concentrated in the cell body, in particular in the perinuclear region, whereas uKHC is more uniformly distributed between the cell body and the processes. These findings suggest that the two kinesins might bind to and transport distinct

types of organelles, although immunoelectron microscopy will be needed to explore this issue further.

Inhibition of uKHC and/or nKHC will be important for determining whether the two KHCs have distinct or overlapping functions in the nervous system. To investigate kinesin function, anti-kinesin antibodies have been used for inhibition studies (Brady et al., 1990) and antisense oligonucleotides have been used to inhibit KHC expression in hippocampal neurons in vitro (Ferreira et al., 1992) and retinal ganglion cells in vivo (Amaratunga et al., 1993). The preparation and characterization of reagents for such experiments have been predicated on the notion of there being only one KHC. In light of the present findings, however, the specificity of antibodies and antisense oligonucleotides for the two isoforms must be determined to establish whether one or both KHCs are affected in such experiments. Genetic analysis constitutes another approach toward resolving the respective roles of the two KHCs. At present, mutations in a Drosophila KHC, which appears more closely related to uKHC than nKHC based upon its size, sequence homology, and tissue distribution, have been generated. These mutant flies display impaired action potential propagation and neurotransmitter release at neuromuscular junctions, but are still capable of transporting certain membranes, including synaptic vesicles, to the nerve terminal (Gho et al., 1992). It will be interesting to determine whether a neuron-specific KHC is also present in Drosophila and what role it may have in neuronal morphology and axonal transport.

## Experimental Procedures

### Cloning and Sequencing of Neuronal KHC

The EST257 clone (Adams et al., 1991) was obtained from the American Tissue Culture Collection (#37774). To obtain a cDNA that contained the entire coding sequence, a 140 bp EcoRI–ApaI DNA fragment from the 5′ end of EST257 was radiolabeled using the random priming protocol (Feinberg and Vogelstein, 1983) and used as a probe to screen by plaque hybridization (Sambrook et al., 1989) the same human hippocampal library (Stratagene, La Jolla, CA) from which EST257 was isolated. Of the cDNAs isolated, two clones, clones 25 and 1b1, were fully characterized and sequenced.

The region of the nKHC gene that was deleted from clone 1b1 (nucleotides 404–432; see Figure 1) was isolated subsequently from a whole human brain λgt10 cDNA library (obtained from R. Myers, Stanford University) using PCR (Mullis et al., 1986). The 5′ oligonucleotide consisted of nucleotides 79–99 (see sequence in GenBank, accession number U06698) with a change at position 85 from an A to a T to create an SpeI site for cloning purposes. The 3′ oligonucleotide consisted of the reverse complement of nucleotides 496–516. The reaction was carried out by combining 2 × $10^7$ pfu of the cDNA library, 660 pmol of each oligonucleotide, and 0.2 U of Taq polymerase (Amplitaq; Cetus, Emeryville, CA) in 10 mM Tris (pH 8.3), 50 mM KCl, 2 mM $MgCl_2$, 0.2% gelatin, and 0.2 mM dNTP. The reaction was first incubated at 94°C for 10 min and then for 30 cycles at 94°C (60 s), 50°C (60 s), and 72°C (60 s). The PCR products were then cloned into pBluescript SK (Stratagene) at the SpeI and EcoRI sites. Two clones obtained from different PCR reactions were sequenced and found to be identical.

A complete cDNA (pWBC7) was created using the following strategy. To restore the deleted region, clone 1b1 was digested with NsiI (at nucleotide 191) and ApaLI (at nucleotide 466) and then ligated to the corresponding NsiI–ApaLI fragment from the PCR product. The corrected clone 1b1 (5′ half of the gene) was ligated together with clone 25 (the 3′ half of the gene) at the XhoI site (at nucleotide 2420) resulting in a 3.8 kb cDNA containing the entire coding sequence.

Sequencing templates of the clones isolated in the library screen were made by using exonuclease III to generate nested deletions (Henikoff, 1987). Both strands of the clones isolated were sequenced by dideoxy chain termination method (Sanger et al., 1977) using the Sequenase kit (United States Biochemicals, Cleveland, OH).

### Southern Blot Analysis

Genomic HeLa cell DNA (10 μg; obtained from Bruce Cree, University of California, San Francisco) was digested with either BamHI, EcoRI, or SacI and run on a 0.7% agarose gel. The gel was treated with 0.25 M HCl for 20 min; 0.5 M NaOH, 1.5 M NaCl for 30 min; 0.5 M Tris–HCl (pH 7.5), 1.5 M NaCl for 30 min and then blotted onto Hybond N nylon (Amersham, Arlington Heights, IL) with 20× SSC (3 M NaCl, 0.3 M Na-citrate). The blot was ultraviolet cross-linked (0.12 J/$cm^2$) using a Stratalinker (Stratagene) and then prehybridized (55°C) in 3× SSCP (60 mM $NaPO_4$ [pH 6.8], 45 mM Na-citrate, 0.36 M NaCl), 10× Denhardt's solution (0.2% [w/v] Ficoll 400, 0.2% [w/v] polyvinylpyrrolidone, 0.2% bovine serum albumin), 0.5% SDS, 250 mg/ml denatured salmon sperm DNA. Hybridization was performed in the same buffer as prehybridization but with 10% dextran sulfate (Pharmacia; Piscataway, NJ) and the radioactive probe at a concentration of 5 × $10^6$ cpm/ml. Placental library KHC (Navone et al., 1992) probes were as follows: N-terminal domain probe, XmaI–SacI fragment (nucleotides −137 to 1094); and C-terminal domain probe, FspI–EcoRI fragment (nucleotides 2399 to end of cDNA). Hippocampal library KHC probes were as follows: N-terminal domain probe, PstI–PstI fragment (nucleotides −37 to 1466); and C-terminal domain probe, HindIII–HindIII fragment (nucleotides 2231–3061). Blots were hybridized overnight at 55°C, washed at 65°C in 0.2× SSC, 0.1% SDS, and then exposed to Kodak XAR-5 film with intensifying screens at −80°C.

### RNA Isolation and Northern Blot Analysis

RNA was isolated from monolayers of HeLa cells with guanidine isothiocyanate followed by purification using ultracentrifugation through a cesium chloride cushion (Sambrook et al., 1989). The poly(A)$^+$ mRNA fraction was selected using oligo(dT)–cellulose chromatography (In Vitrogen Inc., San Diego, CA). RNA isolation from rat tissues (brains of 1-day-old rats as well as brain, liver, kidney, spleen, heart, and lung from adult rats) was performed according to the acid guanidinium thiocyanate–phenol–chloroform extraction method (Chomczynski and Sacchi, 1987) with modifications (Puissant and Houdebine, 1990). RNA concentration and purity were quantitated spectrophotometrically. HeLa cell poly(A)$^+$ mRNA (3 μg per lane) and rat tissue total RNA samples (10 μg per lane) were electrophoresed on 1% agarose, 0.37 M formaldehyde gels. RNA size standards were obtained from BRL Life Technologies, Inc. (Gaithersburg, MD). Ethidium bromide staining was used to confirm that RNA samples were not degraded and that the expected amount of RNA was loaded. After electrophoresis, gels were treated with 50 mM NaOH for 25 min, 1 M Tris–HCl (pH 7.5) for 30 min, and 20× SSC for 15 min and then transferred to Hybond N nylon (Amersham) with 20× SSC. After transfer, blots were ultraviolet cross-linked (0.15 J/$cm^2$) by a Stratalinker (Stratagene) and then prehybridized (55°C) in the same solution as for the Southern blots. Hybridization was performed in the same buffer as prehybridization but with 10% dextran sulfate (Pharmacia) and the radioactive probe (either the complete cDNA clone for uKHC [Navone et al., 1992]) or clone EST257 for nKHC) at a concentration of 5 × $10^6$ cpm/ml. Domain-specific probes for uKHC were made by the following restriction digests: N-terminal domain probe, XmaI–SacI fragment (nucleotides −137 to 1094); α-helical coiled coil domain probe, SacI–FspI fragment (nucleotides 1095–2398); and C-ter-

minal domain probe, FspI-EcoRI fragment (nucleotide 2399 to the end of the cDNA). Blots were hybridized at 55°C overnight, washed at 55°C in 0.2× SSC, 0.1% SDS, and then exposed to Kodak XAR-5 film with intensifying screens at −80°C.

### Preparation of Antibodies from MBP-Human KHC Fusion Proteins

DNA fragments encoding portions of the stalk region of nKHC and uKHC were synthesized using PCR. For the stalk construct of nKHC, the 5' PCR oligonucleotide included an EcoRI site and the 18 nucleotides encoding amino acids 527–532, and the 3' PCR oligonucleotide included the 18 nucleotides encoding amino acids 770–775, a stop codon, and a HindIII site. For the stalk construct of uKHC, the 5' PCR oligonucleotide included an EcoRI site and the 18 nucleotides encoding amino acids 523–528, and the 3' PCR oligonucleotide included the 18 nucleotides encoding amino acids 768–773, a stop codon, and a SalI site. The PCR reaction was carried out as described earlier. The PCR products were then cloned into pMALcRI (New England Biolabs, Beverly, MA) at the EcoRI and either the HindIII or the SalI sites.

Cells were grown at 37°C in 1 liter of Luria broth plus 0.2% glucose to $OD_{600}$ = 0.5, then induced with 3 ml of 0.1 M isopropyl-β-D-thiogalactopyranoside and grown for an additional 2 hr at 37°C. The cells were centrifuged at 4,000 × g, 4°C for 20 min and resuspended in 50 ml of TNED (10 mM Tris [pH 7.4], 200 mM NaCl, 1 mM EDTA, 5 mM dithiothreitol). The resuspended cells were frozen overnight at −20°C and thawed at 16°C before they were broken by a French press. The resulting extract was centrifuged at 8,000 × g for 30 min at 4°C. The supernatant was diluted 1:5 in TNED before loading onto an amylose resin column (New England Biolabs, Beverly, MA) at the rate of 1 ml/min. The column was washed with 8 column volumes of TNED, and the fusion protein was eluted with 50 ml of 10 mM maltose in TNED. The peak fractions were pooled and dialyzed in 10 mM HEPES (pH 6.9), 50 mM NaCl, and 1 mM dithiothreitol for 8 hr at 4°C.

Polyclonal antibodies against the MBP-kinesin stalk proteins were prepared by injecting rabbits initially with 1 mg of antigen in complete Freund's adjuvent followed by 3 boosts with 0.5 mg antigen in incomplete Freund's adjuvent at 3 week intervals. To remove antibodies that reacted against either uKHC or nKHC, affinity columns of MBP-kinesin stalk proteins were prepared by coupling 80 mg of fusion protein to 4 ml of Affigel-15 resin with overnight incubation at 4°C. The uncoupled protein was removed with several washes of 10 mM HEPES (pH 6.9), 50 mM NaCl, and a final wash with 10 mM Tris (pH 7.5). The rabbit polyclonal antisera were heated to 65°C for 15 min and then diluted 10-fold in 10 mM Tris (pH 7.5), and 1 resin volume of diluted antiserum was combined with 1 volume of resin (anti-uKHC antiserum was applied to a resin of MBP-nKHC stalk protein and vice versa). The mixture was incubated overnight at 4°C, and then the resin was removed from the supernatant by sedimentation in a clinical centrifuge.

Affinity purified anti-nKHC and anti-uKHC antibodies were isolated by incubating the anti-nKHC and anti-uKHC supernatants with MBP-nKHC and MBP-uKHC resins, respectively, for 12 hr at 4°C. The resins with bound antibodies were washed once with 10 mM Tris (pH 7.5), 0.5 M NaCl followed by 3 washes with 10 mM Tris (pH 7.5). The antibodies were then eluted with 100 mM glycine (pH 2.5) and immediately neutralized with 1/10 volume of 1 M Tris (pH 8).

### Tissue Preparations, Polyacrylamide Gel Electrophoresis, and Immunoblotting

Tissues (6–8 g of adult brain, liver, kidney, spleen, heart, lung, testes, and newborn brain from rats as well as adult human brain; obtained from R. Myers, Stanford University) were added to 20 ml of acetate buffer (100 mM KAc, 150 mM sucrose, 5 mM EGTA, 3 mM MgAc, 10 mM K-HEPES [pH 7.4]) and homogenized by 20 strokes with a type B pestle followed by 20 strokes with a type A pestle in a Wheaton homogenizer. Crude homogenates were either frozen in liquid nitrogen for later use or centrifuged at 5,000 × g for 10 min to make low speed supernatants which were also frozen in liquid nitrogen and stored at −80°C. Adult rat sciatic nerve tissue extracts were prepared by boiling nerve fragments in SDS gel sample buffer. Protein concentration was approximated by comparing this extract to other crude extracts of known concentrations on a Coomassie blue-stained polyacrylamide gel.

The proteins were separated on 8% polyacrylamide gels under denaturing and reducing conditions (Laemmli, 1970). Immunoblotting (Towbin et al., 1979) was performed by transferring to nitrocellulose at 0.5 A for 1 hr. Blots were usually blocked for at least 2 hr in TBST-5% nonfat dry milk (TBST: 20 mM Tris [pH 7.5], 150 mM NaCl, 0.1% Tween-20). Primary antibody incubation (1:1000 dilution for anti-uKHC antibody and 1:500 dilution for anti-nKHC antibody) was performed in the same solution overnight at 4°C. Blots were then washed 4 × 30 min in TBST and then 1 × 15 min in TBST-5% nonfat dry milk followed by a 1 hr incubation with horseradish peroxidase-conjugated donkey anti-rabbit immunoglobulin (Amersham) at a 1:1000 dilution in TBST-5% nonfat dry milk. After washing 4 × 30 min in TBST, blots were developed using the ECL Western blotting detection kit (Amersham) and exposed to Kodak XAR-5 film. For quantitative immunoblotting, samples were run alongside a range of known quantities of either MBP-uKHC or MBP-nKHC. Determinations were made using signals in the linear range. Densitometry of the images was performed using the NIH Image 1.44 VDM program (Wayne Rasband, National Institutes of Health).

### Immunoprecipitation of KHCs

Twenty microliters of either affinity purified anti-nKHC antiserum or anti-uKHC antiserum was added to 0.4 ml of rat brain high speed supernatant (250,000 × g, 30 min) containing 10 mg/ml bovine serum albumin. After incubation for 1 hr on ice, 0.2 ml of 10% (v/v) protein A beads (Zymed Laboratories, South San Francisco, CA) were added and incubated for 1 hr at 4°C. Beads were washed once with 10 mM Tris (pH 7.5), 0.5 M NaCl, then 3 times with TBST, and were finally boiled in SDS gel loading buffer (50 mM Tris [pH 6.8], 100 mM dithiothreitol, 2% SDS, 10% glycerol).

### Kinesin Preparation from Rat Brains

Rat brains (70 g; 36 rats) were homogenized in 1 volume of homogenization buffer (HB: 80 mM K-PIPES [pH 6.8], 5 mM $MgCl_2$, 1 mM EGTA, 1 mM phenylmethylsulfonyl fluoride) with 20 strokes of a type B pestle followed by 20 strokes with a type A pestle in a Wheaton homogenizer. The crude extract was centrifuged at 27,000 × g for 30 min at 4°C giving rise to S1 (supernatant 1) and P1 (pellet 1). S1 was spun at 250,000 × g for 1 hr at 4°C, creating S2 and P2. Taxol (a generous gift from the National Cancer Institute) was added to S2 to a final concentration of 10 μM. Bovine microtubules preassembled for 20 min in HB, 1 mM Mg-GTP and 10 μM taxol at 37°C were added to a final concentration of 100 μg/ml. After a 10 min incubation at 20°C, hexokinase (60 U/ml), glucose (10 mM), and adenylyl-imidodiphosphate (0.2 mM) were added. Twenty minutes later, the microtubules were sedimented through sucrose cushions (HB, 20% sucrose, 5 μM taxol) by centrifuging for 30 min at 100,000 × g at 20°C. The microtubule pellet was resuspended in 1/20 volume (compared with S2) of HB containing 10 μM taxol and then spun again through 20% sucrose cushions as above. The microtubule pellet was then resuspended in 1/40 volume of HB containing 10 μM taxol, 0.1 M KCl, and 10 mM Mg-ATP, incubated for 20 min at 20°C, and centrifuged at 40,000 × g for 30 min (ATP release). The final microtubule pellet was resuspended in 1/40 volume of HB.

### Immunostaining of Frozen Tissue Sections

Sprague-Dawley albino rats 175–200 g were anesthetized and fixed by transcardial perfusion as previously described (De Camilli et al., 1983). In brief, animals were perfused for 5 min with ice-cold 120 mM sodium phosphate buffer (pH 7.4) and then for 10–15 min with fixative (4% formaldehyde [w/v] freshly prepared from paraformaldehyde) in the same buffer. Following perfusion, brains were removed, cut into small blocks, and immersed in the same fixative for 3 hr at 0°C. Excess fixative was removed by several washes in 120 mM sodium phosphate buffer,

and the tissue specimens were infiltrated with sucrose by passing them through a series of increasing concentrations of sucrose (12%, 15%, and 18% w/v) in the same buffer. Tissue was then frozen in isopentane chilled with liquid nitrogen and sectioned at a thickness of 10 μm with a Reichert-Jung (Vienna, Austria) cryostat. Sections were then mounted on glass microscope slides, which were previously treated with 0.5% gelatin and 0.05% chromium potassium sulfate solution to obtain good adhesion of the sections.

Immunostaining of the sections was performed by an indirect immunofluorescence procedure as described (De Camilli et al., 1983) with minor modifications. Frozen sections were first washed in low salt PBS (150 mM NaCl, 10 mM $NaPO_4$ [pH 7.4]) and then incubated for 30 min in the presence of 0.1 M glycine buffered at pH 7.4 with Tris base. Sections were incubated subsequently for 30–40 min with goat serum dilution buffer (0.8% [w/v] Triton X-100, 0.45 M NaCl, 0.02 M sodium phosphate buffer [pH 7.4] containing 6-fold diluted normal goat serum) followed by an incubation for 2–3 hr with the affinity purified, rabbit anti-nKHC antibody (1:50 dilution) and anti-MAP2 monoclonal antibody (Boehringer Mannheim) diluted in goat serum dilution buffer. The sections were then washed 4 × 15 min in high salt PBS (450 mM NaCl, 20 mM $NaPO_4$ [pH 7.4]) containing 0.3% Triton X-100, followed by an incubation for 45 min with Texas Red-conjugated, affinity purified goat anti-rabbit IgG and fluorescein-conjugated, affinity purified goat anti-mouse IgG (Jackson ImmunoResearch Laboratories, Inc., West Grove, PA) diluted in goat serum dilution buffer. Sections were then washed as before in high salt PBS containing 0.3% Triton X-100 followed by low salt PBS and then 5 mM $NaPO_4$ (pH 7.4). All antibody solutions were spun for 4 min in an Eppendorf microfuge to remove aggregates. At the end of the immunostaining, the glass slides were mounted with 70% glycerol (v/v) in PBS containing 1 mg/ml p-phenylenediamine (Sigma Chemical Co., St. Louis, MO), observed with a Zeiss Axioplan equipped with epifluorescence optics with a 20× Plan Neofluar objective, and photographed with T-Max 400 ASA film (Eastman Kodak Co., Rochester, NY).

### Hippocampal Cell Culture and Immunostaining

Primary neuronal cultures were prepared from hippocampi of 18-day-old fetal rats (4 day cultures shown in Figures 7g and 7h) as described by Banker and Cowan (1977) and Bartlett and Banker (1984). Cultures from newborn rats (in Figures 7a–7f) were prepared by dissecting hippocampal regions CA3–CA1 from 2- to 4-day-old rat brains according to Malgaroli and Tsien (1992).

Hippocampal cultures were fixed by immersing glass slides for 20–30 min in a 4% formaldehyde solution (freshly prepared from paraformaldehyde) in 120 mM $NaPO_4$ (pH 7.4) buffer containing 4% sucrose (prewarmed to 37°C) (Matteoli et al., 1992). After fixation, cells were washed extensively with PBS. Fixed cells were detergent permeabilized and immunolabeled according to the same protocol described for tissue sections except that the wash steps were in high salt PBS without Triton X-100. Primary antibodies used in this study were affinity purified rabbit polyclonal antibodies against nKHC (1:50 dilution), the rabbit antiserum against uKHC (depleted of nKHC antibodies; 1:20 dilution), the mouse anti-MAP2 monoclonal antibody from Boehringer Mannheim, a mouse anti-tubulin monoclonal antibody (DM1α; 1:1000 dilution; a gift from Dr. M. Kirschner, Department of Cell Biology, Harvard Medical School, Boston, MA), and a monoclonal antibody against synaptotagmin (1:60 dilution; a gift from Dr. A. Malgaroli). Secondary antibodies and microscopy were the same as described above for the immunostaining of frozen brain sections, except that a Zeiss 63×, 1.4 numerical aperture Planapochromat objective was used for imaging.

### Acknowledgments

This work was supported by grants from the Rita Allen and Klingenstein Foundations and the National Institutes of Health (GM38499). We are indebted to Dr. A. Malgaroli and Dr. M. Matteoli for providing primary cultures of hippocampal neurons. We also would like to thank Dr. M. Kirschner and Dr. A. Malgaroli for antibodies, M. T. Sprocati and P. Tinelli for technical and photographic assistance, Dr. Eugenio de Hostos and Dr. James Sabry for making comments on this manuscript, Dr. A. Zanini and Dr. G. Vignali for helpful and stimulating discussions, and Jon Kull for performing secondary structure predictions.

The costs of publication of this article were defrayed in part by the payment of page charges. This article must therefore be hereby marked "*advertisement*" in accordance with 18 USC Section 1734 solely to indicate this fact.

Received June 11, 1993; revised February 28, 1994.

### References

Adams, M. D., Kelley, J. M., Gocayne, J. D., Dubnick, M., Polymeropoulos, M. H., Xiao, H., Merril, C. R., Wu, A., Olde, B., Moreno, R. F., Kerlavage, A. R., McCombie, W. R., and Venter, J. C. (1991). Complementary DNA sequencing: expressed sequence tags and human genome project. Science *252*, 1651–1656.

Aizawa, H., Sekine, Y., Takemura, R., Zhang, Z., Nangaku, M., and Hirokawa, N. (1992). Kinesin family in murine central nervous system. J. Cell Biol. *119*, 1287–1296.

Amaral, D. G., and Witter, M. P. (1989). The three dimensional organization of the hippocampal formation: a review of anatomical data. Neuroscience *31*, 571–591.

Amaratunga, A., Morin, P. J., Kosik, K. S., and Fine, R. E. (1993). Inhibition of kinesin synthesis and rapid anterograde axonal transport in vivo by an antisense oligonucleotide. J. Biol. Chem. *268*, 17427–17430.

Andrews, S. B., Gallant, P. E., Leapman, R. D., Schnapp, B. J., and Reese, T. S. (1993). Single kinesin molecules crossbridge microtubules in vitro. Proc. Natl. Acad. Sci. USA *90*, 6503–6507.

Banker, G. A., and Cowan, W. M. (1977). Rat hippocampal neurons in dispersed cell culture. Brain Res. *126*, 379–425.

Bartlett, W. P., and Banker, G. A. (1984). An electron microscopic study of the development of axons and dendrites by hippocampal neurons in culture. I. Cells which develop without intercellular contacts. J. Neurosci. *4*, 1944–1953.

Bloom, G. S., Wagner, M. C., Pfister, K. K., and Brady, S. T. (1988). Native structure and physical properties of bovine neuronal kinesin and identification of the ATP-binding subunit polypeptide. Biochemistry *27*, 3409–3416.

Brady, S. T. (1991). Molecular motors in the nervous system. Neuron *7*, 521–533.

Brady, S. T., Pfister, K. K., and Bloom, G. S. (1990). A monoclonal antibody against kinesin inhibits both anterograde and retrograde fast axonal transport in squid axoplasm. Proc. Natl. Acad. Sci. USA *87*, 1061–1065.

Chomczynski, P., and Sacchi, N. (1987). Single-step method of RNA isolation by acid guanidinium thiocyanate-phenol-chloroform extraction. Anal. Biochem. *162*, 156–159.

Cyr, J. L., Pfister, K. K., Bloom, G. S., Slaughter, C. A., and Brady, S. T. (1991). Molecular genetics of kinesin light chains: generation of isoforms by alternative splicing. Proc. Natl. Acad. Sci. USA *88*, 10114–10118.

De Camilli, P., Cameron, R., and Greengard, P. (1983). Synapsin I (protein I), a nerve terminal-specific phosphoprotein. I. Its general distribution in synapses of the central and peripheral nervous system demonstrated by immunofluorescence in frozen and plastic sections. J. Cell Biol. *96*, 1337–1354.

De Camilli, P., Miller, P. E., Navone, F., Theurkauf, W. E., and Vallee, R. B. (1984). Distribution of microtubule-associated protein 2 in the nervous system of the rat studied by immunofluorescence. Neuroscience *11*, 819–846.

De Cuevas, M., Tao, T., and Goldstein, L. S. B. (1992). Evidence that the stalk of Drosophila kinesin heavy chain is an α-helical coiled coil. J. Cell Biol. *116*, 957–965.

Endow, S. A., and Hatsumi, M. (1991). A multimember kinesin gene family in Drosophila. Proc. Natl. Acad. Sci. USA *88*, 4424–4427.

Endow, S. A., and Titus, M. A. (1992). Genetic approaches to molecular motors. Annu. Rev. Cell Biol. *8*, 29-66.

Feinberg, A. P., and Vogelstein, B. (1983). A technique for radiolabeling DNA restriction endonuclease fragments to high specific activity. Anal. Biochem. *132*, 6-13.

Ferreira, A., Niclas, J., Vale, R. D., Banker, G., and Kosik, K. S. (1992). Suppression of kinesin expression in cultured hippocampal neurons using antisense oligonucleotides. J. Cell Biol. *117*, 595-606.

Finer-Moore, J., and Stroud, R. M. (1984). Amphipathic analysis and possible formation of the ion channel in an acetylcholine receptor. Proc. Natl. Acad. Sci. USA *81*, 155-159.

Gho, M., McDonald, K., Ganetzky, B., and Saxton, W. M. (1992). Effects of kinesin mutations on neuronal functions. Science *258*, 313-316.

Goldstein, L. S. B. (1991). The kinesin superfamily: tails of functional redundancy. Trends Cell Biol. *1*, 93-98.

Goldstein, L. S. B. (1993). Functional redundancy in mitotic force generation. J. Cell Biol. *120*, 1-3.

Hackney, D. D., Levitt, J. D., and Wagner, D. D. (1991). Characterization of $\alpha_2\beta_2$ and $\alpha_2$ forms of kinesin. Biochem. Biophys. Res. Commun. *174*, 810-815.

Hall, D. H., and Hedgecock, E. M. (1991). Kinesin-related gene *unc-104* is required for axonal transport of synaptic vesicles in C. elegans. Cell *65*, 837-847.

Henikoff, S. (1987). Unidirectional digestion with exonuclease III in DNA sequence analysis. Meth. Enzymol. *155*, 156-165.

Hirokawa, N., Pfister, K. K., Yorifuji, H., Wagner, M. C., Brady, S. T., and Bloom, G. S. (1989). Submolecular domains of bovine brain kinesin identified by electron microscopy and monoclonal antibody decoration. Cell *56*, 867-878.

Hirokawa, N., Sato-Yoshitake, R., Kobayashi, N., Pfister, K. K., Bloom, G. S., and Brady, S. T. (1991). Kinesin associates with anterogradely transported membranous organelles. J. Cell Biol. *114*, 295-302.

Hollenbeck, P. J. (1989). The distribution, abundance and subcellular localization of kinesin. J. Cell Biol. *108*, 2335-2342.

Justice, M. J., Gilbert, D. J., Kinzler, K. W., Vogelstein, B., Buchberg, A. M., Ceci, J. D., Matsuda, Y., Chapman, V. M., Patriotis, C., Makris, A., Tsichlis, P. N., Jenkins, N. A., and Copeland, N. G. (1992). A molecular genetic linkage map of mouse chromosome 18 reveals extensive linkage conservation with human chromosomes 5 and 18. Genomics *13*, 1281-1288.

Kato, K. (1990). A collection of cDNA clones with specific expression patterns in mouse brain. Eur. J. Neurosci. *2*, 704-711.

Kosik, K. S., Orecchio, L. D., Schnapp, B., Inouye, H., and Neve, R. L. (1990). The primary structure and analysis of the squid kinesin heavy chain. J. Biol. Chem. *265*, 3278-3283.

Kuznetsov, S. A., Vaisberg, E. A., Shanina, N. A., Magretova, N. N., Chernyak, V. Y., and Gelfand, V. I. (1988). The quaternary structure of bovine neuronal kinesin. EMBO J. *7*, 353-356.

Laemmli, U. (1970). Cleavage of structural proteins during assembly of the bacteriophage T4. Nature *227*, 680-685.

Leopold, P. L., McDowall, A. W., Pfister, K. K., Bloom, G. S., and Brady, S. T. (1992). Association of kinesin with characterized membrane-bounded organelles. Cell Motil. Cytoskel. *23*, 19-33.

Malgaroli, A., and Tsien, R. W. (1992). Glutamate-induced long-term potentiation of the frequency of miniature synaptic currents in cultured hippocampal neurons. Nature *357*, 134-139.

Matteoli, M., Takei, K., Perin, M. S., Südhof, T. C., and De Camilli, P. (1992). Exo-endocytic recycling of synaptic vesicles in developing processes of cultured hippocampal neurons. J. Cell Biol. *117*, 849-861.

Matthew, W. D., Tsavaler, L., and Reichardt, L. F. (1981). Identification of a synaptic vesicle-specific membrane protein with a wide distribution in neuronal and neurosecretory tissues. J. Cell Biol. *91*, 257-269.

Mercer, J. A., Seperack, P. K., Strobel, M. C., Copeland, N. G., and Jenkins, N. A. (1991). Novel myosin heavy chain encoded by murine dilute coat colour locus. Nature *349*, 709-713.

Mullis, K., Faloona, F., Scharf, S., Saiki, R., Horn, G., and Erlich, H. (1986). Specific enzymatic amplification of DNA in vitro: the polymerase chain reaction. Cold Spring Harbor Symp. Quant. Biol. *51*, 263-273.

Mundigl, O., Matteoli, M., Daniell, L., Thomas-Reetz, A., Metcalf, A., Jahn, R., and De Camilli, P. (1993). Synaptic vesicle proteins and early endosomes in cultured hippocampal neurons: differential effects of brefeldin A in axon and dendrites. J. Cell Biol. *122*, 1207-1221.

Navone, F., Niclas, J., Hom-Booher, N., Sparks, L., Bernstein, H. D., McCaffrey, G., and Vale, R. D. (1992). Expression of the human kinesin heavy chain gene in CV-1 cells: interaction of the C-terminal domain with cytoplasmic microtubules. J. Cell Biol. *117*, 1263-1275.

Puissant, C., and Houdebine, L.-M. (1990). An improvement of the single-step method of RNA isolation by acid-guanidinium thiocyanate-phenol-chloroform extraction. Biotechniques *8*, 148-149.

Sambrook, J., Fritsch, E. F., and Maniatis, T. (1989). Molecular Cloning: A Laboratory Manual (Cold Spring Harbor, New York: Cold Spring Harbor Laboratory Press).

Sanger, F., Nicklen, S., and Coulson, A. (1977). DNA sequencing with chain terminating inhibitors. Proc. Natl. Acad. Sci. USA *74*, 5463-5467.

Schnapp, B. J., Reese, T. S., and Bechtold, R. (1992). Kinesin is bound with high affinity to squid axon organelles that move to the plus-end of microtubules. J. Cell Biol. *119*, 389-399.

Schroer, T. A., and Sheetz, M. P. (1991). Functions of microtubule-based motors. Annu. Rev. Physiol. *53*, 629-652.

Skoufias, D. A., and Scholey, J. (1993). Cytoplasmic microtubule-based motor proteins. Curr. Opin. Cell Biol. *5*, 95-107.

Stewart, R. J., Pesavento, P. A., Woerpel, D. N., and Goldstein, L. S. (1991). Identification and partial characterization of six members of the kinesin superfamily in Drosophila. Proc. Natl. Acad. Sci. USA *88*, 8470-8474.

Towbin, H., Staehelin, T., and Gordon, J. (1979). Electrophoretic transfer of proteins from polyacrylamide gels to nitrocellulose sheets: procedure and some applications. Proc. Natl. Acad. Sci. USA *76*, 4350-4354.

Toyoshima, I., Yu, H., Steuer, E. R., and Sheetz, M. P. (1992). Kinectin, a major kinesin-binding protein on ER. J. Cell Biol. *118*, 1121-1131.

Wagner, M. D., Pfister, K. K., Bloom, G. S., and Brady, S. T. (1989). Copurification of kinesin polypeptides with microtubule-stimulated Mg-ATPase activity and kinetic analysis of enzymatic properties. Cell Motil. Cytoskel. *12*, 195-215.

Wright, B. D., Henson, J. H., Wedaman, K. P., Willy, P. J., Morand, J. N., and Scholey, J. M. (1991). Subcelluar localization and sequence of sea urchin kinesin heavy chain: evidence for its association with membranes in the mitotic apparatus and interphase cytoplasm. J. Cell Biol. *113*, 817-833.

Yang, J. T., Saxton, W. M., and Goldstein, L. S. B. (1988). Isolation and characterization of the gene encoding the heavy chain of Drosophila kinesin. Proc. Natl. Acad. Sci. USA *85*, 1864-1868.

Yang, J. T., Laymon, R. A., and Goldstein, L. S. B. (1989). A three domain structure of kinesin heavy chain revealed by DNA sequence and microtubule binding analyses. Cell *56*, 879-889.

Yang, J. T., Saxton, W. M., Stewart, R. J., Raff, E. C., and Goldstein, L. S. (1990). Evidence that the head of kinesin is sufficient for force generation and motility in vitro. Science *249*, 42-47.

# APPENDIX 3

# Differential Expression of Ubiquitous and Neuronal Kinesin Heavy Chains During Differentiation of Neuroblastoma and PC12 Cells

The following work is the product of a collaboration between our lab and the lab of Francesca Navone. Giovanna Vignali, a post-doctoral fellow in Francesca's lab, did most of the work in this manuscript which has been submitted for publication. My contribution includes the generation of many of the reagents used in this study, technical expertise, and taking part in many discussions with Francesca and Giovanna about experimental strategy. I am including this manuscript as an appendix since this work derives from the work presented in Chapter 2. In Chapter 2, the discovery of a new kinesin heavy chain (nKHC) that is only expressed in neurons was discussed. We were interested in determining if the expression of neuronal kinesin is regulated in the course of neuronal differentiation as a preliminary step to get at the question of whether neuronal kinesin plays a role in this process. Analysis of both nKHC protein and mRNA levels revealed that levels of both increase dramatically in neuroblastoma and pheochromocytoma cells when they are pharmacologically induced to differentiate into neurons. In contrast, levels of uKHC protein and mRNA do not change under these conditions. These results suggest that nKHC plays an important role in organelle motility during neuronal differentiation.

**ABSTRACT**

Kinesin is a microtubule-based motor protein involved in intracellular organelle transport. Neurons are characterized by the presence of at least two isoforms of conventional kinesin: ubiquitous kinesin (uKHC), expressed in all cells and tissues, and neuronal kinesin (nKHC), whose pattern of expression is confined to neuronal cells. In order to investigate whether the two kinesin motors, which are encoded by different genes, may play distinct biological roles in neurons, we studied their expression during neuronal differentiation. Human neuroblastoma SH-SY5Y and IMR32 cells and rat pheochromocytoma PC12 cells were used as an *in vitro* system for neuronal differentiation and were induced to differentiate in the presence of retinoic acid, a combination of dibutyryl cAMP and 5-bromodeoxyuridine and nerve growth factor, respectively. The expression level of each kinesin isoform was evaluated by quantitative immunoblot analysis before and after pharmacological treatment. We found that in all cells types expression level of nKHC, but not uKHC, is stimulated during differentiation. In particular, SH-SY5Y cells show a 4.5-fold, IMR32 cells a 3-fold and PC12 cells a 7-fold increase in the level of expression of nKHC. By Northern blot analysis, we found that the selective increase in the expression of nKHC is paralleled by an increase in its mRNA, indicating that there is a transcriptional control of the expression of this kinesin isoform during differentiation of neuroblastoma and PC12 cells. Our results suggest that these cells represent an adequate model to study the function of conventional kinesin and its isoforms.

## INTRODUCTION

The kinesins constitute a superfamily of motor proteins that are thought to be involved in the intracellular translocation of membrane-bounded organelles, chromosomes and other subcellular cargo along microtubules (Walker and Sheetz, 1993). All members of this family are encoded by different genes and their sequences show a high similarity in the 350 amino acid "motor domain". The motor domains are linked to "tails" of variable lengths and of diverse amino acid sequences, which are thought to define the specificity of the motor cargo. Although the majority of kinesins appear to be involved in force-generating events in mitosis and meiosis (Endow, 1991; Goldstein, 1993; Hoyt, 1994), several are thought to participate in organelle transport (Aizawa et al., 1992; Pesavento et al., 1994). Moreover, some organelle-moving kinesins appear to be predominantly associated with specific subsets of membrane bounded-organelles (Hall and Hedgecock, 1991; Kondo et al., 1994; Nangaku et al., 1994; Noda et al., 1995; Okada et al., 1995).

Kinesin itself is the founding member of the kinesin family and it is generally referred to as conventional kinesin (Brady, 1991; Vale, 1987). It can be isolated from a variety of neuronal and non-neuronal tissues and cells, and it is a tetramer composed of two identical heavy chains of ~120 kDa and two nearly identical light chains of ~70 kDa (Cole and Scholey, 1995). The heavy chains of conventional kinesin are thought to interact with the light chains (Hirokawa et al., 1989), with microtubules (Andrews et al., 1993; Navone et al., 1992) and with membrane receptors via their C-terminal tail domain (Skoufias et al., 1994; Toyoshima et al., 1992; Yu et al., 1992). Several conventional kinesin isoforms of both the heavy and light chains have been identified (Brady, 1995) . These kinesin isoforms have been suggested to be motors for the translocation of specific subclasses of organelles (Elluru et al.,

1995) and/or they may be involved at various steps of intracellular organelle transport (Lippincott-Schwartz et al., 1995).

We have recently identified a human cDNA which encodes a conventional kinesin heavy chain expressed exclusively in neurons: this protein has been named neuronal kinesin (nKHC) to distinguish it form the previously characterized human kinesin, which is ubiquitously expressed (uKHC) (Navone et al., 1992; Niclas et al., 1994). These two kinesin isoforms are encoded by different genes and show 65% amino acid identity throughout the sequence of the heavy chains. The nKHC sequence has a stretch of 69 amino acids at the C-terminal end, which is absent from other conventional kinesin molecules (Niclas et al., 1994). Both proteins are present in the central nervous system, but have different patterns of distribution: while uKHC is uniformly distributed, nKHC is concentrated in subpopulations of neurons (Niclas et al., 1994) (Vignali et al., unpublished observations). These observations indicate that neurons possess at least two distinct conventional kinesin motors that may play partially distinct biological roles *in vivo*. So far, however, specific roles for nKHC and uKHC have not been determined.

Human neuroblastoma cell lines have often been used for *in vitro* studies of neuronal differentiation. Although these cells already show several characteristics of neuronal cells, they undergo major morphological, biochemical and functional changes following exposure to differentiating agents (Haussler et al., 1983; Robson and Sidell, 1985; Sidell, 1982; Spinelli et al., 1982). For example, treatment with retinoic acid (RA) stimulates neurite outgrowth, expression of various membrane receptors, the activity of ion channels, the synthesis and release of peptides and neurotransmitters, and an increase in the number of secretory granules (Adem et al., 1987; Giudici et al., 1992; Gotti et al., 1987; Sher et al., 1989). PC12 cells, a neural crest derived

clonal cell line from a rat pheochromocytoma (Greene and Tischler, 1976) have also been widely used as a cellular model for neuronal differentiation. They respond to nerve growth factor (NGF) by projection of long neurites and induction of differentiated properties characteristic of sympathetic neurons (Drubin et al., 1988; Greene and Tischler, 1976; Jacobs and Stevens, 1986; Kongsamut and Miller, 1986).

In order to clarify the function of nKHC and to investigate whether nKHC and uKHC may be involved in different aspects of organelle transport during neurite outgrowth, we studied the pattern of expression of the two proteins in two different human neuroblastoma cell lines (SH-SY5Y and IMR32) and in rat PC12 cells which were pharmacologically induced to acquire a neuronal phenotype. We found that in all cell lines examined, neuronal differentiation is accompanied by a selective increase in the level of expression of nKHC, while that of uKHC remains unchanged. This effect on protein level is paralleled by an increase in the mRNA level of nKHC, but not of uKHC. These observations indicate that the tissue specificity of the expression of nKHC can be reproduced in cell culture and that neuroblastoma and PC12 cells may provide a useful system to study the function of this kinesin isoform.

## MATERIALS AND METHODS

*Cell Culture and Differentiation*

Human neuroblastoma SH-SY5Y cells were grown as previously described (Giudici et al., 1992) in RPMI-1640 medium, supplemented with 10% fetal calf serum, 4 mM L-glutamine, 0.075% sodium carbonate buffer, 100 U/ml penicillin, 100 mg/ml streptomycin, in an atmosphere of 5% $CO_2$ in air, at 37°C. The IMR32 cell line was grown according to Sher *et al.* (Sher et al., 1989) in MEM containing Earle's salts, 10% fetal calf serum, 4 mM L-glutamine and the same concentration of antibiotics as above. PC12 cells were grown in DMEM supplemented with 5% fetal calf serum, 10% donor horse serum, 4 mM L-glutamine, 100 U/ml penicillin and 100 mg/ml streptomycin. All media and supplementing agents were purchased from Gibco (Gibco/BRL, Grand Island, NY).

In the absence of differentiation, all cells were plated at a concentration of 12-15 x $10^3$/ $cm^2$ in 10 cm Falcon Petri dishes and were harvested 3-4 days later when they reached confluency. To induce differentiation, all cells were plated at the same dilution as above and treated with their corresponding differentiating drugs. For SH-SY5Y cells, medium containing 10 μM retinoic acid (Sigma Chem. Co., St. Louis, MO) and for IMR32 cells medium containing 1 mM $N_6$,2',O-dibutyrryladenosine 3':5'-cyclic monophosphate ($Bt_2$cAMP)/2.5 μM 5-bromo-2'-deoxyuridine (BrdU) (Sigma Chem. Co.) was added at the moment of plating. For PC12 cells, 100 ng/ml NGF (nerve growth factor) ( Boehringer, Mannheim/Germany) was added to the culture medium the day after plating. All drugs were added every 2-3 days at each medium change, and neuroblastoma cells were collected 12-13 days after the beginning of differentiation, while PC12 cells were used 7 days later. Control and differentiated cells were observed with a Leitz microscope equipped with

phase contrast optics and photographed with T-Max 100 film (Eastman Kodak Co., Rochester, NY).

*Preparation of low speed supernatants*

Undifferentiated cells were harvested from 2-4 Petri dishes 3-4 days after plating, when they reached 90% confluency. Differentiated cells were collected at the end of pharmacological treatment from the same number of dishes. All cells were first rinsed twice with MEM-Hepes (pH 7.25) without serum and then scraped from the Petri dish surface with a rubber policeman. They were pelleted by centrifugation at 15,000xg in a SA 600 rotor (Sorvall, Norwalk, CT) for 10 min at 4°C to sediment cells and fragments of neuronal processes. The resulting pellet was gently washed with homogenizing buffer (HO: 0.25 M sucrose, 5 mM Hepes, pH 7.4) containing protease inhibitors [0.5 mM PMSF (Sigma Chem. Co.) previously solubilized in ethanol, 2 μg/ml pepstatin (Sigma Chem. Co.) previously solubilized in DMSO, 1 mM EGTA] prior to resuspension in a small volume (approx. 150-200 μl) of HO. Homogenization was performed first by forcing the resuspended pellet up and down through a 22 G needle mounted on a 1 ml syringe and then by 10-15 strokes in a glass-glass homogenizer. The homogenate was centrifuged at 800xg for 5 min at 4°C in a SA 600 rotor (Sorvall) to remove cell debris and nuclei, and then the resulting low speed supernatant was collected and used for immunoblotting analysis. Brain and kidney low speed supernatants were prepared from adult rats according to the procedure described in Niclas *et al.* (1994).

*SDS Gel Polyacrylamide Electrophoresis and Immunoblotting*

Equal amounts of proteins [determined by the Bio-Rad Protein Assay (Bio-Rad Laboratories GmbH, Munchen, Germany) using bovine serum albumin as a standard] of control and differentiated cell homogenates were separated on 7.5% SDS-polyacrylamide gels according to Laemmli (1970). After electrophoresis, the gels were either stained with Coomassie brilliant blue or blotted onto nitrocellulose paper (Towbin et al., 1979) at 0,4 A for 3 hr. Immunolabelling of blots was performed essentially as described in Niclas *et al.*, (1994) except that antibody incubation was at room temperature for 2.5 hr. Primary antibodies were polyclonal sera against ubiquitous kinesin heavy chain (uKHC) and neuronal kinesin heavy chain (nKHC). These antibodies were originally raised against fusion proteins containing portions of the two kinesin heavy chains and they were affinity purified and characterized as described in Niclas *et al.*, (1994). The dilutions were 1:400 for the anti-uKHC and 1:300 for the anti-nKHC antibodies. The secondary antibody was a horseradish peroxidase-conjugated donkey anti-rabbit IgG (Sigma Chem. Co.). After secondary antibody incubation, blots were washed 4 x 15 min in TBST-5% non-fat dry milk (TBST: 20 mM Tris, pH 7.5, 150 mM NaCl, 0.1% Tween-20) and 2 x 10 min in TBS (TBS: 20 mM Tris, pH 7.5, 150 mM NaCl) and then developed using the ECL Western blotting detection kit (Amersham Int., England) and exposed to Kodak XAR-5 film. Immunoreactivity of the kinesin bands was quantitated by densitometric analysis in a LKB Ultrascan XL laser densitometer. Determinations were made using signals in the linear range.

*RNA Isolation and Northern Blot Analysis*

RNA was purified form monolayers of HeLa, neuroblastoma and PC12 cells according to the RNA Fast$^{TM}$-II isolation system (Molecular Systems, San

Diego, CA), which is based on the use of specific RNA binding resin to purify total RNA form homogenized cells. RNA concentration and purity were quantitated spectrophotometrically. Total RNA samples (30 μg per lane) were electrophoresed on 1% agarose. 0.37 M formaldehyde gels. Ethidium bromide staining was used to confirm that RNA samples were not degraded and that the expected amount of RNA was loaded. After electrophoresis, gels were treated with 50 mM NaOH for 25 min, 1 M Tris-HCl (pH 7.5) for 30 min, and 20X SSC for 15 min and then transferred to Hybond N nylon (Amersham) with 20X SSC. After transfer, the blot was baked at 80°C for 2 hrs to allow the RNA to crosslink. Blots were then prehybridized (68°C for 20 min) and then hybridized (68°C for 1 hr) in the QuickHyb Hybridization Solution (Stratagene, La Jolla, CA) in the presence of the radiolabelled probe. To detect the uKHC mRNA, we probed the blot with the complete cDNA clone for uKHC (Navone et al., 1992) at a concentration of $5 \times 10^6$ cpm/ml, whereas for nKHC mRNA, the previously described 1.5 kb EST 257 clone (Adams et al., 1991; Niclas et al., 1994) was used at the same concentration. The same blot was sequentially hybridized with the uKHC and the with the nKHC radiolabelled probe. Between the two hybridization steps, soaking in boiling 0.1% SDS until cooling to room temperature stripped the blot of the first probe. After hybridization, blots were first washed twice at room temperature for 15 min with 2X SSC buffer containing 0.1% (w/v) SDS, then once at 60°C for 30 min with 0.1X SSC containing 0.1% (w/v) SDS for a high stringency wash. Finally, blots were exposed to Kodak X-OMAT AR film with intensifying screens at -80°C. Molecular sizes of the mRNA species detected by the probes were evaluated by comparing their positions in the blot with those of the 18S and 28S rRNA bands.

## RESULTS

### *Pharmacological Differentiation of Neuroblastoma and PC12 cells*

The morphological appearance of control and differentiated SH-SY5Y, IMR32 and pheochromocytoma cells is illustrated in Figure 1. Undifferentiated SH-SY5Y cells were predominantly oval or polygonal in shape (Fig. 1a), and some presented short neurites. A few hours after addition of retinoic acid, cells became elongated and spindle-shaped; at the end of a 12-day differentiation, they displayed very long and ramified neurites (Fig. 1b). Virtually all control IMR32 cells were either round or oval with a few short neurites (Fig. 1c); 10 days after incubation with $N_6$,2',O-dibutyrryladenosine 3':5'-cyclic monophosphate ($Bt_2$cAMP) and 5-bromo-2'-deoxyuridine (BrdU), they showed maximal morphological differentiated with long neurites that connect several cells in the same dish and sometimes present discrete swellings along their length (arrow in Fig. 1d). Treatment of control PC12 cells (Fig. 1e) with nerve growth factor (NGF) for a 7-8 day period resulted in a dramatic increase in the neurite network with the development of long and branched processes that often showed growth cone-like structures at their extremities (arrowheads in Fig. 1f).

### *Expression of ubiquitous and neuronal kinesin proteins in neuroblastoma and in PC12 cells*

The expression of ubiquitous kinesin heavy chain (uKHC) and of neuronal kinesin heavy chain (nKHC) during differentiation was studied by immunoblot analysis of low speed supernatants prepared from homogenates of human neuroblastoma SH-SY5Y and PC12 cells before and after pharmacological treatment. Equal amounts of total protein of undifferentiated and differentiated cells were assayed for immunoreactivity

for either the ubiquitous or the neuronal isoform of kinesin using antibodies that recognize specifically each protein. Different amounts of total protein were solubilized and loaded in the two gels for each experimental condition. Fig. 2a and 2b show immunoblots of SH-SY5Y cell extracts and Fig. 3a and 3b show immunoblots of PC12 cell extracts analyzed with the anti-uKHC and the anti-nKHC antibody, respectively. Coomassie blue staining of identical samples showed that no major changes in the patterns of protein expression occurred with differentiation (Fig. 2c and 3c). The affinity-purified polyclonal antibody against uKHC recognized a single band of approximately 120 kD in brain, kidney, SH-SY5Y and PC12 cell extracts (Fig. 2a and 3a), while the anti-nKHC antibody reacted against a doublet of 120-130 kD in brain, in neuroblastoma and PC12 cells, but not in kidney (Fig. 2b and 3b). The two bands of the nKHC doublet varied slightly in their relative intensities among the various cell lines. In general, in SH-SY5Y the upper band was always more intense (Fig. 2b), whereas in PC12 cells, the opposite was true (Fig. 3b). With equal protein loading, the band corresponding to uKHC always appeared more intense than the doublet corresponding to nKHC. These data are in agreement with our previous observation that adult human brain contains slightly more uKHC and nKHC (Niclas et al., 1994).

The levels of expression of nKHC, but not if uKHC, were affected by differentiation in both neuroblastoma and PC12 cells. The intensity of uKHC bands did not show any modification before and after retinoic acid or NGF treatment (Fig. 2a and 3a), while the intensity of the nKHC doublet always increased after in vitro differentiation (Fig. 2b and 3b). Similar results were obtained with another neuroblastoma cell line (IMR32). Quantitative densitometry (Table I) indicated that in three separate experiments with SH-SY5Y cells, the level of expression of nKHC increased 3 to 5 fold, while that of

uKHC remained unchanged. In IMR32 cells, nKHC expression was selectively stimulated 2 to 4 fold upon pharmacological differentiation (not shown), while in PC12 cells, nKHC expression was 5 to 8 fold higher in differentiated versus control cells. Fig. 4 summarizes the mean and standard deviation of the data obtained from the different experiments with the three cells lines.

*Expression of ubiquitous and neuronal kinesin RNAs in neuroblastoma and PC12 cells*

In order to establish whether the increase of nKHC expression observed after differentiation of neuroblastoma and PC12 cells is the result of transcriptional regulation, we performed Northern blot analysis of total RNAs obtained from SH-SY5Y and PC12 cells before and after pharmacological treatment. Northern blots were hybridized with cDNA probes which specifically recognize either the uKHC or the nKHC mRNAs, i.e. the entire ubiquitous kinesin cDNA and the EST257 cDNA, respectively. Fig. 5 shows the expression of the transcripts of the two kinesin isoforms in the two cell lines before and after differentiation, as well as in HeLa cells.

Both the uKHC and nKHC cDNAs hybridized most strongly to ~8.2 kb and to ~4.1 kb mRNAs in neuroblastoma and in PC12 cells. In HeLa cells, a strong signal with the uKHC probe was obtained, while no bands were detected with the nKHC cDNA. mRNA species of approximately the same molecular weight were previously obtained by Northern blot analysis of total RNA from various rat tissues (Niclas et al., 1994). The size differences noticed between the bands might be due to the different procedures used to calculate their molecular weights. At present, we don't know the significance of the faint band recognized by the nKHC probe at around 5 kb in HeLa cells.

While both ubiquitous and neuronal KHC mRNA were detected in nondifferentiated and differentiated SH-SY5Y and PC12 cells, their levels after the induction of differentiation was different (Fig. 5a and 5b). While the expression level of the uKHC transcripts did not vary in the pharmacologically treated cells, both nKHC transcripts were markedly increased in differentiated cells. Quantitative densitometry of the blot revealed that differentiated SH-SY5Y cells had 6 times more nKHC transcripts than the control cells, while PC12 cells displayed a 4-5 fold increase.

## DISCUSSION

In the present study, we looked at the expression of two kinesin isoforms during the process of differentiation induced by specific pharmacological treatments of neuroendocrine and neuronal cell lines. Ubiquitous and neuronal kinesins are conventional kinesins encoded by genes with different tissue expression patterns (Niclas et al., 1994). Whereas the uKHC gene is expressed in all tissues, the nKHC gene is expressed only in neurons, thereby suggesting that nKHC may serve a neuron-specific function. We found that in three different cell lines, the acquisition of a mature neuronal phenotype is accompanied by an increase in the expression neuronal, but not ubiquitous kinesin. The increase in nKHC protein is paralleled by an increase of its specific message. This is the first report suggesting that the expression of different isoforms of kinesin may be differentially regulated during the *in vitro* differentiation of neuronal and neuroendocrine cells.

Both isoforms of kinesin are present in neuroblastoma cells. Ubiquitous, but not neuronal kinesin, is also present in non-neuronal cell lines such as MDCK and NRK (not shown). These observations are in agreement with our previous results which show that uKHC is expressed in all tissues, while nKHC is specific for neuronal cells (Niclas et al., 1994). It is interesting that nKHC is expressed in undifferentiated PC12 cells, which are neuroendocrine cells and can be regarded as potential neurons. Although the presence of kinesin in PC12 cells has already been reported (Kondo et al., 1994; Lee and Hollenbeck, 1995; Nangaku et al., 1994), this is the first time that a neuron-specific KHC has been found in wild-type PC12 cells. This observation is not surprising, since several lines of investigation have provided evidence that neuron-specific proteins and functions are already

present in neuroendocrine cells(Le Douarin, 1988). In this respect, it would be interesting to study whether nKHC can be detected in endocrine cells, such as insulinoma cells (Polak et al., 1993), that have a different embryological origin from PC12 cells (Le Douarin, 1988) and that are also known to undergo a neuron-like differentiation upon NGF treatment (Porter et al., 1987; Sher et al., 1995).

Determination of the relative amounts of uKHC and nKHC in neuroblastoma and PC12 cells revealed that both cell lines contain more uKHC than nKHC. This result is in agreement with those of our previous study in adult human brain. As in brain homogenates, we observed that the anti-nKHC recognizes a doublet in our cell lines. We previously suggested that the upper band (~130 kD) of the neuronal kinesin doublet most likely corresponds to the full length protein, while the lower band (~120 kD) probably represents a degraded of specifically processed product (Niclas et al., 1994). In the cell lines used in this study, one of the two bands appears to be more prominent: the upper one in the case of neuroblastoma cells and the lower one in the case of PC12 cells. Some variations, however, were noticed in the same cell line in the course of differentiation (not shown). Although the significance of these two bands is still unclear, ,they may reflect different protein processing or different RNA splicing in the two cell lines at different stages of differentiation.

The increase in protein level of nKHC, but not of uKHC, observed after pharmacological differentiation suggests that this neuron-specific motor protein might be important for the acquisition of a mature neuronal phenotype. The fact that the increase in nKHC level was paralleled by an increase of its mRNA indicates that either transcription or mRNA stability are enhanced during differentiation of SH-SY5Y and PC12 cells. At present,

we cannot say whether only one or both of these mechanisms contribute to the increase in the relative amount of nKHC mRNA.

All events involved in neuronal differentiation require newly synthesized proteins that must be transported along the rapidly growing neruonal processes via their storage organelles. In fact, organelle transport is enhanced in the course of neuronal maturation (Greene and Tischler, 1976; Jacobs and Stevens, 1986), and one might expect that both the number and the type of vesicles being translocated are increased. On our study, the expression of two different isoforms of kinesin, one of which is neuron-specific, is shown to be differentially regulated during the acquisition of neuronal characteristics. The finding that the expression of the neuron-specific conventional kinesin is selectively stimulated during the differentiation of three distinct cell lines suggests that it may be involved in the movement of organelles whose transport along microtubules is specifically stimulated during this process.

The idea that different kinesin populations may serve as motors for distinct organelle populations has been recently corroborated by several reports on the identification and characterization of kinesin-like proteins, which appear to be involved in the transport of mitochondria (Nangaku et al., 1994), of synaptic vesicle precursors (Hall and Hedgecock, 1991; Okada et al., 1995) and of other still unclassified transport vesicle (Noda et al., 1995). Moreover, mutations in a conventional KHC in *Drosophila* have been shown to interfere specifically with the supply to the nerve terminal of vesicles distinct from synaptic vesicles (Gho et al., 1992). Some conventional kinesin isoforms also have been reported to be predominantly associated with mitochondria (Elluru et al., 1995). Immunoelectronmicroscopy will be required to determine whether nKHC is associated with a specific subset of

transport vesicles in neuronal cells and in cells that undergo neuron-like differentiation. Since the cell lines we have used in this study increase their expression of nKHC after pharmacological induction of differentiation, they should provide a useful system in which to investigate the types of vesicles that interact with nKHC and the role of this kinesin isoform in neuronal differentiation.

**ACKNOWLEDGMENTS**

We are grateful to Dr. A. Zanini for help in the preparation of tables and figures, for stimulating discussions and for critically reading this manuscript. We also would like to thank Prof. N. Borgese for making comments on this manuscript and Dr. D. Fornasari for helpful discussions. We also thank P. Tinelli for photographic assistance.

This work was supported by grants from the C.N.R., Consiglio Nazionale delle Ricerche and of SOCREA, Scientific and Research Society. G. Vignali is the recipient of a SOCREA fellowship.

## TABLE I

Expression of uKHC and nKHC in differentiated versus undifferentiated SH-SY5Y, IMR32 and PC12 cell lines.

| Cells | | uKHC (AU/mg total protein of differentiated: AU/mg total protein of undifferentiated cells) | nKHC (AU/mg total protein of differentiated: AU/mg total protein of undifferentiated cells) |
|---|---|---|---|
| SH-SY5Y | I | 1.10 ± 0.07 | 3.43 ± 0.82 |
| | II | 0.90 ± 0.17 | 4.81 ± 1.68 |
| | III | 1.60 ± 0.13 | 5.40 ± 2.40 |
| IMR32 | I | 1.91 ± 0.51 | 2.42 ± 0.56 |
| | II | 0.84 ± 0.05 | 3.80 ± 0.88 |
| PC12 | I | 1.34 ± 0.13 | 7.58 ± 1.25 |
| | II | 1.47 ± 0.20 | 5.32 ± 0.14 |
| | III | 0.68 ± 0.13 | 8.10 ± 2.82 |

For each experiment, different total protein aliquots (2-20 mg) were analyzed by SDS-PAGE followed by Western blot. uKHC and nKHC band area values, expressed in arbitrary units (AU) according to LKB laser densitometer, are the average of 2-3 determinations ± S.E.M.

**Figure 1.** Morphological appearance of control and differentiated neuroblastoma and PC12 cells by phase contrast microscopy.
**a,b**: neuroblastoma SH-SY5Y cells before (**a**) and after (**b**) pharmacological treatment with retinoic acid; **c,d**: neuroblastoma IMR32 cells before (**c**) and after (**d**) exposure to $Bt_2$cAMP and BrdU; **e,f**: control (**e**) and NGF-treated PC12 cells (**f**). Both neuroblastoma and PC12 control cells are either round of polygonal in shape with a few short neurites originating from their surface (**a** and **c**). After differentiation, all cells have developed a rich neurite network. In **d**, an arrow points to a varicosity along the length of a neuronal process in IMR32 cells; in **f**, arrowheads point to two growth cone-like structures in PC12 cells. Calibration bars: 4 μm.

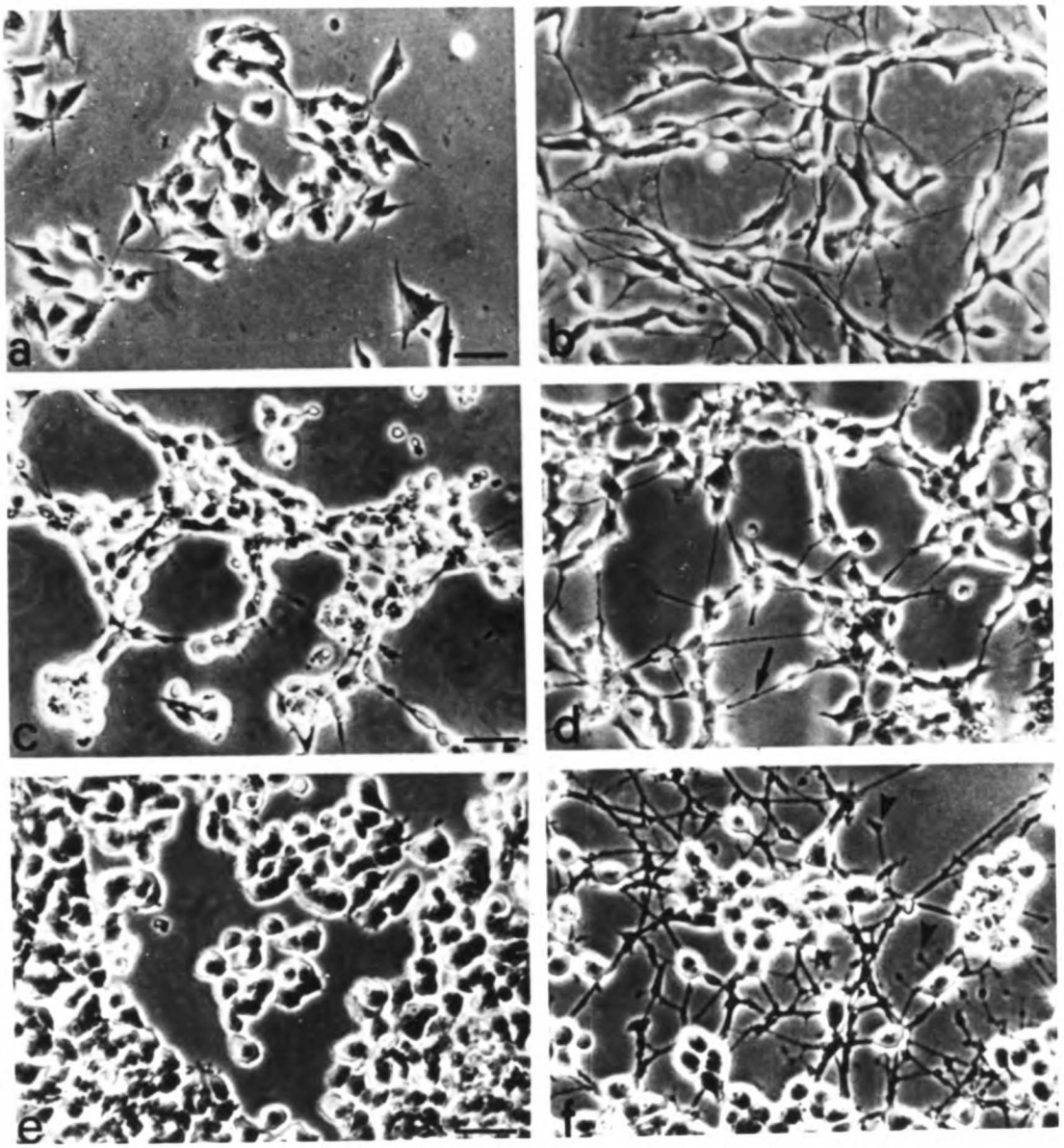

a
b
c
d
e
f

**Figure 2.** Expression of uKHC and nKHC in human neuroblastoma SH-SY5Y cells before and after pharmacological differentiation with retinoic acid. **a**: Western blot immunolabelled with anti-uKHC affinity purified antibody; **b**: Western blot immunolabelled with anti-nKHC affinity purified antibody; **c**: SDS-PAGE protein pattern (same samples as in **b**), stained with Coomassie brilliant blue. 30 µg of rat kidney and brain low speed supernatants were loaded in the first two lanes; equal amounts of total protein of control (-) and differentiated (+) SH-SY5Y cell low speed supernatants were loaded in each of the other three pairs of lanes, with different amounts of total protein loaded in the different pairs of lanes, as indicated. In **c**, molecular weight markers (kD) are shown on the left. Immunoreactivity for uKHC does not vary after treating the cells with retinoic acid, whereas that for nKHC increases after differentiation.

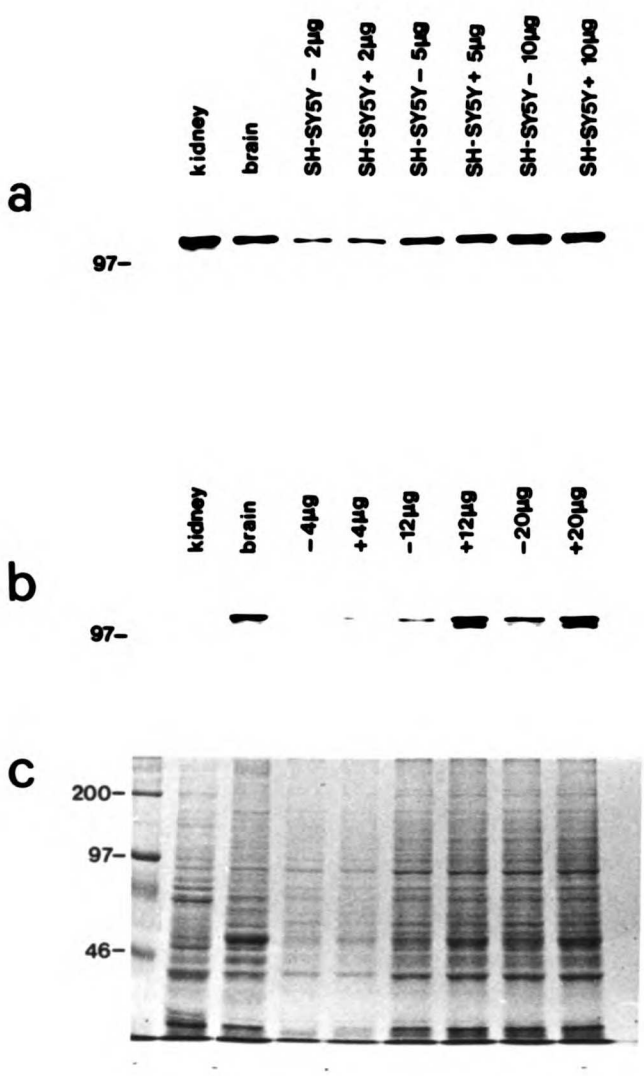

a
kidney
brain
SH-SY5Y – 2µg
SH-SY5Y + 2µg
SH-SY5Y – 5µg
SH-SY5Y + 5µg
SH-SY5Y – 10µg
SH-SY5Y + 10µg
97–
b
kidney
brain
–4µg
+4µg
–12µg
+12µg
–20µg
+20µg
97–
c
200–
97–
46–

**Figure 3.** Expression of uKHC and nKHC in rat pheochromocytoma PC12 cells before and after treatment with NGF.

**a**: Western blot immunolabelled with anti-uKHC affinity purified antibody; **b**: Western blot immunolabelled with anti-nKHC affinity purified antibody; **c**: SDS-PAGE protein stained with Coomassie brilliant blue. 30 μg of rat kidney and brain low speed supernatants were loaded in the first two lanes; equal amounts of total protein of control (-) and differentiated (+) PC12 cell low speed supernatants were loaded in each of the other three pairs of lanes, with different amounts of total protein loaded in the different pairs of lanes, as indicated. In **c**, molecular weight markers (kD) are shown on the left. The intensity of the uKHC immunoreactive bands does not vary after pharmacological treatment of the cells, whereas that of nKHC appears to increase in differentiated cells.

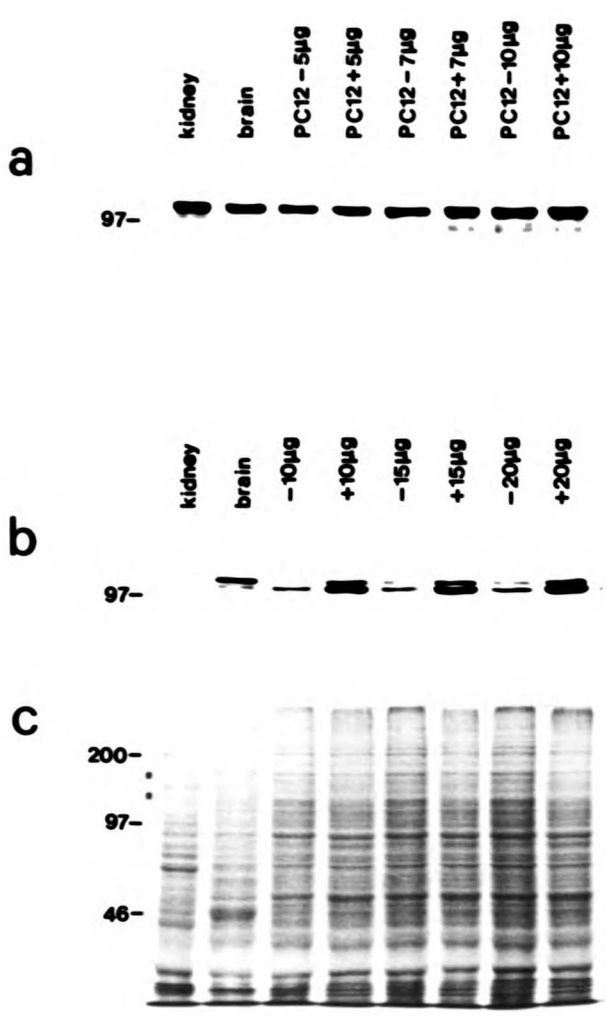

a
kidney
brain
PC12 −5µg
PC12 +5µg
PC12 −7µg
PC12+7µg
PC12 −10µg
PC12+10µg
97−
b
kidney
brain
−10µg
+10µg
−15µg
+15µg
−20µg
+20µg
97−
c
200−
97−
46−

**Figure 4**. Quantitative analysis of the expression of uKHC (black columns) and nKHC (hatched columns) in differentiated versus undifferentiated SH-SY5Y, IMR32 and PC12 cells.

The intensity of the uKHC and of nKHC immunoreactive bands in Western blots was measured as described in Materials and Methods and expressed in arbitrary units (AU)/mg of total protein; the ratio between AU/mg total protein of differentiated and differentiated cells is shown. For each cell line, data are the average of 2-3 experiments (±S.E.M.).

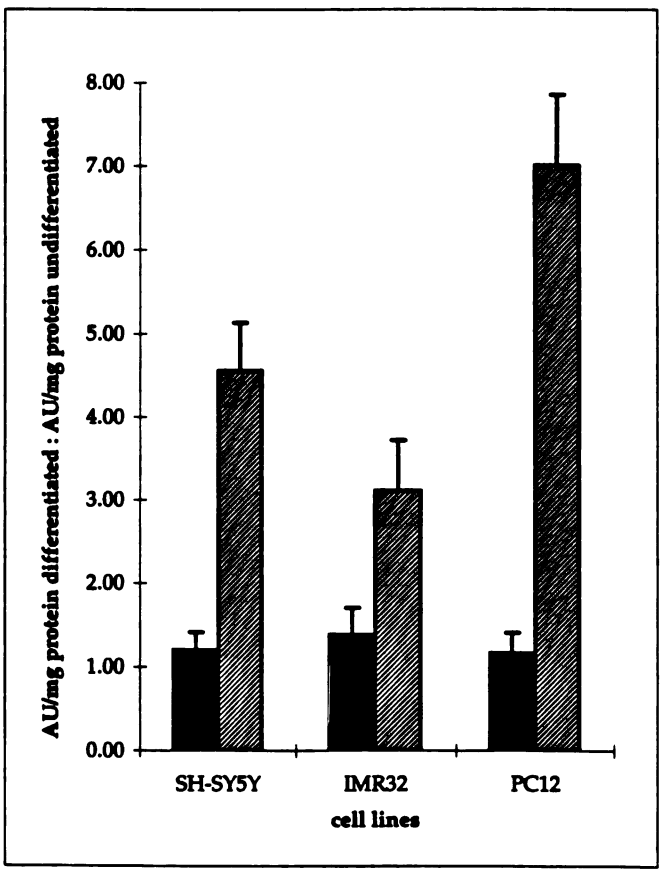
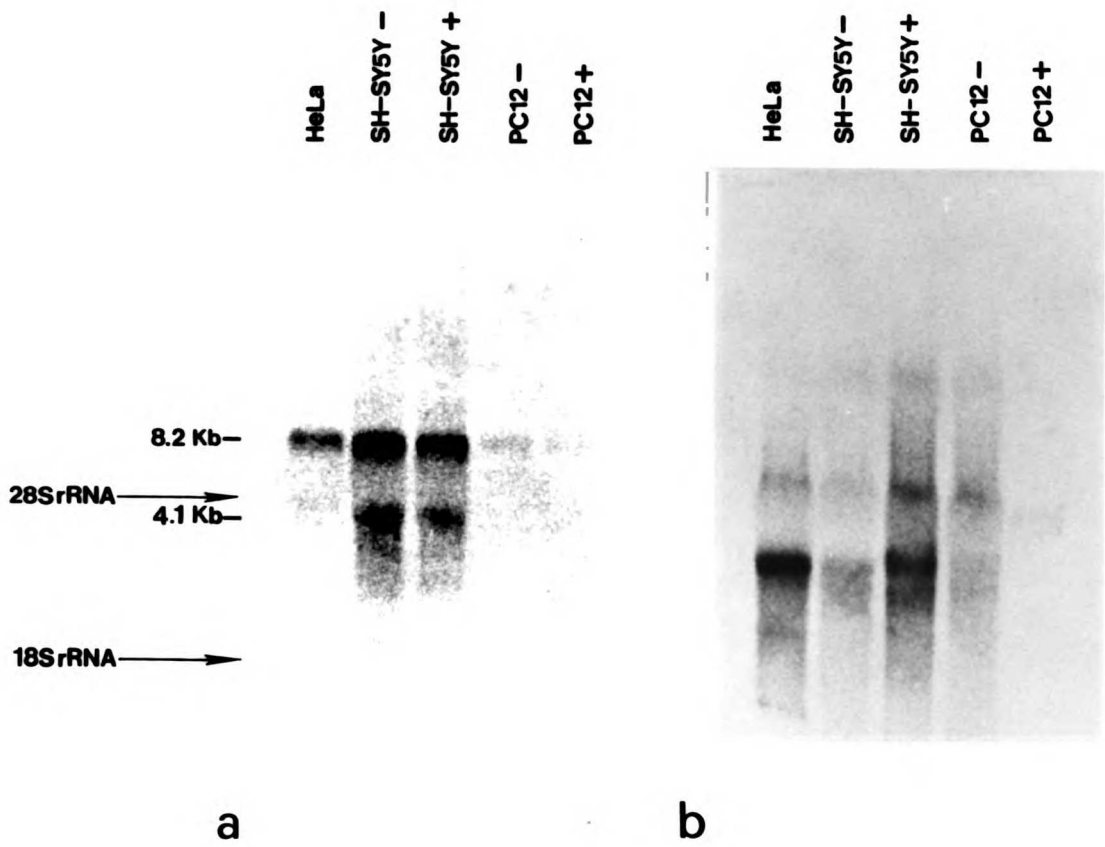

AU/mg protein differentiated : AU/mg protein undifferentiated
8.00
7.00
6.00
5.00
4.00
3.00
2.00
1.00
0.00
SH-SY5Y
IMR32
PC12
cell lines

**Figure 5**. Expression of uKHC and nKHC transcripts in control and differentiated SH-SY5Y and PC12 cells.

In **a**, the Northern blot was probed with the complete human placental library cDNA (nKHC) and, in **b**, with the partial human hippocampal library cDNA EST 257 (nKHC). Total mRNA (30 μg) obtained from SH-SY5Y and PC12 cells before (-) and after (+) pharmacological treatment was loaded in each lane. The same amount of HeLa cell total RNA was loaded in the first lane of both blots. The position of the 28S and the 18S ribosomal RNA species and the molecular size of the bands recognized by the uKHC and the nKHC probes are indicated on the left. The level of expression of the nKHC, but not of the uKHC transcripts, increased in both neuroblastoma and PC12 cells after pharmacological treatment with differentiating agents.


HeLa
SH-SY5Y −
SH-SY5Y +
PC12 −
PC12 +
8.2 Kb
28SrRNA
4.1 Kb
18SrRNA
HeLa
SH-SY5Y −
SH-SY5Y +
PC12 −
PC12 +

a b

# PART 2:

# Regulation of Microtubule-based Organelle Transport

# CHAPTER 3

# Cell Cycle Regulation Of Dynein Association With Membranes Modulates Microtubule-Based Organelle Transport

The work presented in Chapter 3 was done as a collaboration with Viki Allan. In this study, I attempted to determine the mechanism by which minus-end directed transport is regulated by the cell cycle in extracts of *Xenopus* eggs. First, I determined that cytoplasmic dynein is the predominant minus-end motor using a technique that specifically inactivates dynein and then showing that minus ended transport could be restored with purified dynein. Then, I showed that converting an extract from interphase to a metaphase state results in a drastic reduction in both minus-end directed transport as well as the amount of dynein attached to membrane-bound organelles. Viki Allan contributed the studies on cytoplasmic dynein phosphorylation and found that a polypeptide that copurifies with dynein is heavily phosphorylated in metaphase but not interphase extracts.

**ABSTRACT**

Cytoplasmic dynein is a minus-end directed microtubule motor that performs distinct functions in interphase and mitosis. In interphase, dynein transports organelles along microtubules, whereas in metaphase, this motor has been implicated in mitotic spindle formation and orientation as well as chromosome segregation. The manner in which dynein activity is regulated during the cell cycle, however, has not been resolved. In this study, we have examined the mechanism by which organelle transport is controlled by the cell cycle in extracts of *Xenopus laevis* eggs. Here, we show that photocleavage of the dynein heavy chain dramatically inhibits minus-end directed organelle transport and that purified dynein restores this motility, indicating that dynein is the predominant minus-end directed membrane motor in *Xenopus* egg extracts. By measuring the amount of dynein associated with isolated membranes, we find that cytoplasmic dynein and its activator dynactin detach from the membrane surface in metaphase extracts. The 10-fold decrease in membrane-associated dynein correlated well with the 8-fold reduction in minus-end directed membrane transport observed in metaphase versus interphase extracts. Although dynein heavy or intermediate chain phosphorylation did not change in a cell-cycle dependent manner, one of the dynein light chains incorporated ~12-fold more radiolabelled phosphate in metaphase than in interphase extracts. These studies suggest that cell cycle-dependent phosphorylation of cytoplasmic dynein may regulate organelle transport by modulating the association of this motor with membranes.

## INTRODUCTION

A variety of membranous organelles in the cytoplasm are transported along a polarized microtubule array to specific destinations within the cell. The complexity of this membrane traffic must require precise means of regulating both the levels and directionality of such microtubule-based motility. Physiological regulation of organelle transport has been most clearly demonstrated in fish chromatophores, where a cAMP-dependent kinase pathway (Lynch et al., 1986; Lynch et al., 1986; Rozdzial and Haimo, 1986) has been shown to be involved in the plus-end directed dispersion of pigment granules along microtubules. Conversely, dephosphorylation mediated by the phosphatase calcineurin (Thaler and Haimo, 1990) and an increase in intracellular $Ca^{2+}$ (Kotz and McNiven, 1994) have been implicated in the minus-end directed aggregation of these particles. Phosphorylation may control organelle transport in other cells as well, since the protein phosphatase inhibitor okadaic acid enhances minus-end directed ER tubule transport in frog egg extracts (Allan, 1995), bidirectional transport in mammalian cells in culture (Hamm-Alvarez et al., 1993), and plus-end directed lytic granule movements in T-cell extracts (McIlvain et al., 1994). In contrast, phosphorylation mediated by a $p34^{cdc2}$ kinase cascade suppresses organelle motility in metaphase frog egg extracts (Allan and Vale, 1991).

Protein motors, the ATP-hydrolyzing enzymes that power the movement of organelles on microtubules, represent likely targets for regulation of vesicle transport. The two best studied organelle motors, dynein (Paschal et al., 1987; Paschal and Vallee, 1987) and kinesin (Brady, 1985; Vale et al., 1985), move membrane-bound compartments towards the minus ends (slow growing) (Schnapp and Reese, 1989; Schroer et al., 1989) and plus ends (fast growing) (Hollenbeck and Swanson, 1990; Rodionov et al., 1991) of

microtubules, respectively. Both kinesin (Hollenbeck, 1993; Matthies et al., 1993; Okada et al., 1995) and dynein (Dillman and Pfister, 1994) are phosphorylated in cells, although the kinases involved and the functional consequences of such phosphorylation remain largely unresolved. Modulation of dynein and kinesin activity by phosphorylation, however, has been suggested by several studies. In the case of kinesin, specific phosphoisoforms were found to be selectively bound to membranes, and their levels were increased during neurite outgrowth after addition of nerve growth factor (Lee and Hollenbeck, 1995). For dynein, the heavy chain was observed to be less phosphorylated on anterogradely moving vesicles in rat optic nerves compared to the total cellular pool of vesicles, suggesting that dephosphorylation may inactivate dynein so that it could be carried by plus-end directed motors to the nerve terminal (Dillman and Pfister, 1994). In another study, okadaic acid was found to increase phosphorylation of the cytoplasmic dynein heavy chain as well as change the dynein immunofluorescence pattern from a vesicular staining to a more diffuse pattern (Lin et al., 1994). While this result suggests that dynein is released from the organelle surface upon phosphorylation, the stimulation of organelle transport by okadaic acid observed in other studies (Allan, 1995; Hamm-Alvarez et al., 1993; McIlvain et al., 1994) implies that the dynein that dissociated from the membrane in response to okadaic acid could represent an inactivate storage pool of the motor (Lin et al., 1994).

Organelle transport may also be regulated by motor-associated factors, some of which have been purified or partially purified using *in vitro* assays (Schroer and Sheetz, 1991). The best characterized activator is a multi-subunit factor called the dynactin complex which is required for dynein function in organelle motility (Gill et al., 1991) as well as in the mitotic spindle (Muhua et

al., 1994; Plamann et al., 1994). The mechanism by which dynactin regulates dynein activity, however, remains unclear. Three kinesin-associated proteins have also been implicated in regulating organelle movement, since their phosphorylation levels increased concomitantly with a 2-fold increase in lytic granule movement along microtubules after okadaic acid treatment (McIlvain et al., 1994).

In this study, we have examined the mechanism by which organelle transport is regulated by the cell cycle in *Xenopus laevis* eggs. In previous work, metaphase-arrested egg extracts were shown to support 10-fold lower levels of bidirectional organelle motility compared to interphase extracts (Allan and Vale, 1991). This cell cycle regulation of organelle transport is consistent with an overall decrease in vesicular trafficking in the secretory and endocytic pathways in mitosis (Warren et al., 1984; Warren et al., 1983). Here, we have investigated whether the cell cycle regulation of organelle movement involves a change in either the force-generating activity of microtubule motors or the association of motor proteins with membranes. We show that cytoplasmic dynein is the predominant minus-end organelle motor in *Xenopus* egg extracts and that cytoplasmic dynein and its activator dynactin detach from the membrane surface when interphase extracts are converted to a metaphase state. By measuring organelle motility in the same extracts, we find that the reduction in membrane-associated dynein correlates well with the decrease in minus-end organelle transport in metaphase extracts. While cell-cycle dependent phosphorylation of the dynein heavy and intermediate chains was not observed, a substantial increase in the phosphorylation of a dynein light chain was seen in metaphase compared to interphase extracts. These results suggest that dynein-based organelle

## MATERIALS AND METHODS

### *Xenopus Egg Extracts*

Interphase extracts were prepared from electrically activated *Xenopus laevis* eggs (Murray, 1991) with the following modifications. Cycloheximide was used during the egg breakage step to inhibit cyclin synthesis and hence arrest the extract in the interphase state. Final extracts contained 1 mM DTT, 100 μg/ml cycloheximide, *Xenopus* protease inhibitors (10 μg/ml leupeptin, 10 μg/ml chymostatin, 10 μg/ml pepstatin, 10 μg/ml aprotinin) and 10 μg/ml cytochalasin B. Extracts, which were typically 80-100 mg/ml in protein concentration, were stored in liquid nitrogen.

Metaphase extracts were made by treating interphase extracts with partially purified bacterially expressed cyclin Δ90 (0.13 mg/ml final concentration) (Murray et al., 1989), a nondegradable form of cyclin B, for 45 min at 22°C, in the presence of an ATP regenerating system (1 mM ATP, 1 mM $MgCl_2$, 7.5 mM creatine phosphate). Cyclin Δ90 maintains the extract in the mitotic state (Murray et al., 1989).

Histone H1 kinase assays (Murray, 1991) were used to assess the cell cycle state of interphase and metaphase extracts.

### *UV Vanadate Photocleavage of Egg Extracts*

Interphase crude extracts were supplemented with 2 mM ATP, 5 mM Mg-acetate, 2 mM DTT and 20 μM sodium orthovanadate. 40 μl drops of extract on sheets of parafilm taped to aluminum foil on a flat layer of ice were irradiated for 1 hr at a distance of 1 cm with ultraviolet light (366 nm) using a Model UVL-56 Blak-Ray lamp (UVP, Inc., San Gabriel, CA). Norepinephrine was not needed to reduce the orthovanadate ion, since the final concentration of orthovanadate was diluted to <10 μM in the motility assay; such

concentrations did not substantially inhibit organelle transport. High speed supernatants and membrane samples used in microscope assays were made as described below.

*Preparation of High Speed Supernatants and Membranes*

*Xenopus* egg crude extract samples were diluted with 1 volume of acetate buffer (10 mM HEPES, pH 7.4, 100 mM K-acetate, 150 mM sucrose, 5 mM EGTA, 3 mM Mg-acetate) containing protease inhibitors (described above) and 1 mM DTT and then spun at 109,000 x $g_{max}$ for 30 min at 2° C in either a Beckman TLA 120.1 or TLA 100.4 rotor. High speed supernatants and membrane pellets were collected. The membrane pellets were brought up in 3 volumes of 2 M sucrose in acetate buffer and then layered above 2 M sucrose/acetate buffer and below 1.4 M and 0.25 M sucrose/acetate buffer cushions. The membranes were then isolated by floatation up to the 0.25 M/1.4 M sucrose interface by spinning at 260,000 x $g_{max}$ for 30 min in a Beckman TLS-55 rotor.

*Organelle and Bead Transport Assays*

Organelle motility assays were performed in ~5 µl flow cells made from glass coverslips and slides spaced apart by two parallel strips of double-stick tape. Assays were done by pipetting samples sequentially into the flow cell in a 3 step process: 1) First, to polymerize an oriented microtubule array from centrosomes, 5 µl acetate buffer, 4 µl interphase frog egg high speed supernatant, 1 µl crude aster-forming surf clam *(Spisula solidissima)* egg extract (Palazzo et al., 1988; Palazzo et al., 1992) (gift from Robert Palazzo, Dept. of Physiology/Cell Biology, University of Kansas, Lawrence, Kansas) and 0.5 µl 20X ATP regeneration system were flowed into the chamber. 2) Once an

astral array of microtubules was located, it was washed and stabilized with 30 µl acetate buffer containing 0.4 µM taxol and the ATP regeneration system. 3) Finally, the samples of high speed supernatants with added organelles or 0.2 µM carboxylated beads (Polysciences, Inc., Warrington, PA) and the ATP regenerating system were introduced into the chamber. The movement of organelles or beads was then observed on a Zeiss Axioplan microscope equipped with differential interference contrast (DIC) optics, a 50W or 100W mercury arc lamp, and a 63X 1.4 NA Planapochromat objective. Images were detected using a Hamamatsu Newvicon camera, contrast enhancement and background subtraction were performed with a Hamamatsu Argus 10 image processor and recordings made with a Panasonic AG-1960 Super-VHS video tape recorder. Single frame images were captured from video tape onto a Macintosh Quadra 950 using NIH Image software.

Quantitation of organelle and bead motility was accomplished by counting the number of vesicle, membrane tubule or bead movements per min on astral microtubules. If an organelle or bead moved, then paused for more than 2 sec, and then moved again at some later time, it was scored as 2 movements. Recordings of motility were done on centrosome-nucleated microtubule asters of comparable size and microtubule density. These asters enabled the directionality of motility to be determined, since all microtubule minus-ends are located at the center. The polarity of these astral microtubule arrays was confirmed by a motility assay using kinesin-coated 0.2 µm carboxylated beads.

*Polyacrylamide Gel Electrophoresis and Immunoblotting*

Protein samples [quantitated by Bio-Rad protein assay (Bio-Rad Laboratories, Hercules, California) using γ-globulin as a standard] were separated on either 5%, 4-15% or 5-15% gradient polyacrylamide gels under

denaturing and reducing conditions (Laemmli, 1970) and then either Coomassie brilliant blue stained, silver stained or transferred to nitrocellulose. Immunoblotting (Towbin et al., 1979) was performed by electroblotting to nitrocellulose membranes at 0.2 A for 1 hr for 5% gels and 0.3 A for 1 hr for 5-15% gels. Blots were blocked for at least 4 hr in TBST-5% nonfat dry milk (TBST: 20 mM Tris, pH 7.5, 200 mM NaCl, 0.1% Tween-20). Primary antibody incubation with the *Dictyostelium* dynein heavy chain polyclonal antibody (made against a bacterially expressed 115 amino acid segment (Koonce et al., 1992) homologous to the cloned human segment used for antibody production in (Vaisberg et al., 1993) and was a gift from Mike Koonce, Wadsworth Center for Laboratories and Research, Albany, New York) was done overnight at 4°C in TBST-0.5% gelatin (1:5,000 fold dilution). The chicken dynein intermediate chain monoclonal antibody 70.1 (Steuer et al., 1990) was incubated for 1-2 hr at 22°C in TBST-5% nonfat dry milk (1:2,000 fold dilution). The human ubiquitous kinesin heavy chain polyclonal antibody (Niclas et al., 1994) was incubated overnight at 4°C in TBST-5% BSA (1:500 fold dilution). The chicken dynactin monoclonal antibody 150B (a gift from Trina Schroer, Dept. of Biology, The Johns Hopkins University, Baltimore, Maryland) was incubated overnight at 4°C in TBST-5% BSA (1:250 fold dilution). Blots were then washed 4 X 15 min in TBST and then 1 X 10 min in TBST-5% nonfat dry milk followed by a 1 hr incubation at 22°C with either horseradish peroxidase-conjugated donkey anti-rabbit or sheep anti-mouse immunoglobulin (Amersham, Arlington Heights, IL) at a 1:2,000 dilution in TBST-5% nonfat dry milk. After washing 4 X 15 min in TBST, blots were developed using the ECL Western blotting detection kit (Amersham) and exposed to either Kodak XAR-5 film (Eastman Kodak, Rochester, NY) or Hyperfilm-ECL (Amersham). Quantitative analysis of

bands on these films was done either with a LKB soft laser scanning densitometer or by scanning with a UMAX Power Look PS-2400X and then importing the image into the NIH Image software (Wayne Rasband, National Institutes of Health) for densitometric analysis.

*Purification of Frog Egg Cytoplasmic Dynein*

4 ml of crude interphase frog extract (S1) were diluted with 8 ml of BRB80 (80 mM K-PIPES, pH 6.8, 1 mM $MgCl_2$, 1 mM EGTA) containing *Xenopus* protease inhibitors, 0.1 mM PMSF and 1 mM DTT. A high speed supernatant (S2) was made by centrifugation at 109,000 x $g_{max}$ for 30 min at 2°C in a Beckman TLA-100.4 rotor. To the S2, taxol was added to 20 μM and prepolymerized bovine brain microtubules were added to 100 μg/ml. After 20 min at 22°C, apyrase was added to 1 U/ml and AMP-PNP to 0.2 mM, and S2 was incubated another 20 min at 22°C. The nucleotide-depleted S2 was then loaded onto a 20% sucrose cushion (BRB80, 4 μM taxol, 1 mM DTT, *Xenopus* protease inhibitors) and spun at 87,000 x $g_{max}$ for 10 min at 25°C (TLA 100.4 rotor). The microtubule-depleted supernatant (S3) was removed and the pellet resuspended in 0.8 ml BRB80 (4 μM taxol, 1 mM DTT and *Xenopus* protease inhibitors). The resuspended microtubules were spun at 87,000 x $g_{max}$ for 10 min at 25°C through a 20% sucrose cushion again. The supernatant (MT wash) was removed and the pellet brought up in 0.2 ml BRB80 (4 μM taxol, 1 mM DTT and *Xenopus* protease inhibitors) plus 10 mM Mg-ATP followed by a 20 min incubation at 22°C. The microtubules were then pelleted by spinning at 70,000 x $g_{max}$ (TLA 120.1 rotor) and the supernatant collected (ATP release). The ATP release was then loaded onto a 2.2 ml 5-25% sucrose gradient (*Xenopus* protease inhibitors, 1 mM DTT, 0.1 mM Mg-ATP) and spun at 2°C for 3 hr at 259,000 x $g_{max}$ (TLS-55 rotor). 0.2 ml

fractions were collected, and the dynein peak was determined by running the fractions on a polyacrylamide gel and Coomassie staining. The dynein peak fraction was kept on ice for the dynein addback experiment (Fig. 3A).

*Phosphorylation of Cytoplasmic Dynein in Extracts*

A pool of radiolabelled ATP was obtained by adding $^{32}$P-orthophosphate to extracts, and labelled cytoplasmic dynein was then isolated either by immunoprecipitation or by microtubule affinity followed by sucrose density gradient centrifugation.

For immunoprecipitation experiments, 20 µl of extract was pre-incubated with cyclinΔ90 or water for 30 min at 22°C, after which 100 µCi $^{32}$P-orthophosphate was added and the incubation continued for 30 min. The labelling was stopped by adding 1 ml of ice-cold IP buffer (10 mM Tris, 80 mM sodium β-glycerophosphate, 10 mM sodium pyrophosphate, pH 7.5, plus 1% Triton X-100 and protease inhibitors) and incubating on ice for 10 min. All subsequent procedures were carried out at 4°C. After a clarifying spin at 13,000 x $g_{max}$ in a microfuge, half the supernatant was incubated with 2.5 µl monoclonal antibody 70.1 ascites for 1-2 hr, while the other half served as a minus antibody control. Anti-mouse IgM agarose beads (obtained from Sigma) were then added (15 µl packed beads/sample), and the incubation continued for 1-2 hr. The beads were then washed 4x with IP buffer, once with IP buffer plus 500 mM NaCl, and finally once with 50 mM Tris (pH 7.5). Pellets were resuspended in sample buffer and analyzed on 4-15% SDS-PAGE gels. Following staining with colloidal Coomassie (Sigma Chem. Co.), the gels were dried and exposed to Fuji BAS-III imaging plates or Kodak Biomax film. Quantitation of labelled bands was performed on a Fuji BAS 2000 phosphoimager. To correct for differences in loading, the amount of

Coomassie stained cytoplasmic dynein heavy chains was determined by digitizing the bands using a Hewlett-Packard Scan Jet IIcx/T followed by analysis using NIH image software.

Microtubule affinity was used as an alternative method for purifying labelled cytoplasmic dynein. Extracts (100 µl) were pre-incubated with cyclin Δ90 or water for 20 min, supplemented with 200 µCi $^{32}$P-orthophosphate per sample, and then incubated for a further 40 min at room temperature. Labelled extracts were diluted with 220 µl buffer A (120 mM sodium β-glycerophosphate, 15 mM sodium pyrophosphate, 15 mM Hepes, 15 mM EGTA, 7.5 mM $MgCl_2$, pH 7.4) containing 1 mM DTT, protease inhibitors, 10 µg/ml cytochalasin D, and 1.5 µM microcystin. After incubation for 10 min on ice to depolymerize microtubules, supernatants were prepared by centrifugation at 174,000 x $g_{max}$ for 30 min at 4°C in a Beckman TLS-55 rotor. The microtubule affinity protocol was performed as described above but with slight modifications due to the small sample size. The amount of bovine brain tubulin microtubules added was increased to 150 µg/ml, and hexokinase and AMP-PNP were used at 10 U/ml and 0.4 mM, respectively. In addition, BRB80 was replaced in all subsequent steps by buffer B (buffer A diluted 1.5x, plus 4 µM taxol, 1 mM DTT, protease inhibitors, 1 µg/ml cytochalasin D, 1 µM microcystin). Microtubule pellets were resuspended in 100 µl for the wash step, and in 50 µl of buffer B plus 100 mM KCl and 5 mM MgATP for the motor release step. The motor fraction was then loaded onto 600 µl 10-25% sucrose gradients (in 25 mM K-PIPES, 1 mM $MgCl_2$, 1 mM EGTA, pH 6.8, plus 1 mM DTT, protease inhibitors, 100 nM microcystin) and centrifuged in an SW50 rotor with adapters for 5 hr at 200,000 x $g_{max}$, 4°C. Fractions (50 µl) were collected from the top of the gradient and were

## RESULTS

*Dynein is a Minus-end Organelle Motor in Xenopus Eggs*

Extracts from *Xenopus* eggs have been shown to promote high levels of minus-end microtubule-based organelle transport (Allan and Vale, 1991), but the motor responsible for this motility has not been identified. To determine if cytoplasmic dynein drives minus-end organelle transport in the *Xenopus* egg, we examined whether retrograde motility is eliminated after biochemically inactivating this motor. Previous studies in other systems (Schnapp and Reese, 1989; Schroer et al., 1989) have shown that photocleavage of cytoplasmic dynein by UV light in the presence of vanadate greatly reduces retrograde organelle motility. We performed a similar experimental paradigm in interphase-arrested crude *Xenopus* egg extracts by exposing them to UV irradiation (366 nm) for 1 hr in the presence of 2 mM ATP and 20 μM sodium orthovanadate. Under these conditions, 85% of the dynein heavy chain was photocleaved into two smaller fragments. The larger of these two fragments (~250 kDa) known as the heavy UV peptide (HUV) (Gibbons et al., 1987; Lee-Eiford et al., 1986) was recognized by an anti-dynein heavy chain antibody (Fig. 1, lane 4). Incubation with either UV irradiation or vanadate alone did not lead to any detectable cleavage (Fig. 1, lanes 2 and 3). UV-vanadate photocleavage is fairly specific for dynein, since the kinesin heavy chain was immune to photocleavage even at orthovanadate concentrations as high as 100 μM (data not shown).

UV-vanadate photocleaved extracts were tested for their organelle transport activity. Organelle transport activity was assayed by combining high speed supernatants as a source of soluble motor activity, with a crude membrane fraction isolated by floatation through a sucrose step gradient (see Materials and Methods). To establish the directionality of transport,

microtubules polymerized from *Spisula* egg centrosome particles (Palazzo et al., 1992) were used as a substrate for movement (Fig. 2). After extensive washing and stabilization of the microtubule asters with buffer containing taxol, mixtures of high speed supernatants and membranes were applied and plus- and minus-ended vesicle and membrane tubule movements were counted over a 30 min period. UV-vanadate treatment of the extract resulted in a 83% decrease in minus-end transport in comparison to the untreated control (Table 1). UV or vanadate alone had little effect on motility, indicating that the reduction of motility was due to photocleavage. Plus-end movements, on the other hand, were not reduced by UV-vanadate treatment. Similar results were also seen using 0.2 μm carboxylated beads, suggesting that they were also transported by dynein (Table 1). There was a small stimulation in motility seen in the vanadate-treated samples, particularly for bead movement, which could be due to vanadate's ability to inhibit phosphatases. It is known that treating *Xenopus* egg extracts with okadaic acid, another phosphatase inhibitor, results in increased minus-end directed organelle motility (Allan, 1995).

The above results suggested an involvement of dynein in retrograde organelle transport in the *Xenopus* egg extract. However, since the UV-vanadate treatment could potentially inhibit more than one minus-end motor, we sought to determine whether purified dynein could restore minus-end motility to photocleaved extracts. Egg cytoplasmic dynein was purified from interphase extracts via microtubule-affinity followed by centrifugation through a sucrose gradient. As described for purified mammalian brain dynein (Paschal et al., 1987), Coomassie-staining of the 20S fraction revealed a ~450 kD dynein heavy chain, an intermediate chain of ~85 kD, and light chains in the 50-65 kD range (Fig. 3A), although the 50 kDa band was not

observed in all preparations. In addition, a band of ~150 kD was present which appears to be dynactin (Gill et al., 1991) based upon its binding to an anti-dynactin antibody (see Fig. 4B). When this purified 20S dynein was added to the UV-vanadate photocleaved extract, the level of minus-end motility was increased from 9% to 67% and from 14% to 78% of control levels, respectively, in two different assays (Fig 3B). In contrast, the addition of 20S dynein did not have any effect on plus-end motility. Hence, dynein is responsible for the minus-end transport of most if not all of the vesicles and membrane tubules in the cytoplasm of the *Xenopus* egg.

*Dynein Dissociates from Membranes in Metaphase Extracts*

Previous studies have shown that both minus- and plus-end directed microtubule-based organelle transport are dramatically inhibited in metaphase extracts in comparison to interphase extracts (Allan and Vale, 1991). However, minus-end motility of microtubules along glass and beads along microtubules still occurred in metaphase extracts suggesting that the motor domain of soluble dynein is still active. These results suggested that either the motor activity of membrane-bound dynein was selectively inactivated or that dynein dissociated from membranes in mitotic extracts.

To distinguish between the two possibilities described above, the relative quantities of dynein attached to purified total cytosolic membranes isolated from interphase and metaphase-arrested extracts were examined. Interphase-arrested extracts were made from eggs that were electrically activated, and cycloheximide was included in order to inhibit cyclin synthesis. Metaphase extracts were prepared by treating the interphase extract with cyclinΔ90, a nondegradable form of cyclin B that activates $p34^{cdc2}$ kinase (Murray et al., 1989). H1 kinase assays were used to demonstrate conversion

of interphase extracts to metaphase (Fig. 4A). Crude membrane fractions were prepared by floatation through a sucrose step gradient, and equal amounts of interphase and metaphase membranes were then subjected to electrophoresis and immunoblotting. Densitometric analysis of the immunoblots revealed that interphase membranes contained 13-fold (SD=2.2, n=2) more dynein heavy chain compared with metaphase membranes. Similar immunoblotting experiments performed with a dynein intermediate chain antibody revealed 8.7-fold (SD=0.4, n=3) more dynein on interphase compared with metaphase membranes (Figure 4B). Dynactin (p150) of the dynactin complex, which has been shown to stimulate dynein-based organelle transport (Gill et al., 1991), was also similarly reduced (8.5-fold, SD=0.4, n=2) in metaphase compared to interphase membranes. In contrast, there was no difference in the amount of kinesin heavy chain associated with membranes from these two cell cycle states. In order to rule out the possibility that dynein is being degraded in the metaphase state, crude interphase and metaphase extracts were probed with either the anti-dynein heavy or intermediate chain antibodies. No change in the levels of the heavy or intermediate chain were found when comparing these two cell cycle states (Figure 4C).

The differences in association of dynein with membranes correlated with the reduction in minus-end organelle motility seen in the same extracts used for the isolation of membrane for immunoblotting. As shown in Figure 4A, minus-end motility was reduced 8-fold in the metaphase extract when compared to the interphase extract. These results strongly suggest that cytoplasmic dynein-based transport during the cell cycle is controlled by modulating the levels of dynein associated with organelles.

*Regulation of Dynein Phosphorylation by the Cell Cycle*

As many events in the cell cycle are modulated by phosphorylation, we investigated whether dynein is phosphorylated in a cell cycle-dependent manner. When dynein fractions prepared from interphase and metaphase extracts were analyzed by SDS-PAGE, it was clear that the major light chain isoform migrated with a higher apparent $M_r$ in the metaphase dynein (67 kDa versus 62.5 kDa: Fig. 5A). The most prominent lower molecular weight light chain had a $M_r$ of 52 kDa in both metaphase and interphase, unless the purification was performed in the presence of phosphatase inhibitors, in which case the apparent $M_r$ increased to ~57.5 kDa (Fig. 5A: M+ and I+). Since cytoplasmic dynein light chains from chicken and rat (Gill et al., 1994; Hughes et al., 1995) have been shown to migrate more slowly when phosphorylated, these data suggested that phosphorylation of the major light chain occurred in metaphase extracts, and that the other light chain isoforms were phosphorylated in both types of extract.

Incorporation of phosphate into the dynein molecule was assayed directly by incubating metaphase and interphase extracts with $^{32}$P-orthophosphate in order to generate a pool of $^{32}$P-γ-ATP, which then serves as a substrate for endogenous kinases. Dynein was immunoprecipitated using a dynein intermediate chain antibody (Fig. 5B), revealing a prominently phosphorylated band of ~67 kDa in metaphase extracts (lane M+), that was not detected in the absence of antibody (lane M-). In interphase, a band of slightly lower $M_r$ (62.5 kDa) was phosphorylated (not readily seen in Fig. 5B), but to a much lesser extent. These molecular weights correspond well to that of the major light chain described above, but this could not be confirmed by comparison with total protein composition of the immunoprecipitates due to co-migrating antibody bands. Quantitation of the labelled bands from phosphoimager data (with standardization for the amount of Coomassie-

stained heavy chain) revealed that 11.5-fold (± 2.6, n=3) more $^{32}$P-phosphate was incorporated into this putative light chain in metaphase versus interphase. All other labelled polypeptides were also observed in the minus antibody controls. Hence, neither the heavy nor intermediate dynein chains are undergoing phosphate turnover under these conditions.

In order to confirm that the phosphorylated 67 and 62.5 kDa bands observed in metaphase and interphase immunoprecipitates were dynein light chains, dynein was isolated from labelled extracts by microtubule affinity and sucrose density gradient centrifugation. Again, a prominent labelled band of 67 kDa was observed in metaphase dynein (Fig. 5C, left panel), which co-migrated with the major light chain isoforms identified by silver staining (Fig. 5D, left panel). Autoradiography of interphase dynein (Fig. 5C, right panel) revealed a polypeptide of 62.5 kDa which co-migrated with the major interphase light chain isoform (Fig. 5D, right panel), and which had incorporated 13.1-fold less $^{32}$P-phosphate than the metaphase light chain. A high $M_r$ polypeptide in both metaphase and interphase gradients also contained a low level of phosphate, but the peak of this labelled species across the gradient did not match that of dynein (data not shown) and is therefore unlikely to be dynein heavy chain.

One unexpected finding was that preparing the dynein in the presence of phosphatase inhibitors drastically reduced the amount of the p150$^{Glued}$ component of dynactin present in the dynein gradient fractions to levels that were undetectable by silver staining (Fig. 5A: compare M+ and I+ with M- and I-). This makes it highly unlikely that the phosphorylated 67 kDa and 62.5 kDa polypeptides could be components of the dynactin complex.

## DISCUSSION

In this study, we have examined the mechanism by which organelle transport is regulated by the cell cycle in extracts of *Xenopus* eggs. Previous work by Allan and Vale (1991) documented a profound inhibition of minus-end directed membrane motility when an interphase extract was converted to a metaphase state. Here, we have shown that cytoplasmic dynein is the predominant, if not sole, motor that drives minus-end directed organelle transport and have found that the amounts of dynein and its activator, dynactin, that are bound to membranes decrease ~10-fold when extracts enter metaphase. The magnitude of this decrease in membrane-associated dynein is very similar to the reduction in minus-end directed organelle transport observed in the same metaphase extracts. Thus, modulation of dynein association with membranes appears to provide an explanation for how minus-end directed organelle transport is controlled by the cell cycle.

Regulation of both dynein association with membranes and dynein-based organelle transport must be mediated by a post-translational event, since the cell cycle state of extracts can be interconverted in the presence of protein synthesis inhibitors. Although a previous study did not detect any phosphorylation of dynein in crude interphase and metaphase motor fractions (Verde et al., 1991), we detected substantial phosphorylation of dynein isolated from metaphase extracts by either immunoprecipitation or microtubule affinity and velocity sedimentation. The polypeptide that incorporated radiolabelled phosphate is most likely a cytoplasmic dynein light chain isoform, since it cofractionated with dynein heavy chain at 20S by sucrose gradient velocity sedimentation and since the dynactin complex was absent from this fraction. The increase in the incorporation of radiolabelled phosphate into this ~67 kDa light chain in metaphase compared to interphase

extracts (~12 fold) is similar to the magnitude of the changes observed in organelle transport and dynein association with membranes. In contrast, the heavy and intermediate chains incorporated very little radiolabelled phosphate, and labelling did not change in a cell cycle dependent manner. The kinase involved in this light chain phosphorylation is not known. However, $p34^{cdc2}$ kinase may not be directly involved, since incubation of membranes with baculovirus expressed $p34^{cdc2}$/cyclin B did not cause dissociation of dynein from membranes (data not shown).

These findings suggest that light chain phosphorylation may be responsible for decreasing the affinity of dynein for membranes, although phosphorylation of additional proteins might also be involved. The dynein light chains have been considered to be strong candidates for targeting this motor to different intracellular cargoes. In the case of flagellar dynein, the intermediate and light chains may be responsible for anchoring the motor to the A-microtubules of the axoneme (King and Whitman, 1990; King et al., 1991; Mitchell and Rosenbaum, 1986), while the intermediate and light chains of cytoplasmic dynein have been proposed to serve a similar function in docking cytoplasmic dynein to intracellular targets (Gill et al., 1994; Hughes et al., 1995; Paschal et al., 1992). Dynein light chain phosphorylation may cause dissociation of cytoplasmic dynein from membranes and allow this motor to bind to new cargo and perform distinct roles during metaphase. Various studies have provided evidence that dynein is involved in mitotic spindle formation (Vaisberg et al., 1993), spindle orientation and nuclear segregation (Eshel et al., 1993; Li et al., 1993; Plamann et al., 1994; Xiang et al., 1994) and chromosome segregation (Saunders et al., 1995). Furthermore, at least some studies have shown that dynein changes its location from a vesicular staining

in interphase to spindle and kinetochore staining in mitosis (Pfarr et al., 1990; Steuer et al., 1990).

This is the first study, to our knowledge, in which dynein phosphorylation and dynein-based organelle transport have been examined in the same system. However, other studies have indirectly suggested a possible connection between dynein phosphorylation and organelle transport. In some cases, increased phosphorylation is thought to activate dynein-driven membrane movement, in contrast to the results presented here. In interphase *Xenopus* egg extracts, the phosphatase inhibitor okadaic acid increases minus-end directed ER membrane tubule motility without changing the levels of membrane associated dynein (Allan, 1995). Whether this activation is due to increased dynein phosphorylation is not yet known. In addition, studies in the rat optic nerve suggest that phosphorylation of dynein may stimulate membrane transport, since dynein heavy chain phosphorylation is higher on retrograde versus anterograde-moving organelles (Dillman and Pfister, 1994). In both of these cases, phosphorylation during interphase in both these cases seems likely to modulate dynein motor activity rather than dynein binding to the membrane as occurs in the mitotic regulatory mechanism described here.

The effects of dynein phosphorylation may also differ in various cell types. In contrast to interphase *Xenopus* extracts where okadaic acid does not change dynein association with membranes (Allan, 1995), okadaic acid treatment of interphase fibroblasts causes the dissociation of dynein from membranous organelles, an effect that correlates with dynein heavy chain phosphorylation (Lin et al., 1994). How this affects organelle motility in these cells was not investigated. However, as other studies have shown that okadaic acid treatment in interphase increases levels of minus end-directed

movement (Hamm-Alvarez et al., 1993; Allan, 1995), the released population of dynein may represent an inactive storage form of the motor (Lin et al., 1994). Furthermore, the association of dynein with membranous organelles in fibroblasts was not reduced in mitosis, as judged by immunofluorescence microscopy (Lin and Collins, 1992). To resolve these apparent contradictory results, it is clear that both the phosphorylation state and the activity of dynein need to be studied in parallel for each experimental system. Nevertheless, these results, in conjunction with ours, suggest that dynein association with membranes may be regulated differently in different cell types.

Plus-end directed motility in *Xenopus* extracts is also suppressed in metaphase extracts when compared to interphase extracts. A likely candidate for a motor mediating at least a portion of the plus-end directed motility is kinesin. Unlike dynein, levels of this motor on membranes isolated from interphase and metaphase extracts are the same, suggesting that kinesin may be regulated in a different manner than dynein. Further work is required to establish whether plus-end directed organelle transport is regulated by controlling the force-generating activity of kinesin or whether other plus-end directed motors drive organelle transport in the *Xenopus* egg.

## ACKNOWLEDGMENTS

This work was supported by grants from the Medical Scientist Training Program (N.I.H) and the UC Chancellor's Fellowship (both to J.N.) and the National Institutes of Health (R.D.V.). Dr. Viki Allan is a Lister Fellow and her work was supported by the Lister Institute and the Royal Society. We would like to thank Dr. Robert Palazzo for the aster-forming *Spisula* extract

and advice on their use, Drs. Frank McNally and Paul Clarke for the cyclinΔ90, Dr. Trina Schroer for the anti-dynactin monoclonal antibody, Drs. Mike Koonce and Richard McIntosh for the anti-Dictyostelium heavy chain antibody, Dr. Ian Gibbons for advice on the UV-vanadate photocleavage technique, and Dr. Colin Stirling for advice on phosphoimaging and image transfer. We thank Arshad Desai for providing comments on the manuscript.

**Table I.** Organelle and bead transport in UV-vanadate photocleaved interphase *Xenopus* egg extracts.

| | Minus-end directed | | Plus-end directed | |
|---|---|---|---|---|
| | organelles | beads | organelles | beads |
| | *movements/min* | | *movements/min* | |
| No treatment | 4.6 | 5.1 | 0.8 | 0.3 |
| UV | 3.4 | 4.8 | 0.8 | 0.5 |
| Vanadate | 5.5 | 9.4 | 0.9 | 0.8 |
| UV-vanadate | 0.8 | 1.0 | 0.8 | 0.2 |

High speed supernatants and isolated membranes were prepared from the four extract samples described in Figure 1. 8 µl high speed supernatant (14.4 mg/ml) and 2 µl membranes (10 mg/ml) or 2 µl carboxylated beads (1:40 dilution of 2.5% latex solids) were combined, applied to centrosome-nucleated microtubule arrays and assessed for minus- and plus-end directed motility for 30 min periods.

**Figure 1.** UV-vanadate photocleavage of cytoplasmic dynein in *Xenopus* egg extracts. Samples of crude interphase egg extracts containing 2 mM ATP, 5 mM Mg-acetate and 2 mM DTT were incubated for 1 hr on ice under the following conditions. Lane 1, no UV irradiation or vanadate; lane 2, UV irradiation only; lane 3; 20 μM vanadate only; lane 4, UV irradiation and 20 μM vanadate. 100 μg of each sample were run on a 5% polyacrylamide gel, transferred to nitrocellulose and then probed with an anti-Dictyostelium dynein heavy chain polyclonal antibody that only recognizes the larger of the two photocleavage products. Molecular size standards (kDa) are shown on the left side. The dynein heavy chain (DHC) and the larger heavy chain photocleavage product (HUV) are indicated on the right side.


1 2 3 4
kDa
-DHC
-HUV
200-
116-
97-

**Figure 2.** Polarized array of microtubules nucleated by a *Spisula* egg centrosome. These astral microtubules were used to determine the directionality of organelle transport. Centrosome-nucleated microtubules are organized such that their minus-ends are at the center and plus-ends at the periphery. This was confirmed by the observation that kinesin-coated beads moved away from the aster center (data not shown). These asters had the advantage over axoneme-nucleated microtubules of having a much higher microtubule density for capturing vesicles. Microtubules were viewed by video-enhanced differential interference contrast microscopy.

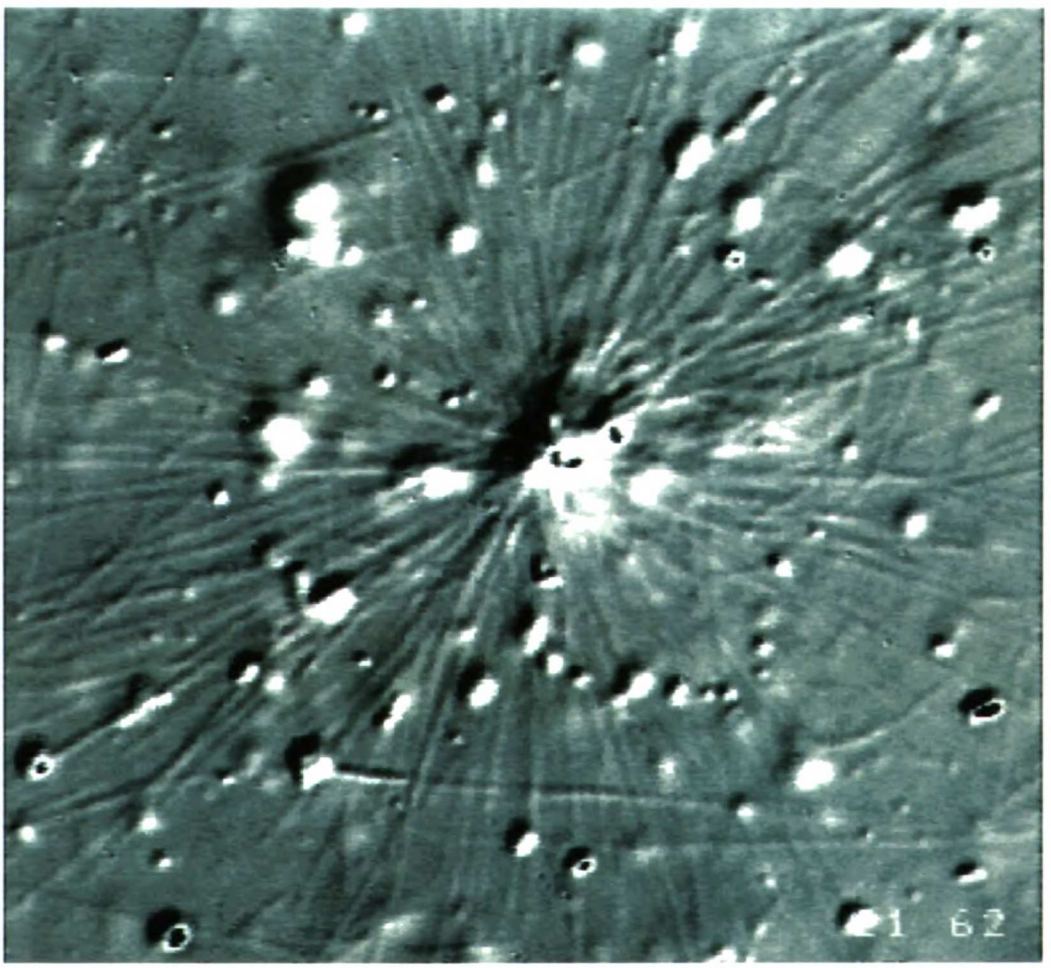
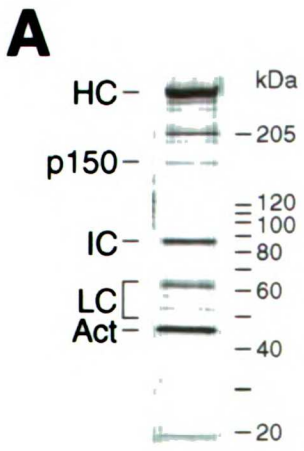

1 62

**Figure 3.** Restoring minus-end directed transport to UV-photocleaved extracts with purified *Xenopus* egg dynein. (A) Cytoplasmic dynein was purified by microtubule-affinity followed by a 5-25% sucrose gradient. 0.8 μg of 20S dynein was run on a 4-15% polyacrylamide gradient gel and silver-stained. The positions of the dynein heavy (HC), intermediate (IC) and light (LC) chains as well as actin (Act) and $p150^{Glued}$ (p150) are indicated on the left. Molecular size standards (205, 120, 110, 100, 90, 80, 70, 60, 50, 40, 30 and 20 kDa) are shown on the right. (B) Stimulation of minus-end directed transport in UV-vanadate treated extracts by addition of purified dynein. Data from two experiments using different concentrations of 20S dynein and UV-vanadate photocleaved high speed supernatant in 10 μl reactions are shown. In the first experiment (solid bars), 6 μl high speed supernatant (14.4 mg/ml) and 2 μl purified total membrane (10 mg/ml) were combined. In the second experiment (hatched bars), 4 μl high speed supernatant (14.4 mg/ml) and 2 μl purified total membrane (10 mg/ml) were used. In both cases, the remainder of the volume was made up with either acetate buffer or sucrose gradient purified dynein (0.12 mg/ml). 20 minute assays were recorded for each sample and organelle movements scored.


A
HC
p150
IC
LC
Act
kDa
205
120
100
80
60
40
20

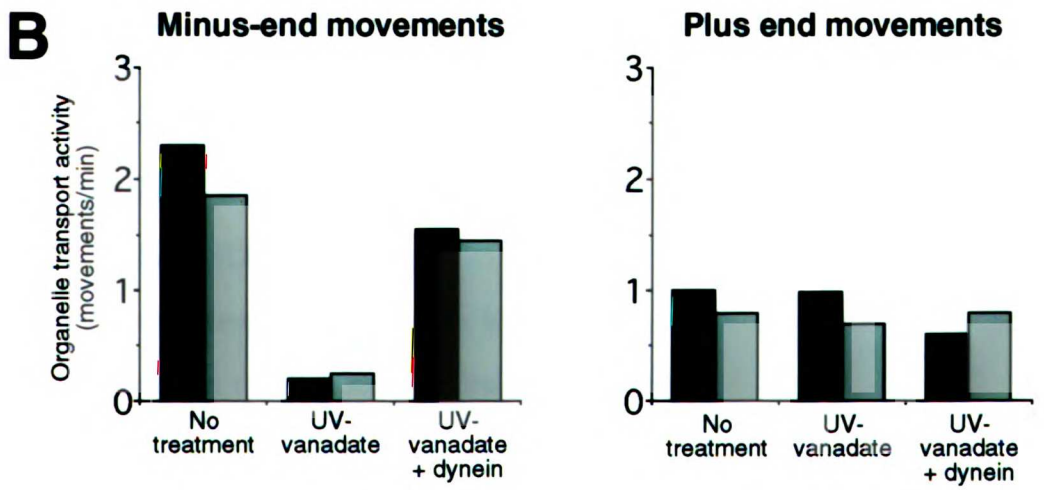
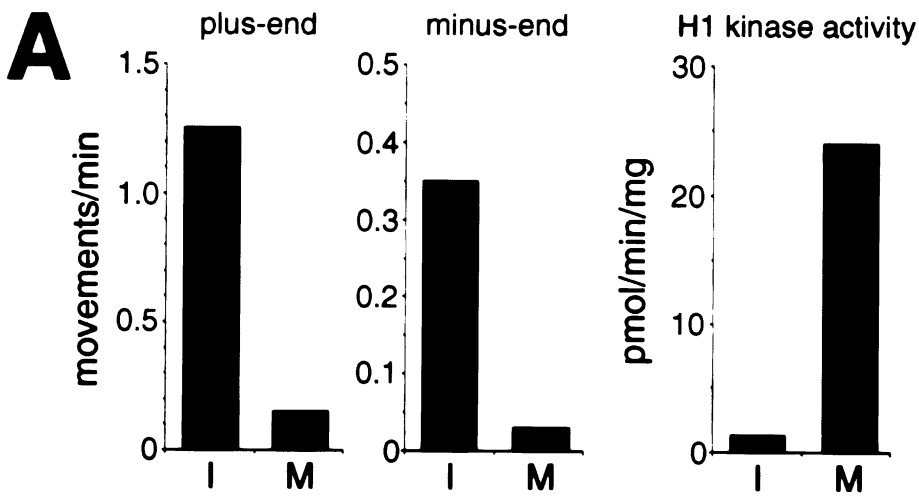
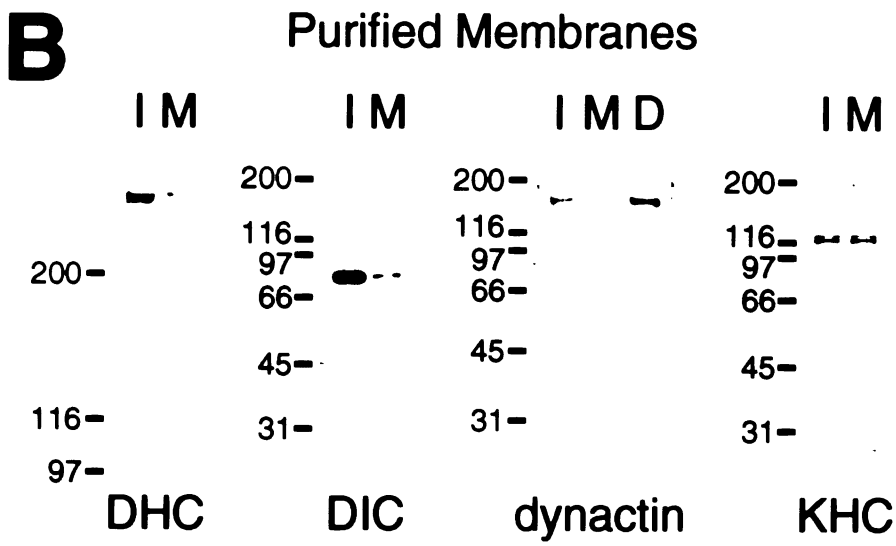

B
Minus-end movements
Plus end movements
Organelle transport activity
(movements/min)
3
2
1
0
No treatment
UV-vanadate
UV-vanadate + dynein

**Figure 4.** Minus-end directed motility and association of dynein with cytosolic membranes decrease in parallel in metaphase versus interphase extracts. (A) Minus- and plus-end directed organelle motility was scored by combining 5 µl of interphase or metaphase high speed supernatant (16.5 mg/ml) with 5 µl isolated interphase or metaphase total membrane (2.5 mg/ml), respectively, and 0.5 µl of a 20X ATP regenerating system. Levels (organelle movements/min) and directionality (minus or plus) of transport of vesicles and membrane tubules were assessed on centrosome-nucleated microtubule asters. (B) Immunoblots of equal loadings (40 µg for all cases except dynactin which had 150 µg) of isolated interphase (I) and metaphase (M) membranes were probed with antibodies directed against either dynein heavy chain (DHC), dynein intermediate chain (DIC), kinesin heavy chain (KHC) or dynactin. The immunoblot for dynactin also had a control lane of 2.5 µg 20S *Xenopus* dynein (marked "D") to show that the anti-chicken dynactin monoclonal antibody recognizes *Xenopus* dynactin (lane marked "D"). (C) Immunoblots of equal loadings (160 µg) of crude interphase and metaphase extracts were probed with anti-dynein heavy chain (DHC) and intermediate chain (DIC) antibodies to show that the total amount of dynein in interphase and metaphase extracts is the same. Molecular size standards (kDa) are shown on the left sides of the immunoblots.


A
plus-end
minus-end
H1 kinase activity
movements/min
pmol/min/mg
1.5
1.0
0.5
0
0.5
0.4
0.3
0.2
0.1
0
30
20
10
0
I
M
I
M
I
M


B
Purified Membranes
I M
I M
I M D
I M
200
116
97
66
45
31
DHC
DIC
dynactin
KHC

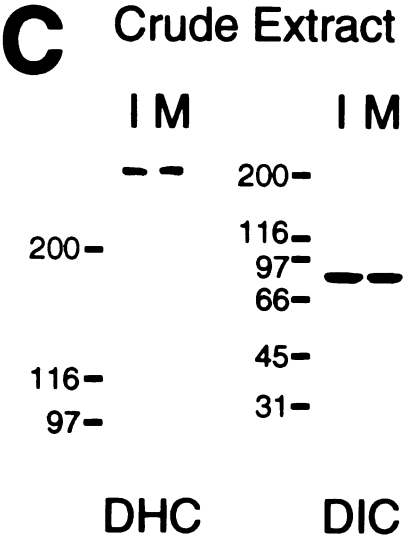
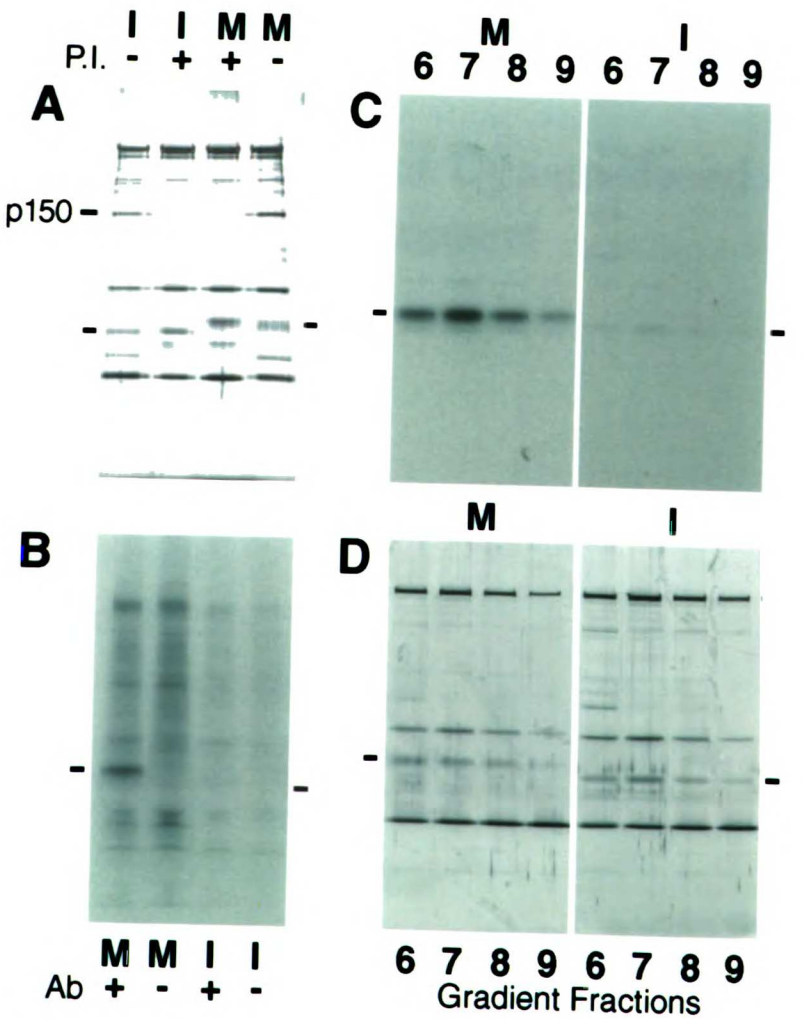

C
Crude Extract
I M
I M
200
116
97
66
45
31
DHC
DIC

**Figure 5.** Cell cycle-dependent phosphorylation of a dynein light chain. The apparent molecular weights of unlabelled dynein light chains were compared by silver staining (A) following isolation from metaphase (M) and interphase (I) extracts in the presence (+) or absence (-) of phosphatase inhibitors (P.I.), revealing substantial changes in light chain mobility. Heavy lines in all panels indicate the position of the major light chain isoform. The 150 kDa dynactin polypeptide (p150) is also indicated. Panels B, C and D: interphase (I) and metaphase (M) extracts were incubated with $^{32}$P-orthophosphate as described in Materials and Methods, and then cytoplasmic dynein was isolated using two different protocols. In panel B, dynein was immunoprecipitated using an intermediate chain monoclonal antibody (lanes marked +), with omission of antibody as controls (lanes marked -). Autoradiography revealed that a 67 kDa band was strongly labelled in metaphase but not in interphase. In panels C and D, dynein was isolated by microtubule affinity and sucrose density gradient centrifugation. Four adjacent fractions (from top to bottom of gradient: 6, 7, 8 and 9) containing the dynein peak are shown, with phosphorylated protein detected by autoradiography (C) and total protein revealed by silver staining (D) (Left panels, metaphase; right panels, interphase). Again, phosphate was strongly incorporated in metaphase into a 67 kDa band that co-migrated with the major light chain.


I I M M
P.I. - + + -
A
p150
B
M M I I
Ab + - + -
M
I
6 7 8 9 6 7 8 9
C
D
6 7 8 9 6 7 8 9
Gradient Fractions

# APPENDIX 4:

# Isolation of Activators of Dynein-Based Organelle Transport

The following section is a brief discussion of efforts to reconstitute organelle transport using components from *Xenopus* egg and *Spisula* egg extracts with the intent to identify factors necessary for dynein-driven organelle transport. Such factors are of great interest since they represent potential regulators of vesicle motility. The purpose of this appendix is to summarize the approach taken to identify such modulators of organelle transport and then to suggest additional pathways that may help in identifying such proteins.

In order to understand how organelle motility occurs, one must identify all the relevant components of the transport machinery. At present, the motor proteins are the best characterized parts of this machinery. However, they are not sufficient for membrane motility, demonstrating that there are additional factors that are necessary for motors to perform their organelle transporting functions. These additional proteins might play roles in regulating the activity of motors or docking motors to organelles and microtubules. Possible approaches to identifying such factors include looking for proteins that interact with motors by affinity chromatography and fractionating extracts into components that when added together are able to reconstitute organelle motility. The latter has the advantage of being a purification method based upon activity and not just protein-protein interactions.

Many attempts have been made by those in the motor protein field to reconstitute organelle transport *in vitro*. It is possible to obtain motility by adding together crude membrane fractions and cytosolic high speed supernatants. However, the addition of purified motors such as kinesin and dynein to purified organelles typically results in little or no motility. The only real successful work at reconstituting organelle transport with a purified motor and purified additional factors involved the identification of the dynactin complex (Gill et al., 1991; Schroer and Sheetz, 1991). This very large complex which runs at 20S in a sucrose gradient is required for the stimulation of organelle motility by cytoplasmic dynein, however, its mechanism of action has not yet been determined. While this work was in progress, I also was trying to identify such a factor(s), but instead of using extracts from avian and mammalian brain, I chose to work with *Xenopus* and *Spisula* (surf clam) egg extracts. These systems were selected because of their

ability to support very active organelle motility in crude extracts, unlike the mammalian brain extracts. In the latter case, microtubule affinity was required to concentrate motor activity so that it was detectable in microscope assays. Hence, the frog and clam eggs appeared to be preferable systems.

The main goal for the fractionation experiments was to purify dynein away from other potential factors that activate minus-end motility in frog and clam egg extracts, and then to recombine dynein with these other fractions to identify activating factors. The method chosen was gel filtration chromatography using Biogel A-1.5m resin. 0.5 ml of high speed supernatant from egg extracts was applied to a 10 ml column and 0.5 ml fractions collected. This column matrix was chosen since cytoplasmic dynein exited the column in the void volume as a result of its very large size (~1.2 X $10^6$ Da) and smaller proteins would come out in later fractions. In order to compensate for the dilution caused by the gel filtration column, the protein-containing fractions were pooled (2 fractions to a pool starting with the first protein-containing fraction) and concentrated 10-fold with Centricon 30 concentrators.

The concentrated pools were then tested for the ability to promote the transport of a rat liver Golgi vesicle fraction (Leelavathi et al., 1970) along polarized microtubules and motility was viewed using video-enhanced DIC microscopy (see Materials and Methods in Chapter 3). Whether frog or clam high speed supernatants were used, it was found that Pool 1 (void volume fraction containing dynein) displayed substantial activity while the subsequent fractions also promoted movement, but to a lesser degree. When Pool 1 was tested in combination with each of the other pools, it was found that Pool 4 seemed to stimulate the activity of Pool 1 in more than just an additive manner (~2 to 3-fold stimulation). Although, this level of stimulation was rather low, it still seemed promising.

Further attempts to repeat and refine this purification method were, however, met with problems of reproducibility. In the ideal scenario, Pool 1 and Pool 4 would have had very little activity on their own, but in combination would have displayed strong synergism. In the many attempts to fractionate both frog and clam egg extracts by gel filtration chromatography, sometimes Pool 1 had a great deal of activity on its own and other times it had much less. Pool 4 activity was also markedly variable. It was also determined by Western blotting that dynein was also present in Pools 2, 3, and 4, but in much smaller quantities. This might explain the variability of activity present in Pool 4. It is possible that reproducibility would have been better had an FPLC chromatography system and higher quality gel filtration columns been used.

In addition to the reproducibility problem, I also found that the frog and clam extracts could not be diluted more than ~8-fold, before organelle motility became nearly undetectable (<0.5 movements/min). In terms of doing successive purification steps, this result suggested that the probability of success was relatively low and that the concentrating of samples would have been necessary at every step. Also, since the microscope-based organelle transport assay is very time and labor-intensive, one round of purification with motility assays to identify active fractions represented a full days worth of work. A multi-step purification would likely take several days to complete. This would be problematic considering that the transport-promoting activity of the extract seemed to be severely diminished after a 24 hour incubation on ice.

I never tried to concentrate motor activity by microtubule affinity followed by ATP release and sucrose velocity gradient as was done by others using brain tissue as an extract source (Gill et al., 1991; Schroer and Sheetz,

1991). It was necessary for the studies of the organelle transport machinery from mammalian brain, since extracts from this tissue do not display any detectable motility. That approach was not chosen because of the concern of losing potentially important factors if this were used as the first step for purification. However, that method proved to be fruitful for the studies using brain extracts and led to the purification of the dynactin complex (Gill et al., 1991). On the other hand, the amount of motility that was obtained in the reconstituted mammalian brain system was very low compared to the activity that one sees in crude extracts from other organisms such as frog and squid, implying that additional stimulatory factors may be missing.

It is possible that other systems may prove to be more user-friendly than frog or clam extracts. Extracts from *Dictyostelium* represent a possible alternative since they have recently been shown in our lab to promote high levels of bidirectional organelle motility (Nira Pollock, personal communication). It is also quite likely that there are regulators of plus and minus-end motility that have not been characterized yet. For example, there is a second activating fraction (dynactin being the first) of organelle motility identified by Schroer et al. (1991), that has yet to be characterized. Perhaps, Dictyostelium extracts may be more amenable to studies involving fractionation than were extracts from frog and clam eggs.

# CONCLUSIONS

**Summary**

The work presented in this thesis includes studies on the two microtubule-based motor proteins, kinesin and cytoplasmic dynein. Part 1 discussed the identification of two conventional kinesin heavy chain genes in mammals, a placental library derived gene (Chapter 1, Appendix 1) later called ubiquitous kinesin (uKHC) based on its universal tissue expression patterns (Chapter 2) and a hippocampal library derived gene called neuronal kinesin (nKHC) (Chapter 2). It should be noted that whenever the term "kinesin" is used, it refers to studies of this motor before the discovery of the second neuronal-specific isoform. In Chapter 1, the cytosolic targets of the motor, rod and tail domains of uKHC were examined in order to gain some understanding of this motor's function in the cell. In Appendix 2, the role of uKHC in neuronal development and axonal transport of certain subpopulations of membrane-bound vesicles was demonstrated. Chapter 2 discussed the discovery of a second conventional kinesin heavy chain in humans as well as its exclusive expression in neurons (nKHC). An extensive immunocytochemical analysis of its distribution in the brain as well as biochemical characterization of the fractionation of both uKHC and nKHC with membranes and microtubules in brain extracts were presented. Part 2 contained the results of a study of the regulation of organelle transport. In chapter 3, the mechanism of cell cycle modulation of cytoplasmic dynein-based transport in *Xenopus* eggs was examined by studying the association of dynein with membranes from interphase and metaphase extracts. In addition, a dynein light chain polypeptide that may be involved in this regulatory mechanism was identified through phosphorylation studies. The following sections discuss the results included in this thesis as well as the questions they raise for future studies.

# Part 1: The Mammalian Conventional Kinesins

## The ubiquitous and neuronal kinesin heavy chain genes

### *The ubiquitous kinesin heavy chain gene*

The kinesin heavy chain (KHC) gene that we cloned from a human placental cDNA library [and later called ubiquitous kinesin heavy chain (uKHC) based upon its expression patterns] demonstrated a high level of sequence identity over the entire molecule to the previously cloned *Drosophila* (Yang et al., 1989), squid (Kosik et al., 1990), and sea urchin (Wright et al., 1991) KHC sequences. The similarity between invertebrate KHCs and human ubiquitous KHC is particularly striking in the motor domain, where long stretches of nearly 100% amino acid identity were found. These regions of high conservation most likely play important roles in microtubule-binding, ATP hydrolysis and force generation. The C-terminal tail domain also displays segments of very high amino acid identity, which may represent regions that could be involved in binding to intracellular cargo. The central rod domain shows far less homology except at its C-terminus.

The characterization of the uKHC gene led to the discovery of an upstream open reading frame (ORF) and a G-C rich leader sequence in the 5' untranslated region that may be involved in translational regulation. This ORF has a perfect consensus sequence for ribosomal initiation of translation (Kozak, 1987). Upstream AUG codons are rare among eukaryotic mRNAs and are absent from the invertebrate KHC sequences. It is known that upstream ORFs (Hinnebusch, 1990) as well as G-C rich regions in the 5'-untranslated region can regulate mRNA translation (Rao et al., 1988). Both

may pose obstacles to translation initiation by ribosome scanning and hence suggest the possibility of internal initiation as has been shown for the mRNAs encoding BiP (Macejak and Sarnow, 1991) and polio virus proteins (Pelletier and Sonnenberg, 1988). Since invertebrates do not have upstream ORFs or a G-C rich leader sequence, these results suggest that vertebrates may have acquired a means of regulating kinesin expression at the translational level. This possibility has yet to be examined and the uKHC gene might represent a useful system for studying internal initiation of translation as well as translational repression of a eukaryotic message.

*The neuronal kinesin heavy chain gene*

Subsequent to the isolation of the ubiquitous kinesin heavy chain gene (Chapter 1, Appendices 1 and 2) (Navone et al., 1992), we discovered a new gene encoding a second human KHC (called neuronal KHC or nKHC; Chapter 2) (Niclas et al., 1994). These two KHCs, which display a high degree of amino acid identity throughout their sequences, are clearly encoded by different genes based on Southern blotting, chromosome mapping, and sequence analysis. Whether the nKHC gene also has translational regulation elements in the 5'-UTR is unknown since none of the cDNA clones isolated contained extensive 5'-UTR sequence. The isolation of the nKHC gene demonstrates that, within the kinesin superfamily, there is more than one conventional KHC.

The human nKHC gene resembles other kinesin cDNAs isolated from mouse brain libraries. Kato (1990) isolated a cDNA (DN40) that was expressed predominantly in the cerebral and cerebellar cortices as well as the motor trigeminal nucleus and encoded a conventional mouse KHC (unpublished but available via Genbank accession number X61435). It is more homologous

to human nKHC (94% amino acid identity) than to human uKHC (71% amino acid identity) and also contains the additional stretch of 69 amino acids that is present in nKHC but not in uKHC. DN40 may be the mouse homolog of human nKHC, but it has not been determined if DN40 is found only in neuronal tissue. In another study (Aizawa et al., 1992), a PCR fragment was isolated that encodes 156 amino acids of a mouse gene (KIF5) which is expressed only in brain and demonstrates 88.5% and 98.7% amino acid identity to the motor domains of human uKHC and nKHC, respectively. KIF5, which is definitely not the mouse homolog of uKHC based on its expression pattern, is also different from mouse DN40 (93.6% amino acid identity in the overlapping region). Hence, there may be two neuron-specific KHC genes, but confirmation will require the sequencing of the non-motor domain of KIF5.

**Expression of the uKHC and nKHC genes**

The expression patterns of the two human KHCs differ dramatically. The uKHC gene is expressed in every tissue that was examined, while the nKHC gene is expressed only in neurons. Despite this difference, the transcript patterns produced by these genes are very similar to one another (6.2, 4.3, 3.9 and 1.7 kb in size). The nKHC and uKHC genes most likely arose from a duplication of a common ancestral gene and nKHC acquired neuronal-specific promoter elements while maintaining similar transcription initiation/processing signals.

It is interesting that the two KHC genes encode multiple transcripts as large as >6 kb considering that the coding region for each is ~3 kb. In the characterization of the cDNAs for both genes, heterogeneity was never seen in the coding region. Thus, the differences between the transcripts imply that

the untranslated regions are of different lengths and hence their translation may regulated in different ways. The smallest transcript (1.7 kb), however, must have differences in the coding region since it is not long enough to encode a full length KHC. This transcript only hybridizes with probes that include sequences from the N-terminal motor domain. Interestingly, the *dilute* gene from mouse (encodes a putative myosin motor) also has several transcripts, including one that corresponds only to the motor region of the protein (Mercer et al., 1991). In contrast, the Drosophila KHC gene only produces a 4 kb message (Yang et al., 1988) implying that the mammalian KHC genes have acquired the capability for more complex transcriptional and/or translational control.

**The uKHC and nKHC proteins**

Using antibodies that are specific for the two kinesins, I found that the uKHC protein is 120 kD in size and expressed in all tissues whereas nKHC runs as a doublet of 133 and 120 kD only in neuronal tissues. In fractionation studies, the majority of both KHCs are present in the soluble fraction although both also cosediment with membranes. Whether the two KHCs interact with different types of membranes could not be determined from this limited subcellular fractionation study. In addition, both uKHC and nKHC can be removed from high speed supernatants of tissue homogenates by microtubule affinity under conditions of ATP depletion and AMP-PNP addition. Mg-ATP is required to release them from microtubules, suggesting that both are microtubule-based motor proteins.

Analysis of kinesin purified from brain by others using single as well as two-dimensional gel electrophoresis has suggested that neuronal tissue contains a mixture of KHC isotypes that differ in charge as well as molecular

weight (Wagner et al., 1989). Although some of these differences are probably caused by posttranslational modifications, the discovery of nKHC demonstrates that KHC diversity in purified kinesin preparations is also generated by the presence of two gene products which differ in size and charge. The presence of two distinct KHCs in neuronal kinesin preparations must be considered as a potentially complicating factor in the analysis of kinesin's ATPase, motility, and binding interactions with microtubules and membranes.

**Cellular roles for uKHC and nKHC**

*uKHC as a microtubule crossbridging and sliding motor*

Unlike the motor domain of conventional kinesin, very little is known about the remainder of the molecule. The tail domain is thought to be the portion of kinesin that interacts with macromolecular structures that are transported along microtubules. The highly conserved nature of this region of kinesin suggests that this domain does bind to specific target proteins, possibly the light chains which have been shown by immunoelectron microscopy to interact with this region of the heavy chain (Hirokawa et al., 1989). In addition, the tail domain may also bind to other proteins which are part of the cargo which kinesin transports.

Although a number of light and electron microscopy immunolocalization studies have suggested that kinesin is membrane associated (Hirokawa et al., 1991; Hollenbeck, 1989; Pfister et al., 1989; Wright et al., 1991) and a biochemical study has shown that the tail domain of sea urchin KHC can bind to microsome membranes (Skoufias et al., 1994), we have shown that when full-length uKHC and uKHC tail domains are expressed in mammalian tissue culture cells, they colocalize with cytoplasmic

microtubules (Chapter 1) (Navone et al., 1992). This distribution was specific for microtubules since there was no colocalization with vimentin filaments and staining patterns were the same with or without Triton X-100 extraction. In addition, the expressed uKHC rod domain did not colocalize with microtubules and was randomly distributed throughout the cytoplasm. The transfected motor domain also stained microtubules, but in the expected Mg-ATP sensitive manner. The uKHC tail domain, on the other hand, does so in a Mg-ATP insensitive manner.

At present, it is unclear if the expressed uKHC tail domain is binding directly to microtubules or indirectly to microtubule-associated proteins. A number of studies using highly purified kinesin, however, suggest that the tail domain can bind directly to microtubules. Studies examining kinesin bound to microtubules by electron microscopy (Amos, 1987; Andrews et al., 1993; Hisanaga et al., 1989) suggested that the tail as well as the motor domain can bind to microtubules *in vitro*. In particular, the dark field scanning transmission electron microscopy study clearly shows that single kinesins can crossbridge two microtubules through interactions at opposite ends of the molecule (Andrews et al., 1993). In addition, the bacterially expressed C-terminal domain of sea urchin KHC cosediments with microtubules in an ATP-independent manner (Skoufias, D. and J. Scholey, personal communication). Hence, our data in combination with the results from other laboratories suggest that the tail domain of uKHC has a microtubule-binding activity.

The localization of whole uKHC and its tail domain to microtubules raises the possibility that ubiquitous kinesin may participate in movements of the microtubule cytoskeleton. The ability of the N-terminal motor domain to bind to and move along microtubules and the C-terminal domain to bind to

microtubules suggests that kinesin could crossbridge and induce sliding between microtubules. In fact, it has been shown that purified kinesin causes microtubule-microtubule bending motions in solution (Vale et al., 1985) and can induce unipolar microtubule asters, presumably by causing sliding between adjacent microtubules (Urrutia et al., 1991). In support of a crossbridging role is our observation that CV-1 cells expressing the intact uKHC display very disorganized arrays of microtubules, possibly due to excessive microtubule movements generated by this expressed motor.

What purpose would the crossbridging and sliding of microtubules serve in the cell? Such sliding may be active in the microtubule overlap zone of the mitotic spindle during anaphase B movements that push the spindle poles apart (Cande and Hogan, 1989). It may also serve the function to move microtubules through the extensive processes of neurons. For example, it has been shown that fluorescently tagged microtubules are transported towards the nerve terminal, the direction of slow axonal transport of the cytoskeleton (Reinsch et al., 1991). The mechanism of this motility is unknown, however, it is plausible that microtubules whose plus-ends are oriented towards the terminal, could be anterogradely transported along a subpopulation of stationary microtubules. This process could be mediated by a plus-end motor, such as ubiquitous kinesin, that is anchored to microtubules via its tail domain and translocates along other stationary microtubules.

Other kinesin-related motors such as KAR3 (Meluh and Rose, 1990), bimC (Enos and Morris, 1990) and cut7 (Hagan and Yanagida, 1992) colocalize to mitotic spindle microtubules and have been suggested to generate force to move microtubules relative to each other. Whether or not kinesin participates in microtubule sliding *in vivo*, however, has yet to be established. We and others (Neighbors et al., 1988; Pfister et al., 1989) have not found an

obvious colocalization of endogenous kinesin with cytoplasmic microtubules by immunofluorescence. Hollenbeck (1989) did, however, document a colocalization with microtubules in cells after saponin permeabilization, but this pattern could have been due to an interaction between kinesin and microtubule-associated membranes. Thus, if ubiquitous kinesin plays a role in microtubule-sliding in cells, the available immunolocalization data suggest that it is driven either by a subset of kinesin motors or must be regulated so that it only occurs under particular circumstances. This might explain the lack of a predominant microtubule-staining pattern for endogenous ubiquitous kinesin when compared to the overexpressed uKHC.

To resolve the issue of microtubule sliding *in vivo*, experiments to determine if the microtubule-binding activity of the tail domain is manifested under physiological conditions are required. The role of the kinesin light chains which associate with the C-terminal half of the KHC (Gauger and Goldstein, 1993; Hirokawa et al., 1989) must be considered. In our experiments, expression of light chains along with the uKHC tail domain was not done. Hence, most of the tails bound to microtubules probably did not have associated light chains and may not have represented a physiological interaction. On the other hand, purified endogenous kinesin has been found to exist with and without associated light chains. Hence, the clear colocalization of the expressed tail domain with microtubules suggests that the subpopulation of ubiquitous kinesin that interacts with microtubules might lack light chains. Further characterization of these endogenous subpopulations in terms of their ability to interact with microtubules in the presence of Mg-ATP must be performed. In addition, in order to determine ubiquitous kinesin's role in *in vivo* microtubule sliding, the effect on this activity of eliminating functional uKHC in the cell must be assessed. Since

movement of microtubules through the axon can be studied in neurons, the effect of suppressing uKHC synthesis (by antisense oligonucleotides, for example) on axonal translocation of microtubules could be studied in these cells.

*uKHC as a vesicle transport motor*

Many studies have suggested that kinesin is a motor that transports organelles in the anterograde direction in the axon. To investigate the role of kinesin in neurons, the phenotype resulting from antisense oligonucleotide suppression of ubiquitous KHC expression was examined (Appendix 2). We found that in untreated or sense-treated cells, synapsin I and GAP-43 were localized to neurites, particularly in the termini. In contrast, in antisense treated cells, both proteins were confined to the cells bodies. Synapsin I and GAP-43 are membrane-associated proteins (De Camilli et al., 1983; Gispen et al., 1985; Valtorta et al., 1988) and are delivered to neuronal termini by fast axonal transport (Baitinger and Willard, 1987; Benowitz et al., 1981; Skene and Willard, 1981). Since microtubules in axons and minor neurites are oriented with their plus ends distal to the cell body (Baas et al., 1989), the translocation of organelles to the neurite terminus of both types of processes requires a plus-end directed motor. The impaired delivery of synapsin I and GAP-43 to the neurite terminus under antisense conditions suggests that ubiquitous kinesin may serve as the plus-end motor for the anterograde transport of vesicles containing these proteins. This conclusion is consistent with the finding that kinesin is associated with vesicles traveling by anterograde transport that accumulate at the proximal side of a nerve ligation (Hirokawa et al., 1991).

Experiments done subsequent to ours have provided additional evidence for ubiquitous kinesin's involvement in anterograde axonal transport. Amaratunga *et al.* injected antisense oligonucleotides into the vitreous humor of rabbit eyes in order to assess the effect on membrane transport in retinal ganglion cells whose axons form the optic nerve. Along with an ~80% reduction in retinal kinesin synthesis, the rapid axonal transport of membrane proteins into the optic nerve was found to be reduced by ~70% (Amaratunga et al., 1993). This included transport of vesicles containing substance P (a marker for peptide containing vesicles), amyloid protein (plasma membrane precursor vesicles) and several integral membrane proteins of synaptic vesicles (Amaratunga et al., 1995). Although the *in vitro* and *in vivo* data strongly support a role for ubiquitous kinesin in anterograde axonal transport, it is still formally possible that uKHC is not directly involved in the transport of these vesicles, but instead transports another protein that traps these vesicles in distal neurites.

An additional phenotype observed in uKHC antisense-treated cells was a reduction in neurite length that affected both the axon and the minor processes that become dendrites (Appendix 2). Normally when dissociated hippocampal neurons are cultured, they create a symmetric array of neurites, one of which eventually becomes an axon while the rest become dendrites. Both classes of neurites were reduced in length by ~50% after 48 hours of antisense treatment. It is generally thought that the addition of new surface membrane necessary for neurite elongation occurs primarily at growth cones (Pfenninger and Maylie-Pfenninger, 1981). If this is the case, then inhibition of anterograde transport of vesicles in uKHC null neurons could result in reduced membrane traffic to the growth cone and consequently a reduced rate of process outgrowth.

Although uKHC expression was virtually eliminated by antisense treatment, neurite elongation was not entirely blocked. This observation implies that there is more than one means of elongating neuritic processes. In the absence of membrane transport to the growth cone, enough membrane addition could be occurring within the cell body to support a reduced rate of process outgrowth, at least for short distances (Small et al., 1984). Another possibility is that an additional anterograde motor transports other organelles that can support neurite elongation. Candidates include the kinesin-related proteins unc-104 a motor that appears to transport synaptic vesicles to the nerve terminal in *C. elegans*(Hall and Hedgecock, 1991), KIF1A (Okada et al., 1995) which is responsible for the transport of synaptic vesicle precursors in mouse neurons, KIF2 (Noda et al., 1995), KIF3A (Kondo et al., 1994) and KIF4 (Sekine et al., 1994), all of which appear to be membrane translocators in axons. Neuronal KHC (this thesis) (Niclas et al., 1994), a second conventional kinesin that is expressed exclusively in neurons, may also have not been repressed in the anti-sense experiments, a point which needs to be examined. Careful identification of which motors transport which axonal vesicles and a full understanding of the membrane addition process required for neurite elongation will be necessary to create a clear picture of the roles that kinesins play in neurons. Antisense experiments designed to suppress the expression of these candidate motors in neurons could be very informative and in fact are currently being done for neuronal KHC.

*Specific roles for nKHC in the nervous system*

Distribution of KHCs in the nervous system

nKHC is present in neurons throughout the central and peripheral nervous systems, although subpopulations of neurons are particularly

enriched in this motor protein. Glial cells, on the other hand, express uKHC, but not nKHC, indicating that nKHC is indeed neuron specific. In hippocampal neurons, nKHC is more concentrated in the cell body particularly in the perinuclear region compared to a more uniform distribution for uKHC in the cell body and processes. These differences suggest that nKHC and uKHC might transport distinct populations of organelles. Studies using the specific KHC antibodies to immunoprecipitate the organelles to which these two motors bind will help in the identification of their respective cargoes. In addition, immunoelectron microscopy on neurons will be required to further explore this issue.

nKHC's role in neuronal differentiation

In addition to studying the expression of uKHC and nKHC in neural tissues, we also examined the regulation of synthesis of these motors during the process of "neuron-like" differentiation in human neuroblastoma (SH-SY5Y and IMR32) and rat pheochromocytoma (PC12) cell lines after treatment with the appropriate pharmacological reagent (Appendix 3). When these cell lines were treated with these reagents, they extend neuritic processes much like a developing neuron. The growth of these processes was found to correlate with an increase in nKHC protein levels of up to 8-fold without any change in uKHC levels. nKHC mRNAs were also observed to increase in cells with the mature "differentiated" phenotype.

The observed increase in nKHC expression after differentiation suggests that this neuron-specific motor might be important for the acquisition of a mature neruonal phenotype. However, its role in this process has yet to be determined. It is known that all events involved in neuronal differentiation require newly synthesized proteins that must be transported

along the rapidly growing neuronal processes via their storage organelles. In fact, organelle transport is known to be enhanced in the course of neuronal maturation (Greene and Tischler, 1976; Jacobs and Stevens, 1986) and one might expect that both the number and the type of vesicles being translocated are increased. The finding that the expression of the neuron-specific conventional kinesin is selectively stimulated during differentiation of the these neuron-like cell lines suggests that it may be involved in the movement of organelles whose transport along microtubules is specifically stimulated during this process.

*Future approaches to identifying the functions of nKHC and uKHC in neurons*

In order to determine if nKHC and uKHC have distinct or overlapping roles in neurons, experiments in which the function of these two motors is inhibited will be necessary. Previous studies investigating kinesin function have used inhibitory antibodies (Brady et al., 1990) and antisense oligonucleotides in hippocampal neurons *in vitro* (Appendix 2) (Ferreira et al., 1992) and in retinal ganglion cells *in vivo* (Amaratunga et al., 1995; Amaratunga et al., 1993). In all of these experiments, it was assumed that there is only one kinesin. Hence, the specificities of these antibodies and antisense oligonucleotides for the two isoforms must be determined to establish whether or not both KHCs were affected in these experiments. The specificity of effects can now be determined using the specific nKHC and uKHC antibodies. It will be interesting to see what effects nKHC-specific antisense treatment will have on neuronal differentiation.

Studying KHC mutants represents another approach to understanding the roles of nKHC and uKHC. So far, the *Drosophila* KHC gene, which

appears to be the homolog of human uKHC rather than to nKHC, is the only KHC gene analyzed by this method. Flies bearing mutations in this gene display impaired action potential propagation and neurotransmitter release, but are still capable of transporting certain membranes such as synaptic vesicles to the nerve terminal (Gho et al., 1992). If a nKHC homolog exists in flies, it will be interesting to determine its roles in neuronal development and axonal transport.

The proteins expressed from the cloned uKHC and nKHC genes represent useful biochemical tools for studying the functions of these two motors. Bacterially expressed uKHC is currently being used to successfully solve the three dimensional structure of the kinesin motor domain (Jon Kull, personal communication), to perform kinetic studies on its ATPase activity (laboratory of E. Taylor), and motility studies on fluorescently-labelled single kinesin molecules (laboratories of R. Vale and T. Yanagida) Expressed proteins could also be used to determine what cytosolic proteins interact with uKHC and nKHC. It has yet to be determined which kinesin light chains associate with which heavy chains and whether nKHC and uKHC associate with unique membrane receptors. In addition, other soluble factors that may specifically regulate one or the other KHC have yet to be identified. *In vitro* assays with expressed uKHC and nKHC could also be used to study the differences in ATPase and force-generating activities as well as the ability of these two KHCs to reconstitute specific plus-end directed organelle transport. Efforts in these directions are currently underway in our laboratory.

## Part 2: Regulation of Microtubule-based Organelle Transport

### Cytoplasmic dynein is the minus-end organelle motor in *Xenopus* eggs

In order to study the regulation of minus-end directed transport in *Xenopus* egg extracts, it was necessary to identify the motor responsible for this movement. Since cytoplasmic dynein was a strong candidate based on work by others (Schnapp and Reese, 1989; Schroer et al., 1989), we examined whether the photocleavage of cytoplasmic dynein in *Xenopus* egg extracts by UV light in the presence of orthovanadate greatly reduces minus-end directed organelle transport. Not only did UV-vanadate cleavage of the dynein heavy chain correlate with greatly decreased levels of minus-end membrane motility, but adding back purified dynein was able to restore a large percentage of the original activity. These results demonstrated that cytoplasmic dynein is the predominant, if not sole, motor that drives minus-end directed organelle transport in the *Xenopus* egg.

**Dynein detaches from membranes during metaphase**

Organelle transport by cytoplasmic dynein appears to be regulated by controlling its ability to associate with membranes. It was found that the amounts of dynein and its activator, dynactin, that are bound to membranes decrease ~10-fold when extracts enter a metaphase state. This decrease in membrane-associated dynein was very similar in extent to the reduction in minus-end directed organelle transport observed in the same metaphase extracts. Thus, modulation of dynein association with membranes appears to provide an explanation for how minus-end directed organelle transport is controlled by the cell cycle.

**Phosphorylation of a dynein light chain increases dramatically during metaphase**

Since the cell cycle state of *Xenopus* egg extracts can be interconverted in the presence of protein synthesis inhibitors, the regulation of both dynein association with membranes and dynein-based organelle transport must be mediated by a post-translational event. Cytoplasmic dynein isolated by either immunoprecipitation or microtubule affinity was found to undergo substantial phosphorylation in metaphase extracts when compared to interphase. The polypeptide that incorporated radiolabelled phosphate appeared to be a dynein light chain isoform since it cofractionated with the dynein heavy chain at 20S in a sucrose velocity gradient. The increase in the incorporation of radiolabelled phosphate into this light chain in metaphase compared to interphase extracts (~12 fold) was similar to the magnitude of the changes observed in organelle transport and dynein association with membranes. This light chain also showed a 5 kDa increase in molecular weight in metaphase versus interphase dynein which may reflect an increase in steady state covalently bound phosphate. In contrast, the heavy and intermediate chains incorporated very little radiolabelled phosphate, and the very low levels of labelling did not change in a cell cycle dependent manner. The kinase responsible for this light chain phosphorylation has not been identified; however, $p34^{cdc2}$ kinase may not be directly involved, since incubation of membranes with baculovirus expressed $p34^{cdc2}$/cyclin B did not cause dissociation of dynein from membranes.

**Phosphorylation of a dynein light chain may decrease dynein's affinity for membranes**

Phosphorylation of this dynein light chain may be responsible for decreasing the affinity of dynein for membranes, although the phosphorylation of additional proteins has not been ruled out. The dynein

light chains have been considered to be strong candidates for targetting this motor to different intracellular cargoes. In the case of flagellar dynein, the intermediate and light chains may be responsible for anchoring the motor to the A-microtubules of the axoneme (King and Whitman, 1990; King et al., 1991; Mitchell and Rosenbaum, 1986), while the intermediate and light chains of cytoplasmic dynein have been proposed to serve a similar function in docking cytoplasmic dynein to intracellular targets (Gill et al., 1994; Hughes et al., 1995; Paschal et al., 1992). Dynein light chain phosphorylation may cause cytoplasmic dynein to dissociate from membranes and allow this motor to bind to new cargo and perform distinct roles during metaphase. In support of this idea are the results from various studies that show that dynein is involved in mitotic spindle formation (Vaisberg et al., 1993), spindle orientation and nuclear segregation (Eshel et al., 1993; Li et al., 1993; Plamann et al., 1994; Xiang et al., 1994) and chromosome segregation (Saunders et al., 1995). In addition, two studies have shown that dynein changes it location from a vesicular staining in interphase to spindle and kinetochore staining in mitosis (Pfarr et al., 1990; Steuer et al., 1990). It will be necessary to determine if the population of dynein that associates with kinetochores is derived from the pool that dissociates from membranes during mitosis. It will also be very interesting to determine if dynein purified from metaphase extracts is able to bind to kinetochores but not to membranes.

**Multiple mechanisms for regulating dynein-based organelle transport**

Although the work in Chapter 3 is the first study in which dynein phosphorylation and dynein-based organelle transport have been examined in the same system, other studies have indirectly suggested a possible connection between dynein phosphorylation and organelle transport. In

certain cases, increased phosphorylation is thought to activate dynein-driven membrane movement, in contrast to the results presented in Chapter 3. In interphase *Xenopus* egg extracts, the phosphatase inhibitor okadaic acid increases minus-end directed endoplasmic reticulum motility without changing the levels of membrane associated dynein (Allan, 1995). Whether this activation is due to increased dynein phosphorylation is not yet known. In addition, studies in the rat optic nerve suggest that phosphorylation of dynein may stimulate membrane transport, since dynein heavy chain phosphorylation is higher on retrograde versus anterograde-moving organelles (Dillman and Pfister, 1994). In both of these cases, phosphorylation during interphase seems likely to modulate dynein motor activity rather than dynein binding to the membrane as occurs in the mitotic regulatory mechanism described in Chapter 3. In the case of *Xenopus* egg extracts, it will be interesting to determine if specific phosphorylation of dynein induced by okadaic acid results in increased motor activity in a microtubule gliding assay.

Mechanisms of dynein regulation by phosphorylation may also differ in various cell types. In contrast to interphase *Xenopus* extracts where okadaic acid does not change dynein association with membranes (Allan, 1995), okadaic acid treatment of interphase fibroblasts causes the dissociation of dynein from membranous organelles, an effect that correlates with dynein heavy chain phosphorylation (Lin et al., 1994). How this affects organelle motility in these cells was not investigated. However, since other studies have shown that okadaic acid treatment in interphase increases levels of minus-end directed movement (Allan, 1995; Hamm-Alvarez et al., 1993), the released population of dynein may represent an inactive storage form of the motor (Lin et al., 1994). Furthermore, the association of dynein with membranous organelles in fibroblasts was not reduced in mitosis, as judged

by immunofluorescence microscopy (Lin and Collins, 1992). To resolve these apparent contradictory results, it is clear that both the phosphorylation state and the activity of dynein need to be studied in parallel for each experimental system. Nevertheless, these results, in conjunction with those in Chapter 3, suggest that dynein association with membranes may be regulated differently in different cell types.

**Kinesin does not detach from membranes during metaphase**

Allan and Vale (1991) found that plus-end directed motility in *Xenopus* egg extracts is also suppressed in metaphase extracts when compared to interphase extracts. Kinesin is a likely candidate for a motor that is responsible for at least a portion of plus-end directed motility in this system. In contrast to dynein, levels of kinesin found on membranes isolated from interphase and metaphase extracts are the same. This result suggests that kinesin may be regulated by the cell cycle in a different manner than dynein. Further work is necessary to establish whether plus-end directed organelle transport is regulated by controlling the force-generating activity of kinesin or whether other plus-end directed motors drive organelle transport in the *Xenopus* egg.

**Future directions**

Although the work in Chapter 3 lead to the discovery that dynein-based transport is regulated by the cell cycle by altering its affinity for membranes, the binding interaction between dynein and membranes is still a mystery. A dynein receptor protein has not been identified and work in some labs suggests that it may also partly interact with membrane phospholipids (Lacey and Haimo, 1994; Lacey and Haimo, 1992). In the *Xenopus* egg system,

preliminary results from my own work show that treating purified cytosolic membrane with trypsin eliminates their ability to bind to cytoplasmic dynein suggesting that a membrane protein is required for dynein association with organelles. Now that we are beginning to understand the control of dynein association with membranes, it may become somewhat easier to identify a receptor. One approach would be to look for a membrane protein in nonionic detergent-solubilized interphase extracts that are able to bind to dynein. It would be expected that a true receptor would only be able to interact with dynein in the interphase extract and not the metaphase extract.

The subunit(s) of cytoplasmic dynein that interacts with membranes has yet to be identified. The results in Chapter 3 suggest that one of the light chain isoforms is involved, but whether its role is direct or indirect is not clear. Experiments in *Dictyostelium* using strains bearing deletions and truncated versions of the dynein heavy, intermediate and light chains will hopefully help to determine which chains are required for membrane binding. At present, the only documented interactions of specific subunits of dynein with structures other than microtubules includes the intermediate chain binding to p150$^{Glued}$ of the dynactin complex (Holzbaur, ASCB meeting abstract, 1994). Dynactin is an activator of dynein's organelle transport activity, but its mechanism of action is unknown. Whether it recruits dynein to the membrane surface still needs to be determined. It will be interesting to see if the dynein light chains interact with the dynactin complex or whether they are capable of binding to membranes directly. In addition, the function of the dynein intermediate chain is also a mystery, but could also play an anchoring role. Challenging different dynein protein mutants to bind to membranes in the *Dictyostelium* system represents a very powerful approach to addressing these questions.

The work presented in Chapter 3 does not resolve the issue of whether modification of dynein or the putative organelle-associated receptor causes the dissociation of this motor from membranes. It was determined that a light chain of dynein was phosphorylated in a cell cycle dependent fashion, but whether this directly leads to the control of dynein binding to membranes is not clear. Hence, experiments in which cytoplasmic dynein isolated from interphase and metaphase extracts is tested for its ability to bind to membranes purified from interphase and metaphase extracts need to be performed. Such analysis might reveal whether cytoplasmic dynein or a membrane receptor is being modified. Although I attempted to do these kinds of experiments several times, they turned out to be very difficult and gave inconsistent results. In some cases, the data indicated that dynein was being modified and in others cases, the results suggested that the membranes were being modified. It is also possible that the regulation of dynein association with membranes is more complicated and involves modifications of both dynein and membranes. If this is the case, then the membrane receptor certainly must be identified in order to determine if cell cycle specific phosphorylation of the receptor as well as dynein is required for dissociation of this motor from organelles.

## Final comments

Presently, the major goals of labs working on motor proteins are to understand how motors move on microtubules, identify which motors associate with which cellular structures, and determine the mechanisms by which each of these aspects of motor function are regulated. However, even if all the organelle targets of the many plus- and minus-end motors are determined and we understand the basic mechanisms of how motors are

turned on and off, there still remains the problem of how each membrane population is targetted to its proper cellular destination. For example, not all plus-end moving organelles travel to the cell periphery or the axonal terminus and not all minus-end organelle movements move completely to the cell center. There must be another level of organization that creates a finer resolution targetting of membranes in the cytoplasm. One might imagine that such organization is maintained by the intricate control of plus and minus-end motor activity as well as through the protein-protein interactions which allow moving organelles to identify their proper destinations. Communication between these machineries might allow for the redirecting of organelles that have missed their destinations. Identifying the components of this undoubtedly complex system of regulation represents a very exciting future area of research in the field of motor protein biology. Once the many organelle motors have been identified and characterized, studies of their behavior in crude extracts, purified systems and in living cells will help us obtain an understanding of how organelle motors function together to create the balance of membrane traffic and organelle positioning that we see in the living cell.

In addition to advances in the understanding of organelle transport and intracellular organization, the field of motor biology will inevitably contribute to the field of medicine. With the ever increasing numbers of identified microtubule-based motors that move organelles and other structures within the cell, it is only a matter of time before defects in some of these proteins are identified as causes of human genetic diseases. At present, there are many uncharacterized neurological diseases that represent good candidates for potential motor protein-based defects. Not only will the matching of human diseases with specific defective motors help in

determining the functions of these proteins *in vivo*, but the knowledge that we obtain from studying motor proteins will allow for the development of more intelligently designed treatments for such diseases.

# REFERENCES

Adams, M. D., Kelley, J. M., Gocayne, J. D., Dubnick, M., Polymeropoulos, M. H., Xiao, H., Merril, C. R., Wu, A., Olde, B., Moreno, R. F., and et al. (1991). Complementary DNA sequencing: expressed sequence tags and human genome project. Science *252*, 1651-6.

Adem, A., Mattsson, M. E., Nordberg, A., and Pahlman, S. (1987). Muscarinic receptors in human SH-SY5Y neuroblastoma cell line: by phorbol ester and retinoic acid-induced differentiation. Brain Res *430*, 235-42.

Aizawa, H., Sekine, Y., Takemura, R., Zhang, Z., Nangaku, M., and Hirokawa, N. (1992). Kinesin family in murine central nervous system. J Cell Biol *119*, 1287-96.

Allan, V. (1995). Protein phosphatase 1 regulates the cytoplasmic dynein-driven formation of endoplasmic reticulum networks in vitro. J Cell Biol *128*, 879-91.

Allan, V. J., and Vale, R. D. (1991). Cell cycle control of microtubule-based membrane transport and tubule formation in vitro. J Cell Biol *113*, 347-59.

Allen, R. D., Allen, N. S., and Travis, J. L. (1981). Video-enhanced contrast, differential interference contrast (AVEC-DIC) microscopy: a new method capable of analyzing microtubule-related motility in the reticulopodial network of Allogromia laticollaris. Cell Motil *1*, 291-302.

Amaratunga, A., Leeman, S. E., Kosik, K. S., and Fine, R. E. (1995). Inhibition of kinesin synthesis in vivo inhibits the rapid transport of representative

proteins for three transport vesicle classes into the axon. J Neurochem *64*, 2374-6.

Amaratunga, A., Morin, P. J., Kosik, K. S., and Fine, R. E. (1993). Inhibition of kinesin synthesis and rapid anterograde axonal transport in vivo by an antisense oligonucleotide. J Biol Chem *268*, 17427-30.

Amos, L. A. (1987). Kinesin from pig brain studied by electron microscopy. J Cell Sci *87*, 105-11.

Andrews, S. B., Gallant, P. E., Leapman, R. D., Schnapp, B. J., and Reese, T. S. (1993). Single kinesin molecules crossbridge microtubules in vitro. Proc Natl Acad Sci USA *90*, 6503-7.

Asai, D. J., Beckwith, S. M., Kandl, K. A., Keating, H. H., Tjandra, H., and Forney, J. D. (1994). The dynein genes of Paramecium tetraurelia. Sequences adjacent to the catalytic P-loop identify cytoplasmic and axonemal heavy chain isoforms. J Cell Sci *107*, 839-47.

Baas, P. W., Deitch, J. S., Black, M. M., and Banker, G. A. (1989). Changes in microtubule polarity orientation during the development of hippocampal neurons in culture. J Cell Biol *109*, 3085-3094.

Baitinger, C., and Willard, M. (1987). Axonal transport of synapsin I-like proteins in rabbit retinal ganglion cells. J Neurosci *7*, 3723-3735.

Benowitz, L. J., Shashoua, V. E., and Yoon, M. G. (1981). Specific changes in rapidly transported proteins during regeneration of the goldfish optic nerve. J Neorosci *1*, 300-307.

Bloom, G. S., Richards, B. W., Leopold, P. L., Ritchey, D. M., and Brady, S. T. (1993). GTP gamma S inhibits organelle transport along axonal microtubules. J Cell Biol *120*, 467-76.

Bloom, G. S., Schoenfeld, T. A., and Vallee, R. B. (1984). Widespread distribution of the major polypeptide component of MAP 1 (microtubule-associated protein 1) in the nervous system. J Cell Biol *98*, 320-30.

Bloom, G. S., Wagner, M. C., Pfister, K. K., and Brady, S. T. (1988). Native structure and physical properties of bovine brain kinesin and identification of the ATP-binding subunit polypeptide. Biochemistry *27*, 3409-16.

Brady, S. T. (1995). A kinesin medley: biochemical and functional heterogeneity. Trends Cell Biol *5*, 159-164.

Brady, S. T. (1991). Molecular motors in the nervous system. Neuron *7*, 521-33.

Brady, S. T. (1985). A novel brain ATPase with properties expected for the fast axonal transport motor. Nature *317*, 73-5.

Brady, S. T., Lasek, R. J., and Allen, R. D. (1982). Fast axonal transport in extruded axoplasm from squid giant axon. Science *218*, 1129-31.

Brady, S. T., Pfister, K. K., and Bloom, G. S. (1990). A monoclonal antibody against kinesin inhibits both anterograde and retrograde fast axonal transport in squid axoplasm. Proc Natl Acad Sci USA *87*, 1061-5.

Cande, Z., and Hogan, C. J. (1989). The mechanism of anaphase spindle elongation. Bioessays *11*, 5-9.

Clark, S. W., and Meyer, D. I. (1992). Centractin is an actin homologue associated with the centrosome. Nature *359*, 246-50.

Cole, D. G., and Scholey, J. M. (1995). Structural variations among the kinesins. Trends Cell Biol *5*, 159-164.

Collard, J. F., Cote, F., and Julien, J. P. (1995). Defective axonal transport in a transgenic mouse model of amyotrophic lateral sclerosis. Nature *375*, 61-4.

Collins, C. A., and Vallee, R. B. (1989). Preparation of microtubules from rat liver and testis: cytoplasmic dynein is a major microtubule associated protein. Cell Motil Cytoskeleton *14*, 491-500.

Corthesy-Theulaz, I., Pauloin, A., and Rfeffer, S. R. (1992). Cytoplasmic dynein participates in the centrosomal localization of the Golgi complex. J Cell Biol *118*, 1333-45.

Cyr, J. L., Pfister, K. K., Bloom, G. S., Slaughter, C. A., and Brady, S. T. (1991). Molecular genetics of kinesin light chains: generation of isoforms by alternative splicing. Proc Natl Acad Sci USA *88*, 10114-8.

De Camilli, P., Cameron, R., and Greengard, P. (1983). Synapsin I (Protein I), a nerve terminal-specific phosphoprotein. I. Its general distribution in synapses of the central and peripheral nervous system demonstrated by immunofluorescence in frozen and plastic sections. J Cell Biol *96*, 1337-1354.

de Cuevas, M., Tao, T., and Goldstein, L. S. (1992). Evidence that the stalk of Drosophila kinesin heavy chain is an alpha-helical coiled coil. J Cell Biol *116*, 957-65.

Dillman, J. F. r., and Pfister, K. K. (1994). Differential phosphorylation in vivo of cytoplasmic dynein associated with anterogradely moving organelles. J Cell Biol *127*, 1671-81.

Drubin, D., Kobayashi, S., Kellogg, D., and Kirschner, M. (1988). Regulation of microtubule protein levels during cellular morphogenesis nerve growth factor-treated PC12 cells. J Cell Biol *106*, 1583-91.

Elluru, R. G., Bloom, G. S., and Brady, S. T. (1995). Fast axonal transport of kinesin in the rat visual system: functionality of kinesin heavy chain isoforms. Mol Biol Cell *6*, 21-40.

Endow, S. A. (1991). The emerging kinesin family of microtubule motor proteins. Trends Biochem Sci *16*, 221-5.

Endow, S. A., and Titus, M. A. (1992). Genetic approaches to molecular motors. Annu Rev Cell Biol *8*, 29-66.

Enos, A. P., and Morris, N. R. (1990). Mutation of a gene that encodes a kinesin-like protein blocks nuclear division in A. nidulans. Cell *60*, 1019-27.

Eshel, D., Urrestarazu, L. A., Vissers, S., Jauniaux, J. C., van Vliet-Reedijk, J. C., Planta, R. J., and Gibbons, I. R. (1993). Cytoplasmic dynein is required for normal nuclear segregation in yeast. Proc Natl Acad Sci USA *90*, 11172-6.

Euteneuer, U., Koonce, M. P., Pfister, K. K., and Schliwa, M. (1988). An ATPase with properties expected for the organelle motor of the giant amoeba, Reticulomyxa. Nature *332*, 176-8.

Fath, K. R., Trimbur, G. M., and Burgess, D. R. (1994). Molecular motors are differentially distributed on Golgi membranes from polarized epithelial cells. J Cell Biol *126*, 661-75.

Ferreira, A., Niclas, J., Vale, R. D., Banker, G., and Kosik, K. S. (1992). Suppression of kinesin expression in cultured hippocampal neurons using antisense oligonucleotides. J Cell Biol *117*, 595-606.

Ferro, K. L., and Collins, C. A. (1995). Microtubule-independent phospholipid stimulation of cytoplasmic dynein ATPase activity. J Biol Chem *270*, 4492-6.

Gauger, A. K., and Goldstein, L. S. (1993). The Drosophila kinesin light chain. Primary structure and interaction with kinesin heavy chain. J Biol Chem *268*, 13657-66.

Gho, M., McDonald, K., Ganetzky, B., and Saxton, W. M. (1992). Effects of kinesin mutations on neuronal functions. Science *258*, 313-6.

Gibbons, B. H., Asai, D. J., Tang, W. J., Hays, T. S., and Gibbons, I. R. (1994). Phylogeny and expression of axonemal and cytoplasmic dynein genes in sea urchins. Mol Biol Cell *5*, 57-70.

Gibbons, I. R., Lee-Eiford, A., Mocz, G., Phillipson, C. A., Tang, W. J., and Gibbons, B. H. (1987). Photosensitized cleavage of dynein heavy chains. Cleavage at the "V1 site" by irradiation at 365 nm in the presence of ATP and vanadate. J Biol Chem *262*, 2780-6.

Gill, S. R., Cleveland, D. W., and Schroer, T. A. (1994). Characterization of DLC-A and DLC-B, two families of cytoplasmic dynein light chain subunits. Mol Biol Cell *5*, 645-54.

Gill, S. R., Schroer, T. A., Szilak, I., Steuer, E. R., Sheetz, M. P., and Cleveland, D. W. (1991). Dynactin, a conserved, ubiquitously expressed component of an activator of vesicle motility mediated by cytoplasmic dynein. J Cell Biol *115*, 1639-50.

Gispen, W. H., Leunissen, J. L. M., Oestreicher, A. B., Verkleij, A. J., and Zwiers, H. (1985). Presynaptic localization of B-50 phospho-protein: the

ACTH-sensitive protein kinase C substrate involved in rat brain phosphoinositide metabolism. Brain Res *328*, 381-385.

Giudici, A. M., Sher, E., Pelagi, M., Clementi, F., and Zanini, A. (1992). Immunolocalization of secretogranin II, chromogranin A, and B in differentiating human neuroblastoma cells. Eur J Cell Biol *58*, 383-9.

Goldstein, L. S. (1993). Functional redundancy in mitotic force generation. J Cell Biol *120*, 1-3.

Goldstein, L. S. (1993). With apologies to scheherazade: tails of 1001 kinesin motors. Annu Rev Genet *27*, 319-51.

Goldstein, L. S. B. (1991). The kinesin superfamily: tails of functional redundancy. Trends Cell Biol *1*, 93-98.

Gotti, C., Sher, E., Cabrini, D., Bondiolotti, G., Wanke, E., Mancinelli, E., and Clementi, F. (1987). Cholinergic receptors, ion channels, neurotransmitter synthesis, and neurite outgrowth are independently regulated during the in vitro differentiation of a human neuroblastoma cell line. Differentiation *34*, 144-55.

Greene, L. A., and Tischler, A. S. (1976). Establishment of a noradrenergic clonal line of rat adrenal pheochromocytoma cells which respond to nerve growth factor. Proc Natl Acad Sci USA *73*, 2424-8.

Hackney, D. D., Levitt, J. D., and Wagner, D. D. (1991). Characterization of alpha 2 beta 2 and alpha 2 forms of kinesin. Biochem Biophys Res Commun *174*, 810-5.

Hagan, I., and Yanagida, M. (1992). Kinesin-related cut7 protein associates with mitotic and meiotic spindles in fission yeast. Nature *356*, 74-6.

Hall, D. H., and Hedgecock, E. M. (1991). Kinesin-related gene unc-104 is required for axonal transport of synaptic vesicles in C. elegans. Cell *65*, 837-47.

Hamm-Alvarez, S. F., Preston, Y. K., and Sheetz, M. P. (1993). Regulation of vesicle transport in CV-1 cells and extracts. Journal of Cell Science *106*, 955-66.

Haussler, M., Sidell, N., Kelly, M., Donaldson, C., Altman, A., and Mangelsdorf, D. (1983). Specific high-affinity binding and biologic action of retinoic acid in human neuroblastoma cell lines. Proc Natl Acad Sci USA *80*, 5525-9.

Hayden, J. H., Allen, R. D., and Goldman, R. D. (1983). Cytoplasmic transport in keratocytes: direct visualization of particle translocation along microtubules. Cell Motil *3*, 1-19.

Hinnebusch, A. G. (1990). Involvement of an initiation factor and protein phosphorylation in translational control of GCN4 mRNA. Trends Biol Sci *15*, 148-152.

Hirano, A. (1991). Cytopathology of Amyotrophic Lateral Sclerosis. Adv Neurol *56*, 91-102.

Hirokawa, N., Pfister, K. K., Yorifuji, H., Wagner, M. C., Brady, S. T., and Bloom, G. S. (1989). Submolecular domains of bovine brain kinesin identified by electron microscopy and monoclonal antibody decoration. Cell *56*, 867-78.

Hirokawa, N., Sato-Yoshitake, R., Kobayashi, N., Pfister, K. K., Bloom, G. S., and Brady, S. T. (1991). Kinesin associates with anterogradely transported membranous organelles in vivo. J Cell Biol *114*, 295-302.

Hisanaga, S., Murofushi, H., Okuhara, K., Sato, R., Masuda, Y., Sakai, H., and Hirokawa, N. (1989). The molecular structure of adrenal medulla kinesin. Cell Motil Cytoskeleton *12*, 264-72.

Hollenbeck, P. J. (1989). The distribution, abundance and subcellular localization of kinesin. J Cell Biol *108*, 2335-42.

Hollenbeck, P. J. (1993). Phosphorylation of neuronal kinesin heavy and light chains in vivo. J Neurochem *60*, 2265-75.

Hollenbeck, P. J., and Swanson, J. A. (1990). Radial extension of macrophage tubular lysosomes supported by kinesin. Nature *346*, 864-6.

Hoyt, M. A. (1994). Cellular roles of kinesin and related proteins. Curr Opin Cell Biol *6*, 63-8.

Hughes, S. M., Vaughan, K. T., Herskovits, J. S., and Vallee, R. B. (1995). Molecular analysis of a cytoplasmic dynein light intermediate chain reveals homology to a family of ATPases. J Cell Sci *108*, 17-24.

Inoue, S. (1981). Video image processing greatly enhances contrast, quality, and speed in polarization-based microscopy. J Cell Biol *89*, 346-56.

Jacobs, J. R., and Stevens, J. K. (1986). Changes in the organization of the neuritic cytoskeleton during nerve growth factor-activated differentiation of PC12 cells: a serial electron microscopic study of the development and control of neurite shape. J Cell Biol *103*, 895-906.

Johnston, G. C., Pendergast, J. A., and Singer, R. A. (1991). The Saccharomyces cerevisiae MYO2 gene encodes an essential myosin for vectorial transport of vesicles. J Cell Biol *113*, 539-551.

Justice, M. J., Gilbert, D. J., Kinzler, K. W., Vogelstein, B., Buchberg, A. M., Ceci, J. D., Matsuda, Y., Chapman, V. M., Patriotis, C., Makris, A., Tsichlis, P. N., Jenkins, N. A., and Copeland, N. G. (1992). A molecular genetic linkage map of mouse chromosome 18 reveals extensive linkage conservation with human chromosomes 5 and 18. Genomics *13*, 1281-1288.

Kato, K. (1990). A collection of cDNA clones with specific expression patterns in mouse brain. Eur J Neurosci *2*, 704-11.

King, S. M., and Whitman, G. B. (1990). Locaization of an intermediate chain of outer arm dynein by immunoelectron microscopy. J Biol Chem *265*, 19807-11.

King, S. M., Wilkerson, C. G., and Witman, G. B. (1991). The Mr 78,000 intermediate chain of Chlamydomonas outer arm dynein interacts with α-tubulin in situ. J Biol Chem *266*, 8401-7.

Kondo, S., Sato-Yoshitake, R., Noda, Y., Aizawa, H., Nakata, T., Matsuura, Y., and Hirokawa, N. (1994). KIF3A is a new microtubule-based anterograde motor in the nerve axon. J Cell Biol *125*, 1095-107.

Kongsamut, S., and Miller, R. J. (1986). Nerve growth factor modulates the drug sensitivity of neurotransmitter release from PC-12 cells. Proc Natl Acad Sci USA *83*, 2243-7.

Koonce, M. P., Grissom, P. M., and McIntosh, J. R. (1992). Dynein from Dictyostelium: primary structure comparisons between a cytoplasmic motor enzyme and flagellar dynein. J Cell Biol *119*, 1597-604.

Kosik, K. S., Orecchio, L. D., Schnapp, B., Inouye, H., and Neve, R. L. (1990). The primary structure and analysis of the squid kinesin heavy chain. J Biol Chem *265*, 3278-83.

Kotz, K. J., and McNiven, M. A. (1994). Intracellular calcium and cAMP regulate directional pigment movements in teleost erythrophores. J Cell Biol *124*, 463-74.

Kozak, M. (1987). An analysis of 5'-noncoding sequences from 699 vertebrate messenger RNAs. Nucleic Acids Res *15*, 8125-8148.

Kumar, J., Yu, H., and Sheetz, M. P. (1995). Kinectin, an essential anchor for kinesin-driven vesicle motility. Science *267*, 1834-7.

Kuznetsov, S. A., and Gelfand, V. I. (1986). Bovine brain kinesin is a microtubule-activated ATPase. Proc Natl Acad Sci USA *83*, 8530-4.

Kuznetsov, S. A., Vaisberg, E. A., Shanina, N. A., Magretova, N. N., Chernyak, V. Y., and Gelfand, V. I. (1988). The quaternary structure of bovine brain kinesin. Embo J *7*, 353-6.

Lacey, M. L., and Haimo, L. T. (1994). Cytoplasmic dynein binds to phospholipid vesicles. Cell Motil Cytoskeleton *28*, 205-12.

Lacey, M. L., and Haimo, L. T. (1992). Cytoplasmic dynein is a vesicle protein. J Biol Chem *267*, 4793-8.

Laemmli, U. K. (1970). Cleavage of stsructural proteins during assembly of the head of bacteriophage T4. Nature *227*, 680-685.

Le Douarin, N. M. (1988). On the origin of pancreatic endocrine cells. Cell *53*, 169-171.

Lee, K. D., and Hollenbeck, P. J. (1995). Phosphorylation of kinesin in vivo correlates with organelle association and neurite outgrowth. J Biol Chem *270*, 5600-5.

Lee-Eiford, A., Ow, R. A., and Gibbons, I. R. (1986). Specific cleavage of dynein heavy chains by ultraviolet irradiation in the presence of ATP and vanadate. J Biol Chem *261*, 2337-42.

Leelavathi, D. E., Estes, L. W., Feingold, D. S., and Lombardi, B. (1970). Isolation of a Golgi-rich fraction from rat liver. Biochim Biophys Acta *211*, 124-138.

Lees-Miller, J. P., Helfman, D. M., and Schroer, T. A. (1992). A vertebrate actin-related protein is a component of a multisubunit complex involved in microtubule-based vesicle motility. Nature *359*, 244-6.

Li, M., McGrail, M., Serr, M., and Hays, T. S. (1994). Drosophila cytoplasmic dynein, a microtubule motor that is asymmetrically localized in the oocyte. J Cell Biol *126*, 1475-94.

Li, Y. Y., Yeh, E., Hays, T., and Bloom, K. (1993). Disruption of mitotic spindle orientation in a yeast dynein mutant. Proc Natl Acad Sci USA *90*, 10096-100.

Lillie S. H. and Brown S. S. (1992). Suppression of a myosin defect by a kinesin-related gene. Nature *356*, 358-61.

Lin, S. X., and Collins, C. A. (1992). Immunolocalization of cytoplasmic dynein to lysosomes in cultured cells. J Cell Sci *101*, 125-37.

Lin, S. X., Ferro, K. L., and Collins, C. A. (1994). Cytoplasmic dynein undergoes intracellular redistribution concomitant with phosphorylation of the heavy chain in response to serum starvation and okadaic acid. J Cell Biol *127*, 1009-19.

Lippincott-Schwartz, J., Cole, N. B., Marotta, A., Conrad, P. A., and Bloom, G. S. (1995). Kinesin is the motor for microtubule-mediated Golgi-to-ER membrane traffic. J Cell Biol *128*, 293-306.

Lye, R. J., Porter, M. E., Scholey, J. M., and McIntosh, J. R. (1987). Identification of a microtubule-based cytoplasmic motor in the nematode C. elegans. Cell *51*, 309-18.

Lynch, T. J., Taylor, J. D., and Tchen, T. T. (1986). Regulation of pigment organelle translocation. I. Phosphorylation of the organelle-associated protein p57. J Biol Chem *261*, 4204-11.

Lynch, T. J., Wu, B. Y., Taylor, J. D., and Tchen, T. T. (1986). Regulation of pigment organelle translocation. II. Participation of a cAMP-dependent protein kinase. J Biol Chem *261*, 4212-6.

Macejak, D. G., and Sarnow, P. (1991). Internal initiation of translation at internal AUG codons in mammalian cells. Nature *353*, 90-93.

Matthies, H. J., Miller, R. J., and Palfrey, H. C. (1993). Calmodulin binding to and cAMP-dependent phosphorylation of kinesin light chains modulate kinesin ATPase activity. J Biol Chem *268*, 11176-87.

McIlvain, J. M., Jr., Burkhardt, J. K., Hamm-Alvarez, S., Argon, Y., and Sheetz, M. P. (1994). Regulation of kinesin activity by phosphorylation of kinesin-associated proteins. J Biol Chem *269*, 19176-82.

Meluh, P. B., and Rose, M. D. (1990). KAR3, a kinesin-related gene required for yeast nuclear fusion. Cell *60*, 1029-41.

Mercer, J. A., Seperack, P. K., Strobel, M. C., Copeland, N. G., and Jenkins, N. A. (1991). Novel myosin heavy chain encoded by murine dilute coat colour locus. Nature *349*, 709-13.

Mikami, A., Paschal, B. M., Mazumdar, M., and Vallee, R. B. (1993). Molecular cloning of the retrograde transport motor cytoplasmic dynein (MAP 1C). Neuron *10*, 787-96.

Mitchell, D. R., and Rosenbaum, J. L. (1986). Protein-protein interactions in the 18S ATPase of *Chalmydomonas* outer dynein arms. Cell Motil Cytoskeleton *6*, 510-520.

Muhua, L., Karpova, T. S., and Cooper, J. A. (1994). A yeast actin-related protein homologous to that in vertebrate dynactin complex is important for spindle orientation and nuclear migration. Cell *78*, 669-79.

Mullis, K. F., Faloona, F., Scharf, S., Saiki, R., Horn, G., and Erlich, H. (1986). Specific enzymatic amplification of DNA in vitro: the polymerase chain reaction. Cold Spring Harbor Symp Quant Biol *51*, 263-273.

Murray, A. W., Solomon, M. J., and Kirschner, M. W. (1989). The role of cyclin synthesis and degradation in the control of maturation promoting factor activity. Nature *339*, 280-6.

Nangaku, M., Sato-Yoshitake, R., Okada, Y., Noda, Y., Takemura, R., Yamazaki, H., and Hirokawa, N. (1994). KIF1B, a novel microtubule plus end-directed monomeric motor protein for transport of mitochondria. Cell *79*, 1209-20.

Navone, F., Niclas, J., Hom-Booher, N., Sparks, L., Bernstein, H. D., McCaffrey, G., and Vale, R. D. (1992). Cloning and expression of a human kinesin heavy chain gene: interaction of the COOH-terminal domain with cytoplasmic microtubules in transfected CV-1 cells. J Cell Biol *117*, 1263-75.

Neighbors, B. W., Williams, R. C., Jr., and McIntosh, J. R. (1988). Localization of kinesin in cultured cells. J Cell Biol *106*, 1193-204.

Niclas, J., Navone, F., Hom-Booher, N., and Vale, R. D. (1994). Cloning and localization of a conventional kinesin motor expressed exclusively in neurons. Neuron *12*, 1059-72.

Noda, Y., Sato-Yoshitake, R., Kondo, S., Nangaku, M., and Hirokawa, N. (1995). KIF2 is a new microtubule-based anterograde motor that transports

membranous organelles distinct from those carried by kinesin heavy chain or KIF3A/B. J Cell Biol *129*, 157-67.

Okada, Y., Sato-Yoshitake, R., and Hirokawa, N. (1995). The activation of protein kinase A pathway selectively inhibits anterograde axonal transport of vesicles but not mitochondria transport or retrograde transport in vivo. J Neurosci *15*, 3053-64.

Okada, Y., Yamazaki, H., Sekine-Aizawa, Y., and Hirokawa, N. (1995). The neuron-specific kinesin superfamily protein KIF1A is a unique monomeric motor for anterograde axonal transport of synaptic vesicle precursors. Cell *81*, 769-80.

Olmsted, J. B. (1986). Microtubule-associated proteins. Annu Rev Cell Biol *2*, 421-57.

Palazzo, R. E., Brawley, J. B., and Rebhun, L. I. (1988). Spontaneous aster formation in cytoplasmic extracts from eggs of the surf clam. Zool Sci *5*, 603-611.

Palazzo, R. E., Vaisberg, E., Cole, R. W., and Rieder, C. L. (1992). Centriole duplication in lysates of Spisula solidissima oocytes. Science *256*, 219-21.

Paschal, B. M., Holzbaur, E. L., Pfister, K. K., Clark, S., Meyer, D. I., and Vallee, R. B. (1993). Characterization of a 50-kDa polypeptide in cytoplasmic dynein preparations reveals a complex with p150GLUED and a novel actin. J Biol Chem *268*, 15318-23.

Paschal, B. M., Mikami, A., Pfister, K. K., and Vallee, R. B. (1992). Homology of the 74-kD cytoplasmic dynein subunit with a flagellar dynein polypeptide suggests an intracellular targeting function. J Cell Biol *118*, 1133-43.

Paschal, B. M., Shpetner, H. S., and Vallee, R. B. (1987). MAP 1C is a microtubule-activated ATPase which translocates microtubules in vitro and has dynein-like properties. J Cell Biol *105*, 1273-82.

Paschal, B. M., and Vallee, R. B. (1987). Retrograde transport by the microtubule-associated protein MAP 1C. Nature *330*, 181-3.

Patel, N., Thierry-Mieg, D., and Mancillas, J. R. (1993). Cloning by insertional mutagenesis of a cDNA encoding Caenorhabditis elegans kinesin heavy chain. Proc Natl Acad Sci USA *90*, 9181-5.

Pelletier, J., and Sonnenberg, N. (1988). Internal initiation of translation of eukaryotic mRNA directed by a sequence derived from poliovirus RNA *334*, 320-325.

Pesavento, P. A., Stewart, R. J., and Goldstein, L. S. (1994). Characterization of the KLP68D kinesin-like protein in Drosophila: possible roles in axonal transport. J Cell Biol *127*, 1041-8.

Pfarr, C. M., Coue, M., Grissom, P. M., Hays, T. S., Porter, M. E., and McIntosh, J. R. (1990). Cytoplasmic dynein is localized to kinetochores during mitosis. Nature *345*, 263-5.

Pfenninger, K. H., and Maylie-Pfenninger, M. (1981). Lectin-labelling of sprouting neurons. II. Relative movement and appearance of glycoconjugates during plasmalemmal expansion. J Cell Biol *89*, 547-559.

Pfister, K. K., Wagner, M. C., Stenoien, D. L., Brady, S. T., and Bloom, G. S. (1989). Monoclonal antibodies to kinesin heavy and light chains stain vesicle-like structures, but not microtubules, in cultured cells. J Cell Biol *108*, 1453-63.

Plamann, M., Minke, P. F., Tinsley, J. H., and Bruno, K. S. (1994). Cytoplasmic dynein and actin-related protein Arp1 are required for normal nuclear distribution in filamentous fungi. J Cell Biol *127*, 139-149.

Polak, M., Scharfmann, R., Seilheimer, B., Eisenbarth, G., Dressler, D., Verma, I. M., and Potter, H. (1993). Nerve growth factor induces neuron-like differentiation of an insulin-secretig pancreatic beta cell line. Proc Natl Acad Sci USA *90*, 5781-5785.

Porter, M. E., Grissom, P. M., Scholey, J. M., Salmon, E. D., and McIntosh, J. R. (1988). Dynein isoforms in sea urchin eggs. J Biol Chem *263*, 6759-71.

Porter, M. E., Scholey, J. M., Stemple, D. L., Vigers, G. P., Vale, R. D., Sheetz, M. P., and McIntosh, J. R. (1987). Characterization of the microtubule movement produced by sea urchin egg kinesin. J Biol Chem *262*, 2794-802.

Rao, C. D., Pech, M., Robbins, K. C., and Aaronson, S. A. (1988). The 5'-untranslated sequence of the c-sis/platelet-derived growth factor 2 transcript is a potent translational inhibitor. Mol Cell Biol *8*, 284-292.

Rasmusson, K., Serr, M., Gepner, J., Gibbons, I., and Hays, T. S. (1994). A family of dynein genes in Drosophila melanogaster. Mol Biol Cell *5*, 45-55.

Rebhun, L. I. (1972). Polarized intracellular particle transport: saltatory movements and cytoplasmic streaming. Int Rev Cytol *32*, 93-137.

Reinsch, S. S., Mitchison, T. J., and Kirschner, M. (1991). Microtubule polymer assembly and transport during axonal elongation. J Cell Biol *115*, 365-379.

Robson, J. A., and Sidell, N. (1985). Ultrastructural features of a human neuroblastoma cell line treated with retinoic acid. Neuroscience *14*, 1149-62.

Rodionov, V. I., Gyoeva, F. K., and Gelfand, V. I. (1991). Kinesin is responsible for centrifugal movement of pigment granules in melanophores. Proc Natl Acad Sci USA *88*, 4956-60.

Rozdzial, M. M., and Haimo, L. T. (1986). Bidirectional pigment granule movements of melanophores are regulated by protein phosphorylation and dephosphorylation. Cell *47*, 1061-70.

Sambrook, J., Fritsch, E. F., and Maniatis, T. (1989). Molecular Cloning: A Laboratory Manual (Cold Spring Harbor, New York: Cold Spring Harbor Laboratory Press).

Sato-Yoshitake, R., Yorifuji, H., Inagaki, M., and Hirokawa, N. (1992). The phosphorylation of kinesin regulates its binding to synaptic vesicles. J Biol Chem *267*, 23930-6.

Saunders, W. S., Koshland, D., Eshel, D., Gibbons, I. R., and Hoyt, M. A. (1995). Saccharomyces cerevisiae kinesin- and dynein-related proteins required for anaphase chromosome segregation. J Cell Biol *128*, 617-24.

Saxton, W. M., Hicks, J., Goldstein, L. S., and Raff, E. C. (1991). Kinesin heavy chain is essential for viability and neuromuscular functions in Drosophila, but mutants show no defects in mitosis. Cell *64*, 1093-102.

Schliwa, M. (1984). Mechanisms of intracellular organelle transport. Cell Muscle Motil *5*, 1-82,403-6.

Schnapp, B. J., and Reese, T. S. (1989). Dynein is the motor for retrograde axonal transport of organelles. Proc Natl Acad Sci USA *86*, 1548-52.

Schnapp, B. J., Reese, T. S., and Bechtold, R. (1992). Kinesin is bound with high affinity to squid axon organelles that move to the plus-end of microtubules. J Cell Biol *119*, 389-99.

Schnapp, B. J., Vale, R. D., Sheetz, M. P., and Reese, T. S. (1985). Single microtubules from squid axoplasm support bidirectional movement of organelles. Cell *40*, 455-62.

Scholey, J. M., Heuser, J., Yang, J. T., and Goldstein, L. S. (1989). Identification of globular mechanochemical heads of kinesin. Nature *338*, 355-7.

Schroer, T. A., and Sheetz, M. P. (1991). Two activators of microtubule-based vesicle transport. J Cell Biol *115*, 1309-18.

Schroer, T. A., Steuer, E. R., and Sheetz, M. P. (1989). Cytoplasmic dynein is a minus end-directed motor for membranous organelles. Cell *56*, 937-46.

Sekine, Y., Okada, Y., Noda, Y., Kondo, S., Aizawa, H., Takemura, R., and Hirokawa, N. (1994). A novel microtubule-based motor protein (KIF4) for organelle transports, whose expression is regulated developmentally. J Cell Biol *127*, 187-201.

Sher, E., Denis-Donini, S., Zanini, A., Bisiani, C., and Clementi, F. (1989). Human neuroblastoma cells acquire regulated secretory properties and different sensitivity to Ca2+ and alpha-latrotoxin after exposure to differentiating agents. J Cell Biol *108*, 2291-300.

Sher, E., Rosa, P., Bassetti, M., and Zanini, A. (1995). Immunolocalization of secretogranin II and insulin in a nreve growth factor-differentiated insulinoma cell line. Eur J Cell Biol *67*, 15-22.

Sidell, N. (1982). Retinoic acid-induced growth inhibition and morphologic differentiation of human neuroblastoma cells in vitro. J Natl Cancer Inst *68*, 589-96.

Skene, J. H. P., and Willard, M. (1981). Changes in axonally transported proteins during axonal regeneration in toad retinal ganglion cells. J Cell Biol *89*, 86-95.

Skoufias, D. A., Cole, D. G., Wedaman, K. P., and Scholey, J. M. (1994). The carboxyl-terminal domain of kinesin heavy chain is important for membrane binding. J Biol Chem *269*, 1477-85.

Skoufias, D. A., and Scholey, J. M. (1993). Cytoplasmic microtubule-based motor proteins. Curr Opin Cell Biol *5*, 95-104.

Small, R. K., Blank, M., Ghez, R., and Pfenninger, K. H. (1984). Components of the plasma membrane of growing axons. II. Diffusion of membrane protein complexes. J Cell Biol *98*, 1434-1443.

Spinelli, W., Sonnenfeld, K. H., and Ishii, D. N. (1982). Effects of phorbol ester tumor promoters and nerve growth factor on neurite outgrowth in cultured human neuroblastoma cells. Cancer Res *42*, 5067-73.

Steuer, E. R., Wordeman, L., Schroer, T. A., and Sheetz, M. P. (1990). Localization of cytoplasmic dynein to mitotic spindles and kinetochores. Nature *345*, 266-8.

Thaler, C. D., and Haimo, L. T. (1990). Regulation of organelle transport in melanophores by calcineurin. J Cell Biol *111*, 1939-48.

Towbin, H., Staehelin, T., and Gordon, J. (1979). Electrophoresis transfer of proteins from polyacrylamide gels to nitrocellulose sheets: procedure and some applications. Proc Natl Acad Sci USA *76*, 4350-4354.

Towbin, J., Staehelin, T., and Gordon, J. (1979). Electrophoretic transfer of proteins from polyacrylamide gels to nitrocellulose sheets: procedure and some applications. Proc Natl Acad Sci USA *76*, 4350-4354.

Toyoshima, I., Yu, H., Steuer, E. R., and Sheetz, M. P. (1992). Kinectin, a major kinesin-binding protein on ER. J Cell Biol *118*, 1121-31.

Urrutia, R., McNiven, M. A., Albanesi, J. P., Murphy, D. B., and Kachar, B. (1991). Purified kinesin promotes vesicle motility and induces active sliding between microtubules in vitro. Proc Natl Acad Sci USA *88*, 6701-5.

Vaisberg, E. A., Koonce, M. P., and McIntosh, J. R. (1993). Cytoplasmic dynein plays a role in mammalian mitotic spindle formation. J Cell Biol *123*, 849-58.

Vale, R. D. (1987). Intracellular transport using microtubule-based motors. Annu Rev Cell Biol *3*, 347-378.

Vale, R. D., Reese, T. S., and Sheetz, M. P. (1985). Identification of a novel force-generating protein, kinesin, involved in microtubule-based motility. Cell *42*, 39-50.

Vale, R. D., Schnapp, B. J., Mitchison, T., Steuer, E., Reese, T. S., and Sheetz, M. P. (1985). Different axoplasmic proteins generate movement in opposite directions along microtubules in vitro. Cell *43*, 623-32.

Vallee, R. B., Wall, J. S., Paschal, B. M., and Shpetner, H. S. (1988). Microtubule-associated protein 1C from brain is a two-headed cytosolic dynein. Nature *332*, 561-3.

Valtorta, F., Villa, A., Jahn, R., De Camilli, P., Greengard, P., and Ceccarelli, B. (1988). Localizationof synapsin I at the frog neuromuscular junction. Neuroscience *24*, 593-603.

Verde, F., Berrez, J. M., Antony, C., and Karsenti, E. (1991). Taxol-induced microtubule asters in mitotic extracts of Xenopus eggs: requirement for phosphorylated factors and cytoplasmic dynein. J Cell Biol *112*, 1177-87.

Wagner, M. C., Pfister, K. K., Bloom, G. S., and Brady, S. T. (1989). Copurification of kinesin polypeptides with microtubule-stimulated Mg-ATPase activity and kinetic analysis of enzymatic properties. Cell Motil Cytoskeleton *12*, 195-215.

Walker, R. A., and Sheetz, M. P. (1993). Cytoplasmic microtubule-associated motors. Annu Rev Biochem *62*, 429-51.

Warren, G., Davoust, J., and Cockcroft, A. (1984). Recycling of transferrin receptors in A431 cells is inhibited during mitosis. EMBO J *3*, 2217-2225.

Warren, G., Featherstone, C., Griffiths, G., and Burke, B. (1983). Newly synthesized G protein of vesicular stomatitis virus is not transported to the cell surface during mitosis. J Cell Biol *97*, 1623-1628.

Waterman-Storer, C. M., Karki, S., and Holzbaur, E. L. (1995). The p150Glued component of the dynactin complex binds to both microtubules and the actin-related protein centractin (Arp-1). Proc Natl Acad Sci USA *92*, 1634-8.

Wright, B. D., Henson, J. H., Wedaman, K. P., Willy, P. J., Morand, J. N., and Scholey, J. M. (1991). Subcellular localization and sequence of sea urchin kinesin heavy chain: evidence for its association with membranes in the mitotic apparatus and interphase cytoplasm. J Cell Biol *113*, 817-33.

Xiang, X., Beckwith, S. M., and Morris, N. R. (1994). Cytoplasmic dynein is involved in nuclear migration in Aspergillus nidulans. Proc Natl Acad Sci USA *91*, 2100-4.

Yang, J. T., Laymon, R. A., and Goldstein, L. S. (1989). A three-domain structure of kinesin heavy chain revealed by DNA sequence and microtubule binding analyses. Cell *56*, 879-89.

Yang, J. T., Saxton, W. M., and Goldstein, L. S. (1988). Isolation and characterization of the gene encoding the heavy chain of Drosophila kinesin. Proc Natl Acad Sci USA *85*, 1864-8.

Yang, J. T., Saxton, W. M., Stewart, R. J., Raff, E. C., and Goldstein, L. S. (1990). Evidence that the head of kinesin is sufficient for force generation and motility in vitro. Science *249*, 42-7.

Yu, H., Toyoshima, I., Steuer, E. R., and Sheetz, M. P. (1992). Kinesin and cytoplasmic dynein binding to brain microsomes. J Biol Chem *267*, 20457-64.

Zhang, Z., Tanaka, Y., Nonaka, S., Aizawa, H., Kawasaki, H., Nakata, T., and Hirokawa, N. (1993). The primary structure of rat brain (cytoplasmic) dynein heavy chain, a cytoplasmic motor enzyme. Proc Natl Acad Sci USA *90*, 7928-32.

UC San Francisco LIBRARY
UNIVERSITY OF CALIFORNIA · UNIVERSITY OF CALIFORNIA

For reference

Not to be taken from the room.

6462231

3 1378 00646 2231